Supported by 日本財団 THE NIPPON FOUNDATION

日 中 笹 川 医 学 奨 学 金 制 度

第３８期研究者研究報告会

研　究　報　告　集

2016 年 4 月～2017 年 3 月

公益財団法人　日中医学協会

２０１７　年　３　月　２８　日

日本財団ビル大会議室 A

目　次(発表順)

The role of endothelial FGFR1 on the homeostasis of endothelial cells

内皮細胞の恒常性において内皮細胞FGFR1が演じる役割

研 究 者 氏 名　　胡　瓊英（第 38期笹川医学研究者）
中国所属機関　　成都中医薬大学附属医院検査科
日本研究機関　　金沢医科大学糖尿病内分泌内科学
指 導 責 任 者　　古家　大祐　教授

Abstract:

Fibroblast growth factor receptor (FGFR)1 in endothelial cells exhibits essential role on the cellular homeostasis via induction of microRNA let-7s, the microRNA displaying anti-endothelial mesenchymal transition (EndMT) program via suppression of transforming growth factor β receptor 1 (TGFβR1). We have shown that the endogenous anti-fibrotic peptide, N-acetyl-seryl-aspartyl-lysyl-proline (AcSDKP) inhibited organs fibrosis by counteracting the EndMT by restoring suppressed levels of FGFR1 and microRNA let-7. The mitochondria is essential for the endothelial homeostasis; the mitochondrial biogenesis is tightly regulated and microRNA let-7b has been shown to display the role for normal biogenesis of mitochondria. Here we found that endothelial FGFR1 and its down stream signaling were essential for the mitochondrial biogenesis and the deficiency in FGFR1 directly disrupted endothelial mitochondria biogenesis and subsequently induced EndMT. When endothelial FGFR1 signaling pathway was inhibited by neutralizing antibody for FGFR1, overexpression of fibroblast growth factor receptor substrate 2 (FRS2) siRNA, or combination of cytokines (TGF-β2, interleukin (IL)-1β, tumor necrosis factor (TNF)-α), we observed mitochondrial biogenesis defects in endothelial cells by MitoTracker Green. Such disruptions of mitochondria in endothelial cells by FGFR1 deficiency were associated with suppression of microRNA let-7b levels and small GTPase proteins critical for mitochondria biogenesis, mitofusin 2 (MFN2) and optic atrophy (OPA1). Furthermore AcSDKP could inhibit mitochondria defects with EndMT phenotype induced by cytokines combination; AcSDKP could not rescue such phenotypes in the endothelial cells without normal FGFR1 signaling. These results indicated that FGFR1 is critical molecule for normal mitochondrial biogenesis and essential for the homeostasis for endothelial phenotype.

Key Words:

FGFR1, mitochondrial biogenesis, microRNA let-7, EndMT

Introduction:

Maintenance of endothelial homeostasis is thought to be necessary for remaining normal endothelial cells and organs biology and function[1]. Endothelial-mesenchymal transition (EndMT) is a fundamental cellular mechanism that occurs in various pathologic conditions such as cancer and fibrosis[2]. Fibroblast growth factor receptor 1 (FGFR1) is a key inhibitor of TGFβ signaling pathway and EndMT development[3]. Chen, et al. demonstrated that disruption of baseline FGF signaling in the endothelium led to a dramatic reduction in microRNA let-7 miRNA levels that increased expression of TGFβ ligands and receptors, subsequently activated of TGFβ signaling leading to EndMT[4]. Therefore, it is thought that targeting the microRNA let-7 biogenesis pathway may lead to the development of endothelial homeostasis. One of the best-studied repressors of microRNA let-7 biogenesis is Lin28, which has crucial and diverse roles in aerobic glycolysis[5]. Mitochondrial bioenergetics and biogenesis are critical for cellular homeostasis and stress responses, including cellular differentiation, host defense and tissue fibrosis[6]. Interestingly, microRNA let-7b contributed in mitochondrial biogenesis. Mitochondrial morphology regulated by fusion and fission machinery is physiologically relevant for cell homeostasis[7]. However, the mechanism of FGFR1 regulating mitochondrial biogenesis via antifibrotic microRNA let-7 family is not clear. In this paper, we demonstrated the AcSDKP-FGFR1 axis promoted mitochondrial biogenesis by upregulation of microRNA let-7 expression to maintain endothelial function.

Methods:

Reagents and antibodies

AcSDKP was from Asabio Bio Technology (Osaka, Japan). FRS2 siRNA and negative control siRNA (Silencer®, Silencer® Select, Ambion™) were from Thermo Fisher Scientific. MitoTracker® Green FM was from invitrogen. 3-isobutyl-1-methylxanthine was from Sigma. Anti-MFN 2 antibody was from abcam. OPA1 antibody was from BD Transduction Laboratories™. DRP1 antibody was from Cell Signaling.

Cell culture

Normal human dermal microvascular endothelial cells (HMVECs,CC-2516, Lonza, Basel, Switzerland) cultured in EGM medium supplemented with EGM^{TM}-2. The cells were grown at 37℃,5% CO_2.

Western blot analysis

Western blot results were detected using an ImageQuant LAS 400 digital biomolecular imaging system (GE Healthcare Life Sciences, Uppsala, Sweden). Images were viewed in ImageJ software for data analysis. Data were exported to GraphPad Prism Software to generate the plot. Error bars showed the calculated standard deviation. P-values of < 0.05 were considered significant.

RNA isolation and qPCR

Complementary DNA (cDNA) was generated by a miScript II RT kit (Qiagen) using the hiSpec buffer method. miR expression was quantified using a miScript SYBR Green PCR Kit (Qiagen). Hs_RNU6-2_1 (Qiagen) was utilized as an internal control.

Immunofluorescence staining and MitoTracker staining

Grow cells in Corning® BioCoat™ Fibronectin 4 Well were mounted using Prolong Gold antifade reagent with 4',6-diamidino-2-phenylindole (DAPI) (Life Technologies P36931). Grow cells in above 4 Well were stained by containing 100 nM MitoTracker® Green. All of them were taken pictures with Confocal Scanning Microscope (Zeiss LSM 710).

Statistical analysis

All graphs were created using GraphPad Prism software, and statistical analyses were calculated using GraphPad Prism. The significance of the differences between the controls and the experimental groups was determined using a two-tailed Student's t-test. For multiple comparisons, one-way ANOVA with Newman-Keuls test or chisquare test was used. The data were presented as means ± SD. A P-value < 0.05 was considered significant ($*P < 0.05$, $**P < 0.01$, $***P < 0.001$). All results were confirmed by three independent experiments.

Results:

1. Deficiency of FGFR1 signaling suppressed mitochondrial biogenesis and microRNA let-7 expression in ECs.

To analyze the relationship between FGFR1, mitochondria, microRNAs in endothelial function, we inhibited FGFR1

signaling by FRS2 siRNA; then measured mitochondrial biogenesis and microRNA let-7 expression in ECs. We found that FRS2 knockdown reduced mitochondrial membrane fusions proteins MFN2 and OPA1 expression in ECs by western blot, while no change of mitochondrial fission protein dynamin-related protein 1 (DRP1) was observed in these cells (Fig. 1A). Meanwhile, inhibition of FGFR1 signaling by FRS2 siRNA also lowered mitochondrial levels by MitoTracker Green (Fig. 1B). Above all, it suggested that inhibition of FGFR1 signaling suppresses mitochondrial biogenesis in ECs, and FGFR1 signaling was tightly related with mitochondrial function. Our previous study performed microRNA microarray and found suppression of antifibrotic microRNA let-7 family levels in fibrotic diabetic mouse kidney and induction of EndMT[8]. Base on them, in this study, to evaluate the microRNAs expression linkage between FGFR1 signaling and mitochondrial biogenesis, we analyzed the let-7b-5p/3p, 7c-5p/3p, 7g-5p/3p genes expression by qPCR. FRS2 deficiency led to a suppression of the level of let-7b-5p/3p, 7c-5p/3p, 7g-5p/3p, moreover, let-7b-5p expression showed the most significant difference in ECs (Fig. 1C).

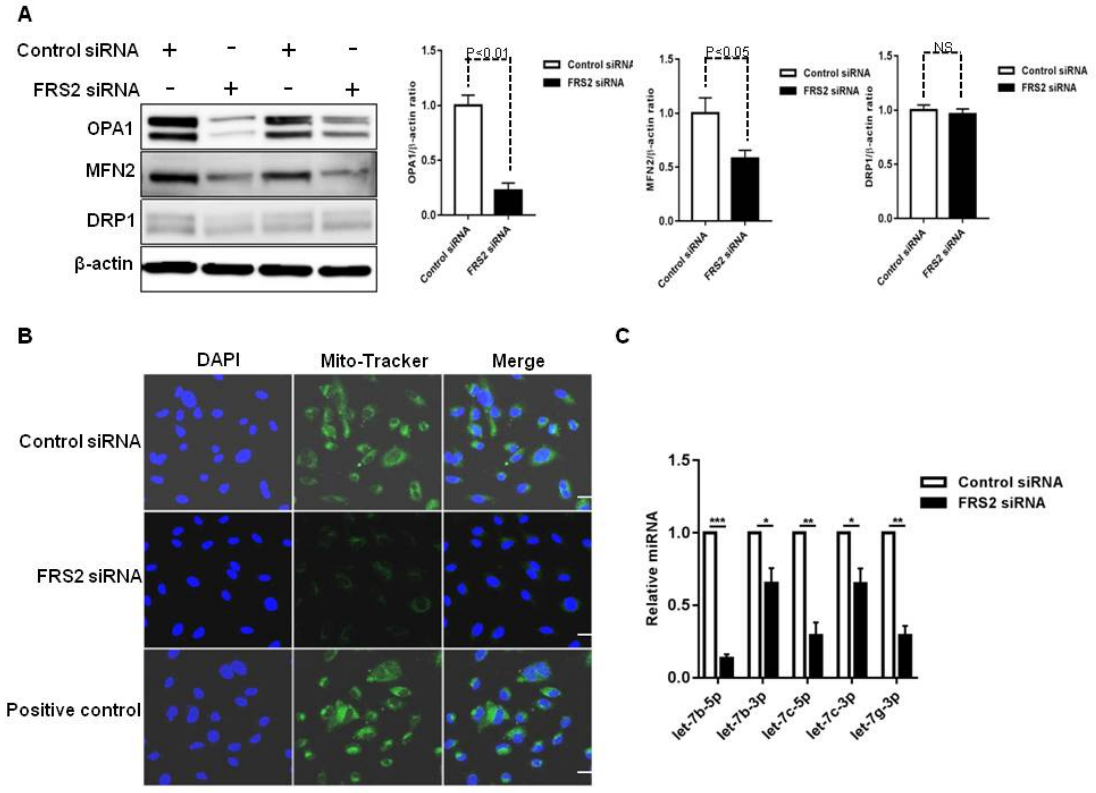

Figure 1. Inhibition of FGFR1 signaling in ECs suppressed mitochondrial biogenesis and microRNA let-7 expression.

(A) Left: Western blot analyzed mitochondrial function markers of FRRS2 deficient in the ECs for 48h. Right: Band intensities of these proteins. **(B)** Confocal microscope analysis of FRS2 deficient in ECs for 48h with MitoTracker®

Green FM, DAPI and overlay images of MitoTracker green and DAPI staining (blue) (Original magnification×400). Isobutyl-1-methylxanthine (IBMX, 5 μM), was used as a positive control10. Scale bar: 25 μm. **(C)** Quantitative real-time PCR analysis of microRNA let-7b family mRNA gene expression in ECs of the control, FRS2 siRNA, n =3 were analyzed in each data set. Results are expressed as means ± SD (*P＜0.05, **P＜0.01 , ***P＜0.001, compared to control siRNA; unpaired two-tailed Student's t-test).

2. AcSDKP regulated mitochondrial biogenesis and microRNA let-7b-5p expression of cytokines combination-induced endothelial EndMT by FGFR1 signaling.

To explored the association between mitochondria biogenesis and microRNA let-7 gene expression in endothelial EndMT, we tested whether by AcSDKP could inhibit cytokines combination (TGF-β2 at 2.5ng/mL, IL-1β at 2ng/mL, TNFα at 1 ng/mL)-induced mitochondrial biogenesis defects and EndMT. Western blot and immunofluorescence analyze revealed that cytokines combination decreased the level of MFN2 and OPA1 proteins while DRP1 had no change associated with EndMT. However, AcSDKP restored the suppression of mitochondrial fusion proteins and mitochondrial levels by MitoTracker into normal levels (Fig. 2A,B) associated with inhibition of EndMT. We continued to analyze the microRNA let-7b-5p gene expression, and found that cytokines combination also suppressed microRNA let-7b-5p gene expression by qPCR in ECs but AcSDKP restored the levels of microRNA let-7b-5p (Fig. 2C). These results supported that the mechanism of AcSDKP antifibrotic effect involved in regulation of mitochondrial biogenesis and miR-let-7b-5p expression. Furthermore, to explore the potential mechanism of AcSDKP recovering mitochondrial biogenesis and microRNA let-7 expression in endothelial EndMT, we analyzed the effect of AcSDKP on FRS2 deficient cells. Western blot and immunofluorescence revealed that AcSDKP failed to restore the reduction of MFN2 and OPA1 proteins and mitochondrial levels by MitoTracker in FRS2 deficient cells (Fig. 2D,E). Finally, AcSDKP could not restore the levels of microRNA let-7b-5p in FRS2 deficient cells (Fig. 2F).

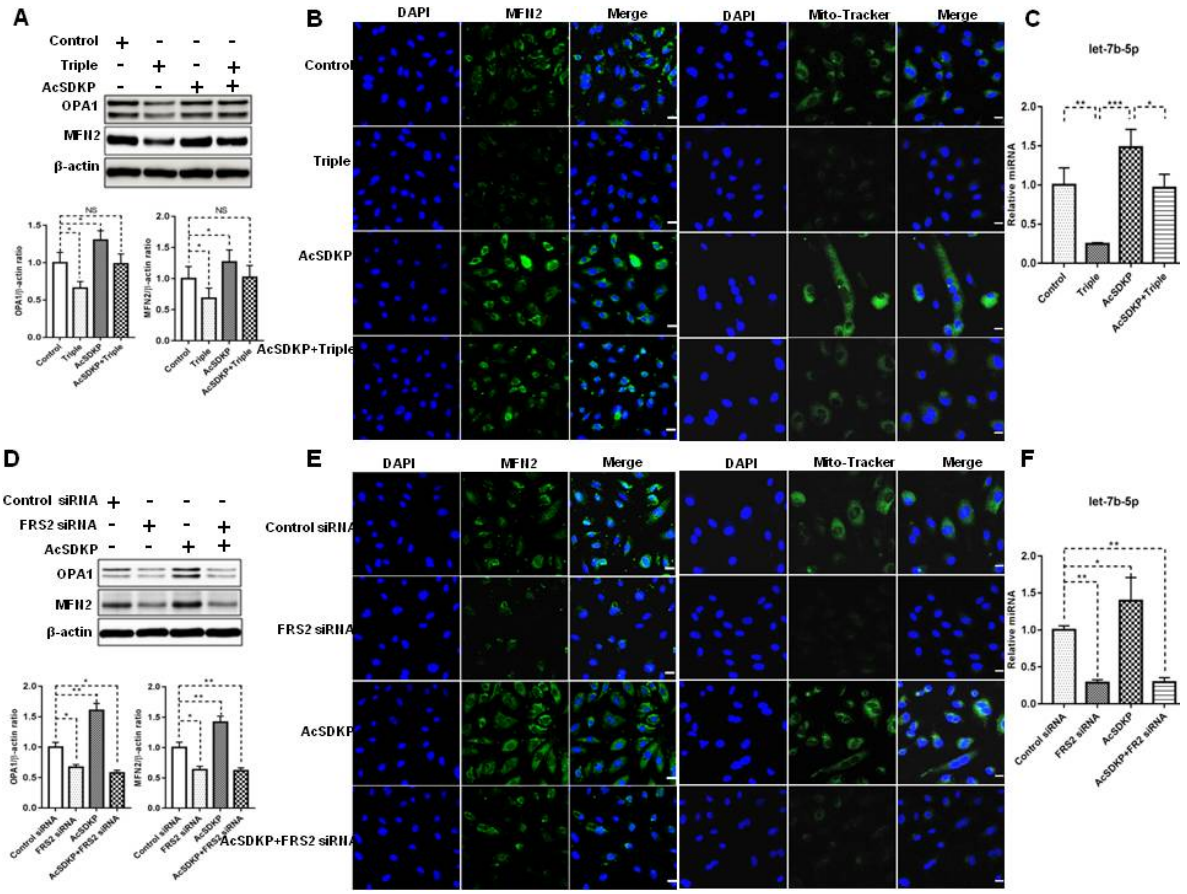

Figure 2. AcSDKP restored mitochondrial biogenesis and microRNA let-7b-5p expression of cytokines combination-induced endothelial EndMT by FGFR1 signaling.

(A) Up panel: Western blot analyzed mitochondrial function markers of AcSDKP treated and cytokines combination-induced EndMT in ECs for 48h. Down panel: Band intensities of these markers. **(B)** Confocal microscope analysis of MFN2 expression and MitoTracker® Green in cytokines combination-induced endothelial EndMT. **(C)** qPCR analysis of miroRNA let-7b-5p mRNA gene expression in these cells. **(D)** Up panel: Western blot analysis of mitochondrial proteins in FRS2 deficient and AcSDKP treated ECs for 48h. Down panel: Band intensities of these proteins. **(E)** Confocal microscope analysis of MFN2 expression and MitoTracker® Green of these cells. **(F)** qPCR analysis of microRNA let-7b-5p mRNA gene expression in these cells. Results are expressed as means ± SD (*P＜0.05, **P＜0.01 as compared to control group, a one-way ANOVA followed by Tukey's test). Original magnification ×400. Scale bar: 25 μm.

Discussion:

In our study, we observed that microRNA let-7 promotes mitochondrial biogenesis and FGFR1 signaling is essential for

the homeostasis of endothelial cells via induction of microRNA let-7. Importantly, our finding first provided that microRNA let-7 itself, played a linkage contribution in mitochondrial biogenesis and endothelial function. Then cytokines combination and blocking FGFR1 signaling provided evidences indicating that endothelial FGFR1 played a key role on the homeostasis of endothelial cells via regulation of microRNA let-7 expression and mitochondrial biogenesis.

MicroRNA let-7 family, was sufficient to prevent and treat impaired glucose tolerance in mice with diet-induced obesity and provide an approach to treating type 2 diabetes[9]. Furthermore, Lin28-suppressed microRNA let-7 played a role in TGFβ-induced collagen accumulation in glomerular mesangial cells under diabetic conditions[10]. A critical another factor for diabetic endothelial dysfunction is impairing mitochondrial biogenesis due to oxidative stress, high production of reactive oxygen species (ROS) and low levels of ATP [11]. Accordingly, mitochondrial dynamic processes, such as mitochondrial biogenesis, fusion, fission and mitophagy, play a key role in maintaining endothelial homeostasis. Here we discovered that mitochondrial fusion proteins were suppressed after blocking FGFR1 signaling associated with suppression of microRNA let-7. In this study, suppression of microRNA let-7 gene expression was associated with the deficiency in mitochondrial fusion proteins and mitochondrial biogenesis. We already reported the anti-EndMT effects of microRNA let-7. These data provide us an opportunity to design the future development of strategy to normalize endothelial FGFR1 signaling by either AcSDKP or new compounds to combat the disease condition associated with mitochondrial defects in endothelial cells.

References:

1 Shi, Y. & Vanhoutte, P. M. Macro- and Microvascular Endothelial Dysfunction in Diabetes. *Journal of diabetes*, doi:10.1111/1753-0407.12521 (2017).

2 Shu, Y. *et al.* Aspirin-Triggered Resolvin D1 Inhibits TGF-beta1-Induced EndMT through Increasing the Expression of Smad7 and Is Closely Related to Oxidative Stress. *Biomolecules & therapeutics* **24**, 132-139, doi:10.4062/biomolther.2015.088 (2016).

3 Chen, P. Y., Qin, L., Li, G., Tellides, G. & Simons, M. Fibroblast growth factor (FGF) signaling regulates transforming growth factor beta (TGFbeta)-dependent smooth muscle cell phenotype modulation. *Scientific reports* **6**, 33407, doi:10.1038/srep33407 (2016).

4 Chen, P. Y., Qin, L., Li, G., Tellides, G. & Simons, M. Smooth muscle FGF/TGFbeta cross talk regulates atherosclerosis progression. *EMBO molecular medicine* **8**, 712-728, doi:10.15252/emmm.201506181 (2016).

5 Ma, X. *et al.* Lin28/let-7 axis regulates aerobic glycolysis and cancer progression via PDK1. *Nature communications* **5**, 5212, doi:10.1038/ncomms6212 (2014).

6 Bernard, K. *et al.* NADPH Oxidase 4 (Nox4) Suppresses Mitochondrial Biogenesis and Bioenergetics in Lung Fibroblasts via a Nuclear Factor Erythroid-Derived 2-like 2 (Nrf2)-Dependent Pathway. *The Journal of biological chemistry*, doi:10.1074/jbc.M116.752261 (2017).

7 Zhang, C. *et al.* Appoptosin interacts with mitochondrial outer-membrane fusion proteins and regulates mitochondrial morphology. *Journal of cell science* **129**, 994-1002, doi:10.1242/jcs.176792 (2016).

8 Srivastava, S. P. *et al.* Effect of Antifibrotic MicroRNAs Crosstalk on the Action of N-acetyl-seryl-aspartyl-lysyl-proline in Diabetes-related Kidney Fibrosis. *Scientific reports* **6**, 29884, doi:10.1038/srep29884 (2016).

9 Frost, R. J. & Olson, E. N. Control of glucose homeostasis and insulin sensitivity by the Let-7 family of microRNAs. *Proceedings of the National Academy of Sciences of the United States of America* **108**, 21075-21080, doi:10.1073/pnas.1118922109 (2011).

10 Park, J. T. *et al.* Repression of let-7 by transforming growth factor-beta1-induced Lin28 upregulates collagen expression in glomerular mesangial cells under diabetic conditions. *American journal of physiology. Renal physiology* **307**, F1390-1403, doi:10.1152/ajprenal.00458.2014 (2014).

11 Han, C. Y. *et al.* NADPH oxidase-derived reactive oxygen species increases expression of monocyte chemotactic factor genes in cultured adipocytes. *The Journal of biological chemistry* **287**, 10379-10393, doi:10.1074/jbc.M111.304998 (2012).

作成日：2017 年 2 月 23 日

Metagenomic analysis of the mucosa-associated microbiota in chronic dacryocystitis
慢性涙嚢炎における粘膜細菌叢のメタゲノム解析

研究者氏名　張　尋（第38期笹川医学研究者）
中国所属機関　北京疾病コントロールセンター
日本研究機関　香川大学医学部分子微生物学
指導責任者　桑原　知巳　教授
共同研究者名　今大路　治之　助教

Abstract

Dacryocystitis is caused by bacterial or fungal proliferation in lacrimal sac or duct. Lacrimal duct obstruction is the most common pathology of dacryocystitis. Most of the dacryocystitis follows the chronic course, and some cases have years of the disease history. During the past years, only few studies had been conducted on the bacteriology of dacryocystitis. In this study, we applied the 16S ribosomal RNA gene (16S rDNA) sequence meta-analysis to the lacrimal sac aspirates from 20 patients with chronic dacryocystitis. We identified 2-11 operational taxonomic units (OTUs) per sample, which showed >1.0% abundance. Of 20 samples, 11 samples contained a dominant OUT that showed >50% abundance, which included the OTUs classified into *Staphylococcus*, *Bacteroides*, *Corynebacterium*, *Pseudomonas*, *Actinomyces* and *Xanthomonadaceae*. Two dacryocystitis cases were monomicrobial (*B. fragilis*) and polymicrobial (*Porphyromonas* sp., *Prevotella* sp., and *Parvimonas* sp.) anaerobic infection, respectively. These results indicate that nearly half of the chronic dacryocystitis is monomicrobial infection and obligate anaerobes share a significant portion of etiology of the disease. These findings are useful for empirical antibiotic treatment of chronic dacryocystitis.

Key words

Dacryocystitis, Microbiome, 16S rDNA, Next generation sequencing

Introduction

Isolation of bacteria or fungi by culture technique is a gold standard for diagnosis of infections. Opportunistic infections are increasing by highly invasive medical treatments or population aging. Compromised hosts are vulnerable to the bacteria of environmental origins as well as to virulent pathogens. It is well known that many of the environmental bacteria are difficult to culture in synthetic media. In addition, culture technique is not suitable for comprehensive bacterial identification of the human samples contaminated by a large amount of commensal bacteria.

Ribosomal RNA gene (rDNA) sequences, especially the 16S rDNA, represent the most important current targets of study in bacterial evolution and ecology, which include the determination of phylogenetic relationships among taxa, the exploration of bacterial diversity in the various environments and the quantification of the relative abundance of taxa of various ranks.

Next-generation sequencing (NGS) technology of 16S rDNA amplicons has been recently applied to a wide variety of environments. For example, the Ion Torrent PGM has been used for community analyses of uranium mine tailings that had particularly high pH and low permeability, recirculating aquaculture systems, hydrocarbon-contaminated Arctic soils, oil sands mining affected sediments and biofilms from the Athabasca River, the rhizosphere of willows planted in contaminated soils, and the microbiota associated with human and animal.

Dacryocystitis is caused by bacterial or fungal proliferation in lacrimal sac or duct. Lacrimal duct obstruction is the

most common pathology of dacryocystitis. Most of the dacryocystitis follows the chronic course, and some cases have years of the disease history. During the past years, only few studies had been conducted on the bacteriology of dacryocystitis. In this study, we applied the 16S rDNA sequence meta-analysis to the lacrimal sac aspirates from 20 patients with chronic dacryocystitis.

Methods

(i) Library preparation

The lacrimal sac microbiomes in the chronic dacryocystitis patients were characterized by 16S rDNA meta-analysis with Ion PGM. DNA extraction was performed using achromopeptidase as described by Morita *et al.* DNA concentration was quantified with Qubit 2.0 instrument by employing Qubit dsDNA BR Assay Kit (Thermo Fisher). PCR amplification of the 16S rDNA hypervariable region was performed with the Ion 16S Metagenomics Kit (Thermo Fisher). PCR conditions consisted of 1 cycle of 95°C for 10 min; 30 cycles of 95°C for 30 s, 58°C for 30 s, and 72°C for 20 s; and then 1 cycle of 72°C for 7 min. The PCR products were purified by electrophoretic separation on a 2% agarose gel and the use of a QIAquick Gel Extraction Kit (QIAGEN). The purified products were end-repaired and ligated with Ion P1 adapter and Ion Xpress Barcode adapters by using the Ion Plus Fragment Library Kit and Ion Xpress Barcode Adapters Kit (Thermo Fisher). These adapters were designed to specify the samples. Purification of the amplicon libraries was performed using the Agencourt AMPure XP Reagent (Beckman), and the library concentration was estimated with the Agilent 2100 Bioanalyzer system using the Agilent High Sensitivity DNA Kit (Agilent).

(ii) Emulsion PCR and sequencing

The emulsion PCR and enrichment was carried out with the Ion OneTouch 2 and Ion OneTouch ES instrument using the Ion PGM Hi-Q OT2 Kit (Thermo Fisher) according to the manufacturer's instructions. Sequencing of the amplicon libraries was performed on an Ion 316 chip v2 using the Ion Torrent PGM system and the Ion PGM Hi-Q Sequencing Kit (Thermo Fisher).

(iii) Data processing

Using the UCLUST algorithm built into the QIIME pipeline, sequences were clustered at > 97 % identity against the Greengenes reference database. Using the QIIME pipeline, unweighted UniFrac distances were produced and used to investigate beta diversity by plotting PCA coordinates.

Results

We analyzed the lacrimal sac microbiomes of the chronic dacryocystitis by Ion PGM-based 16S rDNA sequencing analysis. We identified 2-11 operational taxonomic units (OTUs) per sample, which showed >1.0% abundance. Of 20 samples, 11 samples contained a dominant OUT that showed >50% abundance, which included the OTUs classified into *Staphylococcus*, *Bacteroides*, *Corynebacterium*, *Pseudomonas*, *Actinomyces* and *Xanthomonadaceae*. Two dacryocystitis cases were monomicrobial (*B. fragilis*) and polymicrobial (*Porphyromonas* sp., *Prevotella* sp., and *Parvimonas* sp.) anaerobic infection, respectively (Fig. 1). Principle coordinate analysis (PCoA) basing on the abundance at species level divided the chronic dacryocystitis into five types: (i) *Staphylococcus* predominant type; (ii) *Enterobacteriaceae* predominant type; (iii) *Xanthomonadaceae* predominant type; (iv) Anaerobe type; and (v) Others (Fig. 2).

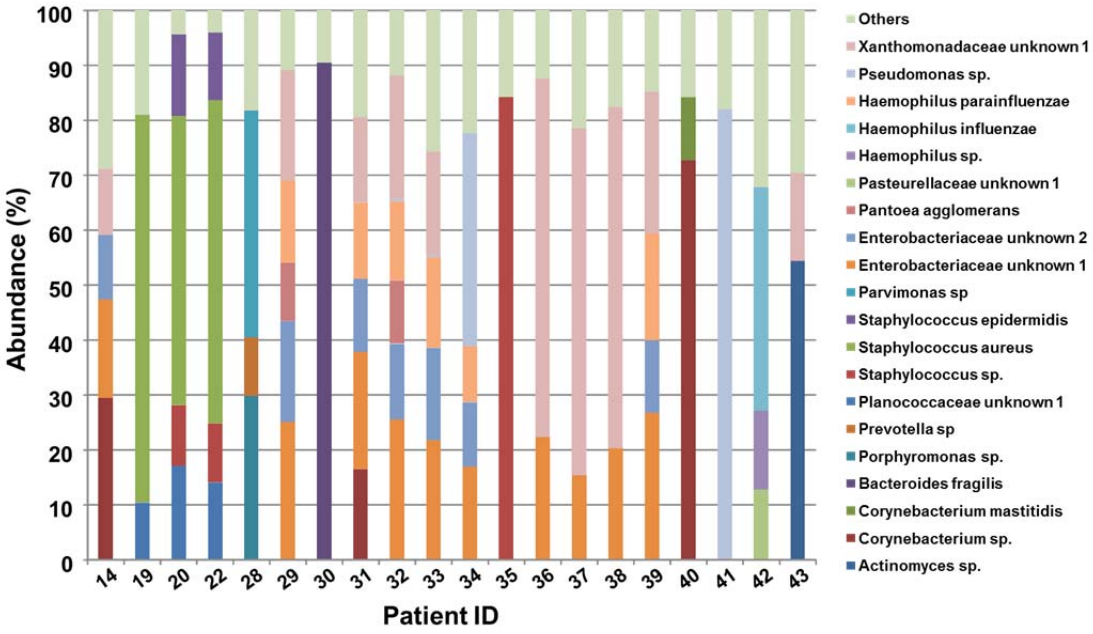

Fig. 1. Comparative microbiota analysis of the lacrimal sac samples. The microbial compositions were compared by Ion PGM-based 16S rDNA sequencing analysis.

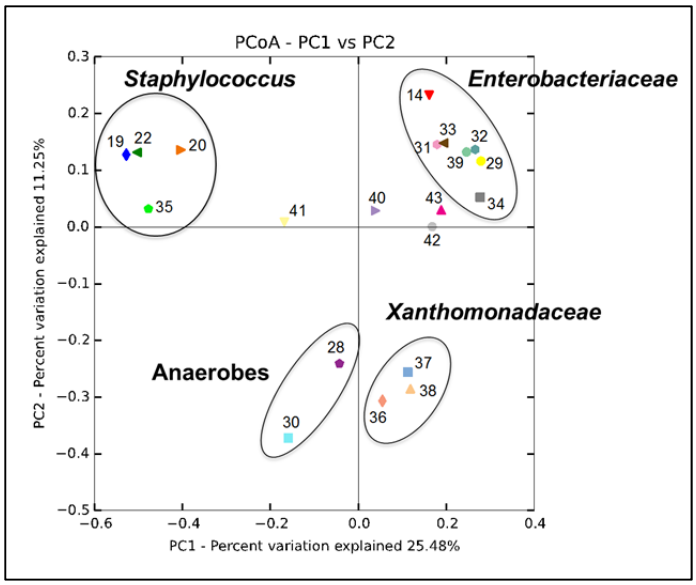

Fig. 2. PCoA plot describing unweighted UniFrac distance among microbial composition in chronic dacryocystitis. Pairwise distances between all samples are projected onto a two dimensional space where the PCA axis describes the highest degree of variation. Samples that are clustered closely together are thus considered to share a larger proportion of the phylogenetic tree compared to samples that have a larger separation.

Discussion

Chronic dacryocystitis is a major clinical type of infection of lacrimal sac or duct. The disease history of chronic dacryocystitis sometimes encompasses several decades of years. However, there are few microbiological surveys for chronic dacryocystitis due to the massive contamination by resident microorganisms in lacrimal canal or sac.

Recently, 16S rDNA meta-analysis employing the NGS technology provides us with the in-depth information about microbial compositions in the samples. In this study, we applied the 16S rDNA sequence meta-analysis to the lacrimal sac aspirates from 20 patients with chronic dacryocystitis. We could identify 2-11 operational taxonomic units (OTUs) per sample, which showed >1.0% abundance.

Staphylococcus and *Pseudomonas* are reported as representative etiologic agents for chronic dacryocystitis. Consistently, *Staphylococcus* was predominant in four of the 20 samples. It was noteworthy that the unknown species in *Enterobacteriaceae* and *Xanthomonadaceae* were predominant in a large proportion of the samples. These results indicate that previously uncharacterized bacterial species might be a common etiologic agent for chronic dacryocystitis.

In addition, anaerobic bacteria should be taken into account for the treatment of chronic dacryocystitis. Oppose to our prediction, many cases of chronic dacryocystitis were monomicrobial infections. These findings are useful for empirical antibiotic treatment of chronic dacryocystitis.

References

[1] Wang Y, Qian P Y. Conservative fragments in bacterial 16S rRNA genes and primer design for 16S ribosomal DNA amplicons in metagenomic studies[J]. PloS one, 2009, 4(10): e7401.e7401

[2] Edwards U, Rogall T, Blöcker H, et al. Isolation and direct complete nucleotide determination of entire genes. Characterization of a gene coding for 16S ribosomal RNA[J]. Nucleic acids research, 1989, 17(19): 7843-7853.

[3] Huws S A, Edwards J E, Kim E J, et al. Specificity and sensitivity of eubacterial primers utilized for molecular profiling of bacteria within complex microbial ecosystems[J]. Journal of Microbiological Methods, 2007, 70(3): 565-569.

[4] Klindworth A, Pruesse E, Schweer T, et al. Evaluation of general 16S ribosomal RNA gene PCR primers for classical and next-generation sequencing-based diversity studies[J]. Nucleic acids research, 2012: gks808.

[5] Yarza P, Yilmaz P, Pruesse E, et al. Uniting the classification of cultured and uncultured bacteria and archaea using 16S rRNA gene sequences[J]. Nature Reviews Microbiology, 2014, 12(9): 635-645.

[6] Yarza P, Yilmaz P, Pruesse E, et al. Uniting the classification of cultured and uncultured bacteria and archaea using 16S rRNA gene sequences[J]. Nature Reviews Microbiology, 2014, 12(9): 635-645.

[7] Manaka A, Tokue Y, Murakami M. Comparison of 16S ribosomal RNA gene sequence analysis and conventional culture in the environmental survey of a hospital[J]. Journal of Pharmaceutical Health Care and Sciences, 2017, 3(1): 8.

[8] Li Q, Wang C, Tang C, et al. Bacteremia in patients with acute pancreatitis as revealed by 16S ribosomal RNA gene-based techniques[J]. Critical care medicine, 2013, 41(8): 1938-1950.

[9] Schloss P D, Jenior M L, Koumpouras C C, et al. Sequencing 16S rRNA gene fragments using the PacBio SMRT DNA sequencing system[J]. PeerJ, 2016, 4: e1869.

[10] Tremblay J, Singh K, Fern A, et al. Primer and platform effects on 16S rRNA tag sequencing[J]. Frontiers in microbiology, 2015, 6: 771.

[11] Nelson M C, Morrison H G, Benjamino J, et al. Analysis, optimization and verification of Illumina-generated 16S rRNA gene amplicon surveys[J]. PloS one, 2014, 9(4): e94249.

[12] Fernandes A D, Reid J N S, Macklaim J M, et al. Unifying the analysis of high-throughput sequencing datasets: characterizing RNA-seq, 16S rRNA gene sequencing and selective growth experiments by compositional data analysis[J]. Microbiome, 2014, 2(1): 15.

[13] Poretsky R, Rodriguez-R L M, Luo C, et al. Strengths and limitations of 16S rRNA gene amplicon sequencing in revealing temporal microbial community dynamics[J]. PLoS One, 2014, 9(4): e93827.

[14] Cole J R, Wang Q, Fish J A, et al. Ribosomal Database Project: data and tools for high throughput rRNA analysis[J]. Nucleic acids research, 2013: gkt1244.

[15] Kennedy N A, Walker A W, Berry S H, et al. The impact of different DNA extraction kits and laboratories upon the assessment of human gut microbiota composition by 16S rRNA gene sequencing[J]. PloS one, 2014, 9(2): e88982.

[16] Mizrahi-Man O, Davenport E R, Gilad Y. Taxonomic classification of bacterial 16S rRNA genes using short sequencing reads: evaluation of effective study designs[J]. PloS one, 2013, 8(1): e53608.

[17] Salipante S J, Sengupta D J, Rosenthal C, et al. Rapid 16S rRNA next-generation sequencing of polymicrobial clinical samples for diagnosis of complex bacterial infections[J]. PloS one, 2013, 8(5): e65226.

[18] D'Amore R, Ijaz U Z, Schirmer M, et al. A comprehensive benchmarking study of protocols and sequencing

platforms for 16S rRNA community profiling[J]. BMC genomics, 2016, 17(1): 55.
[19] Kumar S, Stecher G, Tamura K. MEGA7: Molecular Evolutionary Genetics Analysis version 7.0 for bigger datasets[J]. Molecular biology and evolution, 2016: msw054.
[20] Wang Y, Tian R M, Gao Z M, et al. Optimal eukaryotic 18S and universal 16S/18S ribosomal RNA primers and their application in a study of symbiosis[J]. PloS one, 2014, 9(3): e90053.

作成日：2017 年 3 月 7 日

Role of apoptosis inhibitor of macrophage (AIM) in chronic obstructive pulmonary disease

慢性閉塞性肺疾患における apoptosis inhibitor of macrophage (AIM) の役割

研究者氏名　葛　海燕（第38期笹川医学研究者）

中国所属機関　復旦大学附属華東医院呼吸科

日本研究機関　北海道大学大学院医学研究科
呼吸器内科学分野

指導責任者　西村　正治　教授

共同研究者名　鈴木　雅　助教，木村　裕樹　博士

Abstract:

Rationale: Apoptosis inhibitor of macrophage (AIM) is a multifaceted IgM-binding protein, which has been reported to be involved in the pathogenesis of a variety of inflammatory diseases. We hypothesized that AIM might play a role in the pathogenesis and disease progression of COPD.

Methods: As an animal study, we established cigarette smoke (CS)-induced emphysema mice model, including different time points (0 day, 3 days, 1 week, 2 weeks, 4 weeks, and 16 weeks), using wild type (WT) and AIM-knock out (KO) mice. The degree of emphysema was assessed by the determination of the mean linear intercept (Lm) on hematoxylin and eosin-stained sections. AIM protein in different time points was detected by immunofluorescence and western blotting. As a clinical study, we measured serum AIM and IgM levels in 133 subjects with COPD who participated in the Hokkaido COPD cohort study, and we investigated an association of the serum AIM/IgM ratio with the degree of airflow limitation (GOLD stages) at baseline, COPD exacerbation during the first 5 years, and 10-year mortality using ANOVA and the Kaplan–Meier method with log-rank test.

Results: In the animal study, airspace enlargement (increase in Lm) after 16 weeks of CS exposure was significantly attenuated in AIM-KO mice than in WT mice. Immunofluorescence showed that AIM protein was expressed in airway epithelial cells co-localized with club cell protein 16 (CC16), and its expression was increased after 3 days of CS exposure. In addition, AIM protein levels in the lung tissue homogenate were significantly increased after 3 days of CS exposure. AIM-KO mice showed attenuated cleavage-caspase-3 expression in alveolus when compared with that of WT mice. Inflammation cytokines (IL-1β, IL-6, CCL2 and CXCL5) had significant differences between AIM-KO and WT mice. In the clinical study, serum AIM/IgM ratio was significantly distinguished among different GOLD stages (P<0.05). Furthermore, higher serum AIM/IgM ratio was associated with shorter time to first COPD exacerbation as well as shorter overall survival (P<0.05).

Conclusions: AIM-KO mice showed significantly less emphysema after CS exposure. Furthermore, in patients with COPD, higher serum AIM/IgM ratio was associated with poor prognosis. Collectively, these results suggest that AIM may be involved in COPD and increased inflammation may participate in the process.

Key words: Chronic Obstructive pulmonary disease (COPD), Cigarette Smoke (CS), emphysema, Apoptosis inhibitor of macrophage (AIM).

Introduction:

Chronic obstructive pulmonary disease (COPD) is responsible for substantial and growing morbidity, mortality, and health-care expense worldwide (1). Apoptosis inhibitor of macrophage (AIM)/CD5L, which was initially identified as a supporter of macrophage survival (2), is a member of the scavenger receptor cysteine-rich domain superfamily. AIM has also been reported to be involved in the pathogenesis of a variety of inflammatory diseases. In COPD, AIM expression in association with cigarette smoking was reported to be involved in the accumulation of alveolar macrophages (3). However, it is still unclear what is the exact role of AIM in COPD and how to enhance the inflammatory signals. Here, we hypothesized that AIM might play a role in the pathogenesis and disease progression of COPD. Based on this hypothesis, we investigated whether deletion of AIM affects the degree of emphysema or the inflammatory response after cigarette smoke (CS) exposure.

Methods:

Experimental Animals

AIM-knock out ($AIM^{-/-}$) mice were kindly obtained from Prof. Toru Miyazaki at Tokyo University. $AIM^{-/-}$ mice had been backcrossed to C57BL/6 for at least 13 generations before being used. All experimental protocols and procedures were approved by the Ethical Committee on Animal Research of the Hokkaido University School of Medicine.

CS-induced emphysema mice model

Mice (aged 8-12 weeks) were exposed to mainstream CS generated from filtered cigarettes (Marlboro, 12 mg tar/1.0 mg nicotine; Philip Morris, Richmond, VA, USA) and inhaled CS through their noses using the SIS-CS system (Shibata Scientific Technology, Tokyo, Japan). We used the following experimental settings: 15 ml of stroke volume and 12 puffs/min to generate CS. The CS was diluted with compressed air. The mice were exposed to 5% CS for 60 min/day, 5 days/week for up to 16 weeks.

Participants and clinical study protocol

Subjects with COPD were recruited at Hokkaido University Hospital, Sapporo, Japan, and its nine affiliated hospitals. In this study, 133 COPD patients with available data were analyzed. The Ethics Committee of Hokkaido University School of Medicine approved the study protocol, and written, informed consent was obtained from all participants. We measured serum AIM and IgM levels and investigated an association of the serum AIM/IgM ratio with the degree of airflow limitation (GOLD stages) at baseline, COPD exacerbation during the first 5 years, and 10-year mortality.

Statistical analysis

Data are shown as average ± SEM. Student's *t*-test was used for comparison of two data sets. Comparison between more than two groups was made using one-way ANOVA. Survival rates were analyzed by the Kaplan-Meier method. Significance was defined as $P< 0.05$. All statistical analyses were performed using SPSS software (v22; IBM SPSS, Chicago, IL, USA) and R version 3.1.2 (The R Foundation, http://www.r-project.org/).

Results:

AIM deficiency attenuates cigarette smoke-induced pulmonary emphysema

To obtain an overall view of the roles of AIM in COPD, we chronically exposed *AIM*$^{+/+}$ and *AIM*$^{-/-}$ mice to CS or room air for 16 weeks and evaluated the development of CS-induced emphysema. In *AIM*$^{+/+}$ mice, CS exposure for 16 weeks produced an airspace enlargement with 13.6% increase in mean linear intercept (Figure 1A, 1B, $P<0.05$). On the other hand, *AIM*$^{-/-}$ mice were resistant to CS-induced emphysema and had similar alveolar size as air-exposed *AIM*$^{+/+}$ mice, suggesting that the loss of AIM conferred resistance to CS-induced emphysema in murine lungs.

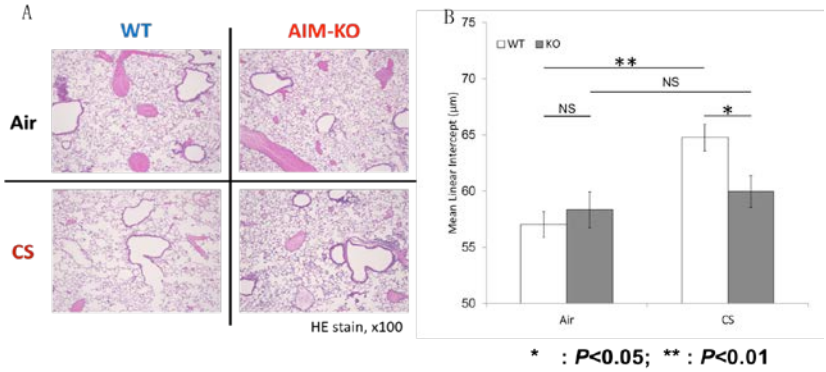

Figure 1. A, Representative hematoxylin and eosin staining of lung tissues of mice after CS exposure for 16 weeks (×100). B, Quantification of mean linear intercept in wild-type (WT, *AIM*$^{+/+}$) and AIM-KO (*AIM*$^{-/-}$) mice.

Effect of CS exposure on AIM protein expression in the lung

We evaluated AIM protein levels in the lung at different time points (0 day, 3 days, 1 week, 2 weeks, and 4 weeks after CS exposure) in *AIM*$^{+/+}$ mice. Western blotting revealed that AIM protein expression was increased after 3 days of CS exposure and it was gradually decreased after 2 weeks of CS exposure (Figure 2A). This observation was further confirmed by immunofluorescence detection of AIM protein in the lung tissue (Figure 2B). The increased AIM protein was colocalized with club cell secretory protein-16 (CC16), an epithelial cell marker, but not with CD31, an endothelial cell marker (Figure 2C). These observations indicate that AIM protein seems to be induced by CS exposure especially in airway epithelial cells during the early time periods after CS exposure.

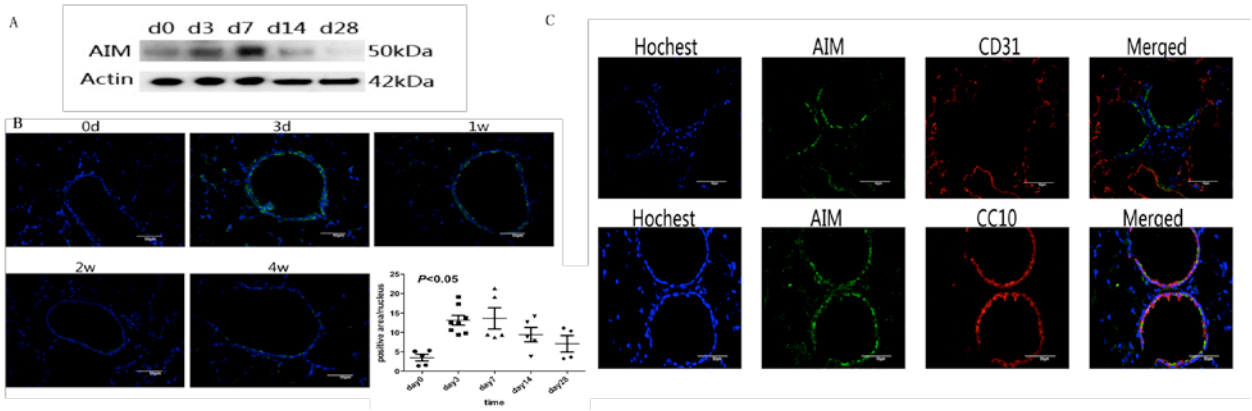

Figure 2. A, AIM protein expression in *AIM*$^{+/+}$ mice after CS exposure by western blotting. B, AIM protein expression in *AIM*$^{+/+}$ mice after CS exposure by immunofluorescence detection. C, Colocalization of AIM protein (green signals) and CC16 (red signals in bottom images) and no colocalization of AIM protein and CD31 (red signals in upper images).

Assessment of cell apoptosis in the lung

We quantified cleaved caspase-3 expression as a marker of apoptosis in *AIM*$^{+/+}$ and *AIM*$^{-/-}$ mice at day 3 after CS exposure. Cleaved caspase-3 expression was significantly increased after CS exposure in *AIM*$^{+/+}$ mice as well as in *AIM*$^{-/-}$ mice (Figure 3A). Interestingly, when we analyzed cleaved caspase-3 expression in the airways and in the alveolus separately, *AIM*$^{-/-}$ mice showed no differences in the airway cleaved caspase-3 expression compared with WT mice (Figure 3B); however, *AIM*$^{-/-}$ mice showed significantly attenuated cleaved caspase-3 expression in the alveolus compared with WT mice (Figure 3C). Thus, AIM may contribute to emphysema via cell apoptosis at early stage.

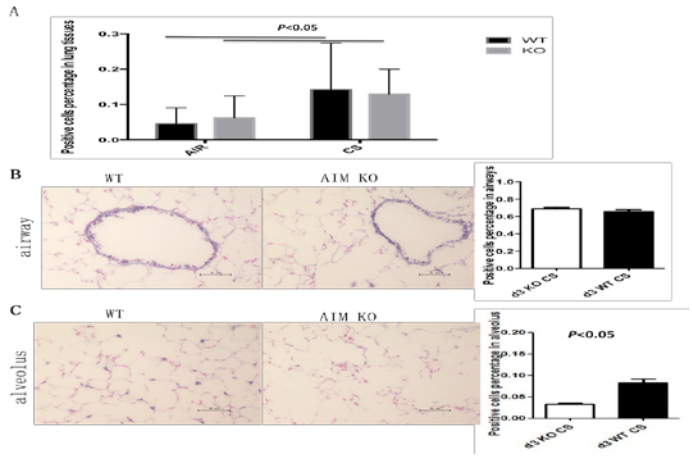

Figure 3. A, Cleaved caspase-3 expression in *AIM*$^{+/+}$ and *AIM*$^{-/-}$ mice after CS or air exposure by immunohistochemistry. B, Cleaved caspase-3 expression in the airway after CS exposure (×400). C, Cleaved caspase-3 expression in the alveolus after CS exposure (×400).

Activation of airway epithelial AIM induces chemokines production

We compared lung inflammatory responses in *AIM*$^{+/+}$ and *AIM*$^{-/-}$ mice exposed to CS. Totally 35 genes related to inflammation and tissue repair were detected in the lung homogenates by real-time PCR. Among them, the levels of a component of inflammasome (NLRP3), cytokines (TNF-α, IL-1β, IL-6, and IL-18), chemokines (CCL3, CCL2, CXCL1, and CXCL5), and chemokine receptor (CXCR2) were increased after CS exposure in the lung of *AIM*$^{+/+}$ mice. On the other hand, *AIM*$^{-/-}$ mice showed decreased levels of two cytokines (IL-1β and IL-6) and two chemokines (CCL2, CXCL5) in the lung compared with *AIM*$^{+/+}$ mice (Figure 4). Taken together, AIM expression in airway epithelial cells is associated with production of several chemokines and may promote emphysema formation.

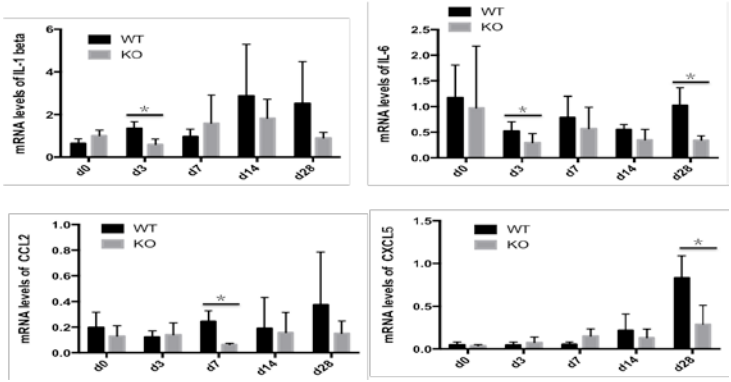

Figure 4. Four chemokines mRNA levels in the lung of different time points after CS exposure in WT and KO mice.

Higher AIM/IgM expression is associated with poor prognosis of COPD

In the clinical study, serum AIM/IgM ratio was significantly different among different GOLD stage (P<0.05) (Figure 5A). Furthermore, higher serum AIM/IgM ratio was associated with shorter time to first COPD exacerbation (Figure 5B) as well as shorter overall survival (P<0.05) (Figure 5C).

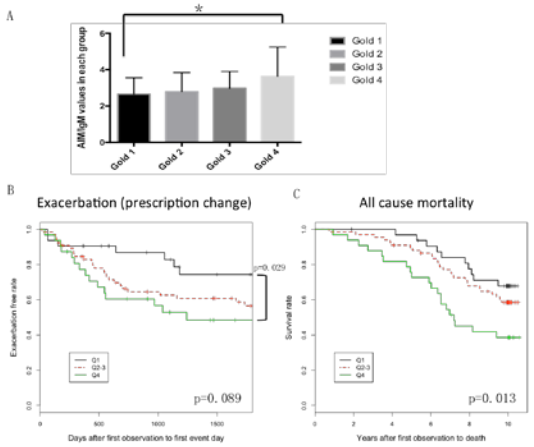

Figure 5. A, Serum AIM/IgM ratio associated with different GOLD stages. B-C, Associations of serum AIM/IgM ratio with COPD exacerbation-free survival (B) and all-cause mortality of COPD patients (C). Subjects were divided into three groups based on quartiles (Q) of serum AIM/IgM ratio.

Discussion:

We demonstrated that the deletion of AIM significantly inhibited development of emphysema in mice. The *AIM*$^{-/-}$ mice showed reduced inflammatory response after CS exposure, and the decreased inflammatory response seemed to be associated with a reduction of alveolar apoptosis and a decrease in airspace enlargement. Furthermore, we also demonstrated that higher serum AIM/IgM ratio was associated with poor prognosis in patients with COPD. These results suggest that AIM plays an important role for inflammation and the development and progression of COPD.

Recent researches have implicated that AIM modulates many aspects of inflammation. In human AIM expression in alveolar macrophages after CS exposure was increased, which may be involved in the accumulation of alveolar macrophages in COPD patients (3). However, the exact role of AIM in COPD is still unclear. The accumulated evidences revealed that treatment during the early stage could repair CS-induced tissue damage, whereas tissue repair failure during the late stage played a role in the progress of emphysema. Lung parenchyma up-regulated tissue repair genes during the first month of CS exposure in mice, but then rapidly down-regulated them, so that expression of most genes necessary for tissue repair was at control levels or below control levels by the time emphysema was well established (4). In human, smokers who quit after the age of 40 years showed a significantly enhanced rate of decline of FEV_1 versus earlier quitters (5). These observations confirm that the early stage of CS exposure is very important for the development of emphysema and earlier intervention for COPD is crucial to prevent emphysema.

We found that AIM expression on mice airway epithelial cells significantly increased after CS exposure. Previous studies showed that AIM was detected in high amounts in serum where it circulated associated with IgM, and AIM appeared to be effective in cell types other than macrophages including epithelial cells (6). In lung tissue from *lac*$^{-/-}$ mice, overexpressed AIM mRNA was detected and it derived from ATII cells (7). Thus, how does AIM located in airway epithelial cells influence the process of emphysema development at the early stage raise our interest and further research is warranted.

An important feature of the pathogenesis of COPD is a chronic inflammatory process mediated by kinds of leukocyte including neutrophils, macrophages and T lymphocytes, and neutrophils play a main role in this process. We found that *AIM*$^{-/-}$ mice showed decreased levels of two cytokines (IL-1β, IL-6) and two chemokines (CCL2, CXCL5) in lung compared with *AIM*$^{+/+}$ mice. It is well known that mediators including cytokines and chemokines will influence the function of special cells by interacting with the cell surface receptors. Previous studies have shown that mediators including IL-1β, CCL2, and CXCL5 are associated with neutrophil recruitment and activation. Whether the different AIM status in airway epithelial cells influences the neutrophil recruitment, thus contributes to continuous inflammation and finally leads to alveolar cells apoptosis and emphysema, still needs to be verified in the following studies. Besides, recombinant AIM protein will also be used to further valid the roles of AIM in CS-induced emphysema mice model.

In summary, AIM-deficient mice demonstrated significantly less emphysema and less inflammatory response after CS exposure. Our data provide the first evidence that AIM plays an important role in the inflammatory response in COPD. The inhibition of AIM could prevent not only inflammation but also CS-induced emphysema.

Main References：

1. Woodruff, P. G., Agusti, A., Roche, N., Singh, D., and Martinez, F. J. (2015) Current concepts in targeting chronic obstructive pulmonary disease pharmacotherapy: making progress towards personalised management. *Lancet* **385**, 1789-1798
2. Miyazaki, T., Hirokami, Y., Matsuhashi, N., Takatsuka, H., and Naito, M. (1999) Increased susceptibility of thymocytes to apoptosis in mice lacking AIM, a novel murine macrophage-derived soluble factor belonging to the scavenger receptor cysteine-rich domain superfamily. *The Journal of experimental medicine* **189**, 413-422
3. Kojima, J., Araya, J., Hara, H., Ito, S., Takasaka, N., Kobayashi, K., Fujii, S., Tsurushige, C., Numata, T., Ishikawa, T., Shimizu, K., Kawaishi, M., Saito, K., Kamiya, N., Hirano, J., Odaka, M., Morikawa, T., Hano, H., Arai, S., Miyazaki, T., Kaneko, Y., Nakayama, K., and Kuwano, K. (2013) Apoptosis inhibitor of macrophage (AIM) expression in alveolar macrophages in COPD. *Respiratory research* **14**, 30
4. Churg, A., Zhou, S., Preobrazhenska, O., Tai, H., Wang, R., and Wright, J. L. (2009) Expression of profibrotic mediators in small airways versus parenchyma after cigarette smoke exposure. *American journal of respiratory cell and molecular biology* **40**, 268-276
5. Kohansal, R., Martinez-Camblor, P., Agusti, A., Buist, A. S., Mannino, D. M., and Soriano, J. B. (2009) The natural history of chronic airflow obstruction revisited: an analysis of the Framingham offspring cohort. *American journal of respiratory and critical care medicine* **180**, 3-10
6. Arai, S., Kitada, K., Yamazaki, T., Takai, R., Zhang, X., Tsugawa, Y., Sugisawa, R., Matsumoto, A., Mori, M., Yoshihara, Y., Doi, K., Maehara, N., Kusunoki, S., Takahata, A., Noiri, E., Suzuki, Y., Yahagi, N., Nishiyama, A., Gunaratnam, L., Takano, T., and Miyazaki, T. (2016) Apoptosis inhibitor of macrophage protein enhances intraluminal debris clearance and ameliorates acute kidney injury in mice. *Nature medicine* **22**, 183-193
7. Lian, X., Yan, C., Qin, Y., Knox, L., Li, T., and Du, H. (2005) Neutral lipids and peroxisome proliferator-activated receptor-{gamma} control pulmonary gene expression and inflammation-triggered pathogenesis in lysosomal acid lipase knockout mice. *The American journal of pathology* **167**, 813-821

作成日：2017年2月15日

First molecular detection and characterization of tick-borne protozoa and bacteria in dogs from Jiangxi province, China

中国江西省のイヌにおけるダニ媒介性原虫および細菌の分子検出と特性評価に関す初報告

研究者氏名　鄭　衛青（第３８期笹川医学研究者）
中国所属機関　南昌市疾病予防控制中心
日本研究機関　帯広畜産大学原虫病センター
指導責任者　玄　学南　教授

Abstract:
Dogs play an important role in transmission of different tick-borne pathogens including protozoa, bacteria and viruses. However, current knowledge on the prevalence of these pathogens in dogs in Jiangxi, China is limited. The aim of the present study is to detect and characterize tick-borne protozoa and bacteria of veterinary and zoonotic importance in thisregion. Blood samples obtained from 162 dogs were employed in molecular screening by PCR and sequencing. *Babesia*spp. gene fragment was detected in 12 (7.41%) dogs while *Mycoplasma* spp. gene fragment was found in one (0.62%) dog. All samples were negative for *Ehrlichia canis*, *Coxiella* spp., *Borrelia* spp., *Rickettsia* spp., *Hepatozoon* spp. and *Anaplasma playts*. Species-specific PCR analysis further confirmed 8 (4.94%) and 4 (2.47%)dogs were infected by *Babeisa canis vogeli* and *B. gibsoni*, respectively. Mixed infections of *B. cani svogeli*, *B. gibsoni* and *Mycoplasma* spp. were not detected. DNA sequences of *Babesia* spp., *B. canis vogeli*, *B. gibsoni* and *Mycoplasma* spp. in this study had 99%-100% identity to the corresponding gene sequences originating from other parts of the world, showing their highly conserved feature. Based on our analyses, tick-borne infections in Jiangxi seemed not related to age, gender, breed, dog use and health status or tick infestation history of the dogs. This is the first molecular report of *B. canis vogeli* and *B. gibsoni* in dogs from Jiangxi, China and the first time to record *M. haemocanis* in dogs from China.

Key Words:
Babesia spp., dogs, Jiangxi,tick-borne pathogens

Introduction:

Many tick-borne protozoan and bacterial agents are significant causes of morbidity and mortality in domestic dogs and potentially of great public health importance. To date, three protozoan (*Theileria*, *Babesia* and *Hepatozoon*) and six bacterial (*Anaplasma*, *Ehrlichia*, *Mycoplasma*, *Rickettsia*, *Coxiella* and *Bartonella*)genera have been reported in domestic dogs around the globe (Buhariwalla et al., 1996; Brown et al., 2006; Yabsley et al., 2008; Compton et al., 2012; Kamani et al., 2013; Loftis et al., 2013;Kawwkong et al., 2014). These pathogens infect blood cells and cause thrombocytopenia, anemia, leukopenia and organ damage. Clinical manifestation mainly includes fever, anorexia and weight loss (Yabsley et al., 2008;Hii et al., 2015). Furthermore, subclinically infected companion dogs have been considered to be a reservoir or carrier for human tick-transmitted infectious agents, such as *Borrelia burgdorferi*, *Rickettisia conori*, *R. rickettsia*, *Ehrlichia chaffeensis*, *E. ewingii*, *Anaplasma phagocytophilum*, *Coxiella burnetii*, *Francisella tularensis*, *Babesia microti* (Shaw et al., 2001;Chomel, 2011; Dantas-Torres et al., 2012; Levin et al., 2012; Baneth, 2014; Chen et al., 2014; Nordstoga et al., 2014;Moreira-Soto et al., 2016).

The current dog population in China is estimated to be between 150 and 200 million (Ma et al., 2012). However, until 2015, very few data were available on tick-borne infections in dogs . In 2015, Xu et al. reported a prevalence of tick-borne pathogens in ten provinces of China, including Xinjiang, Gansu, Shaanxi, Inner Mongolia, Beijing, Henan, Jiangsu, Shanghai, Guangdong and Yunnan. This study, in combination with the previous investigations, evidenced the existence of *Dirofilaria immitis*, *Babesia canis vogeli*, *B.gibsoni*, *Ehrlichia canis*, *Hepatozoon canis* and *Theileria orientalis* infections among the Chinese dog population (Shen et al., 1997;Jin et al., 2005; Shang et al., 2014; Xu et al., 2015). In addition, a large number of ticks, belonging to the genera *Rhipicephalus*, *Haemaphysalis* and *Ixodes* were collected from dogs and detected positive for *B. canis vogeli*, *B. gibsoni*, *B. microti*, *Rickettsia* spp., *Anaplasma platys* and *A. phagocytophilum* infections (Shang et al., 2014; Wei et al., 2012; Wang et al., 2013; Xu et al., 2015). Meanwhile, the seroprevalence of *B. gibsoni* in different types of dogs in East China including Jiangxi, Fujian, Anhui, Jiangsu, Zhejiang, Shanghai and Shandong was assessed in the same year (Cao et al., 2015). Jiangxi, located in the mid-eastern part of China, has a bio-environment that remarkably facilitates tick development and tick-borne pathogen transmission. However, data on tick-borne infections in this area is limited, and therefore this study aimed to achieve a better understanding of these etiological agents. Molecular techniques were used to examine and characterize various tick-borne pathogens in dogs from Jiangxi province.

Materials and methods:

Study area

The study was conducted in two districts: Changbei and Xinjian of Nanchang (28°41′N 115°53′E), the capital of

Jiangxi province (Fig. 1).Jiangxi has its own special features in geography, flora and fauna with Lake Poyang, the largest freshwater lake of China. It is surrounded by mountains on west, south and east sides. The mountainous terrain and large forest coverage of Jiangxi has made it historically one of the more wild places of central China. Wildlife, though not abundant, are more numerous in Jiangxi than in many other areas of China. The current dog population in Jiangxi province is estimated to be between 5 and 6 millions. Most of them comprise police dogs, guard dogs and pet dogs. These dogs have more opportunities to contact humans, compared with stray dogs and free-roaming dogs rarely seen in the study sites.

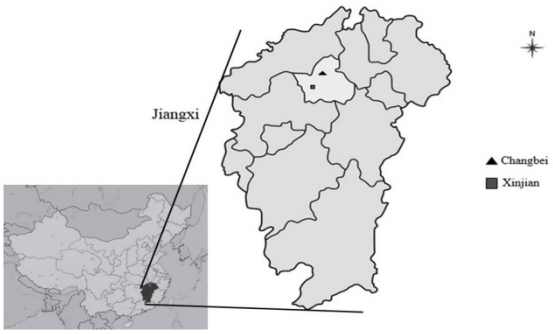

Figure 1. Geographical location of Changbei and Xinjian where dog blood samples were collected. Legends indicate the location of sampling sites. ■ , all samples collected from police dog base or veterinary hospital. ▲ , samples obtained from pet dog owners or in pet dog breeding center.

Sampling of dogs

One hundred and sixty two dogs were selected from 2 districts (counties) of northern area of Nanchang , namely, Changbei (43 samples) and Xinjian (119 samples). Blood sampling was conducted during the peak period of tick infestation in dogs between March and April 2016. Approximately 5 ml aliquot of blood was collected from cephalic vein by using sterile vacutainer tubes with EDTA. The samples were temporarily kept in a sealed cool box with ice pack and transported to the laboratory where they were stored at 4℃for later use. Demographic data, age, gender, breed, dog use, previous history of tick infestation, and health status were recorded for each dog.

DNA extraction from blood samples

Genomic DNA was extracted from a volume of 200µl of whole blood using the QIAamp® DNA blood Mini Kit (QIAGEN, Germany) according to the manufacturer's recommendation. 100µl eluted DNA samples (30 ng/µl -90 ng/µl) were harvested and stored at -30℃ for subsequent PCR analysis. DNA concentrations and purities were determined by measuring the absorbance at 230 nm, 260 nm and 280nm with a NanoDrop Spectrophotometer (Thermo Scientific, USA).

Oligonucleotide primers and PCR amplification

All primers used in this study are summarized in Table 1.Universal and species-specific primers previously described were usedto amplify the target gene fragment of the protozoan and bacterial DNA. The expected size of the products obtained from PCR and annealing temperatures in thermal cycling condition are listed in Table 1.The PCR reactions were carried out in a total volume of 10µl including the primers (Sigma-Aldrich, Japan) at 1µM, 1µltemplateDNA, 250µM dNTP, 1×PCR buffer, 0.5 U Taq-polymerase (EX-Taq DNA polymerase, Takara, Japan) and distilled water added up to the final volume. The PCR amplification program performed by thermocycler (BioRad, USA) included initial denaturation step of 5 min at 94℃, followed by 30 cycles of denaturation at 94℃ for 45 s, annealing at the temperature provided in Table 1 for 45 s, extension at 72℃ for 1 min per1,000 bp of amplicon size, and final elongation at 72℃ for 7 min. Non-template controls and positive controls were included in each PCR assay. DNA extracted from cultured *Rickettsia africa* was used as a positive control for *Rickettsia* spp..Plasmids containing target gene were positive controls for *Babesia* spp., *Babesia canis*, *B. gibsoni*, *Mycoplasma* spp., *E. canis*, *Hepatozoon* spp., *A. platys* and *Coxiella* spp. The PCR products were checked by electrophoresis on1.5% tris-acetate-EDTA buffer (1×TAE) agarose gels,ethidium bromide-stained and visualized under an UV transilluminator and photographed.

Cloning and sequencing

Babesia spp. (n=12), *B. canis* (n=8), *B. gibsoni* (n=4) and *Mycoplasma* spp. (n=3) positive blood DNA samples were randomly selected for cloning and sequencing of amplicons. PCR products were extracted from agarose gel using QIAquick Gel Extraction Kit (QIAGEN, Germany) ligated into pGEM-T Easy Vector (Promega, USA) and then transformed into *Escherichia coli* DH5α-competent cells. For each isolate, at least two clones confirmed positive by colony PCR were multiplied and purified using NucleoSpin® Plasmid QuickPure (MACHERY-NAGEL, Germany). Sequencing reactions were performed using ABI BigDye™ Terminator Kit(ABI Applied Biosystems, USA). DNA fragment sequences were determined using an ABI PRISM 3100 DNA sequencer (ABI Applied Biosystems, USA). Identities and similarities of the nucleotide sequences were analyzed using online GenBank BLASTn.

Table 1 Sequences of oligonucleotides used for target gene PCR amplification

Pathogen	Target gene	Primer	Annealing temperature (℃)	PCR products size (bp)	Reference
Babesia spp	18S rRNA	F: GCATTTAGCGATGGACCATTCAAG R: CCTGTATTGTTATTTCTTGTCACTACCTC	60	209	Kordick et al., 1999
Babesia canis	18SrRNA	F: GTTTATTAGTTTGAAACCCGC R: GAACTCGAAAAAGCCAAACGA	59	456	Inokuma et al., 2004
Babesia gibsoni	TRAP	F: AAGCCAACATCAAGGAAAGC R: TTCTGGTATGCGGCAGTGTA	58	679	This study
Mycoplasma spp.	16S rRNA	F: ATACGGCCCATATTCCTACG R: TGCTCCACCACTTGTTCA	55	595	Criado-Fornelio et al., 2003
Ehrlichia canis	gltA	F: TTATCTGTTTGTGTTATATAAGC R: CAGTACCTATGCATATCAATCC	53	1372	Inokuma et al., 2001
Hepatozoon spp.	18S rRNA	F: ATACATGAGCAAAATCTCAAC R: CTTATTATTCCATGCTGCAG	57	666	Inokuma et al., 2002a
Anaplasma platys	groESL	F: AAGGCGAAAGAAGCAGTCTTA R: CATAGTCTGAAGTGGAGGAC	58	724	Inokuma et al., 2002b
Rickettsia spp	GltA.	F: GCAAGTATCGGTGAGGATGTAAT R: GCTTCCTTAAAATTCAATAAATCAGGAT	50	401	Labruna et al., 2004
Borrelia spp.	Fla	F: ACATATTCAGATGCAGACAGAGGT R: GCAATCATAGCCATTGCAGATTGT	60	665	Stromdahl et al., 2003
Coxiella spp.	16S rRNA	F: ATTGAAGAGTTTGATTCTGG R: CGGCTTCCCGAAGGTTAG	48#	1457	Masuzawa et al., 1997

#, To minimize nonspecific amplification, a so-called touchdown PCR program was used: 3 min at 95 ℃; this was followed by two cycles of 30 s at 95 ℃, 30 s at 58 ℃, and 2 min at 72 ℃ and then two cycles identical to the previous two cycles, but with an annealing temperature of 58 ℃; after every following two cycles, the annealing temperature was lowered by 2 ℃ until it reached 50 ℃. Then, an additional 30 cycles of 30 s at 95 ℃, 30 s at 48 ℃, and 2 min at 72 ℃ were followed by the touchdown PCR program.

Phylogenetic analysis

Phylogenetic analysis was performed using the sequences of this study and those reported from other regions. Both SeqMan and MEGA 7 programs were used to build the alignment of all selected sequences and then we constructed a neighbor-joining phylogenetic tree using MEGA 7 program. The confidence of internal branches was estimated by bootstrapping with 1000 replications.

Statistical analysis

Statistical analysis of the epidemiological data was carried out using the SPSS version 20.0 program. Dogs were grouped as positive or negative for the *Babesia* genus. Exposure variables included age, gender, breed, dog use (companion dogs or police dogs), previous history of tick infestation, and health status. The two-tailed Chi-square test or Fisher's exact test was used to determinate the association between *Babesia* infection and exposure variable. *P-value*<0.05 was considered statistically significant. Odd ratios for exposure variables and their95% confidence interval (CI) were calculated.

RESULTS:

Animals and samples

A total of 162 blood samples were randomly gathered from 4 selected sites in Nanchang city of Jiangxi province, China. 18 samples collected from pet dogs and 25 samples collected in pet dog breeding center were obtained in Changbei district. Meanwhile, 40 samples were gathered in a veterinary hospital and 79 samples in police dog base in Xinjian district. Most (78.40%) of the dogs are young. 46.30% of dogs sampled were femaleand 53.70% were male. The breeds of the study samples were German shepherd (20.37%), Rotterman (12.96%),Samoyed (8.64%),Golden Retriever(8.02%),Rottweiler (7.41%) and Springer (6.79%),and other breeds were 35.81% in total. The majority (63.58%) of the sample dogs were reported as having "absence of previous tick infestation" while 36.42% population were infested by ticks before. Compared with the 75.31% of healthy dogs, 24.69% of the dogs were diseased with leptospirosis, back leg twitches, fungi infection, ascites and /or cough.

Pathogen detection and identification

Overall prevalence of *Babesia* spp. infection was 7.41%(12/162). Amplification of a454bpfragment of the 18S rRNA gene in the *Babesia* spp.-positive samples confirmed the presence of *B. canis vogeli*in 8 (4.94%) dogs. PCR reactions prepared using species-specific primers targeting *B. gibsoni* thrombospondin-related adhesive protein (TRAP) gene revealed 4 (2.47%) positive among the 12 samples containing *Babesia* spp. DNA. However, *B. canis vogeli*/ *B. gibsoni* co-infections were not found in the samples. Of the 162 blood samples tested, one (1.86%) sample was detected with*Mycoplasma* spp. infection by using the 16S rRNA primers. PCR amplification of *E.canis*, *Coxiella* spp., *Borrelia* spp., *Rickettsia* spp., *Hepatozoon* spp. and *A. playts* genes in all the samples were negative.

Exposure variable analyses

Exposure variable analyses revealed that *Babesia* spp. infection in the study population was not significantly associated (P>0.05) to values such as age, gender, breed, dog use, previous history of tick infestation, and health status.

Sequences comparison and phylogenetic analysis

A 209 bp band was amplified with the primers targeting 18S rRNA fragment from *Babesia* spp. positive samples, whilethe species-specific primers yielded a 456 bp product for *B. canis* and a 679 product for *B. gibsoni*. A 595 bp product was isolated from the amplicon of the dog containing *Mycoplasma* spp..

Babesia spp. 18S rRNA, *B. canis* 18S rRNA, *B. gibsoni* TRAP and *Mycoplasma* spp.16S rRNA phylogenetic trees were constructed based on sequences generated in this study and selected sequences from GenBank database.

The *Babesia* spp. tree (Fig.2) found two major clades. Three sequences (KX505275, KX505276 and KX505278) in our study formed clade 1 with *B. canis vogeli* (DQ297390, DQ439545, KX082904, KJ939326) and *B. canis canis* (KF499115) while the remaining sequence (KX505278) was clustered with *B. gibsoni* sequences(KP666168, LC012808, KP901263, LC008285). The sequences generated in the present study were highly (99.99%) conserved and showed 99.98%-100% homology to those from other regions (countries).

Figure 2. Phylogenetic tree of *Babesia* spp. based on 209bp 18S rRNA gene fragment. ●, sequences obtained in this study.

Further phylogenetic analyses (Fig. 3) revealed that the *Babesia canis* gene sequences (KX505279, KX50527980) obtained inthis study were obviously different from *B. canis canis* (KC593878) and formed a clade with the *B. canis vogeli* sequences previously isolated in Europe (JX304677), Middle-east (AY371197), Africa (DQ111766), South America (KU710803), Guangxi in China (KJ939326) and Taiwan (HQ148664, JF682473, HQ148663). Therefore, the isolates classified as *B. canis* in the previous dendogram are considered to be *B. canis vogeli*, not *B. canis canis*.

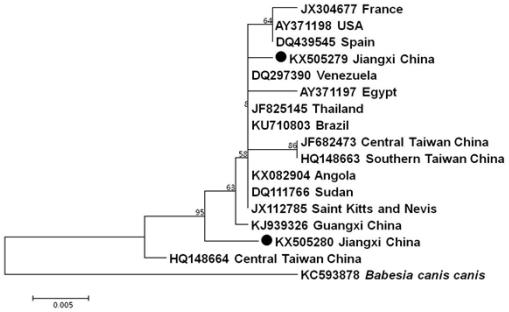

Figure 3. Phylogenetic tree of *Babesia canis vogeli* based on 456bp fragment of 18S rRNA gene. *B. canis canis* was employed as out group.

The 679 bp fragments of TRAP *B. gibsoni* gene isolated in Jiangxi(KX528450, KX528451)showed 99.99% similarity to each otherand shared 99.98%-99.99% homology to sequences deposited in GenBank. Jiangxi isolates formed a sub-cluster with the isolates from Japan (KR013043 , AB478341 , AB478342 and AB478349) and China (JN247443) on the phylogenetic tree, phylogenetically far from the isolates from India (KT750254 and KT750255).The nucleotide sequence of *B. gibsoni* TRAP gene in Jiangxi isolate 1 (KX528450) differed from the homologous sequences deposited in GenBank in 4 bps located at the positions 142, 360, 421 and 671. The *B. gibsoni*Jiangxi isolate 2 (KX528451) and isolate 1(KX528450) were different at 2 nucleotide positions of the sequence, namely, the nucleotides number 420 and 451 (Fig. 4).

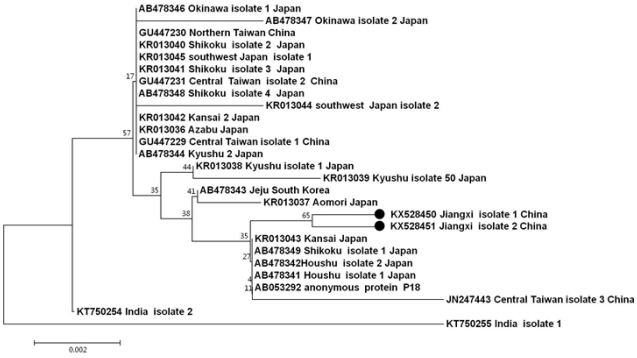

Figure 4. Phylogenetic tree of *B. gibsoni* based on 679 bp fragment of TRAP gene.

The 16S rRNA fragment of *Mycoplasma* Jiangxi isolate (KX519722) were 99.99%-100% identical to the sequences of *M. haemocanis* and *M. haemofelis* available in GenBank. The tree established in this study based on 16S rRNA fragment of *Mycoplasma* spp. presented *M. haemofelis* and *M. haemocanis*in the same clade with Jiangxi *Mycoplasma* spp. isolate. Given that the bacteria was obtained from dogs, *M. haemocanis* was identified in this study (Fig. 5).

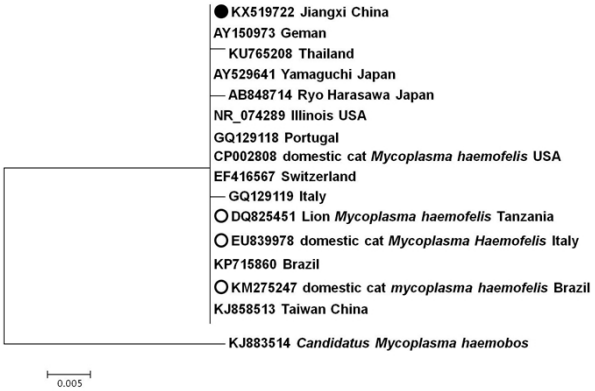

Figure 5. Phylogenetic analysis of *M. haemocanis* based on 595bpof 16S ribosomal RNA gene. *C. M. haemobos* was employed as out group. The marker "○" signifies partial 16s rRNA gene fragment from *M. haemofelis*.

DISCUSSION:

Babesia canis and *B. gibsoni* cause some discomfort, or even more severe clinical manifestations among dog populations. *B. canis vogeli,* like *B. canis canis* and *Babesia canis rossi*, belongs to the *B. canis* subspecies. It is a benign protozoan pathogen of dogs causing mild, often clinically inapparent manifestations, and sometimes thrombocytopenia (Brown et al., 2006). *B. gibsoni* infection, however,is a real threat to canine health. The acute form of the disease in dogs is typically related to fever, anaemia, thrombocytopenia, splenomagaly and hepatomegaly (Mandal et al., 2016).

Existence of *Babesia* spp. DNA in the dogs from Jiangxi in our study provides evidence that members of this genus can be a cause of canine babesiosis in Jiangxi. Overall, 7.41% of the dogs surveyed had *Babesia* spp. infection. Our analyses further confirmed that *B. canis vogeli* (4.94%) was more prevalent than *B. gibsoni* (2.47%) and *B. canis vogeli* /*B. gibsoni* co-infections were not found in 12 dogs positive for *Babesia* spp. infection. The present estimate of *Babesia* spp. infections in dog blood are higher than that reported earlier in Nanjing, but lower than the prevalence in Taixing, east China (Xu et al., 2015). *B. gibsoni* TRAP sequences were amplified from 4 dog samples, corroborating previous seroprevalence of this microorganism in the pet dogs from Jiangxi (Cao et al., 2015). *B. gibsoni* prevalence in this study is almost similar to Luoyang (3.1%), Sanmenxia (3.81%) and Pingdingshan (3.54%), central China (Shang et al., 2014), but higher than Zhejiang (0.27%) and lower than Jiangsu (7.8%), east China (Cao et al., 2015). However, the occurrence of *B. canis vogeli* infection in dogs is not well documented in China, with only two studies having reported this protozoan parasite in tick vectors collected from the police dogs (Wei et al., 2012;Wang et al., 2013).

Rhipicephalus sanguineus, *R. haemaphysoides*. *Haemaphysalis longicornis*, *Dermacentor variabilis* and *Ixodes ricinus* are major vectors of *Babesia* species of dog around the globe (Chomel et al., 2011; Shaw et al., 2011; Schorn et al., 2011;Chen et al., 2014; Shang et al., 2014). In China, *R. sanguineus* is the dominant tick species among dog population, although sometimes *R. haemaphysoides* and *H. longicornis* can be seen on some dogs (Wang et al., 2013;Chen et al., 2014; Shang et al., 2014). *R. sanguineus* ticks frequently occur in the sampling sites of this study

during the tick active season which ranges from March to June. Both *B. canis vogeli* and *B. gibsoni* were found to infect *R. sanguineus*, *H. longicornis* and *R. haemaphysaloides* collected on dogs around China (Wang et al., 2013; Chen et al., 2014; Shang et al., 2014). However, a previous study performed by Wang et al. at the same place withour sampling sites did not detect *Babesia* spp. in *R. sanguineus* removed from police dogs. Other tick species, including *Haemaphysalis campanulata* and *H. verticalis*, which were collected from police dogs, were also tested negative for *Babesia* spp. infection (Wang et al., 2013). The difference in prevalence may be attributed to the geographical distribution and diversity of management programs from one region to the other, in China. Our detection of *Babesia* spp. DNA in dog blood contradicted the absence of *Babesia* spp. in ticks and suggests that the ticks might not play a pivotal role in the transmission. Our hypothesis ispartially supported by other viewpoint that *B. gibsoni* infection was transmitted not only through tick bites, but also by dog bites and blood transfusion, as well as from mother to infant (Shaw et al., 2011;Mandal et al., 2016).

Tick-borne infections are related to detailed exposure variables, such as frequency of contact between animal and parasite, animalor human population, distribution of tick vectors, tick control measures and human behavior/animal management system. In this study, we did not detect any significant association between *Babeisa* spp. infection andage, gender, breed, dog use and health status of the dog hosts and history of exposure to tick infestation. These datasupport a previous survey in Australia that indicated age and breed arenot related to tick infection, as opposed to the pivotal role of ectoparasite infestation history in the transmission of these infections (Hii et al., 2015). Previous history of tick infestation in this study was reported by police dog trainers, pet dog owners or keepers during sample collection and thereforethe reality and accuracy of the information was actually unverifiable.

Dogs are competent reservoir- hosts of several *Mycoplasma* spp. including *M. haemocanis*, *M. Cynos*, *Candidatus M. haemominutum* and *C. M. haematoparvum*. The DNA of these bacteria has been isolated from the nasal cavity or the blood ofdogs (Chalke, 2005; Zhuang et al., 2009; Obara et al., 2011; Compton et al., 2012).The result of this study provides molecular evidence for emergence of *Mycoplasma* spp. in dogs, which was identified as *M. haemocanis*. In fact, it is the first report of *M. haemocanis* in dogs from China, previously *C. M. haemominutum* has been detected in Chinese dogs (Zhuang et al., 2009).This study showed 0.62% infection with *M. Haemocanis* in 162 dogs, consistent with 0.6% prevalence reported in the United States (Compton et al., 2012). Although dogs are considered the main reservoir of *M. haemocanis*, detection of this bacterium in bovines and humans is not entirely surprising(Chalke, 2005).The presence of *M. haemocanis* in humans suggests its zoonotic significance. However, there is no evidence that *M. Haemocanis* infection is associated with any human discomfort or disease.

Despite the fact that *E. canis*, *A. playts*, *Rickettsia* spp., *Coxiella* spp., *Borrelia* spp. and *H. canis* have been detected in blood samples collected from dogs (Buhariwalla et al., 1996; Kamani et al., 2013. Brown et al., 2006; Yabsley et al., 2008; Kaewkong et al., 2014), their presence was not identifiedin any of the samples of our study. This supports the thought that the dogs in the study area, are not important reservoirs/carriers of the above etiological agents.

Babesia spp., *B. canis vogeli* and *M. haemocanis*in this study appear to be remarkably similar to previously described species with 99%-100% homology to the reference sequences from the world. *B. gibsoni* TRAP (BgTRAP) gene is encoding TRAP, a type-Ⅰtransmembrane protein and demonstrates abundant genetic diversity in Asian isolates (Singh et al., 2016). However, fragments of the gene generated in dogs from Jiangxi shared 99.98%-99.99% homology to the sequences deposited in GenBank and formed a sub-cluster with isolates from Japan and other regions of China.

This is the first molecular report documenting the existence of several tick-borne pathogens including protozoan parasites and bacteria in Jiangxi, mainland China. PCR amplification method together with sequence analyses proved efficient for not only distinguishing*B. canis vogeli* and *B. gibsoni*from *Babesia* spp, but also identifing *M. haemocanis* infection in dogs. Further studies regarding the detection of tick-borne infection in other domestic livestock and wild animals, identification of their vector range, and evaluation of their zoonotic potential should be undertaken.

References:

Ball, G., S. Friesen,J.Goedde,B. Henderson, W. Sylvester.2008. Prevalence of *Ehrlichia canis*, *Anaplasma playts*, *Babesia canis vogeli*, *Hepatozoon canis*, *Bartonella vinsonii berkhoffi*, and *Rickettsia* spp. in dogs from Grenada. Veterinary Parasitology **151:**279-285.

Baneth, G. 2014. Tick-borne infections of animals and humans: a common ground. International Journal for Parasitology **44:** 591-596.

Brown, G.K., P.J. Canfield, R.H. Dunstan, T.K. Roberts, A.R. Martin, C.S. Brown, G.K.Brown,R. Irving. 2006. Detection of *Anaplasma platys* and *Babesia canis vogeli* and their impact on platelet numbers in free-roaming dogs associated with remote aboriginal communities in Australia. Australian Veterinary Journal **84:**321-325.

Buhariwalla, F., B. Cann, and T.J. Marrie. 1996. A Dog-Related Outbreak of Q Fever. Clinical infectious diseases **23:**753-755.

Cao, J., Q. Yang, J. Zhang, Y. Zhou, H. Zhang, H. Gong,J. Zhou. 2015. Seroprevalence survey of *Babesia gibsoni* infection and tick species in dogs in East China. Veterinary Parasitology **214:** 12-15.

Chalker, V.J.. 2005. Canine mycoplasmas. Research in Veterinary Science **79:** 1-8.

Chen, Z., Q. Liu, J.Q. Liu, B.L. Xu, S. Lv, S. Xia, X.N. Zhou. 2014. Tick-borne pathogens and associated co-infections in ticks collected from domestic animals in central China. Parasites & Vectors **7:**237.

Chomel, B.. 2011. Tick-borne infections in dogs—An emerging infectious threat. Veterinary Parasitology**179:** 294-301.

Compton, S.M., R.G. Maggi, E.B. Breitschwerdt. 2012. *Candidatus Mycoplasma haemotoparvum* and *Mycoplasma haemocanis* infections in dogs from the United States. Comp. Comparative Immunology, Microbiology & Infectious Diseases **35:** 557-562.
Criado-Fornelio, A., A. Martinez-Marcos, A. Buling-Saraña, J.C. Barba-Carretero. 2003. Presence of *Mycoplasma haemofelis*, *Mycoplasma haemominutum* and piroplasmids in cats from southern Europe: a molecular study. Veterinary Parasitology **93:** 307-317.
Dantas-Torres, F., B.B.Chomel, D. Otranto. 2012. Ticks and tick-borne diseases: a one health perspective. Trends in Parasitology **28:** 437-446.
Hii, S.F., R.J. Traub,M.F. Thompson,J. Henning,C.A. O'Leary,A. Burleigh,M.L. Levin,L.F. Killmaster,G.E. Zemtsova. 2012. Domestic dogs (Canisfamiliaris) as reservoir hosts for *Rickettsia conorii*. Vector-Borne and Zoonotic Diseases**12:** 28-33.
Inokuma, H., P. Brouqui,M. Drancourt,D. Raoult. 2001. Citrate Synthase Gene Sequence: a New Tool for Phylogenetic Analysis and Identification of *Ehrlichia*. Journal of Clinical Microbiology **39:** 3031-3039.
Inokuma, H. K. Fujii,M. Okuda,T. Onishi,J.P. Beaufils,D. Raoult,P. Brouqui. 2002b. Determination of the Nucleotide Sequences of Heat Shock Operon groESL and the Citrate Synthase Gene (gltA) of *Anaplasma* (*Ehrlichia*) *platys* for Phylogenetic and Diagnostic Studies. Clinical and Vaccine Immunology **9:** 1132-1136.
Inokuma, H., M. Okuda,K. Ohno,K. Shimoda,T. Onishi. 2002a. Analysis of the 18S rRNA gene sequence of a Hepatozoon detected in two Japanese dogs. Veterinary Parasitology **106:**265–271.
Inokumaa, H., Y. Yoshizakia, K. Matsumotoa, M. Okudaa, T. Onishia,K. Nakagomeb, R. Kosugib, M. Hirakawab. 2004. Molecular survey of *Babesia* infection in dogs in Okinawa, Japan. Veterinary Parasitology **121:** 341-346.
Jin, L.M., Q.L. Wu,Y.B. Dong,L. Ge. 2005. Investigation on epidemic disease of cannie *Babesia gibsoni* in Nanjing. Journal of Jinling Institute of Technology. **21:**93-96.
Kamani, J., G. Baneth,K.Y. Mumcuoglu,N.E. Waziri,O. Eyal, Y. Guthmann, S. Harrus. 2013. Molecular detection and characterization of tick-borne pathogens in dogs and ticks from Nigeria. PLOS Neglected Tropical Diseases **7:**e2108.
Kawwkong, W., P.M. Intapan,O. Sanpool,P. Janwan,T. Thanchomnang,S. McMahon,R.L. Rees,S.R. Kopp. 2015. Canine tick-borne pathogens and associated risk factors in dogs presenting with and without clinical signs consistent with tick-borne diseases in northern Australia. Australian Veterinary Journal **93:** 58-64.
Kordick, S.K., E.B. Breitschwerdt, B.C. Hegarty, K.L. Southwick, C.M. Colitz, S.I. Hancock, J.M. Bradley,R. Rumbough, J.T. Mcpherson, J.N. MacCormack. 1999. Coinfection with multiple tick-borne pathogens in a Walker hound kennel in North Carolina. Journal of Clinical Microbiology **37:** 2631-38.
Labruna M.B., T. Whitworth, M.C. Horta, D.H. Bouyer, J.W. McBride, A. Pinter, V. Popov,S.M. Gennari,D.H. Walker. 2004. *Rickettsia* species infecting *Amblyomma cooperi* ticks from an area in the states of Sao Paulo, Brazil, where Brazilian spotted fever is endemic. Journal of Clinical Microbiology **42:**90-98.
Ma, D., X. Ding,J. Cao,X. Xun,Z. Cheng. 2012. The situation of dog source in China. China Working Dog **1:** 45-50.
Mokhtar, A.S., S.E. Lim,S.T. Tay. 2013. Molecular detection of *Anaplasma platys* and *Babesia gibsoni* in dogs in Malaysia. Tropical Biomedicine **30:** 345-348.
Kongklieng, A., C. Tantrawatpan, T. Boonmars,V. Lulitanond,P. Taweethavonsawat,S. Chungpivat,W. Maleewong.2014. High throughput pyrosequencing technology for molecular differential detection of *Babesia vogeli*, *Hepatozoon canis*, *Ehrlichia canis* and *Anaplasma platys* in canine blood samples. Ticks and Tick-borne Diseases **5:**381–385.
Moreira-Soto, A., M.V. Carranza,L. Taylor,O. Calderón-Arguedas,L. Hun,A. Troyo. 2016. Exposure of dogs to spotted fever group rickettsiae in urban sites associated with human rickettsioses in Cost Rica. Ticks and Tick-borne Diseases **7:** 748-753.
Mandal, M., P.S. Banerjee,S. Kumar,R. Garg,H. Ram,O.K. Raina. 2016. Development of recombinant BgP12 based enzyme linked immunosorbent assay for serodiagnosis of *Babesia gibsoni* infection in dogs. Veterinary Immunology and Immunopathology **169:** 27-33.
Masuzawa, T., K. Sawaki, H. Nagaoka,M. Akiyama, K. Hirai,Y. Yanagihara. 1997. Identification of rickettsiae isolated in Japan as *Coxiella burnetii* by 16S rRNA sequencing. International Journal of Systematic and Evolutionary Microbiology **47:** 883-884.
Nordstoga, A., K. Handeland,T.B. Johansen,L. Iversen,M.R. Gavier-Widén,K. Wik-Larssen,J.E. Afset,R. Næverdal,A. Lund. 2014. Tularaemia in Norwegian dogs. Veterinary Microbiology **173:**318-322.
Obara, H., M. Fujihara,Y. Watanabe,H.K. Ono,R. Harasawa. 2011. A feline Hemoplasma, '*Candidatus Mycoplasma haemominutum*', detected in dog in Japan. The Journal of Veterinary Medical Science **73:** 841-843.
Schorn, S., K. Pfister.H. Reulen,M. Mahling,C. Silaghi. 2011. Occurrence of *Babesia* spp., *Rickettsia* spp. and *Bartonella* spp. in *Ixodes ricinus* in Bavarian public parks, Germany. Parasites & Vectors **4:**135.
Shang, Z.S., C. Zhang, Z.F. Zhang, S.N. Cuan,Z.J. Yang. 2014. Epidemiological Characteristics of Canine Babesiosis and Main Vector of Infection in West of Henan. Journal of Henan University of Science and Technology:Natural Science **35:**73-78.
Shaw, S.E., M.J. Day, R.J. Birtles, E.B. Breitschwerdt. 2001. Tick-borne infectious diseases of dogs. Trends in Parasitology**17:**74-80.

Shen, Y., Gao, J., Xu, K., Xue, L., Zhang, Y., Shi, B., Li, D., Wei, X., Selichi, H., 1997. Babesiaosis in Nanjing area, China. Tropical Animal Health and Production **29:**19s-22s.
Singh, M.N., O.K. Raina, M. Sankar, A. Rialch, M.N. Tigga, G.R. Kumar, P.S. Banerjee.2016. Molecular detection and genetic diversity of *Babesia gibsoni* in dogs in India. Infection, Genetics and Evolution **41:** 100-106.
Stromdahl, E.Y., P.C. Williamson, T.M. Kollars Jr, S.R. Evans, R.K. Barry, M.A. Vince, N.A. Dobbs. 2003. Evidence of *Borrelia lonestari* DNA in *Amblyomma americanum* (Acari: Ixodidae) Removed from Humans. Journal of Clinical Microbiology **41:** 5557-5562.
J.E. Sykes,L.M. Ball, N.L. Bailiff, M.M. Fry. 2005. '*Candidatus Mycoplasma haematoparvum*', a novel small haemotropic *mycoplasma* from a dog. International Journal of Systematic and Evolutionary Microbiology **55:**27-30.
Wang, W.B. Z.B. Liu, X.J. Bao, W.C. Liu, J.H. Ye. 2013. Epidemiological investigation of tick (Ixodida) on police dogs in some area of China. Chinese Journal of Veterinary Medicine **49:**17-20.
Wei, F.R., Q.X. Lan, D. Zhu, J.H. Ye, Q. Liu, Y. Zhang. 2012. Investigation on Babesia in ticks infested on police dogs in selected areas of China. Chinese Journal of Parasitology and Parasitic Diseases **30:**390-392.
Xu, D., J. Zhang, Z. Shi, C. Song, X. Zheng, Y. Zhang, Y. Hao, H. Dong, L. Wei, H.S. EI-Mahallawy, et al. 2015. Molecular detection of Vector-borne agents in dogs from ten provinces of China. Parasites & Vectors **8:**501.
Yabsley, M.J., J. McKibben, C.N. Macpherson, P.F. Cattan, N.A. Cherry, B.C. Hegarty, E.B. Breitschwerdt, T. O'Connor, R. Chandrashekar, T. Paterson, et al. 2013. Tick-borne pathogens and disease in dogs on St. kitts, West Indies. Veterinary Parasitology **196:** 44-49.
Zhuang, Q.J., H.J. Zhang,R.Q. Lin,M.F. Sun, X.J. Liang, X.W. Qin, W.J. Pu, X.Q. Zhu. 2009. The occurrence of the feline " *Candidatus Mycoplasma haemominutum*" in dog in China confirmed by sequence-based analysis of ribosomal DNA. Tropical Animal Health and Production **41:** 689-692.

注：本研究は 2017 年 2 月 4 日「The Journal of Veterinary Medicine Science」にて掲載した。

作成日：2017 年 2 月 25 日

Ripasudil (K-115), a Rho kinase inhibitor, blocks VEGF-induced disruption of retinal vascular barrier: a new candidate drug for diabetic macular edema

Rho キナーゼ阻害剤であるリパスジル(K-115)は、VEGF 誘導性の網膜血管バリアー破綻を抑制する：糖尿病黄斑浮腫に対する新規治療薬候補

研 究 者 氏 名　馮　浩（第 38 期笹川医学研究者）
中国所属機関　中国医科大学附属第一医院眼科
日本研究機関　九州大学大学院医学研究院眼科学
指 導 責 任 者　園田　康平　教授
共同研究者名　有馬　充　特任助教、中尾　新太郎　講師

Abstract:

Diabetic macular edema (DME) is a major cause of visual impairment in diabetes patients. Impairment of retinal vascular barrier triggered by vascular endothelial growth factor (VEGF) is a core of pathophysiology of DME. Although anti-VEGF treatment using neutralizing antibody is the standard therapy in clinics to control DME, its effect is transient. Therefore, it is necessary to establish other treatment strategy. Here, we demonstrate that ripasudil (K-115), a highly selective and potent ROCK inhibitor, is a new candidate drug for VEGF-induced vascular barrier impairment of DME. In vitro data with neural microvascular endothelial cells indicated that K-115 prevents the VEGF-induced formation of stress fibers, and rescues the degradation of claudin-5 by stabilizing the interaction between ZO-1 and claudin-5. In vivo data using trVEGF029 (Kimba) mice shown the VEGF-induced vascular hyperpermeability was clearly normalized by K-115 eye drop. This study has highlighted K-115 as a potent inhibitor for VEGF-induced impairment of retinal vascular barrier, which can be a new strategy to the treatment of DME.

Key Words:

Diabetic macular edema, Blood retinal barrier, Rho kinase, Tight Junction and Claudin-5

Introduction:

Despite the advancement of medical technology, diabetic retinopathy (DR) is still a common disease leading decline of visual acuity in adults worldwide [1]. Diabetic macular edema (DME) is one of the representative causes of visual loss in DR and it is reported that DME develops in approximately 25% of all diabetes patients [2]. Many researchers have revealed the close association between vascular endothelial growth factor (VEGF) and the formation of DME, and therefore, the intravitreal injection of antibody specific for VEGF is getting to become the first choice among several therapeutic strategies [3].

Although anti-VEGF therapy is certainly effective for the resolution of DME, multiple injections are necessary in most cases and there is no therapeutic reaction in some cases. Prior to the application to DME, anti-VEGF therapy has been used for cancer treatment and nowadays a concept of the resistance for anti-VEGF therapy is raising in this field [4]. Tumor is rich in cytokines in addition to VEGF and it is proved that their downstream pathways attenuate the effect of VEGF neutralization [5]. Because many kinds of cytokines are also upregulated in the retina and the vitreous body of DME, it is speculated the similar mechanism may contribute the resistance for anti-VEGF therapy [6]. In brief, the development of new therapeutic strategies not relying on symptomatic treatment targeting a single secreted cytokine is urgently needed.

To maintain the proper neural microenvironment, vascular vessels in central nervous systems including the retina and the brain have the barrier function which strictly controls the influx of fluid toward neural tissues [7]. This barrier

function depends on the appropriate assembly of tight junction (TJ) between adjacent endothelial cells. It was revealed that claudin-5 is one of the most crucial molecules for the neural vascular barrier among TJ components [8, 9]. Although it is well-known VEGF decreases claudin-5 expression in cell membranes, the proper mechanism is yet to be elucidated completely. The main purpose in this study is to identify the molecule which regulate directly claudin-5 expression and to establish a new strategy for DME.

We have revealed that Rho kinase (ROCK) is closely involved in DR pathogenesis of angiogenesis, adhesion and polarization of leukocytes, endothelial apoptosis and so on [10-15]. However, there is no consensus regarding the role of ROCK on the collapse of retinal vascular barrier function in DR. Claudin-5 is anchored to actin cytoskeleton via ZO-1 and this structure is crucial for stable expression of claudin-5 in cell membranes. Previous report additionally showed that VEGF activates ROCK signaling to induce reorganization of the actin cytoskeleton [16-18]. The above-described data led us to speculate that ROCK could be involved in the disappearance of claudin-5 from cell membranes and the breakdown of retinal vascular barrier in VEGF-stimulated condition. We verified this hypothesis *in vitro* and *in vivo* using K-115, a selective ROCK inhibitor.

Methods:

Cell culture

A mouse brain microvascular endothelial cell line, bEND.3, was grown as a monolayer in Dulbecco's Modified Eagle's medium containing 4500 mg/l glucose supplemented with 10% fetal bovine serum at 37 °C in humidified incubators with 5% CO2 and 95% room air. Cells were cultured in 6-well plates coated with collagen. Experiments were performed in 7 days after confluency. Mouse recombinant VEGF was administrated to the cultured medium 24 hours prior to the start of experiments (the final concentration; 25 ng/ml). K-115 was added into the medium 3 hours prior to addition of VEGF (the final concentration; 3 or 30 μM).

Immunocytochemistry of cultured cells

Cultured cells were fixed with 4% paraformaldehyde (PFA) for 15 minutes at room temperature. Cells were permeabilized with 0.1% Triton X-100 in phosphate-buffered saline (PBS) for 10 min and then were incubated with 10% non-immune goat serum for 30 minutes at room temperature. Then, they were reacted with rabbit polyclonal antibody against claudin-5 at 4 °C overnight. After washing with PBS, they were incubated with Alexa Fluor 488 goat anti-rabbit immunoglobulin G (IgG) for simple staining of claudin-5 or with Alexa Fluor 488 goat anti-rabbit IgG and mouse monoclonal antibody against ZO-1 conjugated with Alexa 594 for double staining of claudin-5 and ZO-1, or with Alexa Fluor 488 goat anti-rabbit IgG and Alexa Fluor 594 phalloidin for double staining of claudin-5 and F-actin at room temperature under light protection for 1 hour. Observation was performed under a Zeiss LSM5 Pascal laser confocal microscope.

Transendothelial electrical resistance

Electrical resistance of a bEND.3 monolayer at confluent state on collagen-coated 0.9 cm^2 inserts of 0.4 μm pore size was measured. We calculated the values of transendothelial electrical resistance (TEER) by subtracting the resistance of blank inserts without cells and multiplying the subtracted values by the surface areas of inserts.

Western blot analyses

Cells were lysed in PBS containing 1% Triton X-100 and 0.2% sodium dodecyl sulfate (SDS). After centrifugation of the lysates at 15000 rpm for 15 minutes at 4 °C, the supernatants were collected. Samples were separated by SDS-PAGE and transferred to PVDF membranes. Membranes were incubated at room temperature for 1 hour in Tris-buffered saline with 0.1% Tween 20 (TBS-T) containing 5% skim milk for blocking. Then, they were reacted with rabbit polyclonal

antibody against claudin-5, rabbit polyclonal antibody against ZO-1 or rabbit polyclonal antibody against GAPDH at 4 °C overnight. After the wash with TBS-T, they were incubated with horseradish peroxidase (HRP) conjugated goat anti-rabbit IgG at room temperature for 1 hour.

Real-time quantitative polymerase chain reaction

Total RNA was extracted from the tissue homogenate with reagent and was exposed to DNase to eliminate potential genomic DNA contamination. Total RNA was reverse-transcribed with a first- strand cDNA synthesis kit. Real-time quantitative polymerase chain reaction was performed with SYBR Premix Ex Taq using LightCycler 96. The primers used were as follows: 5'- GGCACTCTTTGTTACCTTGACC-3' and 5'-CAGCTCGTACTTCTGTGACACC-3' for claudin-5; and 5'- GATGACCCAGATCATGTTTGA-3' and 5'-GGAGAGCATAGCCCTCGTAG-3' for β-actin.

Immunoprecipitaion

A sample was reacted at 4 °C overnight with antibody against ZO-1, and immune complexes were collected by incubating at 4 °C for 2 hours with Protein G Sepharose 4 Fast Flow. Sepharose beads were boiled with Laemmli sample buffer, and the supernatant was used for Western blot analysis. HRP-conjugated rat anti-rabbit IgG Mouse Trueblot® was used as secondary antibodies.

Animals

All procedures were reviewed by the Committee on Ethics in Animal Experiments of the Kyushu University and were carried out according to the Guidelines for Animal Experiments of the Kyushu University and of the Japanese government. We used the trVEGF029 (Kimba) mice (C57BL6 background), in which human VEGF is transiently overexpressed in photoreceptor cells, and wildtype mice for this study.

Visualization of retinal vascular barrier integrity and macular edema

We administered eye drops of 0.8% K-115 into 4 week old Kimba mice and age-matched wild mice for 2 weeks. Then, we evaluated the retinal vascular barrier integrity with fluorescein angiography on a confocal scanning laser ophthalmoscope, Heidelberg HRA. Mice were anesthetized by an intraperitoneal injection of 15 mg/kg ketamine and 7 mg/kg xylazine, and pupils were dilated with 1% tropicamide and 2.5% phenylephrine. Then, 12 μL/g 2.5% fluorescein sodium was injected intraperitoneally. We also evaluated the effect of K-115 on the formation of macular edema using optical coherence tomography, Cirrus HD-OCT.

Statistical Analyses

All data are expressed as the means ± SD. The significance of the differences in the measurements was determined by Student's *t*-tests. Differences were considered statistically significant at $P < 0.05$.

Results:

K-115 blocks the breakdown of vascular barrier function under VEGF-stimulated condition.

To validate the involvement of ROCK signaling on the VEGF-induced impairment of vascular barrier function, we investigated if K-115 could rescued the fall-down of TEERs and the decline of claudin-5 expression in endothelial cell membranes. The values of TEER without VEGF stimulation were not

Fig. 1

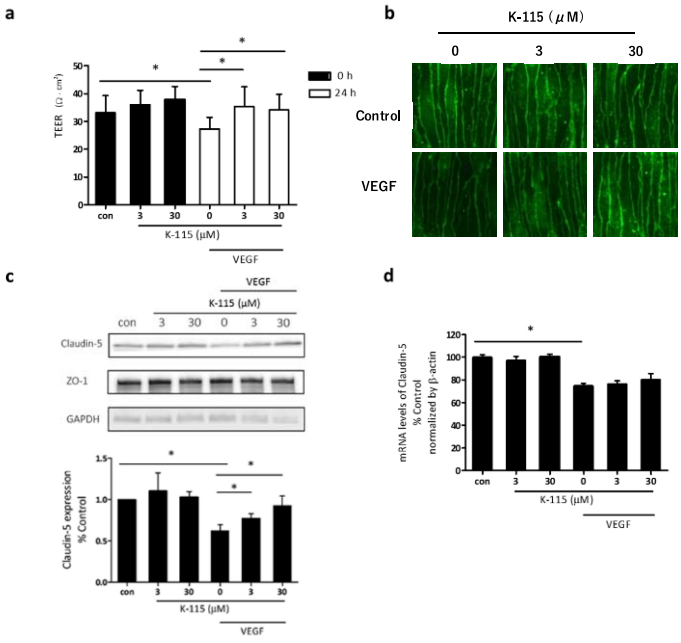

changed by the administration of K-115. On the other hand, K-115 recovered the VEGF-induced decrease of TEER values (Fig. 1a). The results of immunocytochemistry of claudin-5 also revealed the similar phenomenon; K-115 had no influence on claudin-5 expression in cell membranes in normal condition, but blocked claudin-5 disappearance from cell membranes in VEGF-stimulated condition (Fig.1b). The results of immunostainings were closely correlated with the ones of Western blot analyses (Fig.1c). We confirmed that K-115 did not increase the amount of claudin-5 mRNA (Fig. 1d).

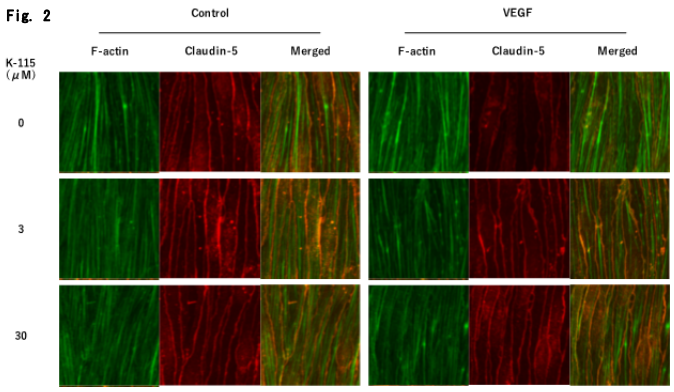

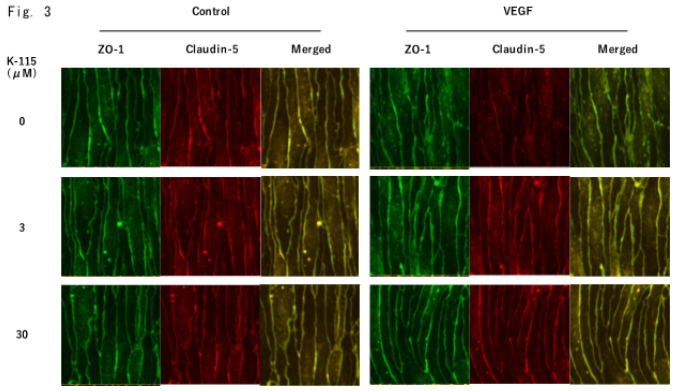

K-115 prevents the dissociation between claudin-5 and ZO-1 by inhibiting to form stress fibers under VEGF stimulation.

The results of double immunostainings revealed (1) VEGF decreased the expression of claudin-5 in cell membranes (2) VEGF had no effect on the expression of ZO-1, and (3) VEGF induced reorganization of the actin cytoskeleton (Fig. 2 and Fig. 3). The results of immunoprecipitation demonstrated that the dissociations between claudin-5 and ZO-1 under VEGF stimulation were retained by the addition of K-115 (Fig 4).

Eye drop of K-115 blocks retinal vascular hyper-permeability and formation of macular edema in Kimba mice.

Although fluorescein leakage from retinal vascular vessels and the formation of macular edema were observed in Kimba mice, these phenomena were clearly disappeared by administration of eye drop of K-115 (Fig 5).

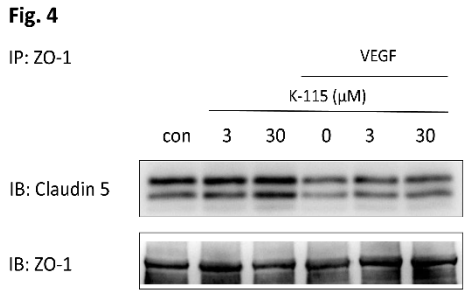

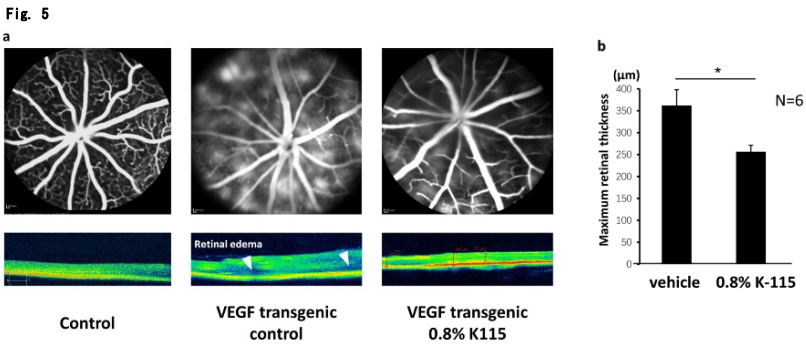

Discussion:

Here, we showed that K-115, a potent ROCK inhibitor, has ability to recover VEGF-induced vascular barrier disruption by inhibiting stress fiber formation and rescuing claudin-5 dissociate from ZO-1. Furthermore, our in vivo data indicated the availability of K-115 as a new candidate drug for DME.

K-115 had no influence on TEER values and claudin-5 expression on endothelial cell membranes in normal condition, and prevented the fall-down of TEER values and claudin-5 disappearance in VEGF stimulated condition. K-115 did not change the level of claudin-5 mRNA, indicating ROCK signaling is involved in VEGF-triggered disruption of vascular barrier function through disappearance of claudin-5 from cell membranes by post-transcriptional

mechanisms.

In order to clarify the molecular mechanisms by which K-115 prevents claudin-5 disassembly, we focused on one of the major roles of ROCK signaling on cytoskeletal dynamics. VEGF can activate ROCK signaling to induce the reorganization of the actin cytoskeleton[17]. Claudin-5 is anchored to actin cytoskeleton via ZO-1 and this structure is crucial for stable expression of claudin-5 in cell membranes. Therefore, we confirmed whether the expression of claudin-5, ZO-1 and F-actin could be changed by VEGF stimulation using immunostaining. VEGF induced the decrease of claudin-5 expression on cell membranes and the formation of stress fiber, but K-115 recovered these phenomena. On the other hand, VEGF did not influence ZO-1 expression. The results of immunoprecipitation revealed K-115 inhibited VEGF-induced claudin-5 dissociation from ZO-1. From these findings, it was speculated that K-115 could rescue claudin-5 degradation through fixing claudin-5 to cytoskeleton.

Encouraged by the results we obtained with vascular endothelia monolayers in vitro BRB model, we continue to move forward to get a more particular knowledge of K-115 in maintenance permeability in the in vivo setting. We found K-115 reduced VEGF-induced retinal hyperpermeability in Kimba mice as measured by fluorescein angiography. Because macular edema is mainly caused by the leakage of fluid from the dilated and tortuous retinal veins to intercellular spaces within the outer plexiform layer of the retina, so we measured the retinal thickness by OCT, the result also indicated K-115 prevent from the formation of macular edema. K-115 has high intraocular permeability which made it could be detected in the retina after eye drop administration in rabbits [19]. The administration route of K-115 which use eye drop instead of intraocular injection compared to traditional anti-VEGF therapies also possess many advantages, such as a lower cost and more safety to mind intraocular infection.

In conclusion, we firstly demonstrated that K-115 has the ability to block VEGF-induced breakdown of vascular barrier function through inhibiting claudin-5 disappearance from cell membranes. K-115 as a novel ROCK inhibitor can effectively suppress cytoskeletal structure reorganization and maintain claudin-5 stabilization. Our findings verify K-115 could be a new candidate drug for diabetic macular edema.

References:

1. Cheung N, Mitchell P, Wong TY (2010) Diabetic retinopathy. Lancet 376: 124-136.

2. Nentwich MM, Ulbig MW (2015) Diabetic retinopathy - ocular complications of diabetes mellitus. World J Diabetes 6: 489-499.

3. Do DV, Nguyen QD, Boyer D, Schmidt-Erfurth U, Brown DM, et al. (2012) One-year outcomes of the da Vinci Study of VEGF Trap-Eye in eyes with diabetic macular edema. Ophthalmology 119: 1658-1665.

4. Kwong TQ, Mohamed M (2014) Anti-vascular endothelial growth factor therapies in ophthalmology: current use, controversies and the future. Br J Clin Pharmacol 78: 699-706.

5. Chung AS, Wu X, Zhuang G, Ngu H, Kasman I, et al. (2013) An interleukin-17-mediated paracrine network promotes tumor resistance to anti-angiogenic therapy. Nat Med 19: 1114-1123.

6. Ciulla TA, Amador AG, Zinman B (2003) Diabetic retinopathy and diabetic macular edema: pathophysiology, screening, and novel therapies. Diabetes Care 26: 2653-2664.

7. Hawkins BT, Davis TP (2005) The blood-brain barrier/neurovascular unit in health and disease. Pharmacol Rev 57: 173-185.

8. Nitta T, Hata M, Gotoh S, Seo Y, Sasaki H, et al. (2003) Size-selective loosening of the blood-brain barrier in claudin-5-deficient mice. J Cell Biol 161: 653-660.

9. Argaw AT, Gurfein BT, Zhang Y, Zameer A, John GR (2009) VEGF-mediated disruption of endothelial CLN-5 promotes blood-brain barrier breakdown. Proc Natl Acad Sci U S A 106: 1977-1982.

10. Hata Y, Miura M, Nakao S, Kawahara S, Kita T, et al. (2008) Antiangiogenic properties of fasudil, a potent Rho-Kinase inhibitor. Jpn J Ophthalmol 52: 16-23.

11. Kita T, Hata Y, Arita R, Kawahara S, Miura M, et al. (2008) Role of TGF-beta in proliferative vitreoretinal diseases and ROCK as a therapeutic target. Proc Natl Acad Sci U S A 105: 17504-17509.

12. Arita R, Hata Y, Ishibashi T (2010) ROCK as a Therapeutic Target of Diabetic Retinopathy. J Ophthalmol 2010: 175163.

13. Arita R, Nakao S, Kita T, Kawahara S, Asato R, et al. (2013) A key role for ROCK in TNF-alpha-mediated diabetic microvascular damage. Invest Ophthalmol Vis Sci 54: 2373-2383.

14. Zandi S, Nakao S, Chun KH, Fiorina P, Sun D, et al. (2015) ROCK-isoform-specific polarization of macrophages associated with age-related macular degeneration. Cell Rep 10: 1173-1186.

15. Yamaguchi M, Nakao S, Arita R, Kaizu Y, Arima M, et al. (2016) Vascular Normalization by ROCK Inhibitor: Therapeutic Potential of Ripasudil (K-115) Eye Drop in Retinal Angiogenesis and Hypoxia. Invest Ophthalmol Vis Sci 57: 2264-2276.

16. Bryan BA, Dennstedt E, Mitchell DC, Walshe TE, Noma K, et al. (2010) RhoA/ROCK signaling is essential for multiple aspects of VEGF-mediated angiogenesis. FASEB J 24: 3186-3195.

17. van Nieuw Amerongen GP, Koolwijk P, Versteilen A, van Hinsbergh VW (2003) Involvement of RhoA/Rho kinase signaling in VEGF-induced endothelial cell migration and angiogenesis in vitro. Arterioscler Thromb Vasc Biol 23: 211-217.

18. He M, Cheng Y, Li W, Liu Q, Liu J, et al. (2010) Vascular endothelial growth factor C promotes cervical cancer metastasis via up-regulation and activation of RhoA/ROCK-2/moesin cascade. BMC Cancer 10: 170.

19. Isobe T, Mizuno K, Kaneko Y, Ohta M, Koide T, et al. (2014) Effects of K-115, a rho-kinase inhibitor, on aqueous humor dynamics in rabbits. Curr Eye Res 39: 813-822.

作成日：2017 年 2 月 28 日

Symptom clusters in breast cancer survivors: A systematic literature review
乳がんサバイバーの症状クラスター：系統的文献検討

研 究 者 氏 名　　張　含鳳（第38期笹川医学研究者）
中国所属機関　　四川省腫瘤医院放射線科
日本研究機関　　広島大学大学院医歯薬保健学研究院老年･がん看護開発学
指 導 責 任 者　　宮下　美香　教授

Abstract

Purpose The aim of this study is to systematically evaluate the literature for symptom clusters in breast cancer survivors.

Methods The MEDLINE, EMBASE, PsycINFO, CINAHL, Web of Science and Elsevier Science Direct databases were searched using key words and synonyms for symptom clusters in patients with breast cancer.

Results Of the 228 articles, 6 relevant articles were reviewed. The six articles were published between 2008 and 2016, with the cluster numbers ranging from three to five. The psychoemotional/depression cluster and gastrointestinal cluster were reported among six articles. The pain, fatigue, and physical/unwellness cluster were mentioned in three of six articles. The hormone/menopausal cluster was named in two studies, while the sleep and increased weight/appetite clusters were only showed in one study respectively. There is no cluster contained identical symptoms in six studies.

Conclusions The psychoemotional/depression cluster and gastrointestinal cluster have been verified in symptom clusters in breast cancer survivors, while the pain, fatigue and physical/unwellness cluster remains inconclusive. Future studies should be implemented to reach some agreements on definition, underlying mechanisms, components, and assessment tools of the symptom cluster in patients with breast cancer.

Keywords Breast cancer· Survivors· Symptom cluster· Symptom management

Introduction

According to the global cancer statistics in 2012, breast cancer is the most common cancer and the leading cause of cancer death among females worldwide, with an estimated 1.7 million cases and 521,900 deaths [1]. Breast cancer accounts for 25% of all cancer cases and 15% of all cancer deaths among females [1]. With the development of treatment methods, the survival rates of breast cancer survivors have increased significantly. However, evidence shows that many inevitable side effects were generated from breast cancer and treatments, which have detrimental effects on patients' functional status as well as quality of life for years [2-3]. As a result, more challenges on long-term management of patients with breast cancer are faced by health professionals, patients, and their families.

Consequently, a large amount of research on breast cancer survivors has been implemented to acquaint symptom experience and its effect on outcomes, with the limitation of focusing on a single symptom or same multiple symptoms preferred by authors [4-5]. Nevertheless, recent articles revealed that breast cancer survivors experienced some concurrent and related symptoms, which could be classified into a same group with the name of a symptom cluster [6-7]. Symptom clusters were initially defined as having three or more coexisting symptoms with some relationship to each other, with or without the same etiology [8]. In 2005, this definition was revised to allow for the presence of only two symptoms in a cluster [9]. Till now, there is no consensus on the definition of symptom cluster.

Although symptom clusters in patients with breast cancer have been widely discussed, the majority of articles were cross-sectional design with diverse participants, various measure tools and inconsistent statistical approaches [10-11]. As a result, the conclusions of literature are various and no agreement has been achieved on the symptom clusters in breast cancer survivors. The latest review about symptom clusters in patients with breast cancer was published in 2011, which stated that there was no common symptom clusters could be derived from the existed reports [12]. Specifically, this review is to update an overview of the literature of symptom clusters in breast cancer survivors from 2008 to 2016.

Methods

Literature Search

A systematic search of the literature was conducted using the MEDLINE, CINAHL, EMBASE, PsycINFO, Web of Science and Elsevier ScienceDirect databases. Search terms 'breast cancer' or 'breast neoplasm' were combined with 'symptom cluster', 'clustering of symptom', 'symptom burden' and so on to elicit relevant literature. The publication language was restricted to English, and the publication date was limited from 2000.

Inclusion and Exclusion Criteria

Articles were included in the review only if the outcomes of symptom cluster derived from the first-hand researches. Articles that did not present data on outcomes (e.g., review) and secondary analysis articles were excluded.

Appraisal and Exclusion Process

The primary author was responsible for reviewing all full text articles and selecting the suitable literature, while exclusion decisions were discussed and determined by two researchers. The quality of articles was assessed using the tool named Standard Quality Assessment Criteria for Evaluating Primary Research Papers [13]. Quality assessment and exclusion decisions of selected articles were completed independently by two researchers. Scores were then compared and discussed until a consensus was reached. Articles that achieved a final score of 70% or greater were included in this review [14]. The screening and exclusion process is presented using an adapted PRISMA (Preferred Reporting Items for Systematic Reviews and Meta-Analyses) flowchart.

Data Extraction and Analysis

The data of included papers were independently derived using data extraction criteria (see Table 1). Papers were listed chronologically by publication data.

Results

Of 230 articles retrieved, 228 potentially relevant articles were identified, 167 were not considered to be related, and 61 were obtained in full text. Eight articles reported data on the symptom cluster of breast cancer that could be extracted for review. After quality assessment, six papers were identified as high quality, which were included for the last review and data extraction.

The publication dates of six articles ranged from 2008 to 2016. The majority of articles reported studies conducted in the United States (n = 4), with one each in Thailand and Brazil. Most articles were cross-sectional design (n=4). A great

variety of data collection tools were used, including Memorial Symptoms Assessment Scale (MSAS), Profile of Mood States (POMS), and so on. The analysis methods used in the six articles were the Factor analysis, Hierarchical cluster analysis and K-medoid clustering. Various time points of collecting data were showed in six studies (see Table 1-2).

Quality assessment

Using the Standard Quality Assessment Criteria for Evaluating Primary Research Papers tool, four papers received a score of 80% or greater. The remaining two articles had a score of 77.3% and 79.6% respectively.

Symptom clusters in patients with breast cancer

As reported in Table 2, the number size of clusters among six articles was ranged from three to five. A cluster was consisted of three to eight symptoms. Among the six articles, only two symptom clusters were same, which were psychoemotional/depression cluster and gastrointestinal cluster. In the psychoemotional/depression cluster, there was only one same symptom across six articles, which was depression. In the gastrointestinal cluster, the highest frequency of symptom was lack of appetite, which was reported in five articles. Moreover, lack of appetite and nausea were associated with each other across four of the six articles, while nausea and vomiting were found together in two articles in this review. Though the symptoms of fatigue and pain were described in all six studies, there were only three studies considered the fatigue and pain as independent symptom cluster respectively. Also, the physical/unwellness cluster was mentioned in three articles. The hormone/menopausal cluster was reported in two studies, while the sleep and increased weight/appetite clusters were only showed in one article.

Discussion

This study is the first to determine the existence of psychoemotional/depression cluster and gastrointestinal cluster in patients with breast cancer. As for the psychoemotional/depression cluster, with some negative feelings of depression, anxiety, worrying and anger, it is often associated with medical, sociodemographic, and psychosocial factors [15]. Previous studies have demonstrated that the negative emotions in breast cancer survivors were frequently occurred during and after treatments, resulting in fewer adherences to therapeutic regimens and lower health outcomes [16]. However, these negative symptoms were found remaining underdiagnosed and undertreated in breast cancer survivors. Thus, the early identification and effective interventions of negative emotional symptoms in patients with breast cancer should be conducted in their long-term survivorships by health professionals. In addition, some studies identified that depression and other symptoms were in the same emotional cluster [17]. However, only depression was the same symptom in the psychoemotional/depression cluster among six reports in this study. Therefore, it necessary to determine and verify the components and mechanisms of psychoemotional/depression cluster in future studies.

In addition to psychoemotional cluster, the gastrointestinal cluster is another same cluster in six articles, characterized by nausea, vomiting, and lack of appetite [16]. Previous studies indicated that the gastrointestinal symptoms were common adverse effects of the anti-cancer treatments [18]. Though nausea and vomiting were mentioned in the same cluster in some studies [12], these two symptoms were found together in only two articles in this review. By contrast, similar with the latest review [12], nausea and lack of appetite were associated together in four articles. More studies should be implemented to confirm which symptoms are within the same gastrointestinal cluster in the future. Also, dealing with symptoms of gastrointestinal cluster is an important issue for medical staffs. As reported, although

previous research has mainly focused on nausea and vomiting in patients, the most burdensome symptom for patients was the taste change of food. Similar to this, the lack of appetite was discovered as the most common symptom in the gastrointestinal cluster in this review. Current data suggests that more comprehensive interventions should be adopted to deal with some invisible symptoms in the gastrointestinal cluster in breast cancer survivors, just like the food taste and lack of appetite.

Previous studies have mentioned that fatigue and pain are frequently observed symptoms in breast cancer survivors [19-20]. Similarly, the symptoms of fatigue and pain were reported in all six studies in this review. Whereas, there were only three studies which considered the fatigue and pain as an independent symptom cluster. The reason of same symptom in different symptom clusters may relate to the diverse causes of symptom (e.g. treatment regimen factor, emotional factor), various research designs and cognition diversities of authors [21]. Future agreements are warranted to reach on the cluster classification of fatigue and pain by using some similar high quality studies.

Regarding to physical/unwellness cluster, it contained some inevitable symptoms which was resulted from cancer treatments, including arm symptom, skin change and so on. Some manifestations of these symptoms are long-term, distressful, and even have huge effects on performance of activities [22]. Based on the regular care for these symptoms in clinical practice, more assessment and guidance of symptom management and rehabilitation exercise in follow-up periods are recommended. Another issue is that some same symptoms, such as skin change, were reported in both physical/unwellness cluster and hormone/menopausal cluster. Therefore, it is confusing to distinguish the differences between these two clusters. More research is needed to determine whether the hormone/menopausal cluster should be included in the physical/unwellness cluster or these two clusters are independent of each other.

Limitations

Among the six articles, four papers were cross-sectional design, which could not reflect the changes of symptom clusters over time. Though the Memorial Symptom Assessment Scale is wildly used in symptom-related studies, it has been criticized for inadequate psychometric properties. Moreover, the discrepancies of research designs and implementations may contribute to the different constructions of symptom clusters among six articles.

Implications for Practice

For research, more empirical studies with an exploratory manner should be designed to identify the changes of symptoms or symptom clusters after treatment over time. For clinical practice, emotion feelings and gastrointestinal symptoms of breast cancer survivors, which have been identified in this review, need more concerns by healthcare providers. It is significant to carry out nonspecific symptom assessment and interventions for patients with breast cancer, and a standard clinical practice followed by some guidelines is required to become a routine work. A regular follow-up should be strengthened to provide an integrated care for patients with breast cancer in their survivorships.

Conclusion

This review is the first to ascertain the existences of psychoemotional/depression cluster and gastrointestinal cluster in breast cancer survivors, while the pain, fatigue and physical/unwellness cluster remains inconclusive. Future studies

should be conducted to reach some agreements on the definition, underlying mechanisms, components, and assessment tools of symptom clusters in patients with breast cancer.

References

1. Torre LA, Bray F, Siegel RL, Ferlay J, Lortet-Tieulent J, Jemal A (2015) Global cancer statistics,2012. CA Cancer J Clin 65:87-108. doi: 10.3322/caac.21262.

2. Jain S, Boyd C, Fiorentino L, Khorsan R, Crawford C (2015) Are there efficacious treatments for treating the fatigue-sleep disturbance-depression symptom cluster in breast cancer patients? A Rapid Evidence Assessment of the Literature (REAL (©)).Breast Cancer (Dove Med Press) 7:267-291. doi: 10.2147/BCTT.S25014. eCollection 2015.

3. Cleeland CS, Bennett GJ, Dantzer R, Dougherty PM, Dunn AJ, Meyers CA, et al (2003) Are the symptoms of cancer and cancer treatment due to a shared biologic mechanism? Acytokine-immunologic model of cancer symptoms. Cancer 97: 2919-2925. doi:10.1002/cncr.11382

4. Cheung YT, Lee HH, Chan A (2013) Exploring clinical determinants and anxiety symptom domains among Asian breast cancer patients. Support Care Cancer 21: 2185-2194. doi: 10.1007/s00520-013-1769-8.

5. Prigozin A, Uziely B, Musgrave CF (2010) The relationship between symptom severity and symptom interference, education, age, marital status, and type of chemotherapy treatment in Israeli women with early-stage breast cancer. Oncol Nurs Forum 37: E411-418. doi: 10.1188/10.ONF.E411-E418.

6. Sanford SD, Beaumont JL, Butt Z2, Sweet JJ, Cella D, Wagner LI (2013) Prospective longitudinal evaluation of a symptom cluster in breast cancer. J Pain Symptom Manage 47:721-730. doi: 10.1016/j.jpainsymman.2013.05.010.

7. So WK, Marsh G, Ling WM, Leung FY, Lo JC, Yeung M, et al (2009) The symptom cluster of fatigue, pain, anxiety, and depression and the effect on the quality of life of women receiving treatment for breast cancer: a multicenter study. Oncol Nurs Forum 36: E205-214. doi: 10.1188/09.ONF.E205-E214.

8. Dodd MJ, Miaskowski C, Paul SM (2001) Symptom clusters and their effect on the functional status of patients with cancer. Oncol Nurs Forum 28: 465-470. PMID: 11338755

9. Kim HJ, McGuire DB, Tulman L, Barsevick AM (2005) Symptom clusters: Concept analysis and clinical implications for cancer nursing. Cancer Nurs 28: 270-282. PMID: 16046888

10. Kim H, Barsevick AM, Tulman L,McDermott PA (2009) Treatment-related symptom clusters in breast cancer: a secondary analysis. J Pain Symptom Manage 36:468-79. doi: 10.1016/j.jpainsymman.2007.11.011.

11. Evangelista AL, Santos EM (2012) Cluster of symptoms in women with breast cancer treated with curative intent. Support Care Cancer 20: 1499-1506. doi: 10.1007/s00520-011-1238-1.

12. Nguyen J, Cramarossa G, Bruner D, Chen E, Khan L, Leung A, et al (2011) A literature review of symptom clusters in patients with breast cancer. Expert Rev Pharmacoecon Outcomes Res 11:533-539. doi: 10.1586/erp.11.55.

13. Kmet LM, Lee RC, Cook LS (2004) Standard Quality Assessment Criteria for Evaluating Primary Research Papers from a Variety of Fields. Canada: Alberta Heritage Foundation for Medical Research. ISBN: 1-896956-71-XX (Online).

14. Paneque M, Turchetti D, Jackson L, Lunt P, Houwink E, Skirton H (2016) A systematic review of interventions to provide genetics education for primary care. BMC Fam Pract 17:89. doi: 10.1186/s12875-016-0483-2.

15. Kim SH, Son BH, Hwang SY, Han W, Yang JH, Lee S, et al (2008) Fatigue and depression in disease-free breast cancer survivors: prevalence, correlates, and association with quality of life. J Pain Symptom Manag 35:644-655. doi: 10.1016/j.jpainsymman.2007.08.012.

16. Mausbach BT, Schwab RB, Irwin SA (2015) Depression as a predictor of adherence to adjuvant endocrine therapy

(AET) in women with breast cancer: a systematic review and meta-analysis. Breast Cancer Res Treat 152:239-246. doi: 10.1007/s10549-015-3471-7

17. Lockefeer JP, De Vries J (2013) What is the relationship between trait anxiety and depressive symptoms, fatigue, and low sleep quality following breast cancer surgery? Psycho-Oncology 22: 1127-1133. doi: 10.1002/pon.3115

18. DibbleSL,CaseyK,NusseyB,IsraelJ,LuiceJ (2004) Chemotherapy-induced vomiting in women treated for breast cancer. Oncol Nurs Forum 31:E1-E8. doi: 10.1188/04.ONF.E1-E8.

19. Romito F, Cormio C, Giotta F, Colucci G, Mattioli V (2010) Quality of life, fatigue and depression in Italian long-term breast cancer survivors. Support Care Cancer 20:2941-2948. doi: 10.1007/s00520-012-1424-9

20. Janz, N.K., Mujahid, M., Chung, L.K., Lantz, P.M., Hawley, S.T., Morrow, M., et al (2007) Symptom experience and quality of life of women following breast cancer treatment. J Womens Health (Larchmt) 16:1348-1361. doi: 10.1089/jwh.2006.0255

21.Hellerstedt-Börjesson S, Nordin K, Fjällskog ML, Holmström IK, Arving C (2016) Women Treated for Breast Cancer Experiences of Chemotherapy-Induced Pain: Memories, Any Present Pain, and Future Reflections. Cancer Nurs 39:464-472. doi: 10.1097/NCC.0000000000000322

22. Burckhardt M, Belzner M, Berg A, Fleischer S (2014) Living with breast cancer-related lymphedema: a synthesis of qualitative research. Oncol Nurs Forum 41: E220- E237. doi: 10.1188/14.ONF.E220-E237.

Tables

Table 1Key Data Extracted From Included Studies Following Quality Appraisal Process

Study and Country	Design and Purpose	Sample and Methods	Tools	Strengths and Limitations	Scores
1.Suwisith et al.,2008 Thailand	Cross-sectional study to explore symptom clusters and their influence on the functional status	320 women; mean age of 47.3 years; time since diagnosis ranged from 1 to 168 months, with a mean of 13.3 months; questionnaires were completed after receiving chemotherapy for seven days	MSAS; IFS-CA	1. Four hospitals and sufficient sample size 2.Validated tools were used 3. Conceptual framework was introduced 4. Symptom clusters were explored across two symptom dimensions 5. Data collection was unclear reported (lacked of the response rate and survey time) 6. Single time point	79.6%
2.Fu et al., 2009 United States	Cross-sectional design to explore ethnicity and persistent symptom burden in breast cancer survivors	139 woman; 58 were non-Hispanic white, 18 were non-Hispanic black, and 63 were Hispanic; median age of 52.5 years; all patients finished treatment ≥3 months. The survey were conducted between August and October 2006	MSAS-SF	1. Diversity of the study population 2. In-depth discussion 3. Excluded data explained 4. Single time point 5. Absence of a non-cancer control group 6. Limited disease stage (stage 0-III)	81.7%
3.Evangelista et al., 2012 Brazil	Cross-sectional study to verify cluster of symptoms in patients treated with curative intent	138 patients; mean age of patients was 51 years	POMS; EORTC-QLQ-C30; EORTC-BR23	1. Medium sample size 2. Focus on symptom clusters of patients after treatment 3. One hospital site 4. Description of exclusion was unclear 5. Result unclear reported (response rate)	77.3%

Table 1 Key Data Extracted From Included Studies Following Quality Appraisal Process (continued)

Study and Country	Design and Purpose	Sample and Methods	Tools	Strengths and Limitations	Scores
4.Lengacher et al., 2012 United States	Two-armed randomized controlled design to investigate symptom clustering in patients who attended MBSR	Control group: (n = 43); MBSR group (n= 41); mean age of 58 years; patients finished questionnaire at baseline and within 2 weeks after the 6-week MBSR intervention	M.D. Anderson Symptom Inventory	1. Randomized controlled design 2. Focus on symptoms of patients received treatment up to 18 months 3. Full discussion of findings and limitations 4. Limited treatment(radiation only or radiation with chemotherapy) 5. Limited disease stage (stage 0-III) 6. Small sample size and single site	87.5%
5.Sarenmalm et al., 2014 United States	Longitudinal study to explore clusters of burdensome symptoms in patients	206 patients (150 early breast cancer; 56recurrence patients); all questionnaire were completed at diagnosis and at one-, three-, and six-month follow-ups	MSAS; Health Status and QoL	1. Sufficient sample size 2. Longitudinal approach 3. Comprehensive discussion of findings and limitations 4. Missing data explained 5. Limited to patients older than 55 years 6. Some severely ill patients were excluded 7. Generalizability of factor analysis might be limited.	93.0%
6.Marshall,et al.,2016 United States	Cross-sectional to explore symptom cluster in patients	653 women; all the patients completed questionnaires by mail	Women's Health Initiative	1. Large sample size 2. Comprehensive discussion of limitations 3. Limited disease stage(stage I-III) 4. Data collected from 2002-2006	83.7%

Table 2 Findings about symptom clusters outcomes among women with breast cancer

Study and Country	Analysis Method	Period of data collection	Findings
1.Suwisith et al.,2008	Factor analysis	Participants received chemotherapy for seven days	1. Emotions related cluster: feeling sad, worrying, feeling irritable, feeling nervous, I don't look like myself, difficulty concentrating, sleeping difficulty, sweating, constipation 2. GI and fatigue related cluster: vomiting, lack of energy, lack of appetite, dizziness, feeling drowsy, shortness of breath, feeling bloated 3. Image related cutaneous cluster: hair loss, changes in food taste, mouth sore, skin change, difficulty swallowing 4. Pain related discomfort cluster: numbness/tingling, pain, dry mouth
2.Fu et al., 2009	Factor analysis	Patients who were ≥3 months post-completion of their adjuvant treatment	1. Depression cluster: sadness/depression, anxiety, grief loss; 2. Chemotherapy cluster: poor appetite, nausea, lymphedema, neuropathy; 3. Hormone cluster: fatigue, poor sex drive, hot flashes, headache, poor memory; 4. Pain-related cluster: insomnia, muscle aches, bone pain
3.Evangelista et al., 2012	Factor analysis	patients have been concluded adjuvant chemotherapy3–24 months prior who may or may not be using hormone therapy	1. Psychoemotional cluster: depression, confusion, anger, tension, fatigue, and breast symptoms 2. Physical cluster: side effects of systemic therapy, pain, dyspnea, arm symptoms, and insomnia 3. Gastrointestinal cluster: inappetence, diarrhea, nausea, and vomiting
4.Lengacher et al., 2012	Hierarchical cluster analysis	patients had been completed treatment within 18 months	1. Gastrointestinal cluster: nausea, vomiting, lack of appetite, shortness of breath, dry mouth, numbness; 2. Cognitive /Psychological cluster: distress, sadness, pain, remembering; 3. Fatigue cluster: fatigue, disturbed sleep, drowsy

Table 2 Findings about symptom clusters outcomes among women with breast cancer (continued)

Study and Country	Analysis Method	Period of data collection	Findings
5.Sarenmalm et al.,2014	Factor analysis	Patients were followed up at one-, three-, and six-month after treatment	1.Emotional cluster: **One-month:** worrying, feeling sad, feeling nervous, feeling irritable, difficulty concentrating, "I don't look like myself", lack of energy, difficult sleeping; **three-month:** worrying, feeling sad, feeling nervous, feeling irritable, difficulty concentrating, "I don't look like myself", lack of energy; **six-month:** worrying, feeling sad, feeling nervous, difficulty sleeping, feeling irritable, sweats, pain, problems with sexual interests, feeling bloated 2.Gastrointestinal cluster: **One-month:** weight loss, change in the way food tastes, nausea, vomiting, lack of appetite, constipation; **three-month:** weight loss, change in the way food tastes, nausea, lack of appetite, hair loss; **six-month:** change in the way food tastes, feeling drowsy, lack of appetite, lack of energy, dry mouth, hair loss, difficulty concentrating 3.Unwellness cluster: **One-month:** changes in skin, swelling of arms or legs, feeling bloated, numbness/tingling in hands/feet, itching; **three-month:** changes in skin, itching, pain, difficulty swallowing; **six-month:** changes in skin, vomiting, swelling of arms or legs, difficulty swallowing
6.Marshall,et al.,2016	K-medoid clustering	Patients diagnosed with cancer in the past eight months	1.Menopausal cluster: hot flashes, night sweats, vaginal dryness 2.Pain cluster: general aches, joint pains, muscle pains, neck-skull aches 3.Fatigue/sleep/gastrointestinal cluster: abdominal pain, constipation, fatigue, headaches, mood changes, nausea, restless sleep, sleeping too much 4.Psychological cluster: avoidance of social affairs, bloating, decreased efficiency, depressed, diarrhea, difficulty concentrating, loss of interest in work, lowered work performance 5.Increased weight/appetite cluster: increased appetite, weight gain

作成日：2017 年 2 月 24 日

TGFβ1 promotes ectopic epithelial cells activation through cadherin-11 to aggravate Invasion joint inflammation in endometriosis

CDH11 は TGFβ1 に活性化され、子宮内膜症上皮細胞の浸潤を促す

研究者氏名　王　煜(第 38 期笹川医学研究者)
中国所属機関　内モンゴル医科大学附属医院婦産科
日本研究機関　東京大学医学部附属病院産婦人科
指導責任者　藤井　知行　教授
共同研究者名　平田　哲也　講師, 練石　和明, 福田 晋也

Abstract:

Background: Endometriotic epithelial cells, which express various growth factors, hormone receptors or inflammatory cytokines, play a major role in the pathophysiology of endometriosis. However, the underlying mechanism for etiology of spread is still unclear. This study was done to elucidate how cadherin11 (CDH11) affects epithelial cells of ectopic endometria and then contributes to spread and implantation beyond uterine.

Methods:

Patients with endometrioma were cystectomized and epithelial cells of ectopic endometria were cultured. The invasion of epithelial cells and expression of interlukin-6 (IL-6) was evaluated at 24 h after the induction of TGFβ1 and after the stimulation of rCDH11. Epithelial cells were treated with TGFβ1, to evaluate the expression of the IL-6 genes.

Result:

CDH11 was preferentially expressed in the endometriotic epithelial cells compared to endometrial epithelial cells. TGFβ1 increased CDH11 expression in endometriotic epithelial cells. Furthermore, the stimulation by rCDH11 promoted invasion of endometriotic epithelial cells.

Conclusion:

These results suggested that CDH11 was involved in the invasion of endometriotic epithelial cells, which contribute to the development of endometriosis.

Key Words: CDH11; endometriosis; epithelial cells; TGFβ1

Introduction

Endometriosis, defined as the proliferation of endometrial tissue outside the uterine cavity, is one of the most common gynecologic disorders, affecting ~10% of all reproductive-age women and 20%–50% of women with chronic pelvic pain and/or infertility. Despite the high prevalence of the disease, optimal treatment of the disease remains challenging owing to the complexity of pathogenesis and diversity of symptoms.

Epithelial cells play a major role in invasion by contributing to endometriosis and they act as the main producers of key inflammatory mediators, such as TGFβ1[1]. Moreover, previous studies showed that TGFβ1 are involved in the modulation of epithelial cells in baboon endometriosis model[2] . Therefore, we hypothesized that TGFβ1 might induce CDH11 expression and inflammation in endometriosis, which may provide new insights into endometriosis diseases.

Cadherins are a group of transmembrane glycoproteins that mediate calcium-dependent homophilic cell to cell adhesion at adherent's junctions. During embryogenesis, cadherin dictate patterns of cell differentiation, morphogenesis, migration, and invasion, in part, through the regulation of epithelial-mesenchymal transition (EMT). Emerging studies

suggest a role for cadherin-11 (CDH11) in the process of cell invasion, corroborated by detecting increased CDH11 levels in epithelial cells[3, 4]. Further, epithelial breast cancer cells often up-regulate CDH11, which correlates with a highly invasive behavior. In fibroblasts cells, cadherin-11 plays an essential role in adhesion and inflammation[5]. Furthermore, CDH11 is also expressed in the epithelial mesenchymal transition of patients with rheumatoid arthritis[6]. Based on our previous study (data not shown), CDH11 have been suggested as an appealing concept for endometriosis. However, the role of CDH11 in the process of EMT and endometriosis has not been investigated.

Therefore, we further hypothesized that TGFβ1 might promote ectopic epithelial cells through potentiating CDH11 to aggravate invasion and inflammation. In this study, we explored whether TGFβ1 could upregulate cadherin-11 and promote inflammation and invasion in endometriosis.

Methods

Tissue Specimens

Human ectopic endometrial tissues were derived from ectopic endometrial tissues of patients with endometriosis (n=13). Human endometrial tissues were obtained from patients during hysterectomies for benign disease (n=3). All women experienced regular menstrual cycles and did not receive hormonal treatment for at least 3 months before surgery. The experimental procedures were approved by the Institutional Review Board of the University of Tokyo. Signed informed consent for the use of the endometrial tissue was obtained from each woman.

Histology and immunohistochemistry

Endometrioma and endometria were removed and fixed in 4% paraformaldehyde and embedded by paraffin. The embedded blocks were sectioned (5μm) and stained with H&E, and we histologically evaluated the endometriosis. Sections were subjected to antigen retrieval with immunosaver at 98 ˚C for 45 min. The sections were blocked with peroxidase for 15 min at room temperature and incubated overnight at 4˚C with cadherin-11 Abs (1:250, QK219821; Thermo). After extensive washing with PBS, the sections were incubated with liker at room temperature for 15 min and HRP-conjugated secondary Abs and visualized using diaminobenzidine (DakoCytomation, Denmark). Nuclei were counterstained with hematoxyline.

Cell Culture and stimulation

Human endometriotic epithelial cell line were derived from ovarian endometrioma as H1 and F3 and cultured as described previously[7]. Cultures of endometriotic epithelial cells between passage 28 and passage 36 were used for our experiments. The H1 and F3 cell line was cultured in phenol red free DMEM/F12 with 10 % FBS (Gibco) and 1 % penicillin/streptomycin at 37 °C under 10% CO2. Cells were treated with 5 ng/ml of TGFβ1 (AV6915101; R&D Systems) or recombinant CDH11 (ab192296; Abcam), respectively. After incubation with TGFβ1 for 6h, 12h, 24 h and 48h, the cells and culture medium was collected to measure the CDH11 and IL-6 levels. After incubation with rCDH11 for 6h, 12h, 24 h and 48h, the cells and culture medium was collected to measure the TGFβ1 and IL-6 levels.

Quantitative real-time PCR

Total RNA was isolated from cells with NucleoSpin Kit (MACHEREY-NAGEL) and converted to cDNA (ReverTra Ace RT kit, TOYOBO) according to the manufacturer's instructions. Quantitative RT-PCR (TOYOBO) was performed to analyze the levels of CDH11 and IL-6. A housekeeping gene GADPH was used as an internal standard for normalizing the relative mRNA expression.

The sequences of the commercially synthesized primers are as follows:

Human GADPH sense/antisense: 5'-ACCACAGTCCATGCCATCAC-3'/5'-TCCACCACCCTGTTGCTGTA-3';

Human CDH11 sense/antisense: 5'-CAAGCCACTTTCCAACCAGC-3'/5'-ACAATGACCAGGAGAATGACG-3';
Human IL-6, sense/antisense: 5'-CAATATTAGAGTCTCAACCCCCA-3'/5'-TGTTTTCTGCCAGTGCCTCT-3';
The following primers were designed with the Primer Premier 5.0 software and commercially synthesized.

Western blot analysis

Protein extraction and Western blotting were performed according to manufacturer's instructions. Antibodies to β-actin (1:1000, Santa Cruz) and Abs cadherin-11 (1:400, Thermo) were used. Bands were visualized by using an ECL Prime detection system (GE Healthcare). Actin served as a loading control.

IL-6 secretion assay

The IL-6 levels in the culture medium were quantified with an ELISA kit (R&D Systems) according to manufacturer's instructions.

Invasion assay

Culture medium was added into each well of 24-well plates, then matrigel coated transwells were inserted TGFβ1 (+) or TGFβ1 (−) and rCDH11 (+) or rCDH11 (−) were seeded on the top transwells (pore size is 8 μm) at 7×10^5/ml were seeded on each transwell. After 24h incubation, transwells were washed, fixed, and stained. Cells that migrated to the bottom side of membranes were counted in ten representative areas via microscope (×100 fold).

Statistical analysis

Statistical analyses were performed with SPSS 16.0 using a two-tailed Student t test. A value of $P < .05$ was considered statistically significant.

Results

Expression of CDH11 in endometrioma and endometria

To identify CDH11 expression between the endometrioma and endometrial tissues, we stained endometriosis and endometrial sections with CDH11 antibody. The endometriotic epithelial cells from endometrioma presented with a higher expression of CDH11 (Fig. 1).

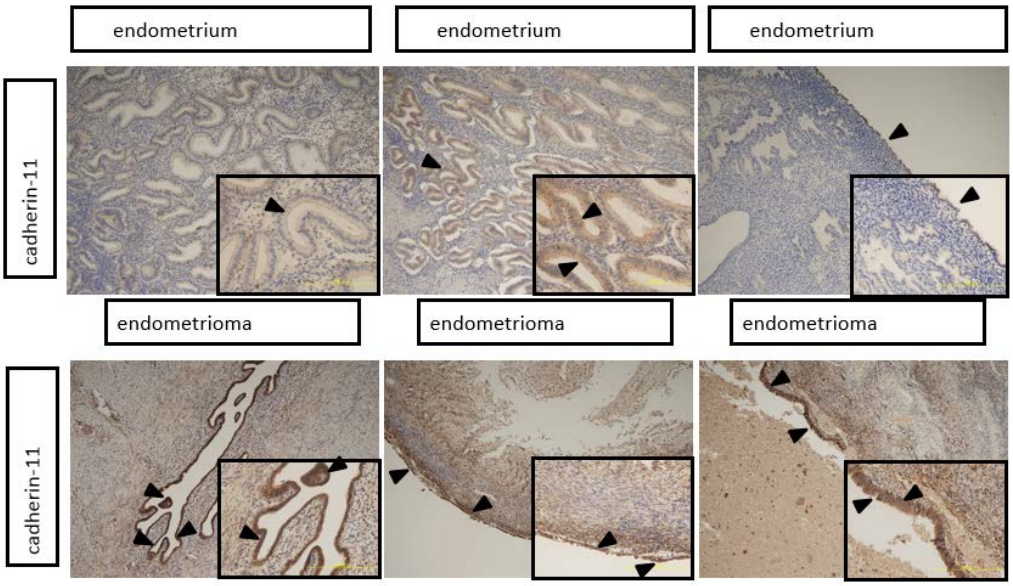

FIGURE 1. Immunohistochemistry of CDH11 in endometria and endometrioma. (A) CDH11 is expressed on the top of epithelial cells in endometria. (B) CDH11 is highly expressed on the top of ectopic epithelial cells in endometrioma.

TGFβ1 promoted upregulation of CDH11 in ectopic epithelial cells

In the previous literature[8], EMT appeared to exhibit adhesion abnormalities affected by TGFβ1 induction. We speculated that TGFβ1 might promote the invasion of epithelial cells by upregulation of CDH11. To verify our hypothesis, we stimulated two epithelial cell lines with TGFβ1, which is one of the key signals of TGFβ1Smad3 signaling pathway[2]. As shown in Fig. 2, after stimulated with TGFβ1, the expression of CDH11 was increased in mRNA and protein level.

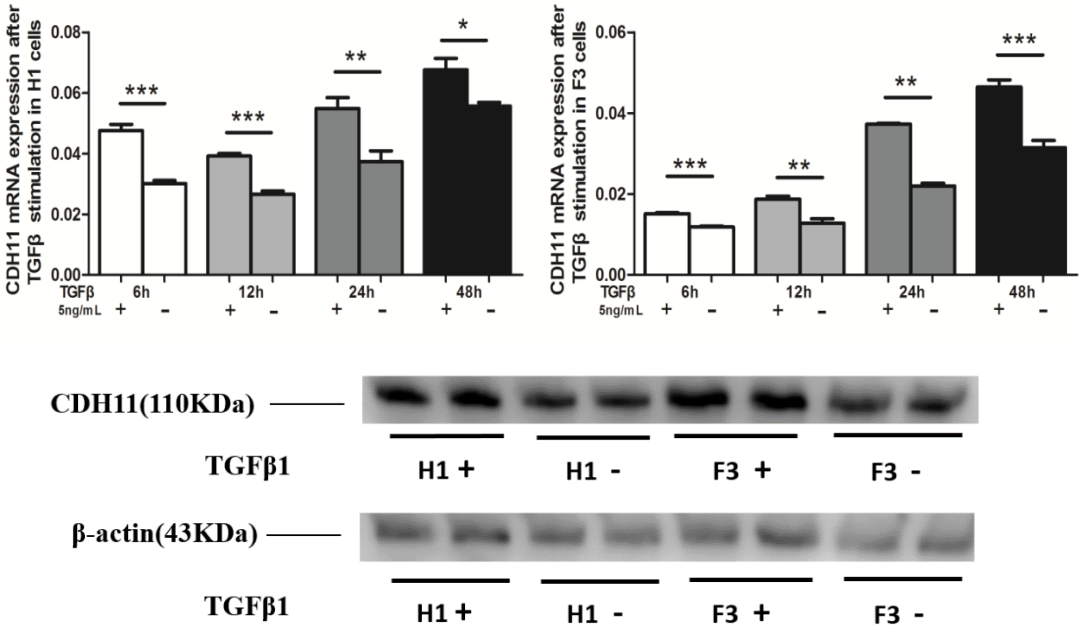

FIGURE 2. TGFβ1 promoted CDH11 in epithelial cells. (A) Expression of CDH11 in H1 and F3 cells. The mRNA expressions were assessed by real-time PCR and normalized to GAPDH. Error bars are standard error. (B) Protein level of CDH11 in H1 and F3 cells detected by Western Blot. Cells were treated with increasing time course of 5mg/ml TGFβ1 *p<0.05, **p<0.01, ***p<0.001.

TGFβ1 promoted epithelial cells in inflammation by upregulating IL6

Cadherin-11 plays an essential role in EMT [9]. We speculated that cadherin-11 might be involved in TGFβ1-mediated proinflammation activation. As shown in Fig. 3, two epithelial cell lines stimulated with TGFβ1 also time-dependently upregulated IL-6 mRNA expression. And the protein level of IL-6 was increased in the ectopic epithelial cells of endometrioma. Therefore, TGFβ1 enhanced the expression of IL-6 in the ectopic epithelial cells of endometrioma.

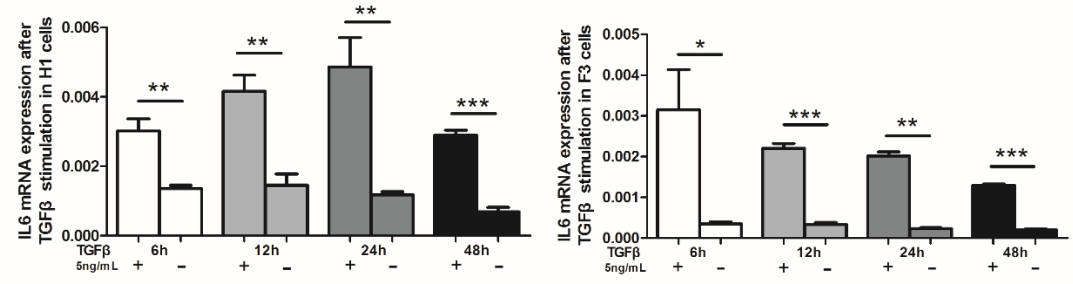

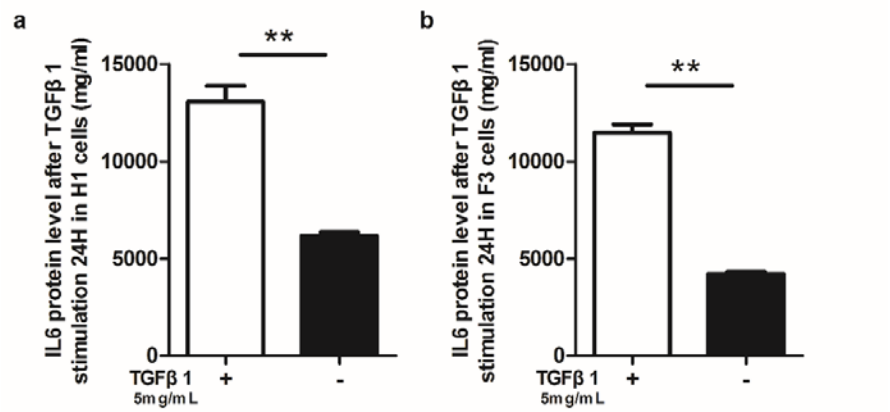

FIGURE 3. TGFβ1 promoted IL6 in epithelial cells. (A) Expression of IL6 in H1 and F3 cells. The mRNA expressions were assessed by real-time PCR and normalized to GAPDH. Error bars are standard error. (B) Protein level of IL6 in H1 and F3 cells detected by ELISA. Cells were treated with increasing time course of 5mg/mL TGFβ1 *p<0.05, **p<0.01, ***p<0.001.

CDH11 promoted epithelial cells in invasion

At 24 h after induction of TGFβ1, invasion assay showed the more epithelial cells invasion (Fig. 5A). To verify the effect of cadherin-11 on ectopic epithelial cells during invasion of endometriosis, we performed invasion of rCDH11. At 24 h after induction of rCDH11, invasion assay showed the more epithelial cells invasion (Fig. 5B).

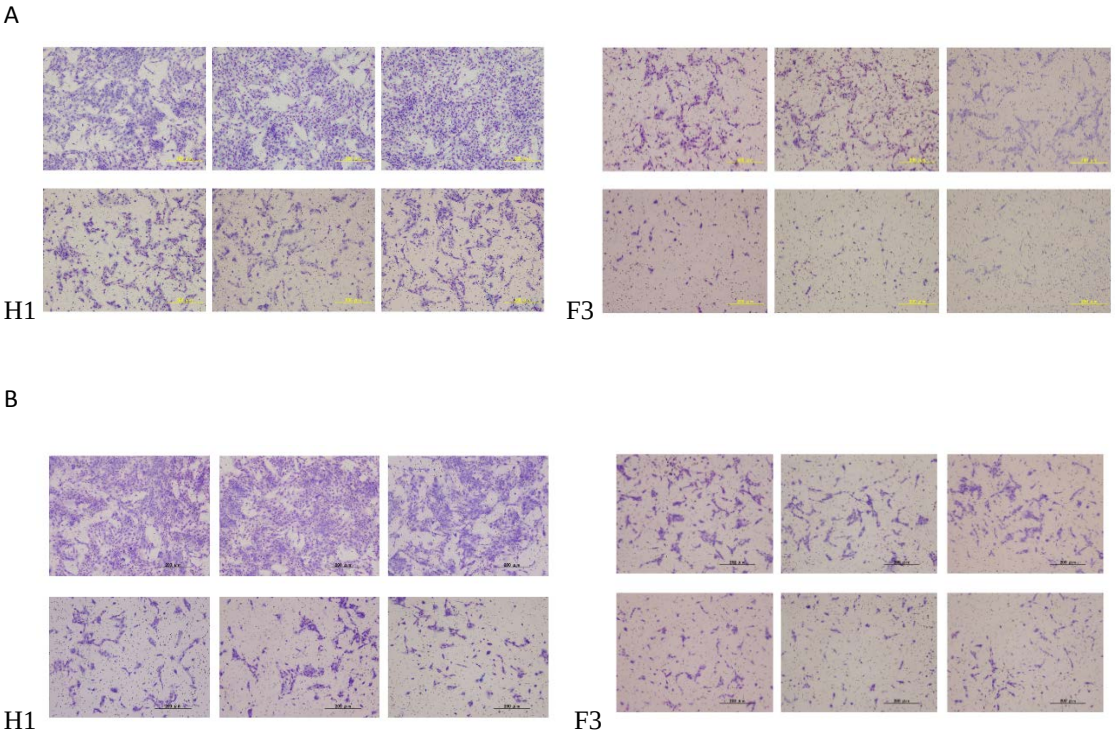

FIGURE 4. Invasive capacity was evaluated after stimulated with TGFβ1 and CDH11 24h, respectively. 7×10^5 cells from each group were seeded on the top chamber of 24-well plate culture inserts coated with 20 μL of matrigel in duplicate. Cells were cultured for additional 24 h. Invaded cells on the bottom of insert were stained and quantified. (A)After stimulated with TGFβ1, H1 and F3 were more invaded. (B) After stimulated with rCDH11, H1 and F3 were more invaded.

Discussion

In this study, we provided several lines of evidence to show that TGFβ potentiates cadherin-11 expression in ectopic endometrial epithelial cell line, thereby contributing to epithelial cell invasion and aggravating inflammation. First, CDH11 is highly expressed in the epithelial cells of endometrioma comparing to normal endometria. Second, TGFβ1 upregulated the expression of CDH11 and increased the expression of IL-6 in a time-dependent manner. Third, invasion results demonstrated that TGFβ1 and CDH11 could increase the number of infiltrated epithelial cells with a predominant profile of proinflammatory in endometriosis.

Cadherins are a group of transmembrane glycoproteins that mediate calcium-dependent homophilic cell-to-cell adhesion at adherent junctions[10]. During embryogenesis, cadherins dictate patterns of cell differentiation, morphogenesis, migration, and invasion, in part, through the regulation of EMT[11]. CDH11 is a classical cadherin adhesion molecule that mediates homophilic cell-to-cell adhesion[12-14]. CDH11 is involved in embryogenesis, bone formation, tumor invasion and metastasis. mRNA transcripts for CDH11 are detected in placenta, brain, lung, and heart [15, 16]. CDH11 could be involved in cell and matrix recognition that may facilitate cell motility and may also be essential for the loose aggregation of cell types that is necessary in tissue morphogenesis. These hypotheses are supported by several observations. The expression pattern of CDH11 was reported to be mainly restricted to mesenchymal tissues rather than to epithelia[17, 18]. However, some type of epithelial cancer cells has been reported to express CDH11[19-21]. Our result also showed CDH11 preferentially expressed in the epithelial cells of endometrioma. The expression of a mesenchymal cadherin CDH11 on epithelial cells may represent an EMT process in endometriosis as well as these cancer cells. Previously, the epithelia of endometrioma was reported to express lower cytokeratin and higher mesenchymal marker S100A4, which represent EMT process was involved in the pathogenesis of endometriosis[22]. Our result may be in line with this report. Previously, we found that CDH11 differently expressed between normal endometrial epithelial cells and ectopic epithelial cells by transcriptome analysis (data not shown). Because CDH11 is expressed primarily on epithelial cell in endometriosis, these findings suggest a key role for epithelial cell in invasion in endometrioma[23]. We postulate that CDH11 plays an important role in the pathogenesis of endometriosis.

As CDH11 has not been noted on leukocytes[24, 25], these findings support a role for epithelial cell in inflammatory mechanisms. Although epithelial cells are not typically considered to be inflammatory cells, many studies have revealed their capacity to produce inflammatory factors that may be important in endometriosis such as cytokines. Previous study showed that mice deficient in CDH11 showed markedly reduced damage to the articular cartilage[25]. Unexpectedly, CDH11-directed therapeutics also markedly reduced synovial inflammation[25].

Here, we show that TGFβ1-mediated activation of epithelial cell results in their production of CDH11, suggesting that CDH11 may be an important modulator of epithelial cell in endometriosis. IL-6 is known to be a key cytokine in endometriosis on the basis of its efficacy in clinical trials[26], and IL-6 is reported to plays a role in endometriosis-related pelvic inflammation which is increased in peritoneal fluid in women with endometriosis[27].

CDH11 is also associated with a mesenchymal and invasive phenotype. Namely, CDH11 expression correlates with developmental cell migration [28] and promotes invasive behavior of synovial fibroblasts[24]. Furthermore, epithelial breast cancer cells often up-regulate CDH11, which correlates with a highly invasive behavior [21]. However, the role of CDH11 in the process of EMT and endometriosis has not been investigated. In our study, the epithelial cell increased to invade after TGFβ1 and rCDH11 stimulated. Together, our findings reveal that CDH11 plays a critical role in evoking epithelial cell invasion and inflammatory factors that may contribute to endometriosis.

In conclusion, TGFβ1 promotes epithelial cell through CDH11 to aggravate invasion and inflammation. These results

may improve our current understanding of the clinical predominance in endometriosis patients. We found CDH11 may actually enhance epithelial cell invasiveness and may be a new target for endometriosis treatment.

References

[1] Gu H, Mickler EA, Cummings OW, et al. Crosstalk between TGF-beta1 and complement activation augments epithelial injury in pulmonary fibrosis. FASEB journal : official publication of the Federation of American Societies for Experimental Biology. 2014; 28: 4223-34.

[2] Zhang Q, Duan J, Olson M, Fazleabas A, Guo SW. Cellular Changes Consistent With Epithelial-Mesenchymal Transition and Fibroblast-to-Myofibroblast Transdifferentiation in the Progression of Experimental Endometriosis in Baboons. Reprod Sci. 2016; 23: 1409-21.

[3] MacCalman CD, Furth EE, Omigbodun A, Bronner M, Coutifaris C, Strauss JF, 3rd. Regulated expression of cadherin-11 in human epithelial cells: a role for cadherin-11 in trophoblast-endometrium interactions? Developmental dynamics : an official publication of the American Association of Anatomists. 1996; 206: 201-11.

[4] Chen GT, Getsios S, MacCalman CD. Cadherin-11 is a hormonally regulated cellular marker of decidualization in human endometrial stromal cells. Molecular reproduction and development. 1999; 52: 158-65.

[5] Chang SK, Noss EH, Chen M, et al. Cadherin-11 regulates fibroblast inflammation. Proceedings of the National Academy of Sciences of the United States of America. 2011; 108: 8402-7.

[6] Zhao C, Zhang L, Kong W, et al. Umbilical Cord-Derived Mesenchymal Stem Cells Inhibit Cadherin-11 Expression by Fibroblast-Like Synoviocytes in Rheumatoid Arthritis. Journal of immunology research. 2015; 2015: 137695.

[7] Izumi G, Koga K, Nagai M, et al. Cyclic stretch augments production of neutrophil chemokines, matrix metalloproteinases, and activin a in human endometrial stromal cells. Am J Reprod Immunol. 2015; 73: 501-6.

[8] Hahn JM, McFarland KL, Combs KA, Supp DM. Partial epithelial-mesenchymal transition in keloid scars: regulation of keloid keratinocyte gene expression by transforming growth factor-beta1. Burns & trauma. 2016; 4: 30.

[9] Zhao N, Sun H, Sun B, et al. miR-27a-3p suppresses tumor metastasis and VM by down-regulating VE-cadherin expression and inhibiting EMT: an essential role for Twist-1 in HCC. Scientific reports. 2016; 6: 23091.

[10] Wheelock MJ, Johnson KR. Cadherins as modulators of cellular phenotype. Annual review of cell and developmental biology. 2003; 19: 207-35.

[11] Kokkinos MI, Murthi P, Wafai R, Thompson EW, Newgreen DF. Cadherins in the human placenta--epithelial-mesenchymal transition (EMT) and placental development. Placenta. 2010; 31: 747-55.

[12] Takeichi M. Cadherins: a molecular family important in selective cell-cell adhesion. Annual review of biochemistry. 1990; 59: 237-52.

[13] Gumbiner BM. Regulation of cadherin-mediated adhesion in morphogenesis. Nature reviews Molecular cell biology. 2005; 6: 622-34.

[14] Takeichi M. Cadherin cell adhesion receptors as a morphogenetic regulator. Science. 1991; 251: 1451-5.

[15] Shibata T, Ochiai A, Gotoh M, Machinami R, Hirohashi S. Simultaneous expression of cadherin-11 in signet-ring cell carcinoma and stromal cells of diffuse-type gastric cancer. Cancer letters. 1996; 99: 147-53.

[16] Kawaguchi J, Takeshita S, Kashima T, Imai T, Machinami R, Kudo A. Expression and function of the splice variant of the human cadherin-11 gene in subordination to intact cadherin-11. Journal of bone and mineral research : the official journal of the American Society for Bone and Mineral Research. 1999; 14: 764-75.

[17] Kimura Y, Matsunami H, Inoue T, et al. Cadherin-11 expressed in association with mesenchymal morphogenesis in the head, somite, and limb bud of early mouse embryos. Developmental biology. 1995; 169: 347-58.
[18] Hoffmann I, Balling R. Cloning and expression analysis of a novel mesodermally expressed cadherin. Developmental biology. 1995; 169: 337-46.
[19] Tomita K, van Bokhoven A, van Leenders GJ, et al. Cadherin switching in human prostate cancer progression. Cancer research. 2000; 60: 3650-4.
[20] Markus MA, Reichmuth C, Atkinson MJ, et al. Cadherin-11 is highly expressed in rhabdomyosarcomas and during differentiation of myoblasts in vitro. The Journal of pathology. 1999; 187: 164-72.
[21] Pishvaian MJ, Feltes CM, Thompson P, Bussemakers MJ, Schalken JA, Byers SW. Cadherin-11 is expressed in invasive breast cancer cell lines. Cancer research. 1999; 59: 947-52.
[22] Matsuzaki S, Darcha C. Epithelial to mesenchymal transition-like and mesenchymal to epithelial transition-like processes might be involved in the pathogenesis of pelvic endometriosis. Hum Reprod. 2012; 27: 712-21.
[23] Row S, Liu Y, Alimperti S, Agarwal SK, Andreadis ST. Cadherin-11 is a novel regulator of extracellular matrix synthesis and tissue mechanics. Journal of cell science. 2016; 129: 2950-61.
[24] Valencia X, Higgins JM, Kiener HP, et al. Cadherin-11 provides specific cellular adhesion between fibroblast-like synoviocytes. The Journal of experimental medicine. 2004; 200: 1673-9.
[25] Lee DM, Kiener HP, Agarwal SK, et al. Cadherin-11 in synovial lining formation and pathology in arthritis. Science. 2007; 315: 1006-10.
[26] Kashanian M, Sariri E, Vahdat M, Ahmari M, Moradi Y, Sheikhansari N. A comparison between serum levels of interleukin-6 and CA125 in patients with endometriosis and normal women. Medical journal of the Islamic Republic of Iran. 2015; 29: 280.
[27] Jin CH, Yi KW, Ha YR, et al. Chemerin Expression in the Peritoneal Fluid, Serum, and Ovarian Endometrioma of Women with Endometriosis. Am J Reprod Immunol. 2015; 74: 379-86.
[28] Borchers A, David R, Wedlich D. Xenopus cadherin-11 restrains cranial neural crest migration and influences neural crest specification. Development. 2001; 128: 3049-60.

作成日：2017 年 1 月 30 日

Potentiating activity of herbal derived tetrandrine on glucocorticoid effect and its action mechanism in mitogen-activated human peripheral blood mononuclear cells

生薬成分テトランドリンによる活性化ヒト末梢血単核細胞に対するグルココルチコイド増強作用とその作用機序

研究者氏名　許　文成（第 38 期笹川医学研究者）

中国所属機関　湖北省中医院薬局

日本研究機関　東京薬科大学薬学部和漢薬物学講座

指導責任者　山田　陽城　教授，平野　俊彦　教授

共同研究者名　杉山　健太郎　准教授，田中　祥子　助教

Abstract:

Glucocorticoids (GC) play significant roles in treatments of inflammatory and autoimmune diseases. Some patients show a poor or absent response even to high doses of GC. The purpose of this study was to find GC potentiating constituent in Chinese and Japanese traditional medicine, and whether the active substance combined with GC could be a new treatment strategy to resolve GC resistance. Information on GC sensitivity was usually obtained through mitogen-activated human peripheral blood mononuclear cells (PBMCs) in cell culture procedures. Thus, PBMCs was chosen as a model to study the immunosuppressive effect and the underlying action mechanisms. The significant synergic effect was discovered in the combination of tetrandrine (TET) from a medicinal plant, *Stephania tetrandra* S. Moore and methylprednisolone (MP). TET decreased the IC_{50} value of MP significantly, but it showed little toxic effect on the concanavalin A-activated PBMCs. Both TET and MP inhibited the secretion of pro-inflammatory cytokines TNFα and IL-6 significantly and the synergic inhibitory effect could be observed. TET and/or MP did not increase the percentage of $CD4^+$ $CD25^+$ $Foxp3^+$ regulatory T cells in $CD4^+$ T cells. However TET with or without MP significantly inhibited the function of drug efflux pump P-glycoprotein 170 of $CD4^+$, $CD8^+$ T cells and lymphocytes. TET suppressed the phosphorylation of mitogen-activated protein kinase (MAPK) and this effect was potentiated by MP. These TET effects were suggested to be beneficial for improving the immunosuppressive efficacy of GC. GC combined with TET could be a new therapeutic approach to resolve GC-resistance via inhibiting the function of P-glycoprotein and blocking MAPK signaling pathway from but not affecting on $CD4^+$ $CD25^+$ $Foxp3^+$ regulatory cells.

Key Words:

tetrandrine, glucocorticoid pharmacodynamics, P-glycoprotein, mitogen-activated protein kinase, peripheral blood mononuclear cells, cytokine

Introduction:

GC play significant roles in treatments of inflammatory and autoimmune diseases based on their anti-inflammatory and immunosuppressive efficacies. A considerable number of patients with these diseases, especially with chronic inflammatory or autoimmune diseases, show a poor or absent response even to high doses of GC, GC resistance or insensitivity represents an important barrier for the effective treatment of these patients [1]. New therapeutic approaches to increase the GC sensitivity is, thus, urgent to be developed for GC resistant patients.

Multiple factors regulate GC sensitivity and the ultimate responses to GC, which include the drug efflux pump P-glycoprotein 170 encoded by the multidrug-resistance gene 1 and the post-translational modification of the GC receptor. P-glycoprotein transports GC out of cells, thereby reducing intracellular GC concentration, permitting blunted or absent efficacies despite high concentration of GC that otherwise would give risk of adverse events [1]. The phosphorylation *via* MAPK modulates trafficking of GC receptor and also impairs its transcriptional activity [1, 2].

In the present study, we discovered that TET (Figure 1) which was derived from a medicinal plant *Stephania tetrandra* S. Moore potentiated GC sensitivity *via* inhibition of P-glycoprotein function and MAPK signaling pathway by using PBMC system *in vitro*.

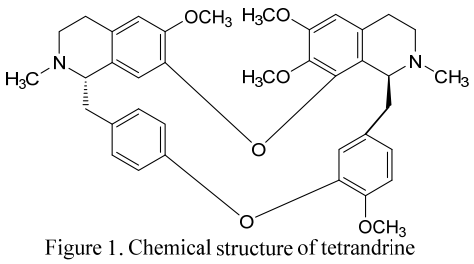

Figure 1. Chemical structure of tetrandrine

Methods

1. *PBMC proliferation*: Twenty milliliters of venous blood were taken from healthy subjects between 9:00 and 11:00 in the morning and heparinized. Then PBMCs were separated and suspended with RPMI 1640 medium to a final density of 1×10^6 cells/mL. After the culture with drugs, 10 μL of WST-8 assay reagent solution were added to each well, and the plate was incubated for another 3 h. The result was calculated by (Test-Blank)/(Control-Blank)×100%.

2 *Functional assays for P-glycoprotein*. P-glycoprotein function of PBMCs was measured *in vitro* by Rhodamine 123 efflux assay using flow cytometry.

3. *Quantification of human cytokines*. The concentrations of cytokines were measured with beads-array procedures using the Human Th1/Th2/Th17 Cytokine Kit, followed by flow cytometry according to the instructions of BD Biosciences.

4. *$CD4^+$ $CD25^+$ $Foxp3^+$ regulatory T cell analysis.* The analysis was carried out according to the manufacturer's instructions (BD Biosciences). The data were analyzed with FACSCanto ™ II (BD Biosciences), using BD FACSDiva™ software. $CD4^+$ cells in the lymphocyte fraction were gated, and the percentages of $CD4^+$ $CD25^+$ $Foxp3^+$ cells, as Treg cells, in the $CD4^+$ cell fraction were calculated

5. *Assessment of phosphorylation of MAPK isoforms.* Phosphorylation of ERK1/2, P38 and JNK as indicative of mitogen-activated protein kinase was determined using Cell Lysates ELISA kits (Ray Biotech Inc, USA) according to the manufacturer's instructions.

Results

1. Effects of MP in the presence or absence of TET on mitogen-activated proliferation of PBMCs. MP dose-dependently inhibited the PBMC proliferation, and TET significantly potentiated the suppressive effects of MP at the doses of 0.05 and 0.5 ng/mL as shown in Figure 2A ($P<0.05$). The synergistic effects from the different concentrations of TET for MP were obvious according to the IC_{50} values of MP ($P<0.01$, Figure 2B). However, TET at 0.3 to 300 nM without MP exhibited no or little toxic effect (Figure 2C).

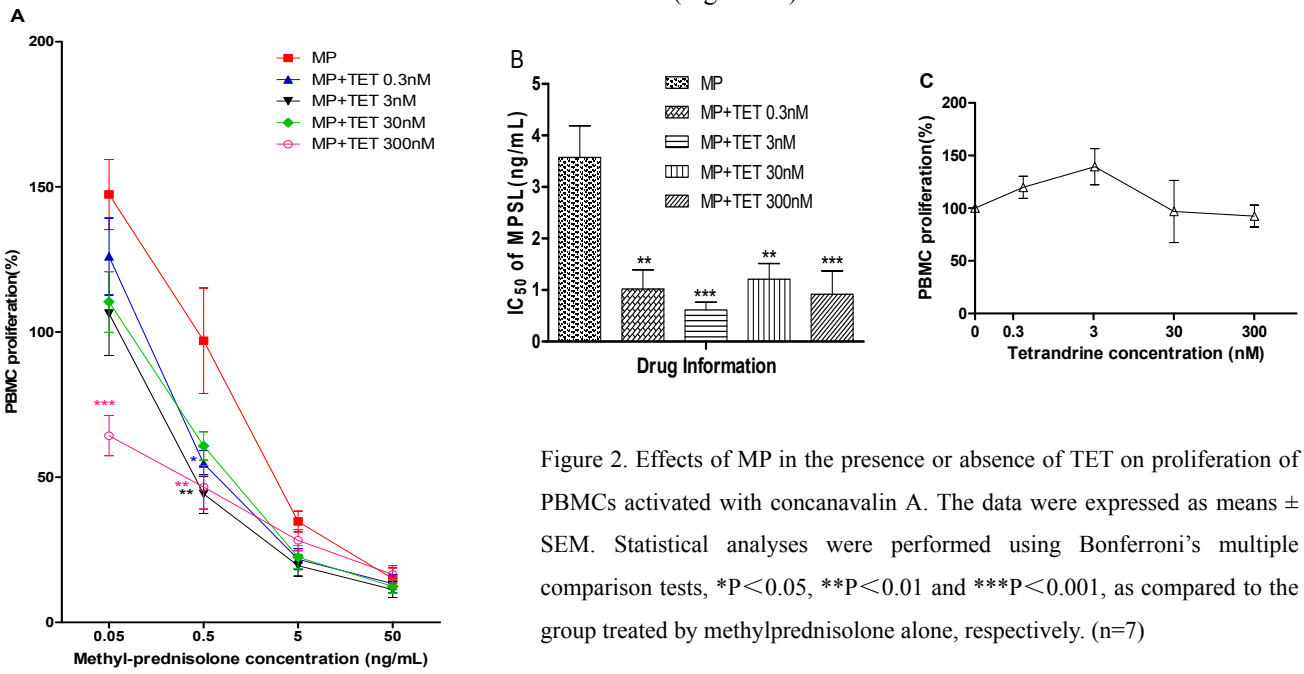

Figure 2. Effects of MP in the presence or absence of TET on proliferation of PBMCs activated with concanavalin A. The data were expressed as means ± SEM. Statistical analyses were performed using Bonferroni's multiple comparison tests, *$P<0.05$, **$P<0.01$ and ***$P<0.001$, as compared to the group treated by methylprednisolone alone, respectively. (n=7)

2. *Effects of TET in the presence or absence of MP on P-glycoprotein function of PBMCs.* As shown in Figure 3A, 5 μM of verapamil, the positive P-glycoprotein blocker, increased the accumulation of Rhodamine 123, which indicated to decrease the intracellular dye efflux of $CD4^+$ T cells, $CD8^+$ T cells and lymphocytes significantly and thus, inhibit the P-glycoprotein function strongly. After treatment with TET, the Rhodamine 123 accumulation also increased significantly by 300 nM and 3 μM of TET ($P<0.001$, Figure 3A). 300 nM of TET exhibited similar inhibitory ability

when comparing with 5 μM of verapamil. However, as shown in Figure 3B, 0.5 ng/mL of MP had little effect on P-glycoprotein function of $CD4^+$ T cells, $CD8^+$ T cells and lymphocytes. Meanwhile, verapamil or TET in the presence of 0.5 ng/mL of MP blocked P-glycoprotein efflux obviously.

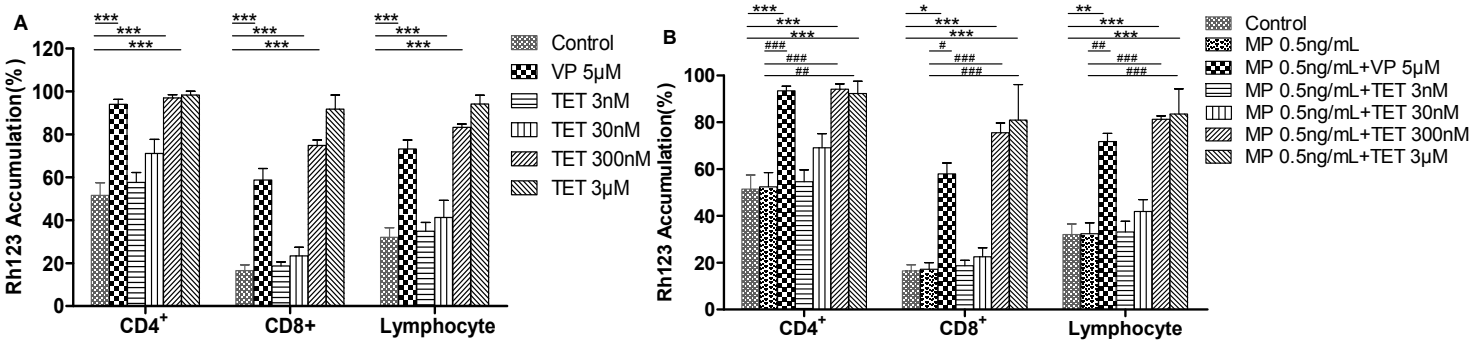

Figure 3. Rhodamine 123 accumulation in the PBMCs by TET. The results were expressed as means ± SEM. Statistical analyses were performed using Bonferroni's multiple comparison tests, $^{*}P<0.05$, $^{**}P<0.01$ and $^{***}P<0.001$, as compared to the group without drugs, respectively. $^{\#}P<0.05$, $^{\#\#}P<0.01$ and $^{\#\#\#}P<0.001$, as compared to the group treated with methylprednisolone alone, respectively. (n=3)

3. ***Effects of MP in the presence or absence of TET on cytokine production from mitogen-activated PBMCs.*** Both tetrandrine and methylprednisolone showed the similar ability to repress Th1/Th2/Th17 related cytokine productions. For pro-inflammatory cytokines IL-6 and TNF-α, the strong synergic inhibitory effects of tetrandrine combined with methylprednisolone could be observed ($P<0.05$, Figure 4). However the results of other cytokines did not show synergic efficacy (data not shown).

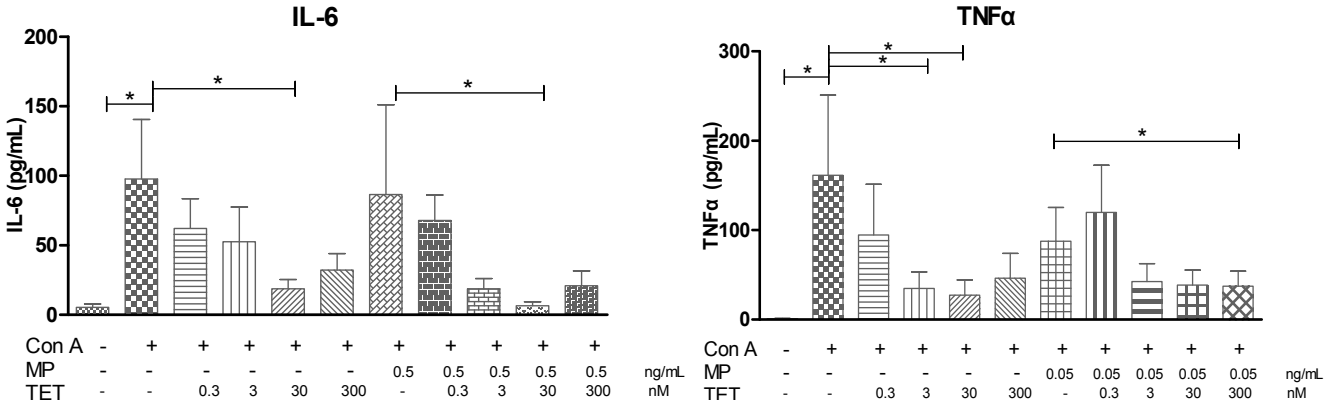

Figure 4. Cytokine concentrations in the supernatant of T-cell mitogen-activated PBMCs treated with TET and/or MP. Averaged results obtained using peripheral blood mononuclear cells from 7 healthy subjects were shown (± SEM). Statistical analyses were performed using Wilcoxon matched-pairs signed rank tests to analyze the differences between each groups.

4. ***Effects of MP in the presence or absence of TET on the frequency of $CD4^+$ $CD25^+$ $Foxp3^+$ Treg cells in mitogen-activated PBMCs.*** TET, MP and their combination tended to decrease the percentages of $CD4^+$ $CD25^+$ $Foxp3^+$ Treg cells in $CD4^+$ cells in lymphocytes, but the changes were not statistically significant (Figure 5).

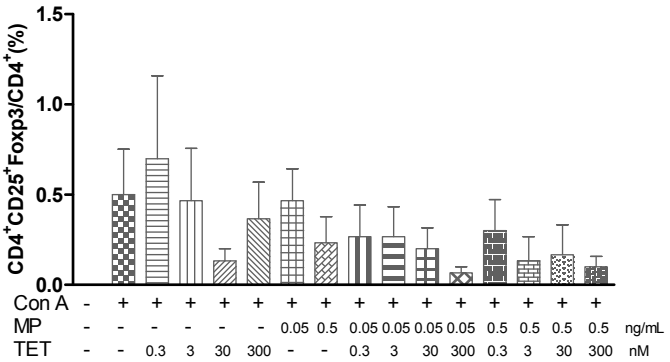

Figure 5. Flow cytometric analysis of $CD4^+$ $CD25^+$ $Foxp3^+$ Treg cells in concanavalin A-stimulated PBMCs treated with TET and/or MP. The data were indicated as the mean ± SEM. Statistically significant changes, as compared to PBMCs treated with concanavalin A without drugs, were not observed using Wilcoxon matched-pairs signed rank tests. (n=3)

5. ***Effect of MP in the presence or absence of TET on phosphorylation of MAPK isoforms in mitogen-activated PBMCs.*** Relative phosphorylation of ERK1/2 and P38 increased by the stimulation with concanavalin A for 5 min. MP at concentration of 0.5 ng/mL tended to repress the ERK1/2 activity. Meanwhile, 3 μM of TET suppressed the phosphorylation of ERK1/2, though the effect was not statistically significant (Figure 6A). The synergic inhibitory effect by the combination of MP (0.5 ng/mL) with TET (3 μM) was observed significantly ($P<0.05$) when comparing with the group treated by MP alone. Similarly, the tendency of synergic suppressing effect on P38 was observed by the same combination of MP with TET, though the effect was not statistically siginigicant. (Figure 6B). On the other hand, concanavalin A did not stimulate significantly the phosphorylation of JNK by 15 min (data not shown).

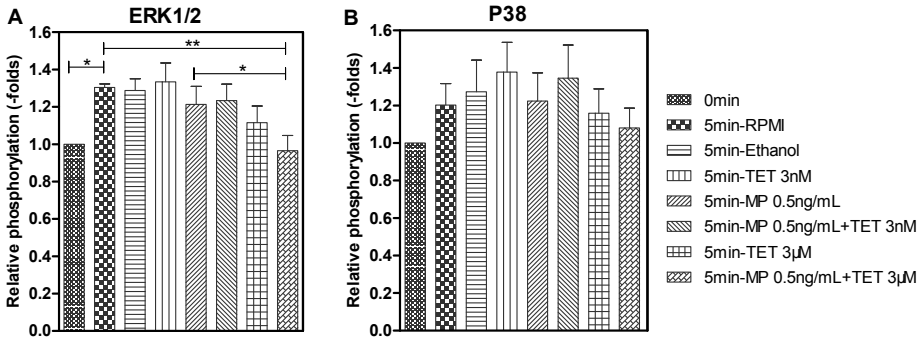

Figure 6. Effect of MP in the presence or absence of TET on phosphorylation of MAPK isoforms in concanavalin A- activated PBMCs.

Discussion

Our results suggested that TET, even at the lowest concentration of 0.3 nM, increased the sensitivity of the mitogen-activated PBMCs to the proliferation-suppressing efficacy of MP by decreasing the IC_{50} value of the drug significantly (Figure 2B). However, TET itself (≤300 nM) showed no toxic effect on the ability of normal PBMCs (Figure 2C). TET (≥300 nM) significantly enhanced the accumulation of Rhodamine 123 in $CD4^+$ T cells, $CD8^+$ T cells and lymphocytes in PBMCs of healthy subjects (Figure 3A). TET with or without MP exhibited the similar tendency of the inhibiting effect, suggesting that MP had little influence on the inhibitory effect of tetrandrine (Figure 3B). Considering the function of inhibiting P-glycoprotein by TET, 300 nM of TET significantly potentiated 0.05 and 0.5 ng/mL of MP inhibitory activity on T-cell proliferation (Figure 2A). Both TET and MP inhibited the pro-inflammatory cytokines TNFα and IL-6 significantly. In the present study, we showed that the combination of TET

and MP shows stronger inhibitory effect on pro-inflammatory cytokines TNFα and IL-6 than MP alone. (Figure 4), which might account for the synergic effect of TET for MP.

Either TET or combination of TET and MP did not increase but rather decreased the percentage of $CD4^+$ $CD25^+$ $Foxp3^+/CD4^+$ cells (Figure 5). This result was also consistent with the effect of TET to decrease the Treg related cytokine IL-10 production (data not shown).

TET at 3 μM was potent of synergistically inhibiting both ERK1/2 and P38 when combining with 0.5 ng/mL MP. For this reason, TET is an ideal candidate to increase the sensitivity of activated PBMCs to GCs *via* suppression of MAPK-NF-κB pathways, which was consistent with our results from the PBMCs proliferation assay shown in Figure 2. As mentioned above, secretion of the pro-inflammatory cytokine IL-6 was inhibited significantly by TET and/or MP, which means that IL-6/ERK1/2 cascades can be other possible action target for TET to decrease the IC_{50} value of MP, since IL-6 was reported to stimulate phosphorylation of ERK1/2 (Figure 7) [3].

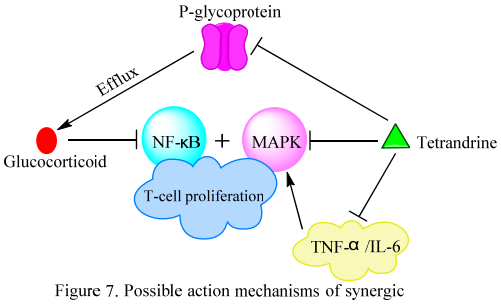

Figure 7. Possible action mechanisms of synergic effect of TET to potentiate GC pharmacodynamics in immune cells.

In conclusion, these effects of TET were suggested to be beneficial for treatment of GC-resistant patients, and thus GC combined with TET could be a new therapeutic approach to resolve GC-resistance.

Reference

[1]. Barnes, P.J. and I.M. Adcock, Glucocorticoid resistance in inflammatory diseases[J]. Lancet, 2009. **373**(9678):1905.

[2]. Quax, R.A., L. Manenschijn, J.W. Koper, et al., Glucocorticoid sensitivity in health and disease[J]. Nat. Rev. Endocrinol., 2013. **9**(11):670.

[3]. Heinrich, P.C., I. Behrmann, S. Haan, et al., Principles of interleukin (IL)-6-type cytokine signalling and its regulation[J]. Biochem. J., 2003. **374**(1):1.

注：本研究は 2017 年 03 月 25 日「日本薬学会第 137 年会（仙台）」にて口演発表する予定

作成日：2017 年 02 月 25 日

A role of the Ubiquitin-modifying enzyme A20 in regulatory T cells

制御性 T 細胞におけるユビキチン修飾酵素 A20 の役割

研 究 者 氏 名　陳　富強（第 38 期笹川医学研究者）
中国所属機関　山東省血液センター
日本研究機関　広島大学大学院医歯薬保健学研究院
指 導 責 任 者　菅野　雅元　教授
共同研究者名　郭　芸　助教

Abstract:

A20, also known as TNFAIP3 (tumor necrosis factor α-induced protein 3), is a ubiquitin-modifying enzyme, which has a key role in the negative regulation of inflammation and innate immune response. Previous studies reported that A20 is highly expressed in lymphoid organs, such as thymus, spleen and lymph nodes. However, its function in T cells, especially in regulatory T cells (Treg), is still unclear. To assess this, we crossed A20 floxed mice with CD4-Cre Tg mice. As a result, we found that there is no clear defects appeared in the conventional T cell development in A20 conditional knockout mice. However, we noticed that the frequency and cell number of $Foxp3^+$ regulatory T cells were significantly increased in both thymus and periphery of A20 deficient mice. A20 deficient Treg cells in periphery were mostly derived from thymus (tTreg), and exhibited the normal suppressive function as control in vivo. Moreover, this increase may be related with the enhanced IL-2 signal, but not be caused by the cell proliferation and death. These results illustrate that A20 plays an important role in regulatory T cells and its survival, and more precise mechanisms still needs further study.

Key Words:

A20, regulatory T cells, Foxp3, IL2, adaptive immunity

Introduction:

Regulatory T (Treg) cells are a specialized subset of immunosuppressive $CD4^+$ T cells which modulate the immune system, maintain tolerance to self-antigens, and prevent autoimmune disease by suppressing excessive and aberrant immune reactions harmful to the host [1]. They can suppress a variety of immune cells including B cells, NK cells, NKT cells, $CD4^+$, and $CD8^+$ T cells, as well as monocytes and dendritic cells (DCs), and act as critical negative regulators of inflammation in various biological contexts, including infection, metabolic disease, tissue repair, and cancer[2]. Treg cells express the biomarkers CD4, CD25, CTLA-4, GITR, LAG-3, CD127 and Foxp3, and are thought to be derived from the same lineage as naïve CD4 cells. While the majority of Treg cells develop in the thymus (tTreg: agonist - selected T cell lineages in thymus), some are induced from naïve $CD4^+$ T cells in the periphery (pTreg). In order for Treg cells to exert their regulatory functions, constitutive expression of the transcription factor Foxp3 is essential. Foxp3 controls a substantial part of Treg cell development and function. There is accumulating evidence that concurrent induction of Treg-specific epigenetic changes and Foxp3 expression is crucial for lineage specification and functional stability of Treg cells. The pivotal roles of Foxp3 in Treg cell function and development are best illustrated by the

manifestation of multi-organ autoimmune inflammation in Foxp3-deficient Immunodysregulation Polyendocrinopathy Enteropathy X-linked syndrome (IPEX) patients and Scurfy mice.

Ubiquitination, a post-translational modification of proteins, has emerged as an omnipresent factor at all levels of transcriptional regulation, including the activation of NF-κB [5]. Ubiquitin is covalently attached to other proteins in a highly regulated process involving the stepwise activity of an E1 ubiquitin activating enzyme, E2-conjugating enzymes and E3 ubiquitin ligases. The latter confer substrate specificity and enable the attachment of ubiquitin to a specific lysine in the target substrate.

A20 is an ubiquitin-editing enzyme that ensures the transient nature of inflammatory signaling pathways induced by cytokines like TNF-α and IL-1 or pathogens via Toll-like receptor (TLR) pathways. A20 has been demonstrated to remove K63-linked ubiquitin chains from specific target substrates in the NF-kB signaling pathway, thus negatively regulating NF-κB activation which is central to many cellular processes. Therefore, tight regulation of NF-κB signaling pathways is an absolute requirement. One of the proteins known to play a key role in the termination of NF-κB signaling is A20 [3].

Multiple studies over the past few years have identified A20/TNFAIP3 as a susceptibility locus for human inflammatory and autoimmune pathology, including rheumatoid arthritis (RA), systemic lupus erythematosus (SLE), inflammatory bowel disease (IBD), psoriasis, type I diabetes, coronary artery disease, rheumatic heart disease, and systemic sclerosis[4]. However, A20's function in T cells, especially in regulatory T cells, is still unclear. In this study, we want to show that the relationship between expression of A20 and Treg proliferation and apoptosis.

Methods:

1. We crossed A20 floxed mice with CD4-Cre Tg mice, and got $A20^{flox/flox}$ mice as control, CD4-Cre $A20^{flox/flox}$ mice as cKO mice. All mice were maintained in accordance with the laboratory animal science guidelines of Hiroshima University.

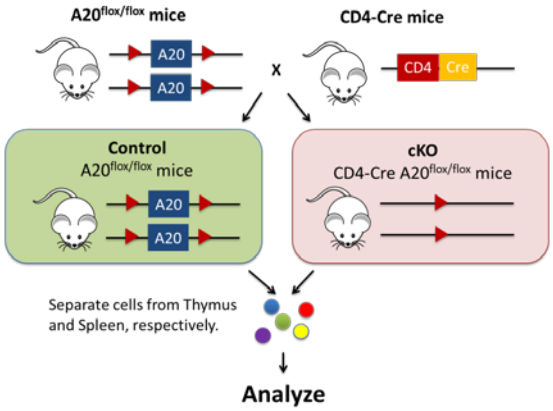

2. 6-8 weeks mice were sacrificed for isolating thymus, spleen and lymph nodes. Treg cells' were detected by flow cytometry to analyze many facets, such as the frequency and number in thymus and periphery, the signature molecules CTLA-4, CD73, FR4, GITR. To assess the proliferation, we injected mice with 2mg BrdU by i.p., overnight and injected 2mg BrdU again 1 H before scarified mice. To assess IL-2 signaling pathway, we treated cells with IL-2 (R&D) 100ug/ml at 37 degree centigrade for 20 min, then stained with pStat5, pERK1/2 and pAKT antibody.

3. Treg cells' suppression function was assayed in vivo. To evaluate the function of Treg cells, three kinds of T cells were sorted by FACS Aria from different kinds of mice. Con Treg cells were isolated from Ly5.2 (CD45.2) $A20^{flox/flox}$ mice, in which A20 gene was normal. A20 cKO Treg cells were isolated from Ly5.2 (CD45.2) CD4-Cre $A20^{flox/flox}$ mice which A20 gene was conditional knocked out in T cells. Effector T cells (Teff) were isolated from Ly5.1 (CD45.1) mice.

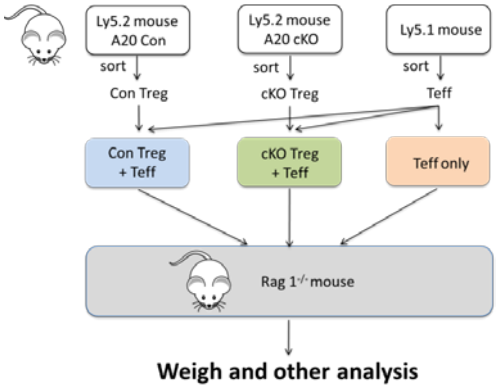

Combined the abovementioned cells to three injection group: Con Treg+Teff, cKO Treg+Teff, Teff only, and then injected into different Rag $1^{-/-}$ mouse respectively. After injection, weight loss was checked twice per week to assay the suppression function of Treg.

Results:

1. Treg were increased in A20 cKO mice both in thymus and periphery

In A20 deficient mice, there was no clear defects appeared in the conventional T cell. However, the frequency and number of $Foxp3^{+}$ regulatory T cells were significantly increased in thymus and periphery (figure 1). These results provide evidence that A20 gene may has important function in Treg.

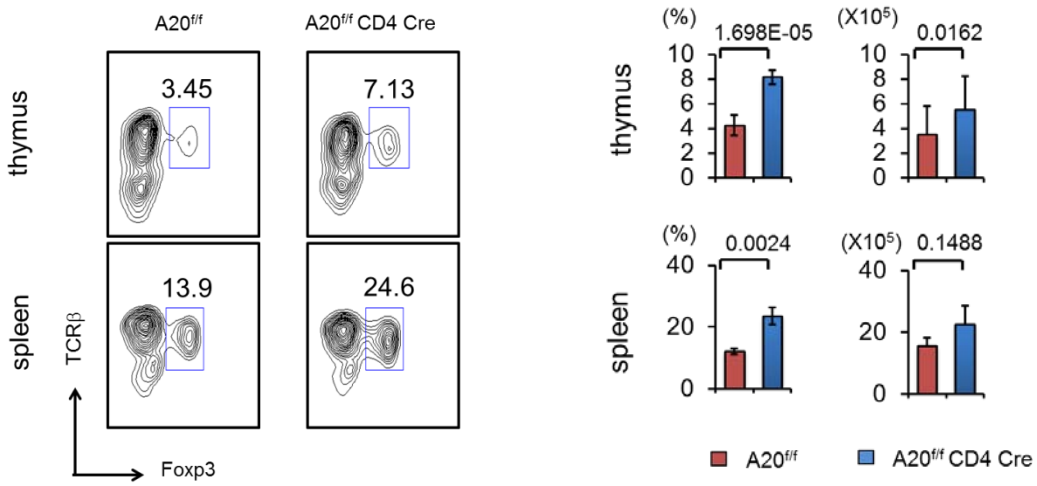

Figure 1. Treg cells were increased in A20 cKO mice both in thymus and periphery

2. Analyze the surface molecules' expression on Treg

We questioned whether the function of Treg in A20 cKO mice was changed, we examined the expression of CTLA-4, CD73, FR4, GITR which are the signature molecules of Treg, and found that the expression of these molecules have no significant difference both in thymus and in spleen. Although the number of Treg in A20 deficient cKO mice is increased, the expressions of Treg surface molecules are stable. Thus, we next want to check whether their suppressive function is intact in vivo.

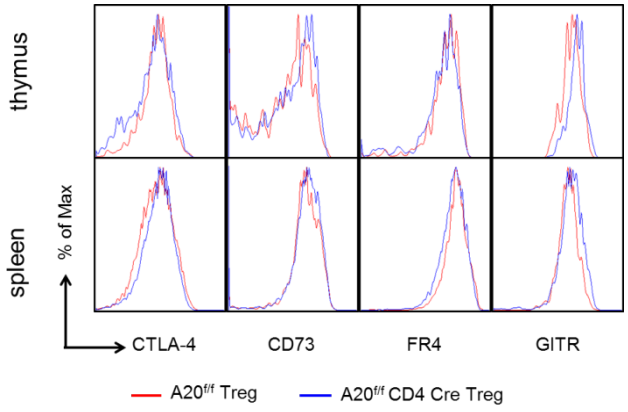

Figure 2. The expression of Treg signature molecules have no significant difference

3. Weight loss of mice in different injection groups

Determining the activity of a regulatory T-cell population in vitro is often the first step in analyzing its function. However in vitro culture conditions cannot replicate the complex in vivo microenvironment. Consequently, assessing Treg function in vivo is more physiologically relevant, and in vivo assays provide more insights of biological significance for Treg than in vitro assays. Therefore, we took a step to assess their suppressive activities in vivo[6]. As mentioned in methods, we FACS-sorted three population of T cells from abovementioned mice and then injected into immune-deficient Rag $1^{-/-}$ mice. Weight losses were monitored twice per week for four weeks, and drew weight loss curves of these three groups (figure 3). A20 deficient Treg maintain the suppressive function in vivo as control.

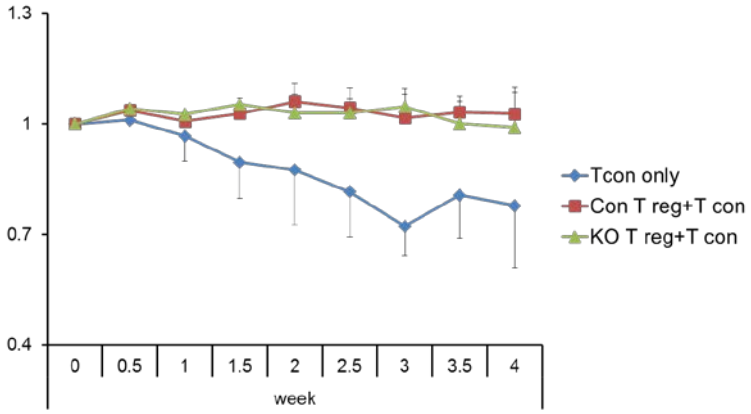

Figure 3. Weight loss in mice in different injection groups

4. Assay of Treg in periphery

Next, we would like to know the source/origin of the increased Treg cells in A20 deficient mice whether from thymus (tTreg) or induced from peripheral (pTreg). The surface expression of Neuropilin 1(Nrp 1) is known to be preferentially up-regulated on tTreg in WT mice, in contrast, low levels of Nrp 1 expression on pTreg. Therefore, we used the Nrp 1 as a specific surface marker for thymus-derived tTreg [7]. More $Nrp1^{+}$ Treg in periphery were found in A20 deficient mice, illustrating that the increased Treg were mostly derived from thymus (figure 4).

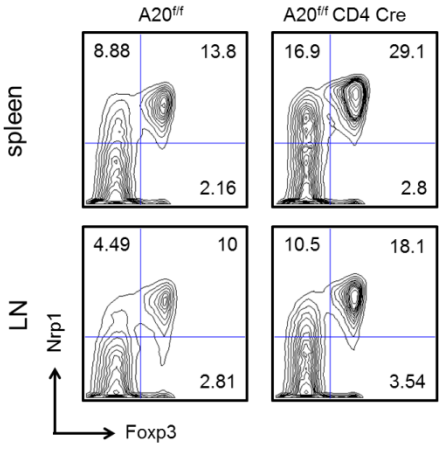

Figure 4. The expression of Nrp 1^{+} Treg in periphery of A20 cKO and control mice

5. Assay of tTreg proliferation and apoptosis

If the increased Treg in periphery of A20 cKO mice were mostly from thymus, what is the real outcome of the tTreg influenced by A20 deficiency? To go further, another FACS analysis was performed with BrdU and Annexin V to check the proliferation and apoptosis of tTreg respectively. Figure 5 demonstrates normal proliferation and cell death in

A20 deficient tTreg, which means A20 has no big effects on the proliferation and apoptosis at the generation of tTreg on the thymus.

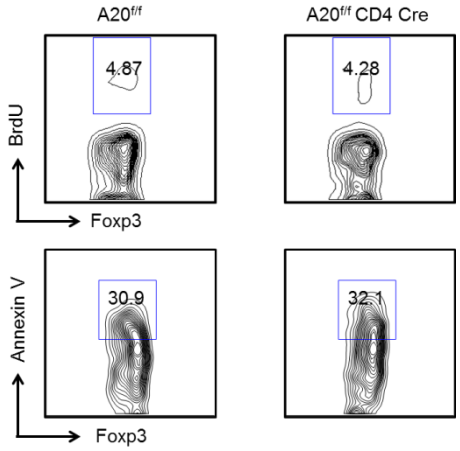

Figure 5. The proliferation and apoptosis of Treg in thymus

6. Effect of A20 in the IL-2 signaling pathways

Interleukin-2 (IL-2) is an O-glycosylated four alpha-helix bundle cytokine that is primarily produced by activated T cells and necessary to support T cell growth (therefore, former named as TCGF: T cell growth factor). The maintenance of T cell homeostasis and prevention of self-reactivity is the primary function of IL-2 signaling. There are three main IL-2 signaling pathways which use Stat5, ERK1/2, and Akt as important mediating molecules. Functionally, IL-2 induces the expression of both IL-2 and IL-2 R alpha on activated $CD4^+$ and $CD8^+$ T cells and stimulates their proliferation. In contrast, IL-2 also plays an important role in the maintenance of peripheral self-tolerance both by initiating Fas-mediated activation-induced cell death of $CD4^+$ T cells following antigen restimulation and by its ability to promote the differentiation and survival of Treg. Rather than displaying a severe immunodeficient phenotype, mice lacking IL-2, IL-2 R alpha, or IL-2 R beta have reduced numbers of Treg, and develop autoimmune diseases. To assess the function of A20 in the IL-2 signaling pathways, the expression of phosphorylated form of Stat5, ERK1/2, and Akt were examined among abovementioned mice. We found that enhanced phosphorylation of Stat5 in A20 deficient mice, while on the other hand there is no significant difference of ERK1/2 and Akt, which illustrate that A20 may influence the expression of several Stat5-target genes (including Cd25, IL-2 receptor alpha chain which create high affinity IL-2 receptor) by regulating phosphorylation of Stat5(figure 6). This high sensitivity of IL-2 is known to be crucial for Treg survival.

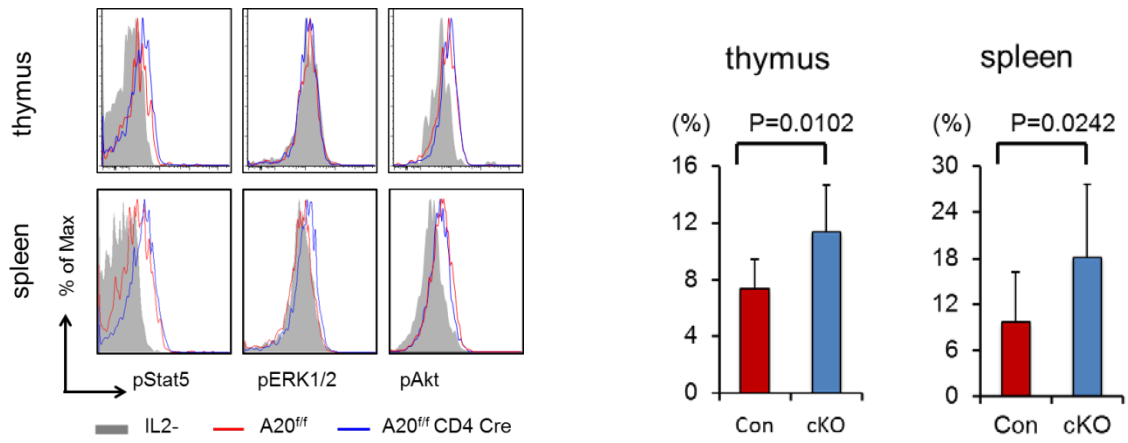

Figure 6. The phosphorylation of Stat5 was enhanced in A20 deficient mice

Discussion:

Our experiments revealed that there were no clear defects appeared in the conventional T cell development in A20 conditional knockout mice. Interestingly, the frequency and number of $Foxp3^+$ regulatory T cells (Treg) were significantly increased in thymus and periphery of A20 deficient mice. This observation suggests that A20 may influence the number of Treg. A20 deficient Treg in periphery were mostly derived from thymus, and exhibited the normal suppressive function as control. This increase may be related with the enhanced both IL-2 signal and TCR signal and its sensitivity. These results illustrate that A20 plays an important role in regulatory T cells and its survival, and more precise mechanisms still needs further study.

References:

1. Josefowicz, S.Z., Lu, L.F., and Rudensky, A.Y. (2012). Regulatory T cells: mechanisms of differentiation and function. Annu. Rev. Immunol. 30, 531–564.

2. Buenrostro, J.D., Giresi, P.G., Zaba, L.C., Chang, H.Y., and Greenleaf, W.J. (2013). Transposition of native chromatin for fast and sensitive epigenomic profiling of open chromatin, DNA-binding proteins and nucleosome position. Nat. Methods 10, 1213–1218.

3. Ingrid E. Wertz, Karen M. O'Rourke, Honglin Zhou, et al(2004). De-ubiquitination and ubiquitin ligase domains of A20 downregulate NF-κB signaling. Nature. 430, 694–699.

4. Ma, A. and Malynn, B.A. (2012). A20: linking a complex regulator of ubiquitylation to immunity and human disease. Nat. Rev. Immunol. 12, 774–785.

5. Iwai, K. (2012). Diverse ubiquitin signaling in NF-kappaB activation. Trends Cell Biol. 22, 355–364.

6. Creg J. W. Lauren W. C., Maria B, Meenu R. P, Jerold E. R, and Dario A.A. V. (2011). In Vivo Treg Suppression Assays. Methods Mol Biol. 707: 119–156.

7. Jonathan M. W., et. (2012). Neuropilin 1 is expressed on thymus-derived natural regulatory T cell, but not mucosa-Generated induced $Foxp3^+$ T reg cells. J. Exp. Med. 209: 1723-1742.

作成日：2017 年 2 月 24 日

A study on vestibular-evoked myogenic potentials via galvanic vestibular stimulation in normal people

正常人電刺激前庭誘発筋電位の研究

研究者氏名　成　顕（第 38 期笹川医学研究者）
中国所属機関　西安交通大学第二附属医院耳鼻咽喉科
日本研究機関　東京医療センター
指導責任者　加我　君孝　名誉臨床研究センター長
共同研究者名　木村　優介　研究員

Abstract: Objectives: Our aim of the study is to show the galvanic vestibular stimulation elicited vestibular-evoked myogenic potentials (VEMPs) on the sternocleidomastoid muscle(SCM) in healthy subjects for later cilinical application. **Methods:** We enrolled six healthy subjects to record the average responses in the electromyograph(EMG) of the SCM to galvanic vestibular stimulation(3mA, 1ms). SPSS18.0 software was used to analyze the data. **Results:** In all healthy subjects mastoid-forehead galvanic vestibular stimulation produced a positive-negative biphasic EMG responses on the SCM ipsilateral to the cathodal electrode. The latency of p13 was 11.15±2.37ms . The latency of n23 was 17.07±2.75ms. The amplitude of p13-n23 was 98.13±44.62μV. **Discussions:** The galvanic vestibular stimulation could elicited a biphasic EMG responses on the SCM via vestibular nerve but not otolith organs. The galvanic stimulation together with ACS or BCS stimulation elicited VEMPs may enable us to differentiate labyrinthine lesions from retrolabyrinthine lesions.

Key Words: galvanic vestibular stimulation; vestibular-evoked myogenic potentials; vestibular nerve; the sternocleidomastoid muscle

Introduction:

Auditory stimulated vestibular-evoked myogenic potentials (VEMPs) recorded by surface electrodes can be used clinically to assess vestibular function.[1,2] It could be classified two types: cervical vestibular-evoked myogenic potentials (cVEMPs) and ocular vestibular-evoked myogenic potentials (oVEMPs). Both VEMPs are elicited by auditory stimulus such as click, short tone burst or tapping. Cervical vestibular-evoked myogenic potentials (cVEMPs), which are recorded from the sternocleidomastoid muscles (SCMs), have been used to evaluate the function of the saccule and the inferior vestibular nerve, since physiological and clinical studies have shown that cVEMPs to air conducted sound (ACS)reflect the function of saccular afferents[3-6]. Ocular vestibular-evoked myogenic potentials (oVEMPs), which are recorded from extraocular muscles beneath the eyes in response to ACS and bone-conducted vibration (BCV) [7,8] have been used to evaluate the function of the untricule and the superior vestibular nerve.[9-11]

Three types of stimulation had been used to elicited VEMPs: air conducted sound (ACV,click and tone burst), bone-conducted vibration(BCV), galvanic vestibular stimulation(GVS). Galvanic stimulation has long been used as a non mechanical means of activating the vestibular apparatus[12]. Vestibular nerve collic evoked by galvanic stimulation in human have been described for clinical application rarely.

Our study was designed to investigate vestibular nerve collic induced by galvanic vetibular stimulation in normal people.

Subjects and Methods:

1 subjects Six normal voluneers (twelve healthy ears) aged from 29-60years old into this study. They are healthy without hearing loss or vertigo. The neck of all subjects was not fixed and could rotate freely. All subjects gave informed consent.

2 Test methods **Recording:** Active recording electrodes were placed on the middle of the SCM while indifferent electrodes were placed on the lateral end of the upper sternum. The ground electrode was on the forehead. **Galvanic stimulation:** Electrodes for galvanic stimulation were placed on the mastoid (cathode), and the forehead (anode). We used 3 mA (1 ms) galvanic stimulation. The thresholds of responses by galvanic stimulation were measured in electromyographic (EMG) activities were amplified and bandpass-filtered (20–2000 Hz). The stimulation rate was 5 Hz, and the analysis time was 50 ms. The responses to50 stimuli were averaged twice with and without contraction of the SCM by the rotation of the neck.When these galvanic stimuli were presented, the subjects felt a slight tapping sensation but no pain.[13-15]

To remove artifacts, we subtracted the average obtained without contraction of the SCM from the average obtained with contraction of the SCM[13,14] (figure 1).

3 Statistical methods SPSS18.0 software was used to analyze the data.

Results: All of the normal subjects showed biphasic responses. In this study we call the first positive peak by galvanic stimulation ‘p13’ and the first negative peak by galvanic stimulation ‘n23’. The latency of p13 was 11.15±2.37ms . The latency of n23 was 17.07±2.75ms. The amplitude of p13-n23 was 98.13±44.62μV. The statictics were showed in the table 1. Our record of the responses on the SCM with and without contraction and the wave after subtraction were showed in the figure 2.

Discussion: VEMPs elicited by ACS and BCS evaluate the function of the untricule, saccule and vestibular nerve.Watson and Colebatch reported that galvanic stimulation of the forehead and mastoid region could evoke myogenic responses in the SCM[13,14,16]. The responses in the SCM were abolished by the selective vestibular nerve section[14]. Their results indicated that these responses were of vestibular nerve origin. They supposed that galvanic stimulation could activate the most distal portion of the vestibular nerve. ACS and BCS could activate the receptor level of vestibule-- untricule and saccule (Fig 3, 4) [17]. Murofushi et al[15] have reported that combined use of click- and galvanic-VEMPs is useful in the differential diagnosis of labyrinthine lesions from retrolabyrinthine lesions in patients with vestibular deficits. In their study,all the 10 patients who were diagnosed as having Meniere’s disease or delayed endolymphatic hydrops showed normal galvanic-evoked myogenic responses on the affected side although they did not show click-evoked myogenic responses on this side. In contrast, 16 of the 18 patients who were diagnosed as acoustic neuroma or other cerebello-pontine angle tumors did not show any responses on the affected side even to galvanic stimulation. Murofushi et al[18]examined 11 patients with vestibular neuritis using click-VEMP and galvanicVEMP testing. In their study, 8 of the 11 patients showed absence of click-VEMPs and galvanic-VEMPs on the affected side, suggesting that the site of the lesion in vestibular neuritis was primarily within the vestibular nerve. Therefore the use of galvanic stimulation together with ACS or BCS stimulation may enable us to differentiate labyrinthine lesions from retrolabyrinthine lesions. The accurate position of lesion is useful to study the pathogenesis. By the record of healthy subjects, we can establish galvanic vestibular stimulation evoked VEMPs criteria for later clinical application. Then the vestibular diseases could be diagnosed and treated by the use gVEMPs with ACS- or BCS-VEMPs such as auditory

neuropathy, vestibular neuropathy and neurofibromatosis Type Ⅳof "normal" subjects.

References:

1 Colebatch JG, Halmagyi GM. Vestibular evoked potentials in human neck muscles before and after unilateral vestibular deafferentation. Neurology. 1992; 42:1635–1636.

2 Welgampola MS, Colebatch JG. Characteristics and clinical application of vestibular-evoked myogenic potentials. Neurology. 2005; 64:1682–1688.

3 McCue MP, Guinan JJ Jr. Acoustically responsive fibers in the vestibular nerve of the cat. J Neurosci. 1994; 14:6058–6070.

4 Murofushi T, Curthoys IS, Topple AN, Colebatch JG, Halmagyi GM. Responses of guinea pig primary vestibular neurons to clicks. Exp Brain Res. 1995; 103:174–178.

5 Murofushi T, Halmagyi GM, Yavor RA, Colebatch JG. Absent vestibular evoked potentials in vestibular neurolabyrinthitis; an indicator of inferior vestibular nerve involvement ? Arch Otolaryngol Head Neck Surg. 1996; 122:845–848.

6 Welgampola MS, Colebatch JG. Characteristics and clinical application of vestibular-evoked myogenic potentials. Neurology. 2005; 64:1682–1688.

7 Rosengren SM, Todd NPM, Colebatch JG. Vestibular-evoked extraocular potentials produced by stimulation with bone-conducted sound. Clin Neurophysiol. 2005; 116:1938–1948.

8 Todd NPM, Rosengren SM, Aw ST, Colebatch JG. Ocular vestibular evoked myogenic potentials (OVEMPs) produced by air-and bone-conducted sound. Clin Neurophysiol. 2007; 118:381–390.

9 Iwasaki S, Chihara Y, Smulders YE, Burgess AM, Halmagyi GM, Curthoys IS, Murofushi T. The role of the superior vestibular nerve in the generation of ocular vestibular-evoked myogenic potentials to bone conducted vibration. Clin Neurophysiol. 2009a; 120:588–593.

10 Iwasaki S, Murofushi T, Chihara Y, Ushio M, Suzuki M, Curthoys IS,Yamasoba T. Ocular vestibular evoked myogenicpotentials to bone-conducted vibration in vestibular schwannoma. Otol Neurotol. 2009b; 31:147–152.

11 Curthoys IS, Kim J, McPhedran SK, Camp AJ. Bone conducted vibration selectively activates irregular primary otolithic neurons in the guinea pig. Exp Brain Res. 2006; 175:256–267.

12 Camis M. The Physiology of the Vestibular Apparatus. Oxford University Press, London, UK. 1930; pp: 209–212.

13 Watson SRD, Colebatch JG. Vestibulocollic reflexes evoked by short-duration galvanic stimulation in man. J Physiol 1998; 513:587–597.

14 Watson SRD, Fagan P, Colebatch JG. Galvanic stimulation evokes shortlatency EMG responses in sternocleidomastoid which are abolished by selective vestibular nerve section. Electroenceph clin Neurophysiol. 1998; 109:471–474.

15 Toshihisa Murofushi, Hideki Takegoshi, Masafumi Ohki et al.Galvanic-evoked myogenic responses in patients with an absence of click-evoked vestibulo-collic reflexes. Clin Neurophysiol. 2002; 113:305-309.

16 Watson SRD, Colebatch JG. EMG responses in the soleus muscles evoked by unipolar galvanic vestibular stimulation. Electroenceph clin Neurophysiol. 1997; 105:476–483.

17 Kaga K. OAE and ABR in newborn and children. Diagnostic and therapeutic press. 2012;58.

18 Murofushi T, Monobe H, Ochiai A, Ozeki H. The site of the lesion in "vestibular neuritis": study by galvanic VEMP.

Neurology. 2003; 61:417-418.

figure 1 The two superimposed traces in A and the single trace in B show responses to transmastoid stimulation(4 mA, 2 ms) with the cathode on the right mastoid. The continuous trace in A is the average with tonic SCM activation and the dashed trace is the average with SCM relaxed. Both traces show stimulus artifact, but the reflex response only occurs with activation. B, trace obtained by subtracting the relaxed average from the active one: p13/n23 response appears free of stimulus artifact[14].

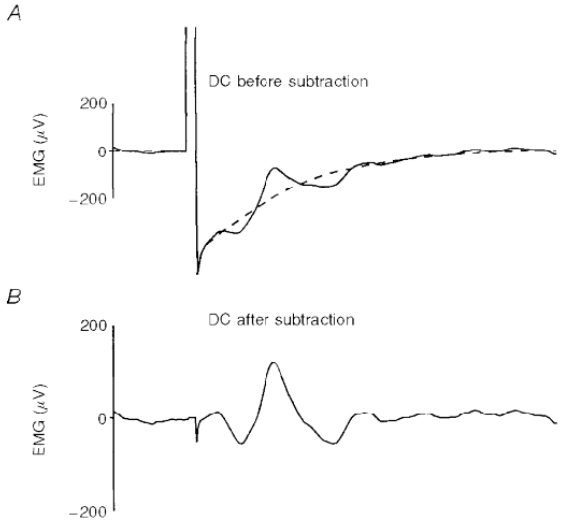

Figure 2 One of subjects was tested of gVEMP. A was the reflex response occured with SCM contraction. B was the reflex response occured without SCM contraction. C was A subtracted to B in order to remove artifacts which was the real trace of gVEMP.

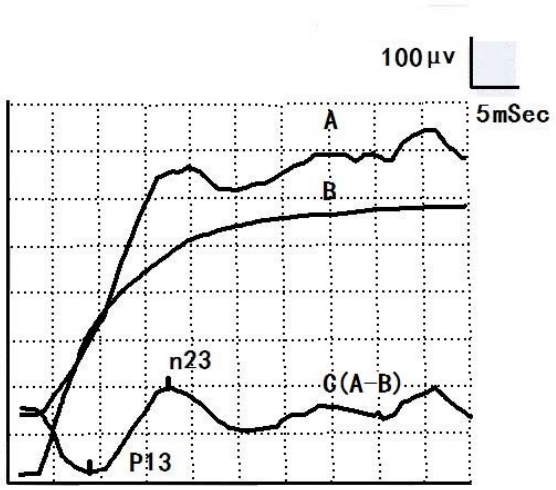

Figure 3 Auditory stimulation(ACS and BCS) could activate the receptor level of vestibule-- untricule and saccule. The galvanic stimulation could activate the most distal portion of the vestibular nerve.[17]

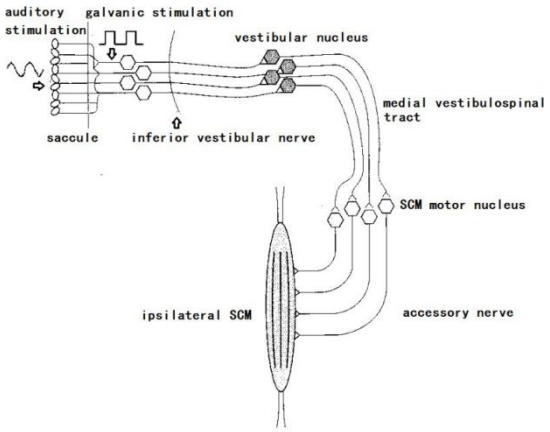

Figure 4 Auditory stimulation could activate the receptor level of vestibule-- untricule and saccule. The galvanic stimulation could activate the most distal portion of the vestibular nerve.(L-SCC: lateral semicircular canal; P-SCC: posterior semicircular canal)

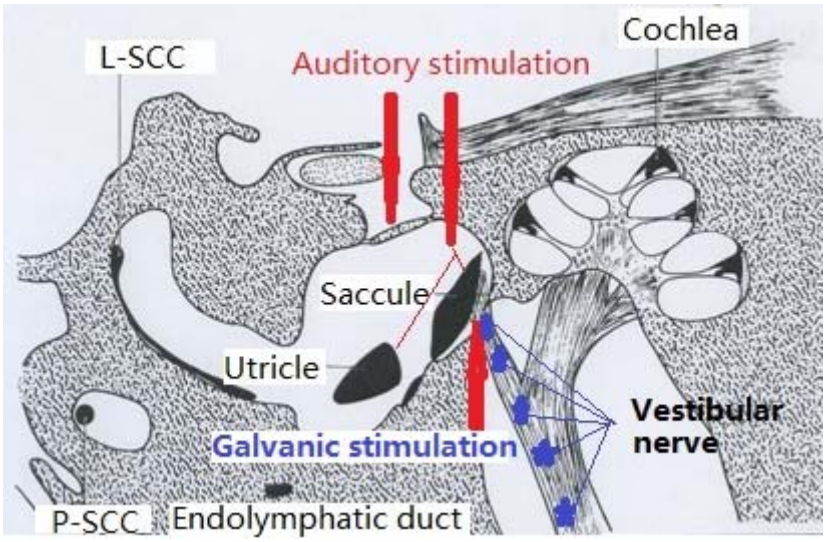

Table 1 The mean and Standard Deviation(SD) of the latecy of p13 and n23, and amplitude of p13-n23 in all subjects.

N=12(ears)	P13 latency(ms)	N23 latency(ms)	Amplitude(μV)
Mean	11.15	17.07	98.13
SD	2.37	2.75	44.62

作成日：2017 年 2 月 23 日

日本と中国の緩和ケア看護の比較

研究者氏名　羅　蕾（第38期笹川医学研究者）
中国所属機関　四川省腫瘤医院·腫瘤内科
日本研究機関　静岡県立静岡がんセンター·看護部
指導責任者　鶴田　清子　副院長

要　旨

【目的】中国ではがん患者死亡患者数が急激に増加し大きな課題となっている。その為がん医療における緩和ケアの重要性が認識されてきた。日本と中国は同じアジア文化圏に属し多くの類似点が見られるので、日本の先進的な緩和ケアを習得するため、静岡がんセンターでの研修を希望した。

【方法】臨床現場で看護師長らの指導下で実地研修を行った。緩和ケア認定看護師教育課程に参加し緩和ケアの知識·技術を習得した。

【結果】実地研修した結果、中国の看護管理や全人ケアの理念の実態は日本とは大きく異なっていた。中国では単一診療科に長期勤務のため専門性が高く、業務内容も日本と大きく異なっていた。がんセンターの PNS（Partnership Nursing System）看護管理方式を習得しその有用性を体験した。日中における医療保険制度も大きく異なっており、日本の緩和ケアの体制を学ぶべきと考えた。日本の認定看護師教育課程に緩和ケアが含まれており、中国で軽視されている家族ケア、終末期ケア教育の重要性を学んだ。

【結論】研修では PNS 看護管理方式、患者・家族とのコミュニケーション技術、がん緩和ケア認定看護師の教育課程・緩和ケアの知識・スキルなどの教育や方法、緩和ケアチームでの看護師の役割などを実地研修した。帰国後、筆者の病院において、PNS 管理法を如何に取り入れていくべきかが、重要な検討課題と考える。看護師と患者間の信頼関係を構築し、緩和ケア認定看護師の教育方法を改善し、医療者と市民への死生観普及活動を実施していきたい。

キーワード

がん緩和ケア、臨死期ケア、PNS、日中看護体制

Ⅰ　はじめに

中国は 65 歳以上の高齢人口が１億人を越える世界で唯一の国となっている[1)]。しかも 65 歳以上の人口比が 7%から 14%に達するまでの所要年数は 27 年と予想され、日本が 24 年間で高齢化が進行したのとほぼ同じスピードで高齢化が進行している[2)]。特に、2020 年から 2050 年間は中国の高齢化が加速され、2050 年には 65 歳以上の高齢者は 25.8%に達すると予測されている。人口が日本の 10 倍多い中国では深刻な問題となっている[3)]。更に、中国では慢性感染症、喫煙、大気汚染などが要因となり、がん患者数が急増している。2015 年にがん罹患率は 429.2 万人となり、死亡者数は 281.4 万人に上昇して、この状態は毎日 12,000 人ががんに罹患し、7,500 人が死亡としていることになる[4)]。このような現状下で、中国全土において腫瘍病院の病床数を急増してきている。筆者の所属する病院も 2017 年に 1,600 床から 2,500 床に増床が予定され、緩和ケアの重要性も認識されてきている。

日本と中国は同じアジア文化圏で、生活習慣や社会生活面など多くの類似点が見られる。従って、筆者は日中医学協会の笹川奨学金制度に応募し、１年間がん緩和ケア看護を勉強するために、日本で最大規模を誇る静岡センターでの研修を希望した。静岡がんセンター内において外来、一般病棟、緩和ケア病棟、IVR 科などでがん看護師業務の実態を見学し研修した。更に、緩和ケア認定看護師教育課程にも参加した。

これらの実体験を通して日中のがん看護の違い、更に、看護教育課程についても比較検討を行ったので報告する。

Ⅱ　目的

日本の先進的緩和ケアモデルを習得し、中国の緩和ケア医療体制内に新しい医療形態を取り入れ、いかに発展させるべきかを、実体験を通して両国間の相違点比較検討する。その成果を中国のがん緩和ケア看護の改善・進化にどのように寄与すべきを検討した。更に、私の専門とする中心静脈専門看護師のトレーニングと腫瘍専門看護師の教課分野におけるがん看護教育方法を習得して、四川省腫瘍病院のがん看護教育の発展に努めたいと考える。

Ⅲ　研修方法・内容

1．実地臨床研修は静岡がんセンターの臨床現場の看護師長らから直接指導下で研修した。緩和ケア認定看護師の教育課程は日本の看護師受講者と一緒に参加し、緩和ケアの知識・技術を習得した。これら、研修した内容を文献検索を加えて考察を行った。

２．各研修期間における研修内容：

1）2016 年４月から 7 月まで、各外来診療部門、通院治療センター、消化器内科病棟、血液·幹細胞移植病棟、IVR 治療科などで実地研修した。具体的には、入院患者の入退院システムと外来患者への対応の手順、通院治療センターでの外来化学療法における看護師の役割、化学療法での副作用の対応、薬剤師らによる抗がん剤の調合方法、骨髄移植患者の看護ケア、IVR の実地臨床を見学した。

2）2016 年８月から 10 月まで、緩和ケア認定看護師教育課程に参加して、がん看護分野の教育方法と知識を習得した。特に終末期のがん患者の看護ケアについて学んだ。

3）2016 年８月から 12 月まで、緩和ケア病棟で患者の医療保険制度がどのよるに適用されているのか、患者・家族へのケアとコミュニケーションの実態などを見学した。特に、緩和ケア病棟における Partnership Nursing System（PNS）看護管理方式やがん緩和ケアの知識とスキルなどがどのように適用されているのかを学んだ。更に、夜勤勤務も実体験した。

4）2016 年 12 月から 2017 年１月まで、一般病棟における緩和ケアチーム活動に参加して、どのように全人的緩和ケア医療が実施され、評価されているかを学習した。特に、緩和ケアチーム員の専門性、組織構成·管理方法やシステムについて学んだ。

Ⅳ　結果と考察

１．日中看護師業務内容の比較（表１）

2016 年 4 月から静岡がんセンターにおいて PNS 看護管理方式が全病棟で実施されていた。その結果、看護師の役割分担と責任がより明確化されていた。二人の看護師は毎日患者 6～8 名のケアを担当し、患者入院処置、通常の輸液、化学療法、褥瘡ケア、口腔ケア、術前·周術期処置、退院処置などが行われていた。その結果、看護師はがん患者治療の全過程においてシームレスにケアが提供されていた。更に、看護師と患者・家族とコミュニケーションをとる時間が多くなり、相互の信頼関係の構築に役立っていた。

一方、表１に示すように中国において看護管理は全人ケアが理念とされているが、実態は日本とは大きく異なっていた。特に、中国では看護師数の不足が大きな問題となっている。看護師数も日本の５分の１と少なく[5)]、介護は全て家族が中心に行われている。業務別の担当制度で、看護基本作業以外に医療秘書ようなの雑用も担当している。仕事量が多く、特に、輸液療法の件数が多く、患者・家族らとコミュニケー

ションをとる時間が極めて少ない現状にある。更に、中国では家族への援助ケアが不充分である。一般的に中国では看護師の地位は低く、給料も日本と比較して相対的に低く、毎月日本円にして5万から25万程度である。診療科間の格差が大きく、職場が不安定でモチベーションや達成感が乏しい現状にある。一方、昇進システムは厳格で、論文・専門知識・技術など審査基準に達成する事が要求されている。また、単一診療科に長期勤務のため専門性が高い。このように、日本と中国のシステムが異なっていた。

がんセンターにおけるPNS看護管理方式の現状を体験し、そのメリットや作業全体の流れ、看護師の役割などを実体験できたことは有意義であった。PNS は日本では2009年に新しい看護管理方式としてパートナーシップ・ナーシング・システム（Partnership Nursing System, PNS）が福井大学医学部附属病院で開発された[6,7]。PNSは看護師が安全で質の高い看護を提供することを目的に、2人の看護師で複数の患者を受け持つのが大きな特徴である[8]。PNSは看護師だけでなく、患者にとっても療養環境が改善され、パートナー同士の業務を補完し合うことで、より質の高い看護を提供できるのが大きなメリットとなっている。今後、中国の看護管理方式を基にして、日本のPNS看護管理方式を如何に導入していくべきかが、重要な検討課題であると考える。そして、医療者と患者・家族とのコミュニケーションを重視していき、看護師と患者間の信頼関係の構築に努めてたいとと考える。

表１　日中看護師業務の内容比較

項目	中　国	日　本
看護師数	2.2/1000 人口	11.0/1000 人口
看護業務	・介護は家族が中心 ・看護は業務別の担当制度 ・単一診療科に長期勤務	・介護を含め全て看護師が担当 Partnership Nursing System (PNS) 看護管理 ・各診療科を経験
仕事特性	・専門性が高い ・看護基本業務以外に雑務が多く、仕事量が多く、輸液療法件数が多い ・患者・家族とのコミュニケーション不足	・看護基本業務が中心 ・看護以外雑務が少なく、輸液療法件数が少ない ・患者・家族とコミュニケーションとの機会が多い
地位給与	・地位が低い ・診療科間の格差が大きい ・給与は相対的に低く、月 5 万から 25 万円程度	・地位は高い ・患者・家族や医師から専門性が認められている ・収入が安定で、格差がない
満足感	・職場が不安定 ・モチベーションや達成感が低い	・職場が安定 ・満足感・モチベーションが高い
昇　進	・競争が厳しい ・論文・ 知識・技術など審査	・年功序列性を重視 ・論文や学術面の評価が低い

２．日中がん緩和ケアと医療保険制度の現状比較（表２）

静岡がんセンターにおける緩和ケアチームは多職種チーム医療と全人的苦痛緩和を基本方針とし、最先端治療から終末期医療まですべてのがん病期に渡り、患者に最善を尽くすことを目標にされていた[9]。2002 年 9 月に開院したがん専門病院である、開院当初より緩和医療科医師、看護師、心理療法士、薬剤師、栄養師らが多職種チームを構成して一般病棟に入院中の患者の緩和ケア活動を行っていた。また、2004 年 4 月からがん看護専門看護師と専従看護師を配置して、緩和医療科、精神腫瘍科との連携がより強化されていた。緩和ケアチームで活動する専従看護師はがん専門看護師 1 名と緩和ケア認定看護師１名で構成されていた。専門看護師は外来患者の看護も担当していた。認定看護師は緩和ケアチームに専従していた。緩和ケアチームにおける看護師の役割は極めて大切な位置づけを占めていた。具体的に、1)患者･家族の情報収集、病態と症状把握、患者の各種苦痛を収集し、緩和ケア専従医師に伝えて、一緒に疼痛症

状緩和を行う。2)医師補助と治療内容などを患者に追加説明する。3)医師診療後に、患者·家族への緩和ケア内容説明、病棟環境·入院費用の説明、面談時間の確認、治療目標と家族へのサポートなどを担当する。4)各病棟の看護師への情報提供。など多方面に渡っていた。

日本では緩和ケアの領域において、緩和ケア病棟は、看護師数は常時入院患者 7 人に 1 人以上，夜勤看護師 2 人以上であることなどが基準看護の要件とされていた[10]。看護師がどれだけ患者·家族の日常生活の援助者となりうるかが重視されていた。

アジア地域で全国民を対象にした医療保険が整備されている国は、日本、韓国、シンガポールのみである[11]。日本は 1961 年に国民皆保険が導入され、1982 年に老人保健制度、2000 年に介護保険も創設された。医療政策として健康増進計画、医療計画、介護計画、医療費適正化計画などが整備されている。更に、2006 年にがん対策基本法案が閣議決定され、この結果緩和ケアが全国的に進展されていた。特に、この法案によって緩和ケアががん治療の重要な一分野と位置づけられていた。更に、病棟診療費・一般病棟におけるチーム医療にも保険診療が加算されていた。

中国においてもは緩和ケアの多職種チーム医療を理念としているが、実態は日本とは大きく異なっていた。緩和ケアチーム構成は腫瘍科医師·看護師·心理療法士のみで構成されている。しかし、緩和ケアにおいては精神面のケアも重要であるが対応が不充分である。緩和ケアチームで活動する看護師の役割分担も不明確である。緩和ケア看護師は一般病棟の看護師と同じであり、専従の緩和ケア看護師は備えていない。

一方、表２に示すように中国にも医療保険は存在するが、実備されておらず、保険で費用は加算されていない。緩和ケアが公的医療保険の対象となっていない、現状は緩和ケアの運営資金が少なく、経営基盤は極めて不安定かつ脆弱である。緩和ケアが公的医療保険制度の対象とされていないことが、日本と中国との緩和ケアにおける最大の相違点であると考える。中国の医療保険制度は「都市住民基本医療保険」「都市労働者基本医療保険」「新型農村合作医療」の 3 つの保険制度で構成されている。しかし、都市部と農村部では保障対象に格差が大きく[12]、近年中国では、医療費が高く「看病難、看病貴」と、社会問題化されており、国民生活の大きな不安定要因となっている。そこで、中国政府は新医療制度改革では、医療衛生を公益性事業と位置付け、国民皆保険という基本医療衛生制度を公共資源として全国民に提供することを基本理念としている。90%の国民をカバーする医療保険制度の基本枠組みを構築する中期目標と、2020 年にすべての国民をカバーする完全な医療保険制度を確立する長期目標を掲げている。

表２　日中がん緩和ケアの現状比較

項 目	中　国	日　本
医療保険制度	・医療保険制度が不備 ・都市部と農村部の格差が大きい	・国民皆医療保険制度 ・自由アクセス・均一 ・保険で保障されている
業務内容	・終末期の緩和ケアに限定 ・鎮痛治療が中心 ・精神的苦痛への対抗不充分 ・早期からの緩和ケアが軽視	・全人的ケア ・看取りの緩和ケア充実 ・精神的苦痛緩和も含め ・がん早期から治療中終末期適用
提供場所	・緩和ケア病棟はない ・がん診療拠点病院はない ・在宅緩和ケアが不充分	・外来患者にも適用 ・緩和ケア病棟 ・一般病棟で緩和チーム ・在宅緩和ケアも保険適用
緩和ケアチームの構成成員	腫瘍科医師·看護師·心理療法士らの集学的検討会のみ	・多専門職種チーム構成されている ・緩和ケアチーム回診治療

３．日中の緩和ケア認定看護師教育課程比較（表３）

日本の緩和ケアにおける看護師の役割と認定看護師の教育分野として身体的苦痛症状のコントロール、コミュニケーションスキルの訓練が大切にされ、家族に対しても基本的な日常生活の援助ケアを提供し、患者・家族の意思決定を支えケアを通して患者の精神的、社会的、心理的に及ぼす影響を把握することが要求されていた。日本看護協会の認定看護師制度は、各専門診療科分野において、熟練した看護技術と知識・スキルを用いて、水準の高い看護が実践できる認定看護師を医療現場に送り出している[13)]。表１、２でも述べたように、日本の緩和ケア看護師数は多く、患者・家族に全人的ケアが提供されていた。そして、緩和ケア看護師の役割と教育課程分野が広範囲に渡っており、患者･家族への社会面、精神面、心理面などの全人的緩和ケアが実施されていた。

表３に示すように日本の認定看護師の教育課程には緩和ケアが含まれており、中国の腫瘍看護認定看護師の育成課程では緩和ケアの内容が少なく、特にがんの終末期患者へのケア教育は全く行れれていない。中国人の死生観は日本と類似点もあるが、相違点も大きい。中国では宗教の思想に影響され、「人生を有意義に、死語は不吉」の言伝えがあるように、死の教育が回避されている。将来死生観を含めた生命の尊厳を重視する啓発が大切と考える。中国では教育課程の講師は病院の医師と認定看護師らのみで構成されて、期間は 2 か月となっている。教科内容は日本のように詳細に書かれていない、主な教育方法は一方向性の講義となっている。2011 年に策定された「中国看護事業発展十二五計画」では、ホスピス・緩和ケア看護が重要な目標となった。2015 年 11 月に、広東省汕頭で国内最初の「中華看護学会・全国の緩和ケア看護トレー二ング」が開設され、今後、中国の緩和ケア看護事業の一層の発展が期待される。緩和ケア看護師が緩和ケアの基本理念を理解して、専門的な技術を習得する研修プログラムに取り入れべきと考える。緩和ケア看護では人材育成は緩和看護ケアの基盤になるので、日本の充実した緩和ケア認定看護師の教育課程を参考にして、筆者の病院における教育方法の改善に努めたいと考える。

表３　日中の緩和ケア認定看護師教育課程比較

項 目	中　国	日　本
専門分野	腫瘍看護（四川）	緩和ケア認定看護（静岡）
対　象	専門分野で 5 年以上の勤務	専門分野で 5 年以上の勤務
定　員	35 名	20 名
費　用	６万円	75 万円
講　師	本院の医師と認定看護師	全国の専門領域講師・本院の医師・認定看護師
期　間	2 か月間	7 か月間
専用教材	全省同一内容、不充分	全講義内容・資料豊富
教育形式	･共通科目 ･専門科目 ･演習実習	･共通科目 ･専門科目 ･演習実習
授業内容	･歴史と現状 ･がん総論と集学的治療 ･症状マネジメントと援助技術 ･臓器別の治療とケア ･心理的ケア	･緩和ケア総論 ･がん総論と集学的治療 ･がんの医療サービス資源 ･症状マネジメントと援助技術 ･患者の心理的ケア ･喪失・悲嘆・死別 ･患者の家族･遺族ケア ･臨死期のケア ･緩和ケアの論理的課題 ･緩和ケアチームのアプローチ
教育方法	一方向性の講義	双方向性の講義
修了試験	全国統一試験	全国統一試験

Ⅴ　結論

日本の看護業務研修から、１）PNS 看護管理方式と臨床実践や患者・家族とのコミュニケーション技術を実地研修した。２）日本におけるがん緩和ケア看護教育･体制と緩和ケアチームで活動する看護師らの臨床を実践で学ぶことかできた。３）がん緩和ケア看護師の教育課程のシステムと教育プログラムを学んだ。

帰国後、筆者の病院で従来の看護管理方式を基に、PNS 看護管理方式を如何に取り入れていくべきかが大切な検討課題と考える。特に、患者・家族とのコミュニケーションを重視し、看護師と患者間の信頼関係の構築に努める緩和ケア認定看護師教育方法を取り入れ、改善に努めたい。医療者と患者・家族への死生観の普及活動を実施していくことも大きな課題と考える。特に、中国のがん緩和ケア看護制度は医療保険制度、死生観、人材育成などの課題が山積しているが、今後緩和ケアに対する「全民医療保障制度」への確立が急務であり、衛生行政へ取り組みを期待したい。

参考文献

１）世界保健機構(WHO)：世界保健における高齢化と健康,2012
http://www.who.int/kobe_centre /mediacentre/forum/forum_whd-2012/ja/index1.html

２）厚生労働省:平成 28 年版厚生労働白書概要版:我が国の高齢者を取り巻く状況,pp3-4,2016
http://www.soumu.go.Jp/johotsusintokei/whitepaper/ja/h25/html/nc123110.html

３）日本貿易振興機構:中国高齢者産業調査報告書,pp1-2,2013
http://www.jetro.go.jp/world/reports/2013/07001397.html

４）Chen WQ, ZhengRS, Baade PD: Cancer Statistics in China, 2015, CA-CANCER J CLIN 2016

５）OECDHealth Data:医師数・看護師数の国際比較,2014
http://www2.ttcn.ne.jp/honkawa/1930.html

６）山香代子:パートナーシップを取り入れた新看護方式 PNS の効果,第 42 回日本看護協会一看護管理一論文集,512,2013

７)橘幸子:福井大学医学部附属病院の新看護方式:PNSPartI.看護展望,37,51,2012

８）松村愛都：福井大学医学部附属病院で開発された PNS の効果：導入 1 年後の病棟看護師の認識.福井大学医学部研究雑誌 16:37-46,2016
http://repo.flib.u-fukui.ac.jp/dspace/bitstream/10098/9888/1/10098-9888.pdf

９）高橋晃子：緩和ケアにおけるコンサルテーション活動の専門性：緩和ケアチームで活動する看護師の役割,pp31-34,2007
http://www.hospat.org/hakusyo/pdf/2007_2_3.pdf

10）宮島俊彦:わが国の医療提供体制と緩和ケア:医療改革の方向と緩和ケア,pp25－28,2008
http://www.hospat.org/hakusyo/pdf/2008_1_5.pdf

11）長谷川和夫:日本の看取り,世界の看取り.国際長寿センター：在宅介護・医療と看取りに関する国際比較研究,2011
http://www.ilcjapan.org/about/doc/report22.pdf

12）日本貿易振興機構:中国高齢者産業調査報告書,pp31-34,2013
http://www.jetro.go.jp/world/reports/2013/07001397.html

13）日本緩和医療学会:緩和ケアチーム登録の実施計画書,2015
http://www.jspm.ne.jp/pct/pct1602. pdf

作成日：2017 年 2 月 15 日

The active ingredients of Shengmaisan that protect PC12 cell injury induced with β-amyloid

生脈散のアミロイドβによるPC12細胞損傷に対する保護活性成分

研究者氏名　韓　瑩（第38期笹川医学研究者）
中国所属機関　黒龍江中医薬大学
日本研究機関　名古屋市立大学大学院薬学研究科
指導責任者　牧野 利明 教授

Abstract:

In this study, we investigated the neuroprotective activities of Shengmaisan (SMS) and its composed crude drugs against amyloid-β (Aβ)-induced neuronal toxicity in differentiated PC12 cells. Extract of SMS significantly altered Aβ-induced reduction of cell activity and neurite-like outgrowth length. Among SMS composed drugs, its monarch drug Ginseng contributed the main activity on up-regulating PC12 cells survival rate and neurite-like outgrowth. Ginseng hot water extract remarkably reversed the decline of survival ratio in Aβ-exposed PC12 cells. MeOH-soluble fraction of Ginseng extract showed the powerful beneficial effects on preventing neurite-like outgrowth from Aβ-induced reduction. By activity-guided fractionation, we focused on the fraction containing ginsenosides which displayed the protective activity. Among several ginsenosides, ginsenoside Rb_1 and F_2 exhibited the significant preventive effects on Aβ-induced neurite-like outgrowth reduction in PC12 cells. These results suggest that SMS and ginseng are the potential agents for preventing Aβ-induced neuropathies, and ginsenoside Rb_1 and F_2 are proposed as two of the active ingredients in ginseng.

Key words:

Shengmaisan, Alzheimer's Disease, PC12 cells, neurite-like outgrowth

Introduction:

Alzheimer's Disease (AD) is a common progressive neurodegenerative disease that gradually deprives the patient of cognitive function, ability, language, visualization skills, eventually causes death[1,2]. There are many hypothesises about AD, and the most accepted one is amyloid hypothesis. It is clarified that an imbalance between amyloid-β (Aβ) production and clearance leads to Aβ accumulation in the central nervous system[3,4]. PC12 cell line is derived from rat adrenal pheochromocytoma. By 1 week's exposure to nerve growth factor (NGF), PC12 cells cease to multiply and begin to extend branching varicose processes similar to those produced by sympathetic neurons in primary cell culture. PC12 cells had been a useful model system for neurobiological and neurochemical studies[5]. Shengmaisan (SMS, 生脈散), which was first recorded in "*Yi Xue Qi Yuan*", is one of the most famous formula in traditional Chinese medicine composed of Ginseng (root of *Panax ginseng*), Ophiopogon Tuber (the enlarged part of the root of *Ophiopogon japonicus*) and Schizandra Fruit (the fruit of *Schisandra chinensis*), it has been used for treatment of cardiovascular disease in Asian countries. My previous study has demonstrated that SMS can improve $AlCl_3$ and D-gal-induced rat cognitive disorders through regulating multiple metabolic pathways. In this study, I employed PC12 cells to investigate the preventive effect and its active ingredients of SMS on Aβ-induced cell injury.

Methods:

1. Materials

Shengmaisan (Ginseng 5.2 g (Daiko, lot number #5D25), Ophiopogon Tuber 3.1 g (Daiko, lot number #4C03M), Schizandra Fruit 1.6 g (Daiko, lot number #6B19M) or each crude drug (Ginseng 10 g, Ophiopogon Tuber 10 g, Schizandra Fruit 10 g) was boiled in a 10-fold weight of water (100 ml, respectively) for 30 min, filtrated and lyophilized. The ratios of yielded were as follows: 31.7% for SMS, 23.8% for Ginseng, 29% for Ophiopogon Tuber and 17.9% for Schizandra Fruit. All the powders were sonicated in 10-fold weight of MeOH for 20 min. After centrifugation (4°C, 3000 *rpm*, 10 min), the supernatants and the residues were collected, and dried to yield MeOH-soluble and MeOH-insoluble fractions of the extract. The weight of each fraction were as follow: MeOH-soluble and insoluble fraction of Ginseng were 1.06 g and 1.34 g, MeOH-soluble and insoluble fraction of Ophiopogon Tuber were 0.48 g and 2.38 g, MeOH-soluble and insoluble fraction of Schizandra Fruit were 1.07 g and 0.61 g. Ginsenosides Rg_1 and Rb_1 were obtained from Wako Pure Chemicals (Osaka, Japan). Compound K was obtained from ChromaDex (Irvine, CA, USA). Ginsenosides F_1, F_2, Rd, Rg_3, Rh_1, Rh_2, protopanaxadiol and protopanaxatriol were obtained from Sichuan Weikeqi Biological Technology (Chengdu, Sichuam, China).

2. Fractionation of ginseng[6]

Ginseng (19 g) was boiled in 380 ml H_2O for 30 min, filtered, and lyophilized to yield 7.1 g extract. 4.7 g MeOH-soluble fraction of the ginseng hot water extract was obtained. The MeOH soluble fraction of the ginseng extract was suspended in water and partitioned three times with n-hexane, with a resulting n-hexane fraction yield of 5.2 mg. The water layer was further partitioned three times with water-saturated BuOH, yielding BuOH and water fractions (0.20 and 4.4 g, respectively).

3. Cell culture

PC12 cells were obtained from the American Type Culture Collection (Manassas, VA, USA). PC12 cells were grown in Dulbecco's modified essential medium (DMEM, Nacalai Tesque, Kyoto) supplemented with 10 % horse serum (HS, Life Technologies, Carlsbad, CA), 5% fetal bovine serum (Sigma, St. Louis, MO, USA), 100 units/ml penicillin and 100 μg/ml streptomycin (both from Nacalai) at 37°C in a 5 % CO_2 atmosphere.

4. MTT assay

PC12 cells (5×10^3 cells/well) were seeded in poly-l-lysine-coated 96-well plate, and incubated at 37°C for 24 h. The cells were exposed to 50 ng/ml mouse NGF 2.5S (Grade II, Alomone Labs, Jerusalem, Israel) without serum for 48 h, and the medium was replaced with serum-free medium containing 50 ng/ml NGF and 0.1 μM $A\beta_{25-35}$ (Nacalai) with or without samples. The cells were further incubated for 24 h, and then the medium was replaced to the one containing 10% MTT reagent (Sigma). After another 4 h incubation, DMSO was added to the medium, and the optical density (OD) value was measured at 570 nm.

5. Neurite-like outgrowth evaluation

PC12 cells (3×10^3 cells/well) were seeded in poly-l-lysine-coated 96-well plate, and incubated for 24 h. The cells were exposed to 200 ng/ml mouse NGF 2.5S without serum for 48 h, and the medium was replaced with serum-free medium containing 200 ng/ml NGF and 3 μM $A\beta_{25-35}$ with or without samples. After 24 h incubation, a morphometric analysis was done on digitalized images of PC12 cells taken with an inverted microscope (Nikon Coolpix 4500, Nikon, Tokyo). Five random fields with more than 50 cells were captured, and the cells that had at least one neurite with a length equal to the cell body diameter were counted. Average neurite-like outgrowth length was determined by manually tracing the neurite using Image J software.

Results:

1. MTT assay results

1.1 Aβ suppressed cell viability.

To investigate the suppression of Aβ on cell viability, we set the concentration of Aβ at 0.01, 0.03, 0.1, 0.3, 1 and 3 μM to determine the rate of cell viability. Aβ-treatment for 24 h significantly reduced the viability of PC12 cells in dose-dependent manners, and the survival percentages of cells incubated with different concentrations of Aβ were from 88% to 31%. Finally, we chose Aβ-concentration at 0.1 μM, which decreased the cell viability rate to approximately 60% (Figure 1).

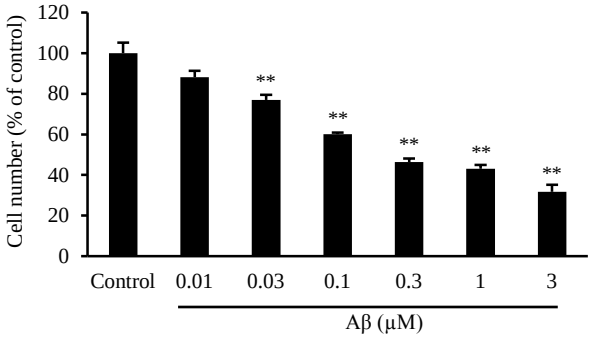

Figure 1 Effects of Aβ on cell viability in PC12 cells. PC12 cells were cultured with nerve growth factor (NGF) (50 ng/ml) for 48 h and then Aβ (0.01, 0.03, 0.1, 0.3, 1 and 3 μM) for 24 h. Each column represents the mean ± SE (n = 6). $^{**}P < 0.01$ *vs* control group treated without Aβ, as evaluated by Bonferroni/Dunnett's multiple t test.

1.2 Extracts of SMS and its composed crude drugs protect cells from Aβ-induced cell injury.

Hot water extract of SMS, MeOH-soluble and MeOH-insoluble fractions of each crude drug were prepared to determine their preventive effects on Aβ-induced cell injury. Incubation with 0.1 μM of Aβ made cell survival percentage declining to 52%, and hot water extract of SMS (1 mg/ml), MeOH-insoluble fraction of Ginseng (1 mg/ml) and MeOH-insoluble fraction of Ophiopogon Tuber (1 mg/ml) displayed the significant preventive effects on Aβ-induced reduction of cell viability. Their recovery rates were 96%, 97% and 72%, respectively (Figure 2).

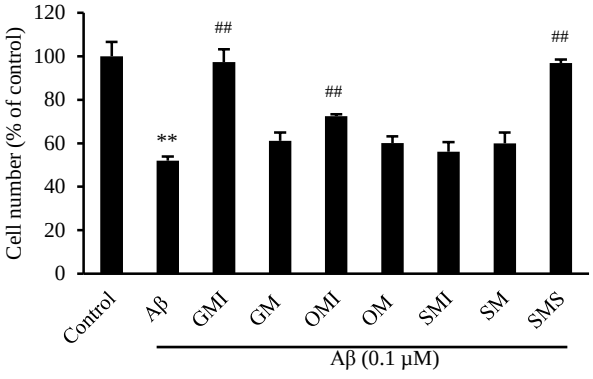

Figure 2 Effects of the extracts of SMS and its composed crude drugs on Aβ-induced reduction of PC12 cells viability. PC12 cells were cultured with nerve growth factor (NGF) (50 ng/ml) for 48 h, and then Aβ (0.1 μM) with or without each sample (1 mg/ml) for 24 h. Each column represents the mean ± SE (n = 6). $^{**}P < 0.01$ *vs* control group without Aβ, $^{\#\#}P < 0.01$ *vs* Aβ-group without samples, as evaluated by Bonferroni/Dunnett's multiple t test. GMI, MeOH insoluble fraction of Ginseng extract; GM, MeOH soluble fraction of Ginseng extract; OMI, MeOH insoluble fraction of Ophiopogon Tuber; OM, MeOH soluble fraction of Ophiopogon Tuber; SMI, MeOH insoluble fraction of Schizandra Fruit; SM, MeOH soluble fraction of Schizandra Fruit.

1.3 Ginseng hot water extract protected cells from Aβ-induced cell injury.

Ginseng hot water extract (GWE) was prepared to examine the possible beneficial effects on the viability of

Aβ-exposed PC12 cells. Treatment with GWE (0.01, 0.03, 0.1, 0.3 and 1 mg/ml) resulted in significantly higher cell viability compared with the Aβ-exposed cells without GWE treatment, the cell survival percentages were from 59% to 110%, and the improving effect was in a concentration dependent manner (Figure 3).

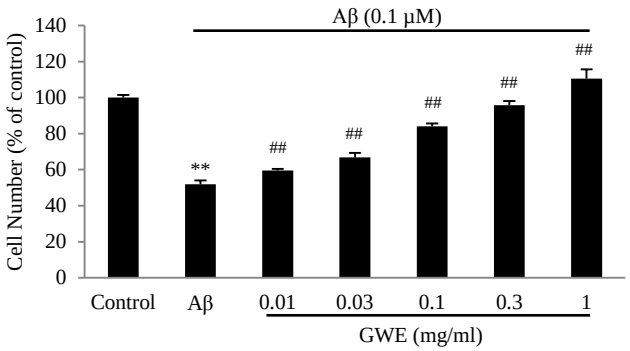

Figure 3 Effects of Ginseng hot water extract (GWE) on Aβ-induced PC12 cells viability reduction. PC12 cells were cultured with nerve growth factor (NGF) (50 ng/ml) for 48 h, and then Aβ (0.1 μM) with or without GWE (0.01, 0.03, 0.1, 0.3 and 1 mg/ml) for 24 h. Each column represents the mean ± SE (n = 6). $^{**}P < 0.01$ *vs* control group without Aβ, $^{\#\#}P < 0.01$ *vs* Aβ group without samples, as evaluated by Bonferroni/Dunnett's multiple t test.

1.4 Ginsenosides and schisandrin protect cells from Aβ-induced cell injury.

We treated cells with ginsenoside Rb_1, Rd, Rh_1, Rh_2, Rg_1, Rg_3, F_1, F_2, schisandrin and the combination use of ginsenoside Rh_1 and schisandrin at 50 μM to investigate their influence on cell injury. All ginsenosides and schisandrin didn't show the protective effects on Aβ-induced reduction of PC12 cells activity (Figure 4).

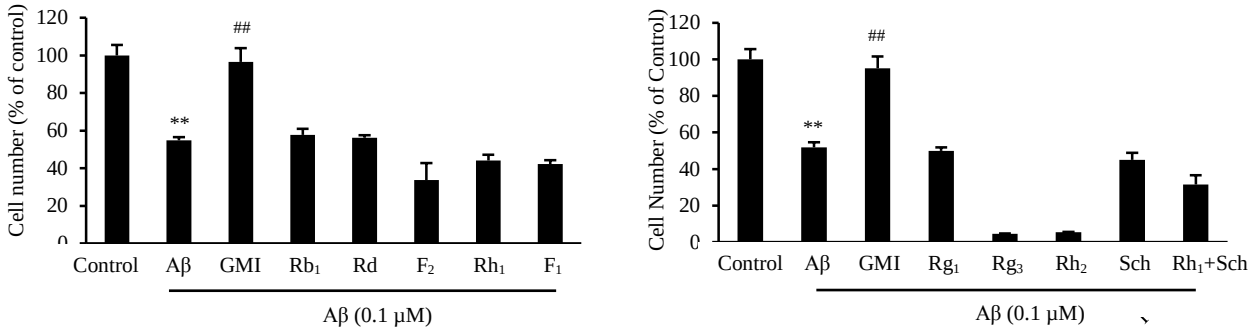

Figure 4 Effects of ginsenosides and schisandrin (Sch) on Aβ-induced reduction of PC12 cells viability. PC12 cells were cultured with nerve growth factor (NGF) (50 ng/ml) for 48 h and then Aβ (0.1 μM) with or without ginsenosides and schisandrin (50 μM) for 24 h. Each column represents the mean ± SE (n = 6). $^{**}P < 0.01$ *vs* the control group without Aβ, $^{\#\#}P < 0.01$ *vs* the Aβ group without samples, as evaluated by Bonferroni/Dunnett's multiple t test.

2. Neurite outgrowth evaluation results

2.1 The extract of SMS and its composed crude drugs protected cells against Aβ-induced reduction of neurite-like outgrowth.

The extract of SMS and its composed crude drugs were prepared to investigate the influence on Aβ-induced cell neurite-like outgrowth reduction. SMS extract (1 mg/ml) and MeOH-soluble fraction of ginseng (1 mg/ml) exhibited significant preventive effects on Aβ-induced reduction of neurite-like outgrowth in PC12 cell. SMS extract could increase the average neurite length to 0.0378 μm, respectively, MeOH-soluble fraction of ginseng extract could increase the average neurite length 0.0381 μm. MeOH-soluble fraction of Schizandra Fruit (1 mg/ml) and MeOH-insoluble fraction of Ophiopogon Tuber (1 mg/ml) treatment also can increase the average neurite length inhibited by Aβ, but there is no significantly statistical difference from Aβ treated cells (Figure 5).

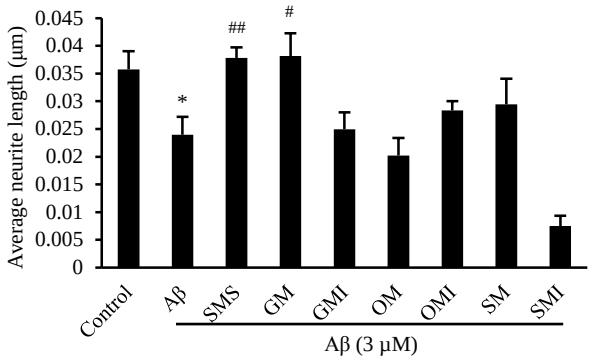

Figure 5 Effects of the extract of SMS and its composed crude drugs on Aβ-induced reduction of neurite-like outgrowth in PC12 cells. PC12 cells were cultured with nerve growth factor (NGF) (200 ng/ml) for 48 h, and then cultured with NGF with or without Aβ (3 μM) and each sample (1 mg/ml) for 24 h. Each column represents the mean ± SE (n = 3). *P < 0.05 *vs* control group without Aβ, $^{\#}P$ < 0.05, $^{\#\#}P$ < 0.01 *vs* the Aβ group without samples, as evaluated by Bonferroni/Dunnett's multiple t test. GMI, MeOH insoluble fraction of Ginseng extract; GM, MeOH soluble fraction of Ginseng extract; OMI, MeOH insoluble fraction of Ophiopogon Tuber; OM, MeOH soluble fraction of Ophiopogon Tuber; SMI, MeOH insoluble fraction of Schizandra Fruit; SM, MeOH soluble fraction of Schizandra Fruit.

2.2 Fractions of Ginseng protect cells against Aβ-induced neurite-like outgrowth reduction.

To elucidate the active ingredients of Ginseng, we partitioned the Ginseng extract into n-hexane-, BuOH-, and water-fractions. The BuOH fraction (40.1 μg/ml) displayed a similar preventive effect as the MeOH soluble fraction (1000 μg/ml) and increased the average neurite length to 0.0375 μm. The water-fraction (959 μg/ml) slightly increased the average neurite length to 0.0316 μm, but its rescue effect is weaker than BuOH-fraction, then we focused on the BuOH-fraction of Ginseng (Figure 6).

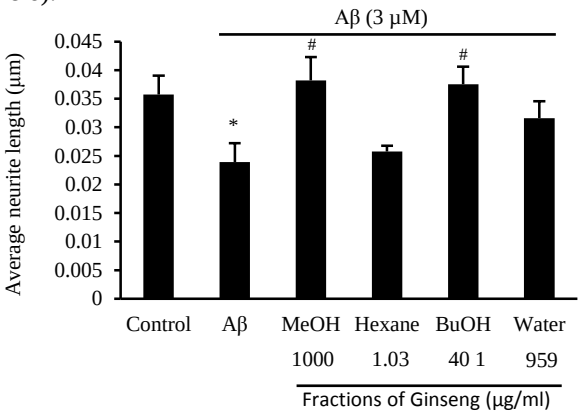

Figure 6 Effects of the fractions of Ginseng on Aβ-induced reduction of neurite-like outgrowth in PC12 cells. PC12 cells were cultured with nerve growth factor (NGF) (200 ng/ml) for 48 h, and then Aβ (3 μM) with or without each fraction for 24 h. Each column represents the mean ± SE (n = 3). *P < 0.05 *vs* control group without Aβ, $^{\#}P$ < 0.05 *vs* Aβ group without samples, as evaluated by Bonferroni/Dunnett's multiple t test.

2.3 Ginsenosides protected the cells against Aβ-induced reduction of neurite-like outgrowth.

HPLC analysis suggested that the BuOH fraction contained ginsenoside Rh_1, Rd, Rb_1, F_1, F_2, compound K. When PC12 cells were treated with each detected ginsenoside at a concentration of 10 μM, ginsenoside Rb_1 and F_2 exhibited slight preventive effects. Ginsenoside Rb_1 increased average neurite length to 0.0312 μm, and ginsenoside F_2 increased to 0.0337 μm. Compound K exhibited excessive cytotoxicity for the PC12 cells and was precluded from measurement of neurite-like outgrowth (Figure 7).

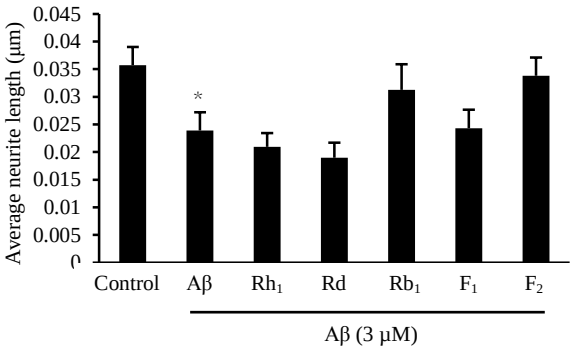

Figure 7 Effects of ginsenosides on Aβ-induced reduction of neurite-like outgrowth in PC12 cells. PC12 cells were cultured with nerve growth factor (NGF) (200 ng/ml) for 48 h, and then cultured with NGF with or without Aβ (3 μM) and ginsenosides (10 μM) for 24 h. Each column represents the mean ± SE (n = 3). *P < 0.05 *vs* control group without Aβ, as evaluated by Bonferroni/Dunnett's multiple t test.

Discussion:

Shengmaisan is a classic formula of traditional Chinese medicine to tonify *qi* and *yin*, and has been applied for heart and blood diseases for thousand years in China. Recent research showed SMS possessing cognitive-enhancing activity[7]. My previous studies also verified that the SMS extract-pretreatment significantly attenuated $AlCl_3$ and D-gal-induced rat learning and memory impairment, inhibited generation of $A\beta_{1\text{-}40}$ plaque, and increased Bcl-2 and ChAT in hippocampus by some key metabolic pathways. Lipid metabolism and energy metabolism were all involved in the improvement of SMS on delaying AD development. Here, I demonstrated that SMS exhibited significant preventive effects against Aβ-induced reduction of PC12 cells activity and neurite-like outgrowth length, and suggested that SMS was effective for preventing neurodegeneration treated with Aβ.

The monarch drug Ginseng in SMS is believed to reinforce vital energy, and its neuroprotective activity on different neurologic diseases has been investigated[8,9,10]. There are many active constituents in Ginseng, such as ginsenosides, ginseng polysaccharides and ginseng peptides[11]. In the present experiment, GWE exhibited significant preventive effects against Aβ-induced reduction of PC12 cells activity. The main constituents in GWE are ginseng polysaccharides, oligosaccharides and peptides, some researches had demonstrated that oligosaccharides and peptides from ginseng root can enhance memory in scopolamine-induced dementia in rats[12.13]. Ginseng pectins, the main active compounds in ginseng polysaccharides, also showed protective effects on neuronal cells against H_2O_2-induced oxidative stress *via* regulating the pro-survival ERK/MAPK and Akt pathways[14].

The NGF-induced differentiation of PC12 cells is a well-established *in vitro* model for neurite outgrowth research. Here, the NGF-induced PC12 cell differentiation model was established for screening effective material in SMS that could promote neurite outgrowth. By activity-guided fractionation, ginseng BuOH-fraction containing ginsenosides showed powerful beneficial effects on preventing Aβ-induced reduction of neurite-like outgrowth from in differentiated PC12 cells, and among several ginsenosides, ginsenoside Rb_1 and F_2 exhibited preventive effects on Aβ-exposed reduction of neurite-like outgrowth in PC12 cells. Ginsenoside Rb_1 has been reported to be the primary ginsenoside responsible for the neuroprotective effects of neurodegenerative diseases, and Rb_1-pretreatment can protect neuronal cells from Aβ toxicity through an antioxidant pathway[15,16]. In my study, cooperated incubation with ginsenoside Rb_1 and Aβ didn't show the protective effects on reduction of PC12 cells activity, this result is consistent with a previous research, which revealed that Rb_1 can't reduce Aβ-induced cytotoxicity in the SK-N-SH human neuroblastoma cell line and suggested that Rb_1 had neurotrophic and selective neuroprotective actions[17]. Ginsenoside F_2 is one of the metabolites of Rb_1 generated by intestinal bacteria, and the previous study revealed the strongest preventive activity of ginsenoside F_2 on

oxaliplatin-induced decrease of neurite-like outgrowths in differentiated PC12 cells[6]. However, the mechanism of which ginsenoside Rb_1 and F_2 regulating Aβ-induced neurotoxicity is still not clearly and should be further studied.

In conclusion, my study reveals that SMS can prevent PC12 cells from Aβ about its reduction of the activity and neurite-like outgrowth, and that the effective compounds in SMS which protect Aβ-induced reduction of neurite-like outgrowth in PC12 cells were ginsenoside Rb_1 and F_2, which would play important roles in regulating Aβ-induced neurotoxicity. Its action mechanisms will be studied in future.

References:

1 Eliezer Masliah. Neuropathology: Alzheimer's in real time [J]. Nature, 2008, 451, 638-639.

2 D.J. Selkoe. Alzheimer’s disease: genes, proteins, and therapy, Physiol. Rev [J]. 2001, 81, 741-766.

3 Kwasi G. Mawuenyega, Wendy Sigurdson, Vitaliy Ovod, et al. Decreased Clearance of CNS Amyloid-β in Alzheimer’s Disease [J]. Science. 2010, 330(6012), 1774.

4 Russell H. Swerdlowa, Jeffrey M. Burnsa, Shaharyar M. Khanc. The Alzheimer's disease mitochondrial cascade hypothesis: Progress and perspectives [J]. Biochim. Biophys. Acta, 2014, 1842, 1219–1231.

5 L. A. T. Greene, A S Tischler. Establishment of a noradrenergic clonal line of rat adrenal pheochromocytoma cells which respond to nerve growth factor [J]. Proceedings of the National Academy of Sciences, 1976, 73(7), 2424-8.

6 Toshiaki Suzuki1, Ayano Yamamoto, Masahiro Ohsawa, et al. Ninjin’yoeito and ginseng extract prevent oxaliplatin-induced neurodegeneration in PC12 cells [J]. J Nat Med, 2015, 69(4), 531-7.

7 Giridharan VV, Thandavarayan RA, Konishi T. Effect of Shengmai-san on cognitive performance and cerebral oxidative damage in BALB/c mice [J]. J Med Food. 2011, 14(6):601-9.

8 Kim J, Kim SH, Lee DS, et al. Effects of fermented ginseng on memory impairment and b-amyloid reduction in Alzheimer’s disease experimental models [J]. J Ginseng Res, 2013, 37, 100e7.

9 Cho IH. Effects of Panax ginseng in neurodegenerative diseases [J]. J Ginseng Res, 2012, 36, 342e53.

10 Zhao Z, Kim YW, Wu Y, et al. Korean Red Ginseng attenuates anxiety-like behavior during ethanol withdrawal in rats [J]. J Ginseng Res, 2014, 15, 256e63.

11 Wenwen Ru, Dongliang Wang, Yunpeng Xu, et al. Chemical constituents and bioactivities of Panax ginseng (C. A. Mey.) [J]. Drug Discoveries & Therapeutics, 2015, 9(1):23-32.

12 Wang Y, Jiang RZ, Li GR, et al. Structural and enhanced memory activity studies of extracts from Panax ginseng root [J]. Food Chem, 2010, 119, 969e73.

13 Ting Xu, Xiangfeng Shen, Huali Yu, et al. Water-soluble ginseng oligosaccharides protect against scopolamine-induced cognitive impairment by functioning as an antineuroinflammatory agent [J]. J Ginseng Res, 2016, 40, 40211e219.

14 Yuying Fan, Chengxin Sun, Xiaoge Gao, et al. Neuroprotective effects of ginseng pectin through the activation of ERK/MAPK and Akt survival signaling pathways [J]. Molecular Medicine Reports, 2012, 5, 1185-1190.

15 Xie X, Wang HT, Li CL, et al. Ginsenoside Rb1 protects PC12 cells against beta-amyloid-induced cell injury [J]. Mol Med Rep, 2010, 3: 635e9.

16 Qian YH, Han H, Hu XD, Shi LL. Protective effect of ginsenoside Rb1 on beta amyloid protein(1-42)-induced neurotoxicity in cortical neurons [J]. Neurol Res, 2009, 31: 663e7.

17 Rudakewich M, Ba F, Benishin CG. Neurotrophic and neuroprotective actions of ginsenosides Rb(1) and Rg(1) [J]. Planta Med. 2001, 67(6):533-7.

作成日：２０１７年２月２４日

Adolescent Idiopathic Scoliosis Patients with Lumbosacral Transitional Vertebra May Associated with High Pelvic Parameters

特発性側弯症における腰仙椎移行椎とペルビックインシデンスの関係

研究者氏名　劉　鉄（第 38 期笹川医学研究者）
中国所属機関　首都医科大学附属北京朝阳医院
日本研究機関　名城病院整形外科/脊椎脊髄センター
指導責任者　川上　紀明　教授
共同研究者名　辻　太一，小原　徹哉，齋藤　敏樹

Abstract

Study design. Retrospective radiographic study on the pelvic parameters in adolescent idiopathic scoliosis(AIS) patients with or without lumbosacral transitional vertebra (LSTV).

Summary of background data LSTV is a common congenital anomaly in spinal pelvic region. There has been a lot of studies on the relationship between LSTV and low back pain or disc degeneration. Little is known of its effect on pelvic parameters and lumbar lordosis in AIS patients. Since it happens in lumbosacral area, which may have potential to influence pelvic parameters.

Objective (1) To study the prevalence of LSTV in AIS patients using CT three-dimensional reconstruction (2) Compare the pelvic parameters in adolescent idiopathic scoliosis patients with LSTV or without LSTV.

Methods This study included all the AIS patients who underwent surgery in a single center dated from 2003 to 2015. Anteroposterior plain radiographs and CT three-dimensional reconstructions were evaluated regarding the presence of LSTV. Castellvi type II, III, IV were identified and chosen for further studies. AIS patients with LSTV were defined LSTV group, while non-LSTV group were defined as those sex, age and curve type matched controls who were selected randomly among AIS patients without LSTV. Pelvic parameters were measured on the lateral radiographs which included pelvic incidence (PI), sacral slope(SS) and pelvic tilt(PT). Pelvic parameters were compared between LSTV group, non-LSTV group and historical data.

Results A total of 491 AIS patients with both full length anteroposterior and lateral radiographs and CT scans were included in this study. Of these patients, 33 patients were found with LSTV Castellvi type II, III, IV. Mean age of the patients with and without LSTV were 15.9±3.2 years old and 15.7±2.6 years old respectively. The mean PI in LSTV group and non-LSTV group were 65.0±10.0˚ and 45.4±8.7˚ respectively, which showed a significant difference between the two groups (P<0.001). The mean PT in LSTV and non-LSTV group were 20.1±9.8˚ and 9.1±9.1˚, and the mean SS in the two groups were 45.7±9.4˚ and 37.4±7.0˚ respectively. The two components PT and SS were also significantly higher in LSTV group than non-LSTV group. Lumbar lordosis in LSTV group was accordingly significantly higher. Compare to historical data in previous reports, the results showed pelvic parameters in AIS patients with LSTV was significantly higher not only than healthy subjects but also than common AIS patients(P<0.001).

Conclusions This study revealed that AIS patients with LSTV had higher pelvic parameters and lumbar lordosis than those without LSTV and historical data. Surgeons should keep an eye on the transitional anomalies and its related high pelvic parameters when make a surgical plan, as they may impact the selection of instrumentation levels as well as surgical results.

Keywords transitional vertebrae; adolescent idiopathic scoliosis; pelvic parameters; pelvic incidence; sagittal balance

Introduction

Pelvic parameters which were first defined by Legaye at al, determine pelvic shape, orientation, lumbar lordosis and even entire underlying sagittal spinal profile. [1, 2] Pelvic incidence(PI) is the most important amongst pelvic parameters, as it plays a key role in maintaining sagittal balance. Abnormal pelvic parameters are considered to be a risk factor for sagittal decompensation and failure after adult scoliosis instrumentation, which is usually related with poor

clinical results. [3, 4]Various factors are thought to have an influence on the magnitude of pelvic parameters: age[5], sex, race,[6] curve type[7] and so on. Besides, malformations within lumbosacral transitional region may also have a potential to change pelvic morphology and pelvic parameters.

Lumbosacral transitional vertebra(LSTV) is a very frequently observed congenital lumbosacral anomaly, which characterized as unilateral or bilateral articulation or osseous bridging between the transverse process of L5 and sacral alar.[8, 9] As a common spinal-pelvic morphological malformation, LSTV has been frequently discussed in the literature.[8, 10-12] Most of these reports were focus on its connection with low back pain and disc degeneration. As lumbosacral structures were thought to play an important role in determination of shear and compressive forces applied on the anterior and posterior elements of lumbar vertebral column. [13] Relative biomechanical studies also have showed a strong correlation between lumbar-pelvic pathologies and pelvic morphology,[14, 15] which indicated LSTV may have a potential impact on pelvic parameters. High clinical value has been put on pelvic parameters nowadays in the evaluation and treatment planning for adolescent idiopathic scoliosis(AIS) correction. However, little is known regarding the impact of LSTV on spinal-pelvic parameters in patients with AIS.

Moreover, in AIS patients, the radiographs we routinely use for clinical treatment are full-spine films, which sometimes would be very obscure to detect structures in lumbosacral region. As computed tomography(CT) three-dimensional reconstruction is becoming more and more popular in surgical planning, which is more accurate, herein, the purpose of this study was to (1) To study the prevalence of LSTV in AIS patients using CT three-dimensional reconstruction (2) Compare the pelvic parameters in adolescent idiopathic scoliosis patients with LSTV or without LSTV.

Materials and Methods

This study has been approved by the Institutional Review Board(IRB). This was a retrospective study which included AIS patients who underwent surgery from a single center between 2003~2015. Inclusion criteria comprised a diagnosis of AIS, treatment of spinal instrumentation, perioperative full length standing radiographs and preoperative computed tomography(CT) three-dimensional reconstruction available. Exclusion criteria comprised scoliosis due to other causes, and incomplete imaging studies. Patients with history of trauma or spine surgery were also excluded. Demographic and radiographic data were reviewed and analyzed. Anteroposterior radiographs and CT were evaluated regarding the presence of LSTV. Classification of LSTV was modified according to Castellvi et al[16]. Castellvi type II, III, IV were identified and chose for further studies, while type I were excluded for little clinical significance. AIS patients with LSTV were defined LSTV group, while non-LSTV group were defined as those sex, age and curve type matched controls who were selected randomly among AIS patients without LSTV.

Pelvic parameters were measured on the lateral radiographs which included pelvic incidence (PI), sacral slope(SS) and pelvic tilt(PT). Pelvic parameters were measured modified according to Legaye et al.[1] Briefly, for patients with Castellvi type II patients, the angle between a line perpendicular to the S1 endplate at its midpoint and the line connecting this point to the middle axis of the femoral heads, since L5/S1 was still mobile. Lumbar lordosis was measured from T12 upper endplate to S1 upper endplate. For patients with over Catellvi type III grade LSTV (Figure 2), L5 instead of S1 was chosen, since the mobility of L5/S1 was seriously limited. LL was measured from T12 upper endplate to L5 endplate. PT was measured as angle between line connecting the center of the bicoxo-femoral axis to the midpoint of the sacral endplate and vertical axis. SS was measured as angle between line passing through the inferior endplate of the sacral endplate and horizontal axis. Figure1 was displayed as our workflow chart. pelvic parameters were compared between LSTV group, non-LSTV group and historical data.

Statistical analysis was done via R GUI version 3.3.1 and Microsoft Excel 2016, with *P* values of less than 0.05 considered to be statistically significant. Independent *t* test was used for sagittal parameter comparisons between LSTV group, non-LSTV group, and historical data.

Results

A total of 491 AIS patients with both full length anteroposterior and lateral radiographs and CT scan three-dimensional reconstructions were included in this study. Of these patients, 33 patients were found with LSTV Castellvi type II, III, IV. The detailed distribution was listed in Table1. All patients with LSTV were paired by sex, age and curve type with

AIS patients without LSTV. There were 2 males and 31 females in each group. Mean age of patients with and without LSTV were 15.9±3.2 years old and 15.7±2.6 years old respectively. Scoliosis curve type was classified following Lenke classification(Table2). [17]

The mean PI in LSTV group and non-LSTV group were 65.0±10.0˚ and 45.4±8.7˚ respectively, which showed a significant difference between the two groups (P<0.001). The mean PT in LSTV and non-LSTV group were 20.1±9.8˚ and 9.1±9.1˚, and the mean SS in the two groups were 45.7±9.4˚ and 37.4±7.0˚ respectively. The two components PT and SS were also significantly higher in LSTV group than non-LSTV group (P<0.001(PT, SS), Table3). Accordingly, LL was significantly higher in LSTV group than in non-LSTV group.

We further compared the pelvic parameters in the current study with AIS patients and healthy subjects in the previous reports (Table 4).[7, 18, 19] The results showed PI in LSTV group was significantly higher not only than healthy subjects but also than AIS patients in previous reports(P<0.001). However, there was no significant difference of theses parameters between non-LSTV group in the current study and Qiu et al study.[18]

Discussion

In this study, we compared the pelvic parameters between AIS patients with and without LSTV. Castellvi type II, III, IV were included, while Castellvi type I was excluded as it usually involved neither an articulation or bony fusion of the transverse process to the sacrum, which suggested a less possible state of a disease or a syndrome that may have no relevant clinical significance. In the general population, the incidence rate of LSTV varies from 4% to 36%. While in this study the LSTV prevalence in AIS patients was 6.57%. As CT three-dimensional reconstruction can provide more anatomical details, thus a more accurate frequency of LSTV in AIS can be obtained. The prevalence of LSTV may be also affected by the different populations and diagnostic criteria.

All spino-pelvic parameters were found significantly higher in LSTV group than non-LSTV group. The mean PI in LSTV group was 65.0±10.0°, defined by Boulay et al as high PI, [14]which might have some significant influence on sagittal plane balance. The two component PT and SS were also found significantly higher than non-LSTV group(Table4). Compare to the independent previous reports, pelvic parameters in LSTV group was also significantly higher than AIS patients and normal subjects. In non-LSTV group, pelvic parameters were quite the similar with Qiu et al study, which were smaller than those from the data of Mac-Thiong et al and Upansani et al. [7, 19, 20]This may be because Asian people have quite similar body shape and pelvic morphology, which also supported that race is a factor that influence on pelvic parameters.

For patients with LSTV, there may have some controversies in measuring pelvic parameter, because sometimes it is very hard to decide whether to measure L5 or S1 for reference due to the anatomical variations. [21, 22]Dominguez et al proposed L5 incidence as a good substitute for traditional pelvic incidence, [22]But there was no standard data for reference. So, here we still chose classic pelvic incidence with some modifications for evaluation, since it has been fully studied in scoliosis patients' population. In this study, pelvic anatomy and L5/S1 motion were both taken into account. In patients with Castellvi II, although there was articulation between transverse process, L5/S1 segment was still mobile. So, in this case, the mid-point of S1 was chosen for PI calculation. For patients with higher grade LSTV(over Castellvi III), there were unilateral or bilateral boney fusion between transverse process. L5/S1 segment was no longer mobile. In this case, L5 acted as the new S1, so L5 was taken into PI calculation.

There are several possible reasons for the high pelvic parameters in LSTV group. LSTV usually includes morphologic characteristic changes such as squaring of upper sacral segment or wedging of the lowest lumbar segment, [23]which represent cranial and cauda shifts of the spine and to a new sagittal balance. Many studies revealed a decreased disc height on radiograph between a lumbar transitional segment and sacrum compared with L5/S1 disc space in normal population. [24-26] In addition, the facet joints between transitional L5 and the sacrum were found usually hypoplastic or even nonexistent.[12] These changes may lead to weight bearing mechanism and a compensation of sacrum orientation which co-changed with increased PI. And the body weight transfer through lumbar-pelvic area result an extension to the sacrum via sacral ligaments.[8] The anatomic malformation on the transferring pathway may have an effect on the pelvic parameters. Furthermore, in a cadaver study, Aihara et al found that iliolumbar ligament at the level

immediately above transitional vertebrae were thinner and weaker in patients with LSTV than those without LSTV. [27] While the stress adjacent to the transitional area was higher than normal, as pseudoarthroses and bony fusion limited transitional segment motion.[10] High pelvic parameters may represent an adaptive mechanism to compensate for the pathological changes related to preserve stability.

To the best of our knowledge, this is the first study to systematically investigate the pelvic parameters in AIS patients with LSTV using age and curve type matched study. Although there were only 491 AIS patients included, the results suggest surgeons to mention LSTV and its related pelvic change in AIS in clinical practice. When making a surgical plan, surgeons should keep an eye on the transitional anomalies and its related high pelvic parameters, as they may impact the selection of instrumentation levels as well as surgical results.

Conclusion

In conclusion, this study showed that pelvic parameters in AIS patients with LSTV were significantly higher than those without LSTV, as well as significantly higher than the historical data. Lumbar lordosis was accordingly significantly bigger in patients with LSTV. Surgeons should keep an eye on the transitional anomalies and its related high pelvic parameters when make a surgical plan, as they may impact the selection of instrumentation levels as well as surgical results.

Reference

1. Legaye J, Duval-Beaupere G, Hecquet J, Marty C. Pelvic incidence: a fundamental pelvic parameter for three-dimensional regulation of spinal sagittal curves. Eur Spine J. 1998;7(2):99-103.
2. Le Huec JC, Aunoble S, Philippe L, Nicolas P. Pelvic parameters: origin and significance. Eur Spine J. 2011;20 Suppl 5:564-71.
3. De Giorgi S, De Giorgi G, Borracci C, Tafuri S, Piazzolla A, Moretti B. Adult scoliosis: age-related deformity and surgery. Eur Spine J. 2014;23 Suppl 6:597-603.
4. Deinlein D, Bhandarkar A, Vernon P, et al. Correlation of Pelvic and Spinal Parameters in Adult Deformity Patients With Neutral Sagittal Balance. Spine Deform. 2013;1(6):458-63.
5. Mac-Thiong JM, Berthonnaud E, Dimar JR, 2nd, Betz RR, Labelle H. Sagittal alignment of the spine and pelvis during growth. Spine (Phila Pa 1976). 2004;29(15):1642-7.
6. Lonner BS, Auerbach JD, Sponseller P, Rajadhyaksha AD, Newton PO. Variations in pelvic and other sagittal spinal parameters as a function of race in adolescent idiopathic scoliosis. Spine (Phila Pa 1976). 2010;35(10):E374-7.
7. Mac-Thiong JM, Labelle H, Charlebois M, Huot MP, de Guise JA. Sagittal plane analysis of the spine and pelvis in adolescent idiopathic scoliosis according to the coronal curve type. Spine (Phila Pa 1976). 2003;28(13):1404-9.
8. Apazidis A, Ricart PA, Diefenbach CM, Spivak JM. The prevalence of transitional vertebrae in the lumbar spine. Spine J. 2011;11(9):858-62.
9. Bron JL, van Royen BJ, Wuisman PI. The clinical significance of lumbosacral transitional anomalies. Acta Orthop Belg. 2007;73(6):687-95.
10. Farshad-Amacker NA, Herzog RJ, Hughes AP, Aichmair A, Farshad M. Associations between lumbosacral transitional anatomy types and degeneration at the transitional and adjacent segments. Spine J. 2015;15(6):1210-6.
11. Lee CS, Ha JK, Kim DG, Hwang CJ, Lee DH, Cho JH. The clinical importance of lumbosacral transitional vertebra in patients with adolescent idiopathic scoliosis. Spine (Phila Pa 1976). 2015;40(17):E964-70.
12. Konin GP, Walz DM. Lumbosacral transitional vertebrae: classification, imaging findings, and clinical relevance. AJNR Am J Neuroradiol. 2010;31(10):1778-86.
13. Roaf R. Vertebral growth and its mechanical control. J Bone Joint Surg Br. 1960;42-B:40-59.
14. Boulay C, Tardieu C, Hecquet J, et al. Sagittal alignment of spine and pelvis regulated by pelvic incidence: standard values and prediction of lordosis. Eur Spine J. 2006;15(4):415-22.
15. Roussouly P, Pinheiro-Franco JL. Sagittal parameters of the spine: biomechanical approach. Eur Spine J. 2011;20 Suppl 5:578-85.

16. Castellvi AE, Goldstein LA, Chan DP. Lumbosacral transitional vertebrae and their relationship with lumbar extradural defects. Spine (Phila Pa 1976). 1984;9(5):493-5.
17. Lenke LG, Edwards CC, 2nd, Bridwell KH. The Lenke classification of adolescent idiopathic scoliosis: how it organizes curve patterns as a template to perform selective fusions of the spine. Spine (Phila Pa 1976). 2003;28(20):S199-207.
18. Qiu Y, Yin G, Cao XB. [The influence of thoracic kyphosis on sagittal balance of the lumbosacral spine in thoracic idiopathic scoliosis patients]. Zhonghua Wai Ke Za Zhi. 2008;46(16):1237-40.
19. Upasani VV, Tis J, Bastrom T, et al. Analysis of sagittal alignment in thoracic and thoracolumbar curves in adolescent idiopathic scoliosis: how do these two curve types differ? Spine (Phila Pa 1976). 2007;32(12):1355-9.
20. Yong Q, Zhen L, Zezhang Z, et al. Comparison of sagittal spinopelvic alignment in Chinese adolescents with and without idiopathic thoracic scoliosis. Spine (Phila Pa 1976). 2012;37(12):E714-20.
21. Crawford CH, 3rd, Glassman SD, Gum JL, Carreon LY. Conflicting calculations of pelvic incidence and pelvic tilt secondary to transitional lumbosacral anatomy (lumbarization of S-1): case report. J Neurosurg Spine. 2017;26(1):45-9.
22. Dominguez D, Faundez A, Demezon H, Cogniet A, Le Huec JC. Normative values for the L5 incidence in a subgroup of transitional anomalies extracted from 147 asymptomatic subjects. Eur Spine J. 2016;25(11):3602-7.
23. Wigh RE, Anthony HF, Jr. Transitional lumbosacral discs. probability of herniation. Spine (Phila Pa 1976). 1981;6(2):168-71.
24. Nicholson AA, Roberts GM, Williams LA. The measured height of the lumbosacral disc in patients with and without transitional vertebrae. Br J Radiol. 1988;61(726):454-5.
25. Hsieh CY, Vanderford JD, Moreau SR, Prong T. Lumbosacral transitional segments: classification, prevalence, and effect on disk height. J Manipulative Physiol Ther. 2000;23(7):483-9.
26. O'Driscoll CM, Irwin A, Saifuddin A. Variations in morphology of the lumbosacral junction on sagittal MRI: correlation with plain radiography. Skeletal Radiol. 1996;25(3):225-30.
27. Aihara T, Takahashi K, Ogasawara A, Itadera E, Ono Y, Moriya H. Intervertebral disc degeneration associated with lumbosacral transitional vertebrae: a clinical and anatomical study. J Bone Joint Surg Br. 2005;87(5):687-91.

Tables

Table 1 Distribution of LSTV Type in AIS Patients Using Castellvi Classification

Castellvi Classification	
IIa	14(2.9%)
IIb	5(0.8%)
IIIa	5(0.8%)
IIIb	8(1.6%)
IV	1(0.2%)

Table 3 Comparison of Pelvic Parameters of AIS Patients with LSTV and without LSTV

Group	**LSTV(n=33)**	**non-LSTV(n=33)**	**P**
PI(˚)	65.0±10.0	45.4±8.7	<0.001
PT(˚)	20.1±9.8	9.1±9.1	<0.001
SS(˚)	45.7±9.4	37.4±7.0	0.001
LL(˚)	55.7±10.4	50.2±10.6	<0.05

Table 2 Preoperative Demographic Data

Group	LSTV	non-LSTV	*P*
Sex			
Male	2	2	-
Female	31	31	-
Age(yrs)	15.9±3.2	15.7±2.6	>0.05
Lenke			
1	19	19	-
2	5	5	-
3	1	1	-
5	5	5	-
6	3	3	-

Table 5 Comparison of Pelvic Parameters in AIS Patients with LSTV Type II and Type III,IV

Group	LSTV II	LSTV III，IV	*P*
PI(˚)	64.8±8.0	71.9±9.2	0.04
PT(˚)	21.1±6.5	25.1±10.1	0.22
SS(˚)	44.1±6.9	47.5±13.8	0.39

Table 4 Comparison of Pelvic Parameters in the current study with Historical Data of patients with AIS and Healthy Subjects

Study	Population	N	Age(yrs)	PI(˚)	PT(˚)	SS(˚)
Current Study	LSTV group	33	15.9±3.2	65.0±10.0*	20.1±9.8*	45.7±9.4*
Qiu et al	AIS	95	14.2±1.6	44.2±10.0†	9.2±8.5†	35.1±7.9†
Mac-Thiong et al	AIS	42	13.4±1.8	57.3±13.8†	8.4±7.9†	47.9±9.2
Upasani et al	AIS	53	14.5±2.0	55.5±12.2†	11.5±7.6†	45.8±11.5
Qiu et al	Health girls	33	13.6±2.1	44.6±11.5†	11.3±8.2†	33.3±8.2†
Upasani et al	Healthy subjects	50	13.5±2.0	45.5±8.5†	8.4±6.7†	37.1±8.5†

**Comparison of PI , PT and SS between historical data and LSTV group of the current study.*
† Significant difference(P<0.05)
PI, pelvic incidence;PT, pelvic tilt; SS, sacrum slope

注：本研究は 2017 年 1 月 7 日「JSDI 学会」にて口演発表

作成日：2017 年 2 月 14 日

Screen of co-activators in mutant EGFR

変異 EGFR 活性化因子のスクリーニング

研究者氏名	李　文雅（第 38 期笹川医学研究者）
中国所属機関	中国医科大学第一附属医院胸部外科
日本研究機関	京都大学医学部呼吸器外科学
	京都大学医学部放射線遺伝学
指導責任者	伊達　洋至　教授
	武田　俊一　教授
共同研究者名	毛受　暁史　助教

Abstract:

Epidermal growth factor receptor (EGFR) plays a critical role in development and various abnormal conditions. Mutations in EGFR attributes to progress of multiple cancers, especially lung cancer. However, the co-activators following mutant EGFR are less known. Thus, we not only detected the some possible markers which may act differently between wild-type and mutant EGFR according to previously reported studies, but also evaluated and screened potential target markers using Receptor Tyrosine Kinases (RTKs) phosphorylation antibody array.

Key Words:

EGFR; GEP100; Arf6; ERK; AKT; RTKs

Introduction:

Epidermal growth factor receptor (EGFR) plays a critical role in development, cell differentiation, proliferation and maintenance in both physiologically normal and cancerous conditions [1]. Mutations in EGFR are among the most common oncogenic mutations in non-small cell lung cancers (NSCLCs), which remains the most cancer both in incidence and in death rate globally (1.35 million deaths annually) [2, 3]. Experimentally and clinically, activated EGFR signal is believed to be involved in the induction of Epithelial Mesenchymal Transition (EMT) and tumor metastasis [4-7], both traditionally regarded as major reasons for bad outcome of various cancers. However, mounting studies have reported that mutant EGFR, which always contains activated EGFR, is associated with better prognosis when compared to wild-type tumors [8, 9]. Thus, it is plausible that there are some underlying mechanisms accounting for the mentioned phenomenal paradox. To evaluate that, we are aimed at screening potential co-activators following mutant EGFR signal.

Methods:

Cell culture and reagents. 293T cells were cultured at 37.0℃ by using Dulbecco's Modified Eagle Medium (DMEM) (Sigma-Aldrich, USA) medium supplemented with 10% fetal bovine serum (FBS)

Transfection. Mutant (Ex19del746-750aa)/wild-type EGFR cDNA transfections were performed by using Lipofectamine 2000 (Invitrogen) according to the manufacturer's instructions. Transfected cells were incubated for 24 h

or 48 h at 37.0℃ with 5% CO_2 using DME medium or starved medium (DMEM with 0.1% FBS) based on different analyses.

Western blotting analysis. Cells were lyzed with RIPA lysis buffer as previously described [10]. Cell lysates were separated with sodium dodecyl sulfate–polyacrylamide gel electrophoresis (SDS-PAGE), and then transferred to membrane, and detected by antibodies using ECL Plus Western blotting detection reagents (ATTO, Tokyo, Japan). The antibodies against EGFR, phospho-EGFR, Akt kinase, phospho-Akt, p44/42 Erk1/2 and phospho-p44/42 Erk1/2 were purchased from Cell Signaling (Beverly, MA, USA). The anti-Arf6 antibody was obtained from Santa Cruz Biotechnology (Santa Cruz, CA, USA).

GST-GGA pull down. Arf6 activities were measured using GST-GGA, as previously described [11]. Firstly, cells were transfected with EGFR-GFP, HA-GEP100, and Arf6-myc, and the cells were incubated for 24 h/48h in starved DME medium. Cells were lysed using GGA3-buffer (50 mM Tris-HCl (pH 8.0), 100 mM NaCl, 10 mM MgCl2, 0.005% SDS, 0.05% sodium deoxycholate, 1% Triton X-100, 10% glycerol with 1 mM phenylmethylsulfonyl fluoride, 1 mM Na3VO4, and 5 μg/ml aprotinin) after with/without 10 ng/ml of EGF stimulation for 10 minutes. Each lysate (500 μg) was precleared by incubation for 30 minutes with the glutathione magnetic beads (Thermo Scientific). Then, each lysate was incubated with 20 ug of GST-GGA3 bound to glutathione magnetic beads at 4°C gently rotated for 40 min, followed by washing three times with GGA3-buffer. Bound proteins were used to detect the presence of Arf6 by Western blotting with the antibody against Afr6 or myc, while total levels of EGFR-GFP, HA-GEP100, and Arf6-myc were measured using 30 ug of the precleared lysate.

Receptor Tyrosine Kinases (RTKs) phosphorylation antibody microarray analysis. The phosphorylation levels of 71 different human receptor tyrosine kinases (RTKs) in cell lysates were simultaneously detected using a RayBio Phosphorylation Antibody Array I Kit (RayBiotech, Inc., USA) briefly as follows. Cells from different groups were lysed and the total proteins were purified using the Cell and Tissue Protein Extraction Reagent. A total of 40 μg of protein extract, recommended by the manufacturer, was incubated with RTK glass slide subarrays spotted with 71 different anti-RTK antibodies. Then, the antibody array chips were washed and Biotin-conjugated anti-phosphotyrosine antibodies were added to each slide. After incubation with Fluorescent dye-Conjugated Streptavidin, the signals were visualized by a fluorescence scanner (GenePix 4000B).

Results:

Proper concentration of plasmid for Transfection. In order to adjust proper concentration of wild-type/mutant EGFR plasmid for 10cm-dish, four concentration were initially administered following 1ul, 2ul, 4ul, 8ul for each. Then, the transfection was confirmed by fluorescence and protein assay by western blotting, where we found 4ul plasmid per dish as optimal concentration to distinguish phophorylated status of EGFR between the wild-type and the mutant (Fig 1).

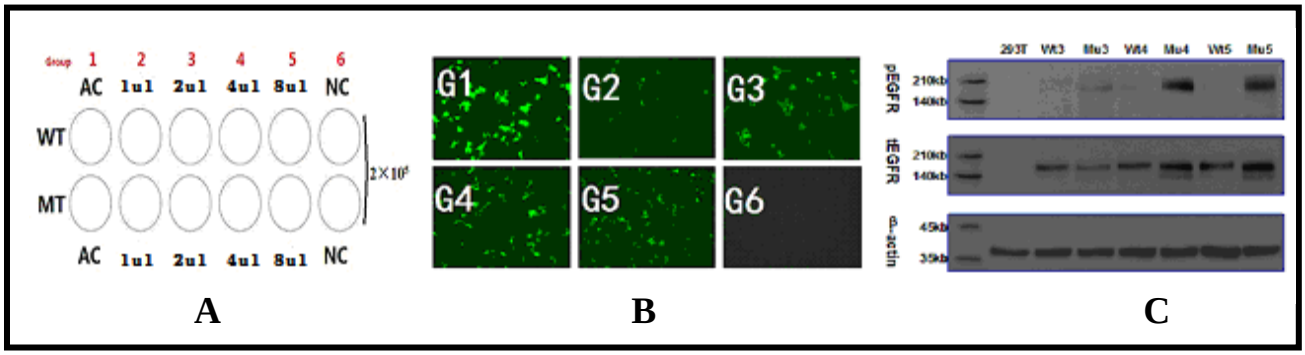

Fig 1. Selection of proper concentration of plasmid for Transfection. A: Different amount of plasmid were shown, AC as active control, and NC as negative control; B: Fluorescence in different concentration; C: Phospho-EGFR, pan-EGFR and β-actin were mainly detected by western blotting in NC, 2ul, 4ul, 8ul groups.

What role does Arf6 play in wild-type and mutant EGFR? Previous studies has illuminated that GEP100 can link EGFR to activate Arf6 and to promote cancer invasion [12], however, whether there is any difference between wild-type (Wt) and mutant EGFR (Mu) is unclear, since the latter always possesses active EGFR signal. Using western blotting, we detected the GST-GGA pull-down protein assay and total protein assay separately (Fig 2). Unfortunately, no band was observed in GST-GGA pull-down protein assay, which may be due to the invalidity of long-term stored GST-GGA probe. We will check it in future.

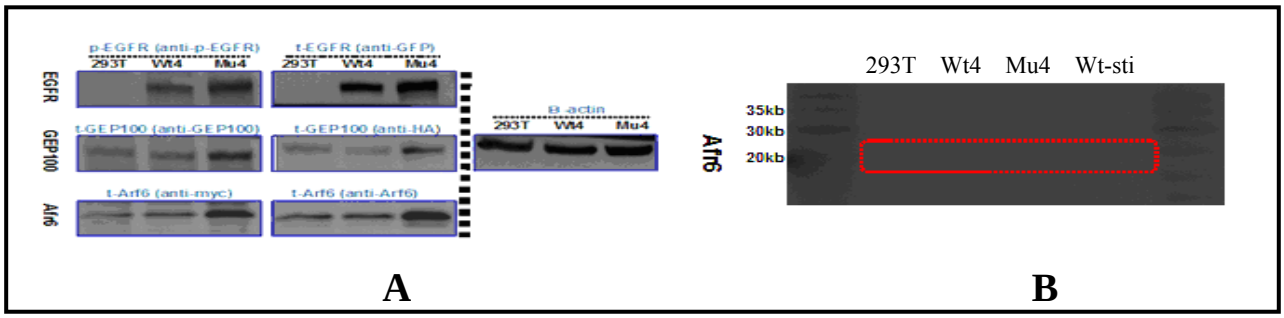

Fig 2. GST-GGA pull-down protein assay and total protein assay by western blotting. A: EGFR, GEP100 and Arf6 in total protein assay; B: Arf6 detected in GST-GGA pull-down protein assay.

The expression of ERK and AKT in wild-type and mutant EGFR. ERK/AKT is reported to be the downstream signals following EGFR activation [13]. In our research, phospho-ERK/AKT and pan-ERK and AKT were detected in 293T (N1), wild-stimulation group (wt-sti), wild-type and mutant EGFR groups after incubated 24h or 48h. The data showed that the expression of phospho-AKT did not associate with the phosphorylation of EGFR; whereas, a similar trend was observed on phospho-protein expression of ERK and EGFR (Fig 3).

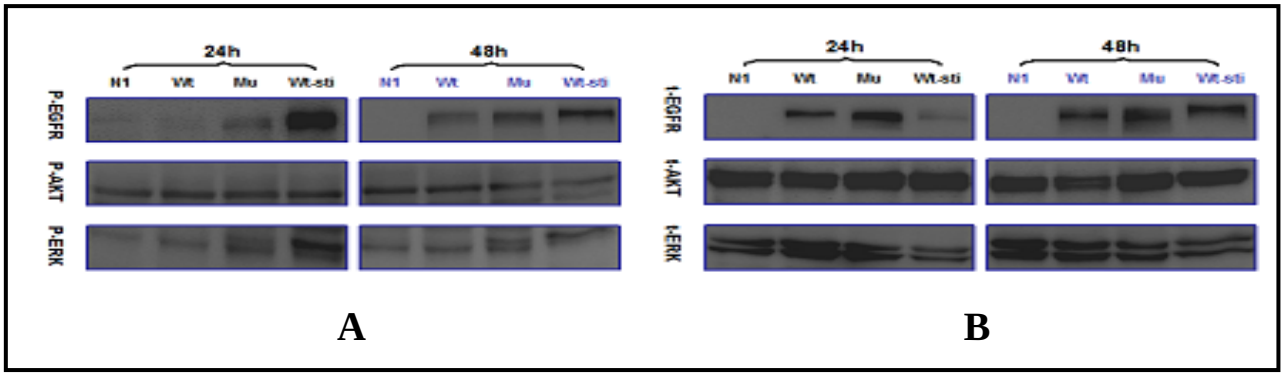

Fig 3. Phospho- and pan- EGFR, ERK and AKT were detected in 293T, Wt, Mu and Wt-sti groups. A: Results of phospho-protein in different groups; B: Results of pan-protein in different groups.

RTKs phosphorylation antibody array analysis. Using RTKs phosphorylation antibody array, 71 RTKs were evaluated among 293T, wild-type and mutant EGFR incubated for 24h, and wild-type with incubation of 48h. When compared the RTKs phosphorylation among N1, Wt-24h and Mu-24h, significant differences were discovered on Blk, EphA1, ErbB2, ErbB4, FGFR2, IGF-1R and SCFR ($P<0.05$). Similarly, PDGFR-β in addition to the above RTKs was expressed with statistical difference ($P<0.05$). It should be noted that FGFR1 and HGFR are always phosphorylated, even in the negative group. (Details in Fig 4)

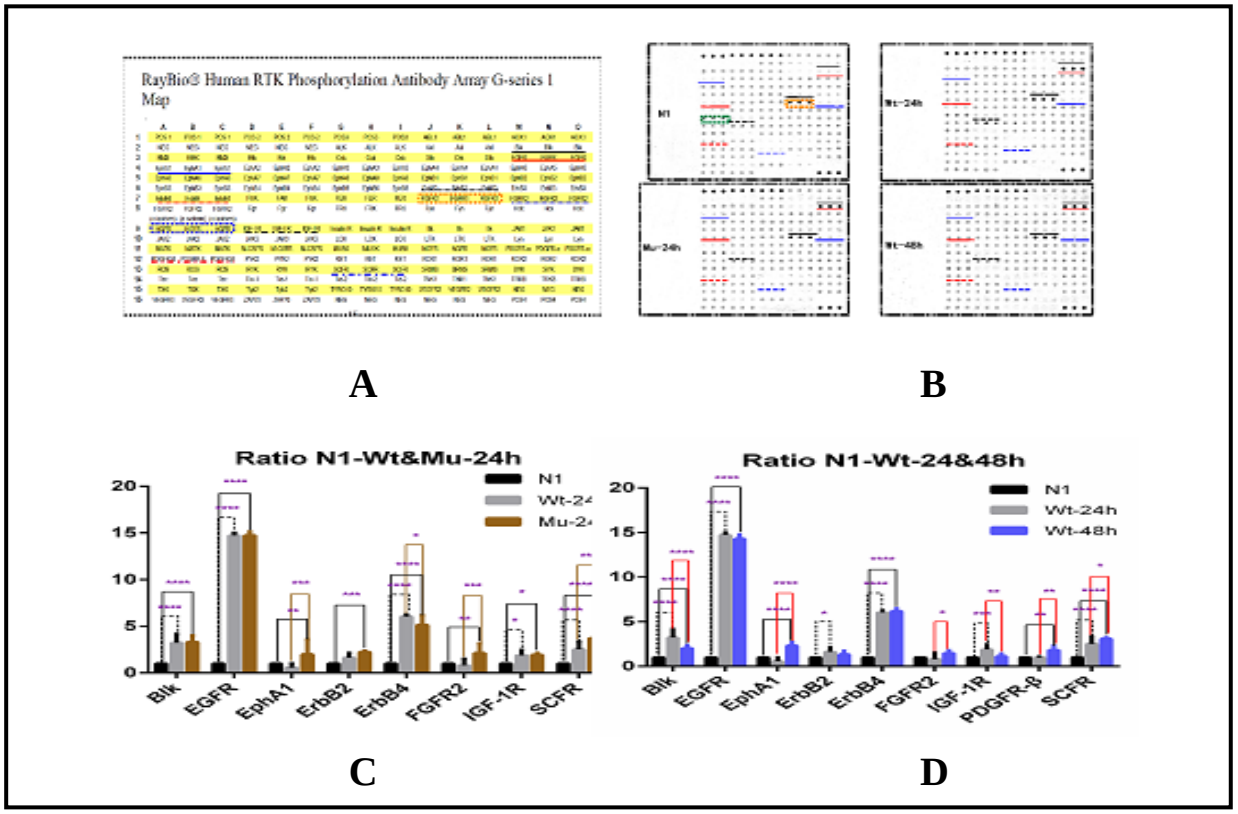

Fig 4. RTKs phosphorylation antibody array analysis. A: RTKs phophorylation antibody array map; B: Detection of spots by fluorescence; C: Markers with significant difference among N1 Vs. Wt-24h Vs. Mu-24h groups; D: Markers with significant difference among N1 Vs. Wt-24h Vs. Wt-48h groups.

Discussion:

In the present study, we first illustrated the role of ERK/AKT and GEP100/Arf6 axis in wild-type and mutant EGFR in 293T cell line. A little different to some literature, where both ERK and AKT cooperate with EGFR [14], here, phosphorated status of AKT was not consistent with EGFR in 293T cell, similar result to Margaret's report [15]. In the subsequent RTKs array analysis, we found FGFR1 and HGFR were always phosphorylated in 293T cell line, it remains unclear whether these two RTKs phosphorylation account for the activation of AKT or it is just due to cell line specificity. It needs to be illuminated in our future work. In addition, Arf6 was detected since after activation by EGFR it plays an important role in development of breast cancer [12]. However, no result was exhibited in our GST-GGA pull-down protein assay. We speculate it originate from the long-term stored GST-GGA probe, for the positive group

presented no result either.

To clarify potential markers acting different role in wild-type and mutant EGFR, RTKs phosphorylation antibody array was administered among four groups, and found that Blk, EphA1, ErbB2, ErbB4, FGFR2, IGF-1R, SCFR and PDGFR-β presented with obvious difference. Among them, EphA1, FGFR2, and SCFR should be noted as they vary markedly between wild-type EGFR and mutant EGFR. Because of the limited time, until now we have not completed the confirmation of these three markers, but already on road.

References:

1 Chapman AM, Sun KY, Ruestow P, Cowan DM, Madl AK. Lung cancer mutation profile of EGFR, ALK, and KRAS: Meta-analysis and comparison of never and ever smokers. Lung Cancer. 2016; 102:122-134.

2 Wang Y, Li RQ, Ai YQ, Zhang J, Zhao PZ, Li YF, He WJ, Xia YX, Li WH. Exon 19 deletion was associated with better survival outcomes in advanced lung adenocarcinoma with mutant EGFR treated with EGFR-TKIs as second-line therapy after first-line chemotherapy: a retrospective analysis of 128 patients. Clin Transl Oncol. 2015; 17:727-736.

3 Sequist LV, Rolfe L, Allen AR. Rociletinib in EGFR-Mutated Non-Small-Cell Lung Cancer. N Engl J Med. 2015; 373:578-579.

4 Thiery JP, Acloque H, Huang RY, Nieto MA. Epithelial-mesenchymal transitions in development and disease. Cell. 2009; 139:871-890.

5 Lu Z, Ghosh S, Wang Z, Hunter T. Downregulation of caveolin-1 function by EGF leads to the loss of E-cadherin, increased transcriptional activity of beta-catenin, and enhanced tumor cell invasion. Cancer Cell. 2003; 4:499-515.

6 Lo HW, Hsu SC, Xia W, Cao X, Shih JY, Wei Y, Abbruzzese JL, Hortobagyi GN, Hung MC. Epidermal growth factor receptor cooperates with signal transducer and activator of transcription 3 to induce epithelial-mesenchymal transition in cancer cells via up-regulation of TWIST gene expression. Cancer Res. 2007; 67:9066-9076.

7 Hsu F, De Caluwe A, Anderson D, Nichol A, Toriumi T, Ho C. EGFR mutation status on brain metastases from non-small cell lung cancer. Lung Cancer. 2016; 96:101-107.

8 Zhou C, Wu YL, Chen G, Feng J, Liu XQ, Wang C, Zhang S, Wang J, Zhou S, Ren S, Lu S, Zhang L, Hu C, Luo Y, Chen L, Ye M, Huang J, Zhi X, Zhang Y, Xiu Q, Ma J, You C. Erlotinib versus chemotherapy as first-line treatment for patients with advanced EGFR mutation-positive non-small-cell lung cancer (OPTIMAL, CTONG-0802): a multicentre, open-label, randomised, phase 3 study. Lancet Oncol. 2011; 12:735-742.

9 Wu YL, Zhou C, Hu CP, Feng J, Lu S, Huang Y, Li W, Hou M, Shi JH, Lee KY, Xu CR, Massey D, Kim M, Shi Y, Geater SL. Afatinib versus cisplatin plus gemcitabine for first-line treatment of Asian patients with advanced non-small-cell lung cancer harbouring EGFR mutations (LUX-Lung 6): an open-label, randomised phase 3 trial. Lancet Oncol. 2014; 15:213-222.

10 Sordella R, Bell DW, Haber DA, Settleman J. Gefitinib-sensitizing EGFR mutations in lung cancer activate anti-apoptotic pathways. Science. 2004; 305:1163-1167.

11 Menju T, Hashimoto S, Hashimoto A, Otsuka Y, Handa H, Ogawa E, Toda Y, Wada H, Date H, Sabe H. Engagement of overexpressed Her2 with GEP100 induces autonomous invasive activities and provides a biomarker for metastases of lung adenocarcinoma. PLoS One. 2011; 6:e25301.

12 Morishige M, Hashimoto S, Ogawa E, Toda Y, Kotani H, Hirose M, Wei S, Hashimoto A, Yamada A, Yano H, Mazaki Y, Kodama H, Nio Y, Manabe T, Wada H, Kobayashi H, Sabe H. GEP100 links epidermal growth factor receptor signalling to Arf6 activation to induce breast cancer invasion. Nat Cell Biol. 2008; 10:85-92.

13 Sevelda F, Mayr L, Kubista B, Lotsch D, van Schoonhoven S, Windhager R, Pirker C, Micksche M, Berger W. EGFR is not a major driver for osteosarcoma cell growth in vitro but contributes to starvation and chemotherapy resistance. J Exp Clin Cancer Res. 2015; 34:134.

14 Zhang Y, Wang L, Zhang M, Jin M, Bai C, Wang X. Potential mechanism of interleukin-8 production from lung cancer cells: an involvement of EGF-EGFR-PI3K-Akt-Erk pathway. J Cell Physiol. 2012; 227:35-43.

15 Soucheray M, Capelletti M, Pulido I, Kuang Y, Paweletz CP, Becker JH, Kikuchi E, Xu C, Patel TB, Al-Shahrour F, Carretero J, Wong KK, Janne PA, Shapiro GI, Shimamura T. Intratumoral Heterogeneity in EGFR-Mutant NSCLC Results in Divergent Resistance Mechanisms in Response to EGFR Tyrosine Kinase Inhibition. Cancer Res. 2015; 75:4372-4383.

作成日：2017 年 2 月 24 日

Literature review of disaster nursing competencies in China
中国の看護師災害看護能力の文献回顧性研究

研究者氏名　胡　沁（第 38 期笹川医学研究者）
中国所属機関　四川大学華西医院
日本研究機関　兵庫県立大学地域ケア開発研究所
指導責任者　山本　あい子　教授

Abstract:

Objective: This paper use literatures review on Chinese disaster nursing competencies. The purpose is to explore the development status and trend of disaster nursing competencies study in China.

Methods: CNKI Data and PubMed were used for the literature search. Key words were “disaster nursing” and “competencies”, “China” has been added when searches have been undertaken with PubMed. All the literatures were published between 2008 and 2016 with Chinese or English.

Results: A total of 29 articles have been discovered by search. With 27 Chinese articles and 2 English articles. Four major themes were emerged from the analysis of the literature. They were competence; skills; knowledge and evaluation tools. 27 out of 29(91.30%) literatures mentioned the request of field first aid skills. 20 (68.96%) articles have described knowledge of psychology after trauma. However, seldom articles (10.34%) paid attention to disaster preparedness.

Conclusions: This literature review indicated the complexity of the criteria for disaster nursing competencies in China. The concern of disaster nursing education is also not enough. Meanwhile, the design of evaluation tools should be more scientific and systematic in the future.

Key words: Literature Review; Disaster Nursing; Competencies; China

Introduction:

Disasters occur every day somewhere in the world，and bring huge damage to individuals, families and communities. Over 2 million people died from natural disasters between 1970 and 2014 in Asia and the Pacific [1]. With the continuous development of human society, the environmental damage caused by human being is getting more and more serious; the frequency of natural disaster is highly increased. In recent years, nuclear weapons, chemical and biological weapons are also constantly threatening human life and safety [2]. The massive casualties caused by various disasters to the world health care system have become a great challenge [3]. As the largest group of disaster rescue, nurses often work in limited resources and play an important role in disaster [4]. In order to minimize the mortality rate, which is directly related to the pre disaster preparedness and disaster response competence [5]. In this paper, the development of disaster nursing competencies in China has been analyzed through the literature review.

Methods:

The literatures were obtained from CNKI (China National Knowledge Infrastructure) Data and PubMed in the field of disaster nursing competencies. Considering the relatively small category of disaster nursing competencies, this study chose a wide range of key words. All the literatures have been published between 2008 and 2016. The key words were “disaster nursing” and “competencies”. “China” has been added when searches have been undertaken with PubMed.

Results:

After reviewing these articles carefully in details. Ultimately, a total of 29 articles have been discovered by search. With 27 Chinese articles and 2 English articles. 4 themes have been classified as follow:

1.What is disaster nursing competence?

Competence is a kind of comprehensive quality that is embodied in practice. The International Council of Nurses (ICN) defined competencies as "a level of performance demonstrating the effective application of knowledge, skill and judgment [6]. In 2003, the International Nursing Coalition for Mass Casualty Education (INCMCE) developed the scale for registered nurse's competence to cope with large-scale disasters, including the core competencies, core knowledge and professional role of the development of the 3 ways. It is one of the first standards for disaster nursing competencies [7]. In 2006, University of Hyogo proposed 5 aspects of disaster nursing competencies, which based on the framework described in a report of the nursing education study group of the Ministry of Education, Culture, Sports, Science and Technology of Japan [8]. In 2009, based on University of Hyogo's 5 aspects, World Health Origination (WHO) and ICN have proposed the "ICN framework of disaster nursing competence". This framework contains with 4 areas (prevention/mitigation; preparedness; response; recovery/rehabilitation) and 10 domains, and became the most meaningful framework in the world [9].

At present, there is a lack of accurate definition of the concept and elements of disaster nursing competence in China [7]. Since 2011 nursing was assessed as a first level subject, the knowledge field gradually trended to be specialized. The system of nursing subject construction became a multi-level and comprehensive knowledge of network [10-12]. However, the disaster nursing field started late in China, many aspects need to be standardized, which has not formed a complete discipline system [13].

2.Widely mentioned skills

Items of skills	No. of Articles	Percentage
Field first aid	27	93.10%
Communicate with different groups	19	65.51%
Able to self-protection	11	37.93%
Leadership	10	34.48%
Cooperation	7	24.13%
Field survival ability	6	20.68%
Foreign language	2	6.89%

Table 1 Widely Mentioned skills

The above table is the skills that widely mentioned in their articles. As can be seen, 27 out of 29(93.10%) articles require competence of field first aid. In addition, the communication, self-protection and leadership are also accounted for a large part of it. The main reason is that these skills are widely used by the nursing staffs in the field of disaster rescue, which are the key for the nurses to participate in disaster relief and rescue the lives of the refugee.

Disaster relief is not a personal behavior, which needs collective efforts and cooperation with different people. Like refugees, own rescue team members and other rescue team members. One research showed Chinese nurses have good ability to communicate and share information in the disaster area of Wenchuan earthquake [14].

Self-protection and field survival ability are the skills of saving ourselves. The nursing staff in disaster relief has been always fighting in the first line, the scene of disaster is totally different from ordinary life. In this case, the nurses should learn the basic ability to protect themselves and skill of the field survival, in order to reduce the unnecessary harm.

Moreover, only little of them require the competencies to speak foreign language. Although in the disaster relief work, this skill may not directly affect the treatment of patients, it makes the rescue more easily for nursing staff in disaster relief. After all, the rescue team has become increasingly international.

Nurses as part of a rescue group, how to maximize their roles in order to improve efficiency and save lives is important. They have to learn these comprehensive skills, so that it can better for the development of the subject.

3.Widely mentioned knowledge

Items of knowledge	NO. of articles	Percentage
Knowledge of psychology after trauma	20	68.96%
Nursing for special vulnerable groups （chronic disease, old, children, pregnant, disable）	7	24.13%
Treatment of chemical, biological, radiological	5	17.24%
Safety management of vaccine, drug	5	17.24%
Quarantine	5	17.24%
Preparedness	3	10.34%

Table 2 Widely Mentioned Knowledge

This table displayed the disaster nursing knowledge, which have been widely mentioned in this literature review. The psychology after trauma (68.96%) has become the main content, which the majority of researchers believe that disaster nurses should have. People lack a sense of security and belonging, often seen as extreme panic and anxiety. If there is no timely intervention, it will be caused by disorders of emotion, cognition, behavior, and the formation of posttraumatic stress disorder [15]. Meanwhile, psychological care is very important both for the victim and the rescue nurse. Fung WM et al.[16] believed that when disaster stroked, the demand of nursing staff was often higher than other types of health professionals. Too much pressure would cause psychological problems of nurses. Moreover, severely traumatized adolescent survivors of the earthquake may suffer from psychological symptoms even 6 years after the disaster [17]. All these have indicated nurses should have knowledge about how to deal with the victims' psychological problems as well as how to control themselves. At the same time, we also need to concern for a long time.

In the process of disaster, people tend to neglect the care of special populations, such as the elderly, pregnant women, children, and chronic disease patients. When the disaster occurs, the threat to them was greater than the ordinary population. A survey showed the concern of nursing care for vulnerable population was low [14]. ICN has made clear recommendation of nursing for those vulnerable groups. Moreover, concern for vulnerable group should run through the whole disaster period.

What's more, table 2 elicits that knowledge like how to treat the chemical, biological, radiological are not high. 《Disaster Nursing and Emergency Preparedness for Chemical, Biological and Radiological Terrorism and Other Hazards》 has been published in 2003, this guideline provided a theoretical basis for us to learn the knowledge. With the rapid development of the world, special disasters have become the focus of all countries. How to master the relevant knowledge of chemical, radioactive, biological material protection in order to calmly face the disaster, has become more and more important.

The important role of nursing staff in disaster nursing is not only reflected during the disaster or post disaster, but also includes the pre-disaster prevention and preparedness. In the disaster preparedness capacity, the average dimension of disaster preparedness is low [14]. Unfortunately, with 10.34% of the demand for disaster preparedness knowledge, which has not attracted enough attention in China.

4.Design of disaster nursing competencies evaluation tool

Under the condition of emergency rescue, the requirement of emergency and response competencies of nurses have been put forward. However, Chinese disaster nursing competence standards and evaluation system are still in the development stage [18]. In order to fit to the development of Chinese national conditions, different institutions were explored evaluation index system on the basis of their own research. For example, Li et al., [19] devised a questionnaire about disaster emergency knowledge scale's item pool, which comprised with 44 items, and contains 6 components. The overall Cronbach's alpha coefficient is 0.975, and retest Cronbach's alpha coefficient is 0.916. Ge et al., [20] designed an evaluation indicators system of nursing ability in emergency rescue, including 5 items in first grade index,

10 items in second grade index, 35 items in third grade index. Coordination coefficients in first, second and third grade index were 0.489, 0.437 and 0.383. There is another scale designed for community nurses by Yang et al., [21]. They used the Delphi method and consult with 36 experts, establish a scale with 35 items, which include 6 parts ultimately. In short, a set of scientific and systematic evaluation standard of disaster nursing competence system is in accordance with the trend of international rescue.

Discussion:

1. Strengthen the education of disaster nursing.

Disaster nursing is an emerging discipline in China. There is no unified education curriculum and textbook. Nursing students mainly learn the relevant knowledge of emergency nursing courses [22]. Zhang [23] has investigated 20 undergraduate nursing colleges and universities. The result shows only small groups have courses related to disaster nursing. Such as the Second Military Medical University has 100 hours of field nursing. A few nursing schools have 2-4 hours of disaster nursing care in emergency care. What's more, the teaching of disaster nursing education in junior college and technical secondary school is almost blank. Moreover, there is no research on graduate education at present [24]. In 2011, the Hong Kong Polytechnic University and Sichuan University established Disaster Management College at the Sichuan University, became the first global cooperation between two universities, and has brought new opportunities for the development of disaster nursing.

In the field of disaster nursing education, Japan has always been in the forefront of the world. In 2005, University of Hyogo began to carry out disaster nursing education of master, which was the only one at that time. They set up with doctor curriculum of disaster nursing as well [25]. From 2014, Japan designed a program found by University of Kochi; University of Hyogo; Tokyo Medical and Dental University; Chiba University and Japanese Red Cross College of Nursing, which called Disaster Nursing Global Leader Degree Program (DNGL). The curriculum is made up of six categories for five years. There are academic foundations of nursing (total of 12 subjects from 5 universities); interdisciplinary courses required for global leaders in disaster nursing (13 subjects); courses related to disaster nursing (9 subjects); disaster nursing seminars (9 subjects); disaster nursing practicum (7 subjects); and research report course related to disaster nursing (3 subjects). Students must complete a standard course of study of 5 years or more, and acquire 50 or more credits. With 15 weeks of classes for per semester, and 90 minutes for each class. They aim to produce 50 global leaders of disaster nursing who can initiate their interdisciplinary and international guidance and appropriately resolve multiple challenges in the vital field of disaster nursing [26].

2. Integrate assessment of evaluation tool

In order to build comprehensive assessment of disaster nursing competencies, nurses need to be verified by the corresponding evaluation and assessment tools. Nevertheless, the evaluation tools in China are random and incomplete in the content nowadays [27]. From this literature review, we can see that there are plenty of evaluation tools, however, not all of them have good validity and reliability test. Due to the lack of an accurate definition of the concept and elements of disaster nursing competencies in China, the research and education related to disaster nursing in our country are lack of convincing theoretical framework [23]. Therefore, it is necessary to combine the scientific analysis with our country's national condition to develop an evaluation tool or scale.

Conclusion：

This systematic review of the literature shows that different professional institutions have been published about disaster competencies in China. Research focuses primarily on the nursing competencies; indicates the complex of the criteria for disaster nursing competencies, mainly due to the variety of institutions. Most articles have proclaimed that Chinese nurses' disaster nursing competencies level is not high [28-33]. In the future study,

we have to base on Chinese real conditions, and design scientific and comprehensive evaluation system. In succession, we should test nurses' disaster nursing competence through practical investigation, in order to determine the content of disaster nursing curriculum, and make sure the teaching methods make effect on nurses' competence of disaster nursing. This will be a long-term challenge to face with disaster nursing research in china.

Reference：

[1]Overview of Natural Disasters and their Impacts in Asia and the Pacific 1970-2014, 2015, P6.

[2]Minami Hiroko, Watanbe Tomoe, Zhang Xiaochun, Yamamoto aiko. The development and current situation of disaster nursing in Japan [J]. Chinese Journal of nursing, 2005,04:27-29.

[3]Zhang Jing, Jiang Anli. Progress of disaster nursing education in theory and practice [J]. Chinese Journal of Nursing, 2009,44 (7): 592-593.

[4]“ICN Framework of Disaster Nursing Competencies，” 2009, piv,1.

[5]Magnaye B, Lindsay S, Ann F, et al. The role, preparednes and management of nurses during disasters[J].E -Int Sci Res J,2011,3(4):269-274.

[6]“ICN Framework of Disaster Nursing Competencies，” 2009, p34.

[7]Dong Chaoqun, GUI Li, Liu Xiaohong. Research status and progress of disaster nursing ability [J]. Nursing Journal of Chinese People's Liberation Army, 2011,28 (5B): 26-29.

[8]Core Competencies for Disaster Nursing, http://www.coe-cnas.jp/english/group_education/core_competencies.html (2006)

[9]“ICN Framework of Disaster Nursing Competencies，” 2009, p40.

[10]Zhang Yan, Jiang Anli. Progress in the study of the discipline system of nursing science [J]. Nursing Research, 2012, 26 (35): 3265-3267.

[11]Li Jing. An exploratory study on the construction of discipline system of nursing [D]. Second Military Medical University, 2010.

[12]Bai Yining. The current situation and development of [J] nursing research in China from the comparison of the nursing literature. China Journal of Practical Nursing, 2005, 21 (5): 58-59.

[13]Li Yule, Li Fan, Shi Donglei, Feng Xiumin, Liu Aihui. The research peogress of disaster nursing in China[J]. Chinese Nursing Management, 2015,01:115-118.

[14]Wang Heng, Hu Xiuying, Disaster nursing competencies of nurses working in area of Wenchuan earthquake[J]. Journal of Nursing Science, 2014,23:48-52.

[15]Flannery RB Jr, Everly GS Jr.Crisis intervention: a review[J] Int J Emerg Ment Health, 2000 Spring:2(2):119-25.

[16]Fung WM, Lai KY, Loke AY. Nurses' perception of disaster: implications for disaster nursing curiculum[J].Clin Nurs,2009,18 (22):3165-3171.

[17]Tanaka, E., et al., Long-term psychological consequences among adolescent survivors of the Wenchuan earthquake in China: A cross-sectional survey six years after the disaster. J Affect Disord, 2016. 204: p. 255-61.

[18]Wang Liqin, Li Simu, Xu Naiwei, et al. Research progress on disaster nursing competency framework of nurses in China [J]. Nursing Research, 2016,08:901-904.

[19]Li Shumei, Wang Yang, Han Jinfeng, Huang Yeli. The establishment of disaster emergency knowledge scale's item pool [J]. Journal of Translational Medicine, 2012,03:170-172.

[20]Ge Xuedi, Li Bing, Huang Ying, Zhu Ya, Ling Xia, Xu Xinju. Construction of evaluation indicators system for emergency rescue nursing capability [J].Nursing Journal of Chinese People's Liberation Army,2013,11:1-4.

[21]Yang Yana, Luo Yu. Study on evaluation index system of community nurses' ability to cope with disasters [J]. Nursing Research, 2010,10:855-858.

[22]Deng Jingyun, Ba Ruiqi, Li Xuguang, Zhu Mengying. Investigation on rescue knowledge level of nurses in disaster

and training strategies [J]. Journal of Nursing, 2010,10:57-59.
[23]Zhang Qing. Analysis and Enlightenment of disaster nursing and disaster nursing education in China [J]. Nursing Research, 2009,10:923-924.
[24]Wang Heng, Hu Xiuying, Chen Yan. Document analysis on research status quo of disaster nursing education teaching in China[J].Nursing Research,2013,8(27)：2421-2423.
[25]Yamamoto Aiko, Xie Hong (Translation). Disaster nursing education in Japan [J]. Chinese Nursing Management, 2009,05:19-20.
[26]Cooperative Doctoral Program for Disaster Nursing Course Guide, 2015,p5,8.
[27]Yang Meifang, Zhong Qingling, Chen Jing. Disaster nursing new progress. Nanchang University. 2013.53(1) 96-98.
[28]Li Yunfeng, Wang Liyuan, Yu Zang pear. Nursing competency and necessity of earthquake disaster:a retrospective study [J]. Liberation Army Nursing Journal, 2013,04:23-25.
[29]Li Zhen, Sheng Yu. An investigation of emergency nurses' preparedness for disasters in China [J]. Chinese Journal of Nursing, 2014,06:699-703.
[30]Zhu Aiqun, Zhang Jingping, Li Lezhi, et al. Investigation on disaster-related competencies and cognition in clinical nurses[J]. Journal of Nursing Science, 2014,29 (17), 47-50.
[31]Yang Yana, Luo Yu, Liu Xiuna, Zhou Juan, Chen Ping. Research of disaster response capabilities and its influencing factor of community nurses in Chongqing municipality[J]. Journal of Nursing Management, 2010,10:698-699.
[32]Yu Luo, Ling Liu, Wen-Quan Huang, Ya-Na Yang, Jie Deng, Chun Hong Yin, Hui Ren, Xiao-Yun Wang. A Disaster Response and Management Competency Mapping of Community Nurses in China[J]. Iranian J Publ Health, Vol. 42, No. 9, Sep 2013, pp. 941-949.
[33]Li Fan, Shi Dong Lei, Li Yule, Sun Pengxia, Feng Xiumin, Liu Aihui. Knowledge Level of Disaster Rescue of Emergency Nursing Managers and Their Attitude Toward Disaster Rescue[J]. Journal of Nursing, 2016,14:32-34.

作成日：2017 年 2 月 23 日

A comparative radiographic and arthroscopic study of Stage 3 varus ankle arthritis

3 期変形性足関節炎の放射線学と関節鏡の比較研究

研 究 者 氏 名　　顧 文奇（第 38期笹川医学研究者）
中国所属機関　　上海第六人民医院東院整形外科
日本研究機関　　奈良県立医科大学整形外科
指 導 責 任 者　　田中　康仁　教授

Abstract

This retrospective study included 45 cases of varus ankle arthritis and 28 cases of normal subjects, which was divided into 3 groups: control group, stage 3a group and stage 3b group. Tibial anterior surface (TAS) angle, talar tilt angle (TTA), tibia lateral surface (TLS) angle, tibiofibular clear space (TFCS) and lateral clear space (LCS) were compared among three groups. The arthroscopic videos of arthritis were also reviewed to investigate the cartilage lesion of talar dome. There was a statistical difference in TAS between normal ankles and arthritis ankles. Difference of TLS was only found between control and stage 3b group. However, no difference was seen in TFCS among three groups. Both of TTA and LCS had a difference among three groups and a correlation between TTA and LCS was also calculated. More severe cartilage involvement was observed in stage 3b from arthroscopic observation. We concluded that for stage 3b varus ankle arthritis, the more severe talar tilt and widened lateral clear space indicated a more unstable ankle joint, leading to a more severe cartilage lesion.

Keywords Instability, varus ankle arthritis, arthroscopy, radiograph, comparative study

1. Introduction

The varus ankle arthritis have been studied for decades, but is still a challenge for foot and ankle surgeons. In 1995, Takakura et al[1] firstly described the classification for varus ankle arthritis, which was modified by Tanaka in 2006[2], who developed stage 3 into two sub-stages. The major difference between two sub-stages is the talar dome involvement, which is confirmed on the weight-bearing AP view.

Radiographic studies for varus ankle arthritis have been reported in recent years. However, most of these studies focus on the axial alignment and subtalar joint[3-5]. Currently, ankle instability has been regarded as an another major factor for ankle arthritis[6,7]. Despite of this, the discussion on instability of varus ankle arthritis is limited, and the parameter for

evaluation of lateral clear space has not been developed.

Ankle arthroscopy is a golden standard for cartilage evaluation with advantage of direct visual of joint facet. However, few study of arthroscopic comparison for stage 3a and 3b varus ankle arthritis has been reported.

Therefore, the purpose of this study is to: (1) investigate the instability of ankle joint in stage 3 varus ankle arthritis; (2) attempt to develop the measurement for lateral clear space; (3) compare the cartilage lesion between stage 3a and 3b to provide a clinical guidance for different sub-stages.

2. Materials and Methods

2.1 Patient recruitment

The plain films of varus ankle arthritis who were treated surgically from 2007 to 2016 in Nara Medical University Hospital were reviewed. The inclusive criteria was: (1) degenerative osteoarthritis; (2) varus deformity; (3) stage 3a and 3b of Takakura-Tanaka classification system (stage 3a, bony contact limited to the medial malleolar; stage 3b, bony contact extended to the talar dome); (4) with intact radiographic and arthroscopic data. The exclusive criteria was: (1) secondary osteoarthritis subsequent to trauma, osteonecrosis, neuropathic arthropathy; (2) other stages of varus ankle arthritis; (3) arthritis with normal alignment or valgus deformity; (4) septic arthritis; (5) rheumatoid arthritis; (6) other inflammatory arthropathy; and (7) previous surgical history of ipslateral foot and ankle joint.

According to the criteria, finally 48 ankles of 45 patients (4 males and 41 females) with a mean age of 64.2 years (range, 42~75 years) were enrolled in this study, including 21 ankles of stage 3a and 27 of stage 3b. Another 28 patients (2 males and 26 females, with an average of 62.2 years, range, 43~77 years) of normal ankle between 2004 to 2016 were selected as control group, who had no history of ankle fracture, generalized arthritis or deformity of hindfoot and ankle joint. The etiology in arthritis group was degenerative osteoarthritis, with 17 of which had a history of sprain ankle.

2. Measurement methods

The radiographic measurements were performed retrospectively with weight-bearing AP and lateral view of ankle joint. All plain films were digitally obtained and assessed through the NexusSif system (Fuji film, Japan).

On weight-bearing AP view, the TAS angle, TTA, TFCS and LCS were measured. The TLS angle was assessed on the lateral weight-bearing view. The TAS angle is the angle between tibia shaft axis and articular surface of tibial plafond (Figure 1), and the TTA is the angle between the articular surface of plafond and talar dome (Figure 2). The tibiofibular

clear space was the space between lateral border of posterior tibia and medial border of fibula, measured 1cm above the plafond (Figure 3). The lateral clear space was the horizontal distance between the lateral border of talus and medial border of fibula, measured at the level of subtalar joint line on talus (Figure 3). TLS angle is the angle between the tibial axis and distal tibia articular surface which is drawn between the anterior and posterior margins of the tibial plafond on the lateral weight-bearing view (Figure 4).

According to the French Society of Arthroscopy (SFA) cartilage grade system[8]: Grade 4 area of talar dome, defined as exposure of subchondral bone was documented (Figure 5).

1

2

Figure 1 and 2. Measurement of TAS angle (Fig. 1) and TTA (Fig.2).

3

4

Figure 3 and 4. Measurement of TFCS, LCS (Fig.3) and TLS angle (Fig.4).

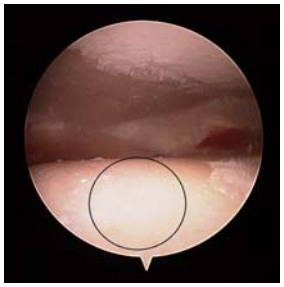

5

Figure 5. Grade 4 cartilage lesion.

2.3 Statistical analysis

All the radiographic parameters were analyzed by one-way analysis of variance (ANOVA) with a Bonferroni test among three groups. The difference of grade 4 cartilage lesion area was compared by independent t-test, and the correlation between TTA and LCS was calculated by Pearson's correlation coefficients. The differences were considered statistically significant if the *P* value was less than 0.05. All statistical analysis were performed using SAS 19.0 (IBM Analytics, USA).

3. Results

The result of radiographic measurement see in table 1. The positive correlation between TTA and LCS was calculated (r=0.834, P<0.001). For the arthroscopic evaluation, the dome involvement was more severe in stage 3b. (mean, 18.36% v.s. 30.52%, *P<0.05*).

Table 1. Results of radiographic measurement

	TAS	TTA	TLS	TFCS	LCS
Control	88.0±1.6° *,**	0.3±0.5° *,**	80.2±2.7° **	4.62±0.84	3.40±0.43*,**
	(85 ~ 90°)	(0 ~ 2°)	(76 ~ 85°)	(2.52 ~ 6.23)	(2.47 ~ 4.25)
Stage 3a	82.2±2.0° *	5.9±3.5° *,***	78.5±2.7°	4.16±0.97	6.16±1.61*,***
	(79 ~ 85°)	(1 ~ 15°)	(75 ~ 84°)	(2.41 ~ 6.11)	(4.13 ~ 10.26)
Stage 3b	82.9±2.8° **	15.4±5.5° **,***	76.7±3.5° **	4.35±0.97	7.52±1.90**,***
	(78 ~ 88°)	(9 ~ 31°)	(70 ~ 83°)	(2.57 ~ 6.23)	(4.17 ~ 10.79)

*Statistical difference between control group and stage 3a group; **Statistical difference between control group and stage 3b group; ***Statistical difference between stage 3a and 3b group.

4. Discussion

The mechanism of deterioration in stage 3 varus ankle arthritis remains uncertain. Lee et al suggested a various alignment of tibial plafond in the varus ankle arthritis[3]. Hayashi[4] and Wang[5] described the mechanism of subtalar compensation in the deterioration of varus ankle arthritis. However, stability of ankle joint was little mentioned in current studies.

Previous study hypothesized that the primary varus ankle arthritis may begin from the inclination of varus plafond[4]. In

our study, a statistical difference of TAS angle was found between control group and arthritis group, indicating a varus change of tibial plafond in stage 3. However, the TAS angle of two sub-stages had no difference (P>0.05). Moreover, no significant difference in TFCS was seen among three groups. Therefore, a normal syndesmosis in stage 3 should be concluded. However, the TTA was obviously different in three groups, which suggested that the severity of talar tilt should be attributed to the peritalar instability.

The stability of talus was maintained by the complex soft tissue and bony structures[9]. Previous studies demonstrated that increased contact pressures on the medial ankle after release of the lateral ligaments[10,11]. And the instability may accelerate the deformity and joint degeneration. In this study, the TTA was significant different during the deterioration among three groups. Therefore, our hypothesis is that the varus ankle arthritis may start with a plafond inclination and a simultaneous lateral instability. With the lateral stabilizers gradually disabled, the deformity exacerbates and directly leads to a talar tilt, which increases the load on the medial weight-bearing surfaces of the joint and accelerates the cartilage lesion. Furthermore, the talar tilt may further aggravate the lateral instability. In this study, 17/45 of patients confirmed a history of sprain ankle, indicating that ankle instability might be a major factor in deterioration of varus ankle arthritis.

The measurement of lateral clear space has not been described previously. In our study, the LCS manifested a statistical difference among three groups. And a positive correlation between LCS and TTA was confirmed, which suggested that the lateral clear space widened with the aggravation of talar tilt. Moreover, we found the medial translation of talus in most cases in stage 3a, with a limited talar tilt and widened LCS. A supramalleolar osteotomy could be indicated to stabilize the mortise and realign the axis in these cases[12]. And sometimes, the soft tissue reconstruction for further stabilization should be considered simultaneously to prevent a recurrence of instability[13,14].

In this study, we compared the cartilage damage between two sub-stages via arthroscopy. A more severe cartilage damage in stage 3b was confirmed. Therefore, we suggested that the lateral instability might be a major factor for talar tilt and cartilage lesion. With the exacerbation of the instability, the cartilage lesion accelerated.

There are still some limitations in this study. First, the sample size was small and the gender was female in majority, which may cause some bias. Moreover, the reliability of LCS also should be tested in a larger sample. Second, the grade 4 cartilage lesion area was measured by subjective observation via arthroscopy, which also may cause some error.

Finally, stage 3b was confirmed on a weigh-bearing AP view. However, we found that for some stage 3a cases, bony contact of talar dome could be seen on a lateral view, and more cartilage lesion was observed under arthroscopy in these patients. We think that these patients may be classified into stage 3b potentially. Therefore, we suggest that weight-bearing lateral view should also be referred to during the classification. All these will be improved in the future study.

We concluded that the instability plays an important role in stage 3 varus ankle arthritis. The arthritis deteriorated with aggravation of ankle instability. And the lateral clear space may be a new predictor for the lateral stability of ankle joint.

References

[1] Takakura Y, Tanaka Y, Kumai T, et al. Low tibial osteotomy for osteoarthritis of the ankle. Results of a new operation in 18 patients. J Bone Joint Surg Br, 1995,77(1):50-54.

[2] Tanaka Y, Takakura Y, Hayashi K, et al. Low tibial osteotomy for varus-type osteoarthritis of the ankle. J Bone Joint Surg Br, 2006,88(7):909-913.

[3] Lee WC, Moon JS, Lee HS, et al. Alignment of ankle and hindfoot in early stage of ankle osteoarthritis. Foot Ankle Int, 2011,32(7):693-699.

[4] Hayashi K, Tanaka Y, Kumai T, et al. Correlation of compensatory alignment of the subtalar joint to the progression of primary osteoarthritis of the ankle. Foot Ankle Int, 2008,29(4):400-406.

[5] Wang B, Saltzman CL, Chalayon O, et al. Does the subtalar joint compensate for ankle malalignment in end-stage ankle arthritis? Clin Orthop Relat Res, 2015,473(1):318-325.

[6] Golditz T, Steib S, Pfeifer K, et al. Functional ankle instability as a risk factor for osteoarthritis: using T2-mapping to analyze early cartilage degeneration in the ankle joint of young athletes. Osteoarthritis Cartilage. 2014,22(10):1377-1385.

[7] Valderrabano V, Hintermann B, Horisberger M, et al. Ligamentous posttraumatic ankle osteoarthritis. Am J Sports Med, 2006,34(4):612-620.

[8] Dougados M, Ayral X, Listrat V, et al. The SFA system for assessing articular cartilage lesions at arthroscopy of the knee. Arthroscopy, 1994,10(1):69-77.

[9] Hintermann B, Knupp M, Barg A. Joint-preserving surgery of asymmetric ankle osteoarthritis with peritalar

instability. Foot Ankle Clin, 2013,18(3):503-516.

[10] Noguchi K. Biomechanical analysis for osteoarthritis of the ankle. Nihon Seikeigeka Gakkai Zasshi, 1985,59(2):215-222.

[11] Bonnel F, Toullec E, Mabit C, et al. Chronic ankle instability: biomechanics and pathomechanics of ligaments injury and associated lesions. Orthop Traumatol Surg Res, 2010,96(4):424-432.

[12] Tanaka Y. The concept of ankle joint preserving surgery: why does supramalleolar osteotomy work and how to decide when to do an osteotomy or joint replacement. Foot Ankle Clin, 2012,17(4):545-553.

[13] Knupp M. The Use of Osteotomies in the Treatment of Asymmetric Ankle Joint Arthritis. Foot Ankle Int, 2017,38(2):220-229.

[14] Krause FG, Henning J, Pfander G, et al. Cavovarus foot realignment to treat anteromedial ankle arthrosis. Foot Ankle Int, 2013,34(1):54-64.

作成日：2017 年 2 月 23 日

Low skeletal muscle is a negative prognostic factor for curative stage I-II non-small cell lung cancer

術前体幹筋肉量は、I-II 非小細胞肺がん根治手術後の不良予後因子となり得る

研 究 者 氏 名　　孫　長博（第 38期笹川医学研究者）
中国所属機関　　中国医科大学附属第一医院胸部外科
日本研究機関　　東京大学医学部附属病院呼吸器外科
指 導 責 任 者　　中島　淳　教授
共 同 研 究 者　　安樂　真樹　特任准教授

Abstract

Background:

Skeletal muscle depletion is closely associated with limited physical ability and high mortality. This study was performed to evaluate the prognostic significance of skeletal muscle depletion in patients with curative stage I–II non-small cell lung cancer (NSCLC).

Method:

We conducted a retrospective analysis of 314 consecutive patients with stage I to II lung cancer who underwent curative resection. The pectoralis muscle index (PMI, area/height^2) at the forth thoracic vertebral (Th4) level, and the lumbar muscle index (LMI, area/height^2) at the first lumber vertebral (L1) level were measured by preoperative computed tomography. Overall survivals (OS) and recurrence-free survival (RFS) were compared between the lowest sex-specific quartile of PMI or LMI and the rest of quartiles. Multivariate Cox proportional hazard model was used to evaluate the indices as prognostic factors.

Results:

Of the total 314 patients, the cutoff values of low pectoralis muscle index and low 1st lumbar skeletal muscle index were calculated with 10.3 and 38 cm^2/m^2 for male, and 8.4 and29.6 cm^2/m^2 for female, respectively. RFS was not statistically significant in patients with loss of muscle of the pectoralis, but OS was significantly shorter in patients with loss of muscle (5-year OS, 64.6% vs. 80.3%, p = 0.009). RFS and OS were significantly shorter in patients with loss of muscle of the 1st lumbar than those without (5-year RFS, 72.1% vs. 82.3%, p = 0.026; 5-year OS, 64.8% vs. 80.1%, p = 0.003). In multivariable models of RFS and OS for LMI group, the 1st lumbar muscle index, preoperative serum albumin level, Neutrophil to Lymphocyte Ratio (NLR), and pathologic stage were independent predictors for overall survival (p=0.016, HR=1.845, CI95%: 1.121-3.038 for LMI), whereas PMI was not. Conclusions:

The LMI was is an independent prognostic factor in patients with stage I-II lung cancer who had curative resection, while PMI was not prognosis. As for the estimation of total body skeletal muscle, The LMI demonstrated a higher

correlation with post-surgical prognosis than PMI. The LMI can be a part of preoperative assessments when surgical intervention is considered for patients with early-stage NSCLC.

Key words: Skeletal muscle depletion, early stage, I–II non-small cell lung cancer, prognosis

Introduction

Lung cancer is one of the most frequently diagnosed cancers and the leading causes of cancer death in the world (*1*). The overall survival of patients with early stage I-II NSCLC is distinctly better than advanced lung cancer (*2*). However, even though in the early I-II stage NSCLC undergoing curative surgery, some patients still have poor survival because some other prognosis-related factors. As a prognostic factor, sarcopenia, as loss of muscle mass and function, contributes to functional decline, disability, injury, and mortality. The poor prognosis due to sarcopenia has been studied mainly in patients with non-malignant diseases and in geriatric populations (*3, 4*). Recently, there are some investigations shows the clinical importance of sarcopenia is also being increasingly recognized in oncologic patients (*5, 6*). As a key component of sarcopenia, low skeletal muscle is closely associated with limited physical ability and high mortality in some cancers (*5, 6*). Nevertheless, the correlation between low skeletal muscle and the prognosis of stage I-II NSCLC is not well understood.

In this study, the aim was to investigate the correlation of low skeletal muscle and prognosis of patients undergoing curative surgery for early stage I–II NSCLC and evaluate the efficiency of pectoralis muscle area on CT slice just above the aortic arch level (T4) and the L1 skeletal muscle area to explore a practical method for patients with stage I–II NSCLC to evaluate skeletal muscle mass on chest computed tomography.

Patients and Methods

We performed a retrospective analysis of 314 consecutive patients with stage I–II NSCLC who underwent lobectomy and lymph nodes dissection at University of Tokyo Hospital (Tokyo, Japan) from January 2009 to December 2013.

Data collected from inpatient and outpatient records included demographic data [age, sex, height, weight, body mass index (BMI)], blood count and serum biomedical data before a week of operation [leucocyte, neutrophil, lymphocyte, albumin(Alb), C-reactive protein(CRP)], tumor-specific data [carcinoembryonic antigen (CEA), tumor location, size], pathologic data (pathological types and TNM staging according to the 2009 International Association for the Study of Lung Cancer (IASLC) staging) and survival data including recurrence free survival(RFS) and overall survival(OS).

The pectoralis muscle area (T4) and the first lumbar vertebra (L1) were measured retrospectively on chest CT scans performed before surgery at the level of the fourth thoracic vertebra (T4) and the first lumbar vertebra (L1), respectively

(Fig. 3). The image analysis system, SYNAPSE VINCENT (Fujifilm Medical, Tokyo, Japan) was used to outline the skeletal muscle area manually and compute the cross sectional area of each in centimeters squared (cm^2) automatically. The cross-sectional area of muscle (cm^2) at the T4 and L1 level computed from each image was normalized by the square of the height (m2) to obtain the skeletal muscle index (cm^2/m^2) as PMI and L1MI, respectively.

All analyses were performed using SPSS, version 22.0 software (IBM Inc., Armonk, New York, USA). $P < 0.050$ was considered statistically significant.

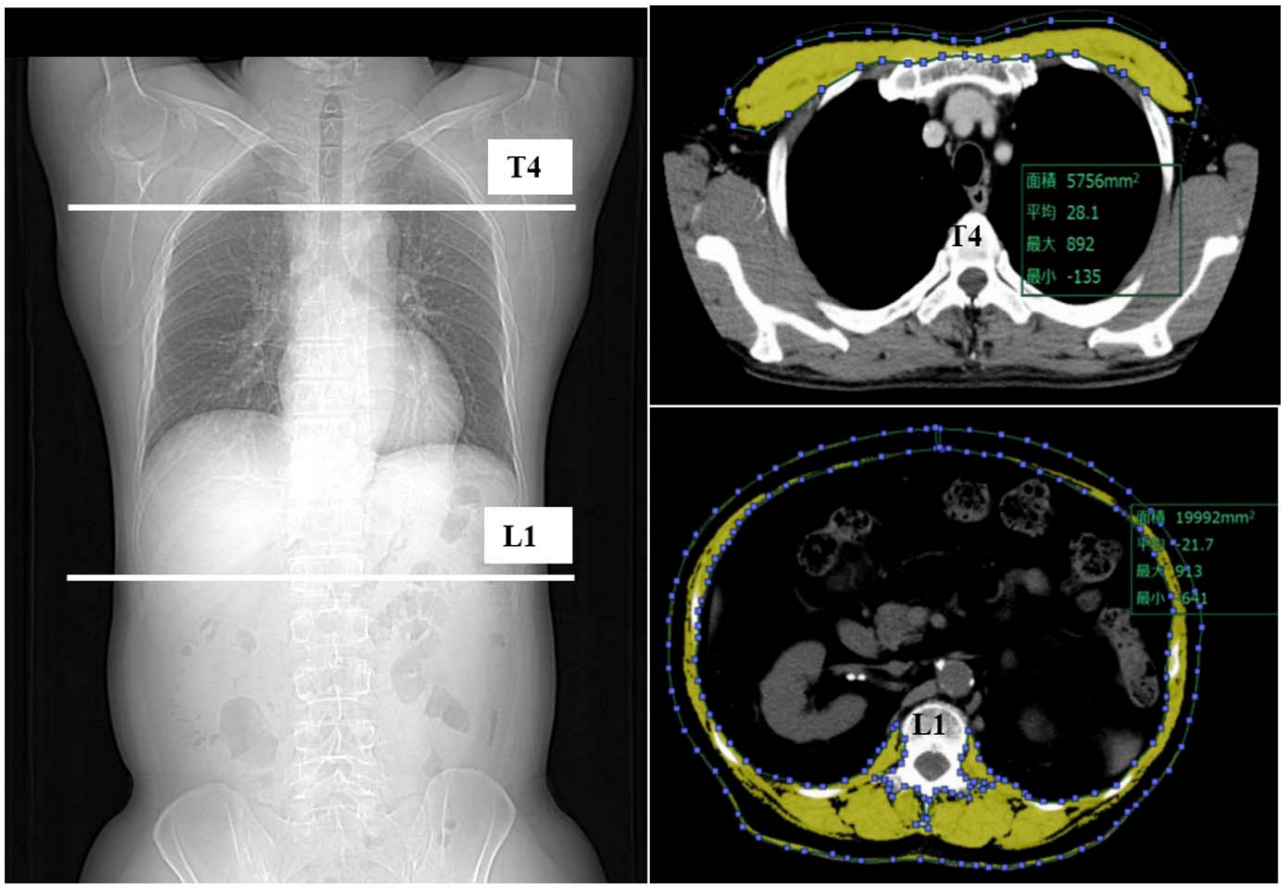

Figure 3: Muscle Area calculation

3 Results

The clinical and pathological characteristics of the 314 patients included in this study are shown in Table 1 with a mean age of 68.1±10.68 years. There were 183(58.3%) male patients and 131(41.7%) female patients. The majority were stage I patients with 254(80.9%), and the rest were stage II patients with 60(19.1%). The corresponding histology confirmed as adenocarcinoma 227 (72.3%), followed by squamous carcinoma 63(20.1%), large cell carcinoma 4 (1.2%)

and other NSCLC 20 (6.4%). Additionally, there were 59 recurrence patients and 77 deaths. Median overall survival was 51 months (1 to 92 months). The median PMI and L1MI for male was 12.3, 41.2, and for female was 9.7, 33.4, respectively. The PMI and L1MI were both significantly higher in males than females ($P < 0.05$). The median albumin, NLR and CEA were 4, 2.2, 4.3, respectively.

Patients were divided into two groups according to the sex-specific lower quartile cutoff value of PMI (12.3 cm^2/m^2 for male, 8.4 cm^2/m^2 for female) because the PMI were significantly higher in males than females ($P < 0.05$). The lower quartile of PMI was defined as low skeletal muscle group, and the rest was defined as normal skeletal muscle group. A comparison of clinicopathological factors in the low skeletal muscle group and normal skeletal muscle group showed that the Age (< 65 vs. ≥ 65, $P < 0.05$), median of BMI (20.7 vs. 22.8 kg/m^2, $P < 0.001$), albumin (<4 vs. ≥ 4g/dl, $P < 0.001$) of patients with low skeletal muscle were significantly lower than those of the patients without low skeletal muscle regardless of gender. (Table 2). In the survival analysis, RFS curves were not statistically significant in patients with and without loss of muscle of the pectoralis (5-year RFS 79.6% vs 80.4%, p=0.869). However, OS curves were statistically significant in patients with and without loss of muscle of the pectoralis (5-year OS, 64.6% vs. 80.3%, p = 0.009).

Based on the sex-specific lower quartile cutoff value of L1MI, patients were divided into two groups (38 cm^2/m^2 for male, 29.6 cm^2/m^2 for female) because the L1MI were also significantly higher in males than females ($P < 0.01$). Compared with normal skeletal muscle patients, those with low skeletal muscle had a significantly lower BMI (median 20.1 vs. 23 kg/m^2, $P < 0.05$), albumin (<4 vs. ≥ 4g/dl, $P < 0.01$). In the Kaplan–Meier analysis, RFS was significantly shorter in patients with low skeletal muscle of L1MI than those without low skeletal muscle (5-year RFS, 72.1% vs. 82.3%, p = 0.026). Similar results of OS were observed between low skeletal muscle group and normal skeletal muscle group (5-year OS, 64.8% vs. 80.1%, p = 0.003).

Multivariate analysis showed that PMI was not an independent prognostic factor for overall survival (p = 0.072). However, multivariate analysis of the OS of patients found that low L1MI was an independent prognostic factor (Hazard Ratio: 1.843, 95%CI: 1.115, 3.047, p=0.017) while adjusting for smoking history, NLR, albumin, CEA, p-Stage II.

Discussion

To our best knowledge, this is the first study about the impact of low skeletal muscle on the outcome of patients with curative early stage I-II NSCLC with Chest CT-defined muscle depletion. In this study, we investigated the potential ability of chest CT-defined muscle depletion of pectoralis muscle at the forth thoracic vertebra (Th4) and cross-sectional

muscle at the first lumbar vertebra (L1) to act as an indicator for survival in patients undergoing curative surgery for with early-stage I-II NSCLC. As a result, the study found that L1MI is an independent prognostic factor with a 1.843 fold increased risk of death in patients, while PMI was not an independent predictor for overall survival.

In the study, we found the advancing age (≥65) is slightly associated with low L1MI, but not significant (p=0.073,). In the univariate analysis, advancing age (≥65) is related to the poor survival with p= 0.016, but not significant in the multivariate analysis after adjusting for gender, low L1MI, NLR, CEA, Alb, and p-stage. Preoperative NLR, as an indicator of systemic inflammation, was demonstrated to be a prognostic factor in resected lung cancer patients in some studies (*23*). Our study showed NLR was an independent predictor for poor survival (0.002), which was consistent with the previous result. But it was not significantly associated with L1MI. As an indicator of nutrition status, serum albumin was evaluated in the study and showed a significant association with L1 muscle index (p=0.046), and it was also proved to be an independently prognostic factor in the multivariate analysis (p=0.001). This possibly indicated that the reason of low skeletal muscle in early stage NSCLC were more susceptible to metabolic status due to nutrition than systemic inflammation owing to early lung cancer. And this might also explain why cancer-specific mortality between low muscle skeletal group and normal skeletal muscle group in early stage I-II was no significant different. The poor survival for the patients with low skeletal muscle in early NSCLC may reflect a metabolic disorder, associate with low insulin sensitivity or diabetes, decreased physical activity, increased risk of cardiovascular diseases, and resistance to therapy(*7, 21, 24*).

The present study identified low skeletal muscle is an independent prognostic factor for poorer survival after early stage I-II surgery. On one hand, such data provide a feasible method of investigation to further study skeletal muscle mass on chest CT. Especially, given the increasing morbidity of lung cancer and prevalence of sarcopenia among older patients. On the other hand, it is still unknown whether treatment of sarcopenia may improve outcomes. It may be a potential modifiable risk factor that could be assessed before surgery so that patients are well informed and adjust their lifestyle to optimize their health prior to undergoing treatments.

In conclusion, our study demonstrated low skeletal muscle, referred to sarcopenia, evaluated on the first lumbar level on chest CT is an independent prognostic factor in patients with stage I-II NSCLC after lobectomy.

作成日：2017 年 3 月 3 日

Sevoflurane pre-conditioning attenuated incomplete hippocampal injury in the rat model of hemorrhagic shock resuscitation via HO-1 by altering Nrf2:Bach1 ratio

出血ショック蘇生モデルへのセボフルラン前投与はNrf2-Bach1系を介したHO-1により海馬の不完全虚血虚血再灌流傷害を改善する

研究者氏名　張　立民（第３８期笹川医学研究者）
中国所属機関　滄州中心医院麻酔科
日本研究機関　岡山大学麻酔蘇生科
指導責任者　森松 博史　教授
共同研究者名　清水 裕子　研究員

Abstract

Objective:

More than 2 million major surgical operations are performed every year worldwide, with increasing frequency of reported incomplete cerebral ischemia induced by hemorrhage shock [1]. The neuroprotective effect of sevoflurane pre-conditioning against cerebral ischemia/reperfusion has been gradually realized, but the underlying mechanism during incomplete cerebral ischemia has not been established [2]. The current studies of neuroprotective mechanism of sevoflurane pre-conditioning mainly focused on attenuation of neuronal apoptosis [3]. As an inducible form of the first and rate-limiting enzyme of heme degradation resulting from the mitochondria cascade, heme oxygenase-1 (HO-1) negatively regulates the development of oxidative stress [4]. As a transcription factor, nuclear factor erythroid 2-related factor 2 (Nrf2) induces the expression of HO-1 mediated by coupling with antioxidant responsive element (ARE) [5]. In contrast, BTB and CNC homology 1 (Bach1), as transcription repressors, down-regulate HO-1 expression [6]. Recent studies have suggested that HO-1 down-regulation is associated with altering the Nrf2-to-Bach1 ratio in alveolar macrophages in patients with severe emphysema or chronic obstructive pulmonary disease (COPD) induced by cigarette smoke [7]. In this study, we examined whether sevoflurane pre-conditioning attenuated hemorrhage shock resuscitation (HSR)-induced neuronal apoptosis via Nrf2:Bach1-HO-1 signal pathway.

Methods:

Rats were subjected to hemorrhagic shock to achieve a mean arterial pressure of 30 mmHg for 60 min by bleeding into a heparinized syringe (10 units/ml), followed by resuscitation with the shed blood and/or sterile saline as necessary until the blood pressure was restored to the baseline level. During sevoflurane preconditioning, rats were performed to inhale 2% sevoflurane for 10 min, and then wash out by air for 10 min before the hemorrhagic shock insult.

Hippocampal neuronal apoptosis was assessed by TUNEL and activated caspase-3 fluorescence assays on 7 days after HSR. Western blot was performed to measure the expression of Nrf2, Bach1 in nuclear and HO-1 in cytosol of hippocampus 1 h, 6 h, 12 h, and 24 h after resuscitation.

Results:

On days 7, HSR increased TUNEL positive cells and activated caspase-3 expression in the hippocampal CA 1 region compared with control ($P<0.05$), whereas sevoflurane pre-conditioning reversed TUNEL positive cells and activated caspase-3 expression ($P<0.05$) (Fig. 1). The ratio of Nrf2:Bach1 6 h and HO-1 12h after resuscitation were significantly increased in HSR group compared with control ($P<0.05$). The ratio of Nrf2:Bach1 6 h and HO-1 12 h after resuscitation were significantly higher in the HSR plus sevoflurane pre-conditioning group than in the HSR group ($P<0.05$) (Fig. 2 and Fig. 3).

Conclusion:

Neuroprotective effects of sevoflurane preconditioning against HSR-induced neuronal apoptosis involved up-regulation of HO-1 via altering Nrf2:Bach1 ratio signal pathway.

Key words:

hemorrhagic shock; heme oxygenase-1; sevoflurane; pre-conditioning

Reference:

1. Lee H M, Lee D H, Choi J H, et al. Sevoflurane-induced post-conditioning has no beneficial effects on neuroprotection after incomplete cerebral ischemia in rats. [J]. Acta Anaesthesiologica Scandinavica, 2010, 54(3):328-36.

2. Krantic S, Mechawar N, Reix S, et al. Apoptosis-inducing factor: a matter of neuron life and death. [J]. Progress in Neurobiology, 2007, 81(3):179-96.

3. Zhang L M, Zhang D X, Zhao X C, et al. Sevoflurane pre-conditioning increases phosphorylation of Erk1/2 and HO-1 expression via inhibition of mPTP in primary rat cortical neurons exposed to OGD/R[J]. Journal of the Neurological Sciences, 2017, 372:171.

4. Fuse Y, Nakajima H, Nakajima-Takagi Y, et al. Heme-mediated inhibition of Bach1 regulates the liver specificity and transience of the Nrf2-dependent induction of zebrafish heme oxygenase 1. [J]. Genes to Cells, 2015, 20(7):590–600.

5. Yamazaki H, Tanji K, Wakabayashi K, et al. Role of the Keap1/Nrf2 pathway in neurodegenerative diseases[J]. Pathology International, 2015, 65(5):210–219.

6. Arimori Y, Takahashi T, Nishie H, et al. Role of heme oxygenase-1 in protection of the kidney after hemorrhagic shock. [J]. International Journal of Molecular Medicine, 2010, 26(1):27-32.

7. Lee H, Park Y H, Jeon Y T, et al. Sevoflurane post-conditioning increases nuclear factor erythroid 2-related factor and haemoxygenase-1 expression via protein kinase C pathway in a rat model of transient global cerebral ischemia. [J]. BJA: British Journal of Anesthesia, 2015, 114(2):307-18.

Figure legend

Figure 1 Sevoflurane pre-conditioning induced decrease of TUNEL-positive cells and cleavage caspase-3 expression after hemorrhage shock resuscitation (HSR) treatment. (A) TUNEL-positive cells (TUNEL, green; nuclear, red) increased after HSR indicating increased neuronal apoptosis, but the value was decreased after sevoflurane pre-conditioning treatment; (C) Cleavage caspase-3 positive neuronal cells (Cleavage caspase-3, green) increased after HSR indicating increased neuronal apoptosis, but the value was decreased after sevoflurane pre-conditioning treatment; (B, D) HSR: Rats were subjected to hemorrhagic shock to achieve a mean arterial pressure of 30 mmHg for 60 min, followed by resuscitation with the shed blood. S+HSR: rats were performed to inhale 2% sevoflurane for 10 min, and then wash out by air for 10 min before HSR treatment. Control: rats without any treatment. Data are presented as mean±SD (n=3/group). Comparisons between groups were using one-way ANOVA with Bonferroni-Dunn tests as post-hoc procedure. $^{*}P<0.05$ vs. Control. $^{**}P<0.05$ vs. HSR

Figure 2 Sevoflurane pre-conditioning induced increase of Nrf2/Bach1 ratio in nuclear after hemorrhage shock resuscitation (HSR) treatment. (A) Optical density (OD) of Nrf2 and Bach1 evaluated by Western blot analysis; (B) Control, HSR and S+HSR denotation were described previously. Data are presented as mean±SD (n=3/group). Comparisons between groups were using one-way ANOVA with Bonferroni-Dunn tests as post-hoc procedure. *P<0.05 vs. control. #P<0.05 vs. control. **P<0.05 vs. HSR 1h. ##P<0.05 vs. S+HSR 1h, HSR 6h.

Figure 3 Sevoflurane pre-conditioning induced increase of HO-1 expression in cytosol after hemorrhage shock resuscitation (HSR) treatment. (A) Optical density (OD) of HO-1 evaluated by Western blot analysis; (B) Control, HSR and S+HSR denotation were described previously. Data are presented as mean±SD (n=3/group). Comparisons between groups were using one-way ANOVA with Bonferroni-Dunn tests as post-hoc procedure. $^{*}P<0.05$ vs. control, HSR 1h, 6h. $^{**}P<0.05$ vs. control, S+HSR 1h, 6h. $^{**}P<0.05$ vs. HSR 12h.

Figure 1

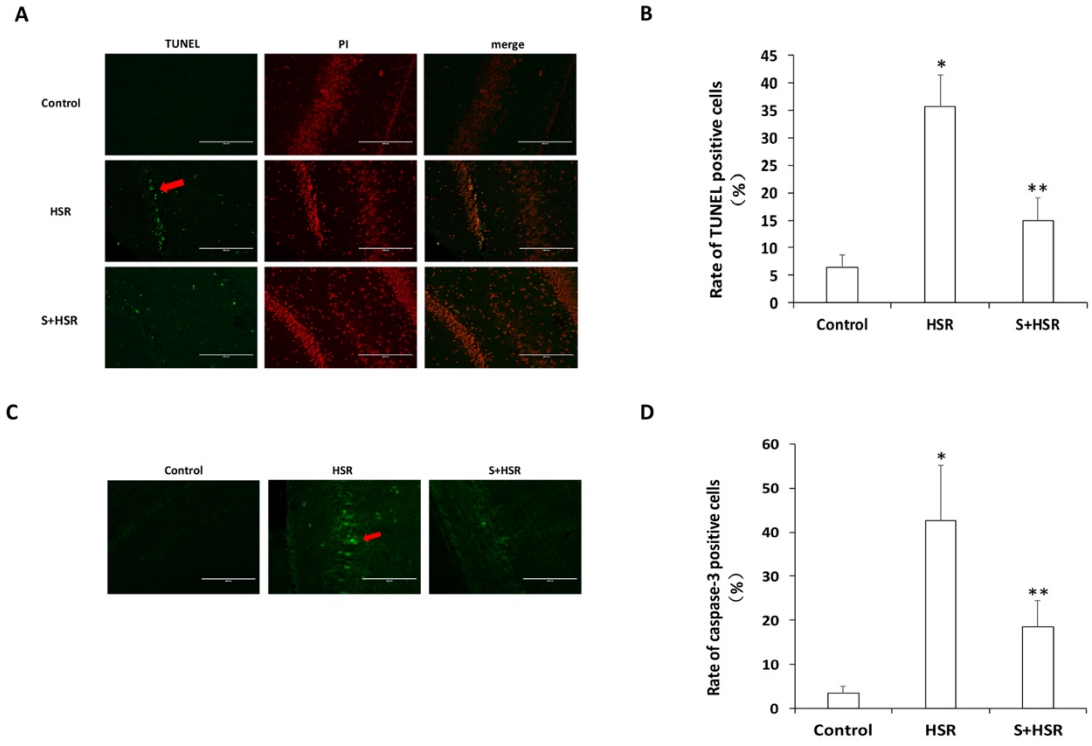

Figure 2

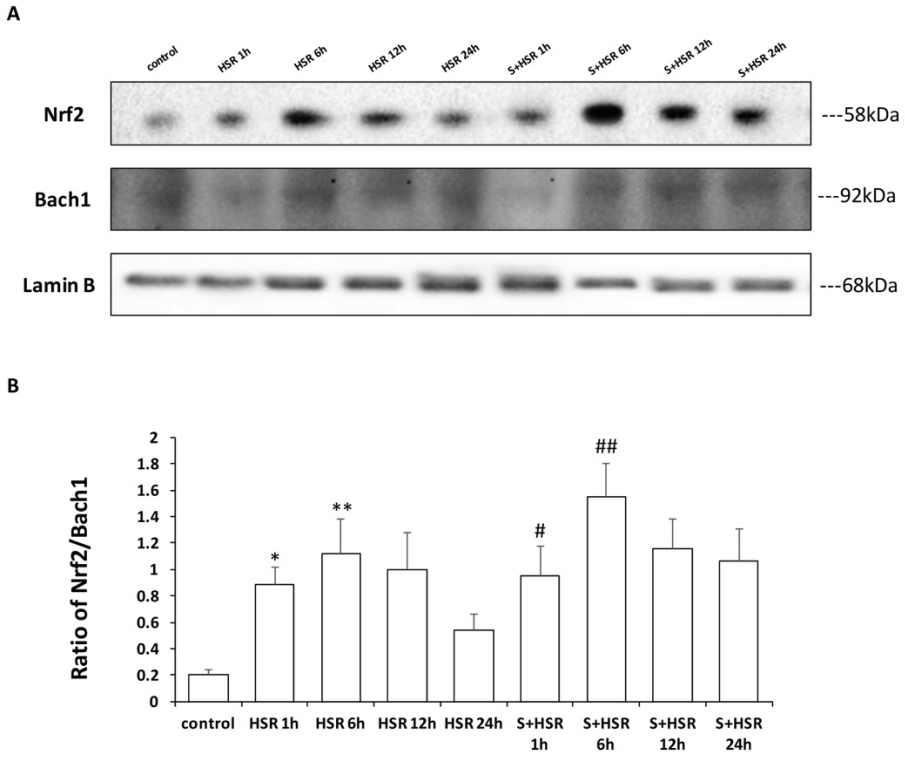

Figure 3

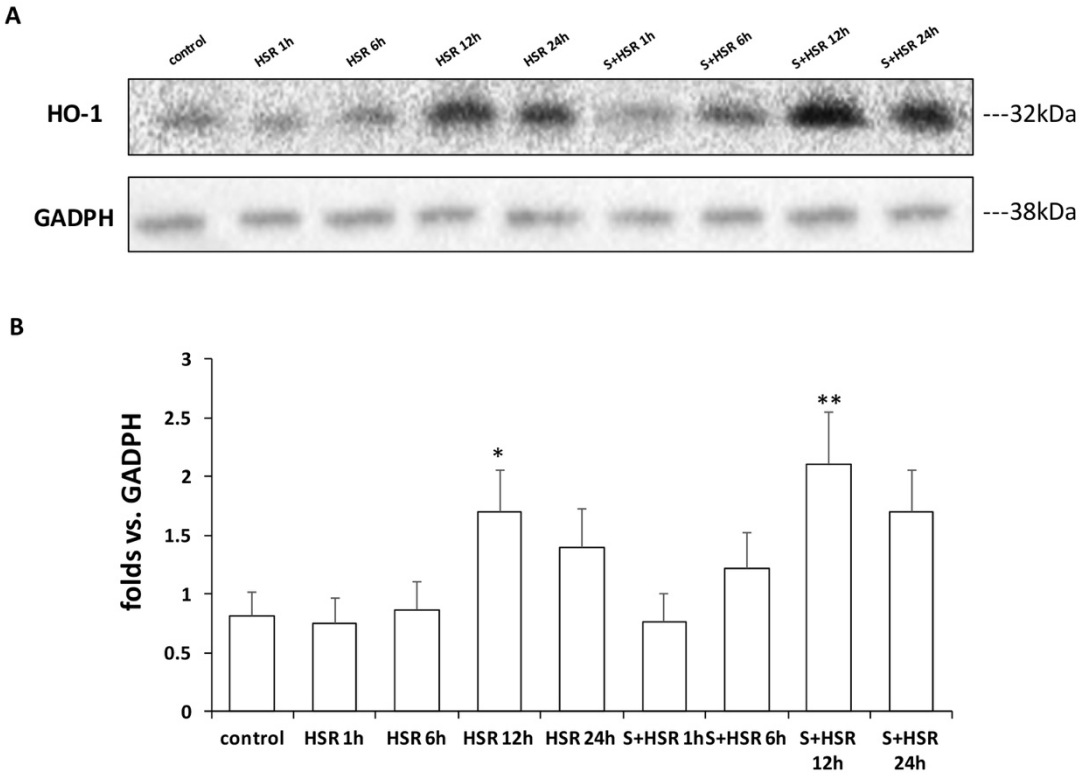

作成日：2017 年 2 月 24 日

日中病院における胃癌手術治療の比較検討

研究者氏名	楊　　光（第３８期笹川医学研究者）
中国所属機関	山西省腫瘤医院普通外科一病区
日本研究機関	埼玉医科大学国際医療センター消化器外科
指導責任者	小山　勇　　教授，山口　茂樹　教授
共同研究者名	桜本　信一　教授，岡本　光順　教授

要旨：2016 年 4 月から 9 月までに、日本の埼玉医科大学国際医療センターと中国の山西省腫瘤医院で胃癌手術を行った症例について比較検討した。両地域の患者に性別の差はなかったが、年齢、発生部位及びステージに差があった。日本の患者より中国の患者は発症平均年齢が若く、噴門部癌の割合が高く、Stage I の発見率は低かった。両地域の胃癌手術患者の特徴が異なることが確認された。術式では、噴門部癌の症例に対して、中国では全例に胃全摘術が行われたが日本では胃全摘術が少なかった。胃癌手術全体の手術時間は中国が短かったがリンパ節郭清個数は少なかった。中国で術後の食事摂取開始時期が遅く、平均入院が長く、術後合併症発生率が高かった。両地域の腹腔鏡手術の導入率について差はなかった。両地域の治療レベルには違いがあり、日本での経験は今後の中国での胃癌診療レベルアップのために有用なものだった。

キーワード： 胃癌, 腹腔鏡手術, EGJ, ERAS

はじめに

著者は 2016 年に日中笹川医学奨学金により、日本の埼玉医科大学国際医療センター(Saitama Medical University International Medical Center, SIMC)で研修の機会を得た。半年間、上部消化器外科桜本教授の指導により胃癌の手術治療を学んだ。SIMC の消化器外科は日本国内屈指の症例数を誇り、2015 年の胃癌に対する手術件数は日本で 9 位である。私の属する山西省腫瘤医院は（Shanxi Tumor Hospital, SXTH）中国の華北地区の大規模癌専門病院の一つで、年間胃癌手術件数は 1000 例以上である。そのうち私が担当する病区は年間300 例以上を行っており、近隣の３つの病区から成る。日本と中国の代表的な二つの病院における胃癌の手術治療を比較することによって、胃癌の臨床病理学的特徴及び治療方法について検討した。

対象および方法

2016 年 4 月から 9 月までに、埼玉医科大学国際医療センター上部消化管外科（SIMC）と山西省腫瘤医院普通外科一病区（SXTH）で治療された原発性胃癌手術症例について、性別、年齢、BMI、腫瘍の位置、ステージおよび手術法について、２つ病院の類似点と相違点を検討した。

結果

胃癌手術症例数は SIMC 群 121 例、SXTH 群 151 例であった。平均年齢は SIMC 群が SXTH 群有意に高い結果となって（$P<0.05$）、身長は有意に低い結果であった（$P<0.05$）。腫瘍位置では、SIMC 群は主に胃体

部と前庭部で発生していたのに対し、SXTH 群では胃食道接合部(esophago-gastric junction, EGJ)近傍の噴門部の割合が多かった（P<0.05）。腫瘍ステージでは、SIMC 群は Stage I が多いのに対し SXTH 群は Stage III が多かった。性別、体重及び BMI では有意差はみられなかった（表１）。

根治胃癌手術は、SIMC 群 111 例、SXTH 群 143 例に行われた。SIMC 群は手術時間が有意に長かったが、SXTH 群はリンパ節郭清個数が有意に少なかった。また SXTH 群は術後食事摂取開始が遅く平均入院期間が長く、さらに術後合併症発生率が高くいずれも有意差を認めた（P＜0.05）（表２）。SIMC 群では 73 例（65.8%）に部分胃切除術が行われたのに対し、SXTH 群では 76 例（53.1%）に胃全摘術が行われていて有意差を認めた（表３）。両群の腹腔鏡手術の施行率には差がなかった（P>0.05）（表４）。

考察

日本と中国は胃癌の発生率が高い国である。 世界保健機関（WHO）の統計によると、2002 年に全世界で日本の胃癌発生率は第一位で、中国は第二位でなった。その後 2014 年のレポートでは、世界で新罹患症例の四分の三がアジアで発生し、アジアの症例の中で中国は五分の二を占め、日本の胃癌発生率が著しく減少した[1]。日本は胃癌の基礎研究及び臨床治療が古くからアジアの最先端を歩んできて、中国の胃癌治療は今まで日本の臨床研究結果を参考にしてきた。日本の先進的な治療を学び中国の欠点を模索して、中国の胃癌治療技術の発展を図るために、二つの病院の胃癌手術の短期成績を比較した。

胃癌発症の特徴からみると、SMIC 群は発症年齢が高く、比較的早期の癌の治療率が高く、腫瘍が胃の遠位で発生していることが認められた。一方、SXTH 群は発症平均年齢が 60 歳未満で、噴門部の発生率が高く、治療時は、多くが進行癌になっていた（P＜0.05）。これらから日中両国の胃癌患者の特徴がみられる。長寿大国と言われる日本は胃癌の対策を重視しており、1970 年代から政府と企業が共同出資して国民に X 線二重造影検査と内視鏡検査を主とする定期健康診断を受けられるようにした。それによって全体に占める早期胃癌の発見率は 42％から現在の 70%までに上がって胃癌の治療効果も大いに向上した。中国では胃癌の定期検査受診率は依然として低く、特に農村地方及び発展の遅れた地区では定期検査という概念の欠如から進行癌で発見されることが多く早期胃癌の比率は 10%以下である。さらに中国の環境汚染と食品安全上の問題は深刻であり、胃癌の発病年齢が早まったという説もある。また術後の合併症などが原因になって術後死亡率は比較的高い。また近年は、中日両国において西洋文化の影響を受け飲食習慣が変わってきた。両国のデータからみて噴門部癌の発病率が増加傾向であり、特に中国で明らかである[2]。これは近年の研究課題の一つでもある。

手術治療は胃癌の主要な治療手段である。治癒手術を受けた2期胃癌患者の5年生存率は60%～80%である[3]。表2の結果からみると、SXTHでは胃全摘術が多いのに対してSMICでは部分胃切除術の方が多かった（P<0.05）。これは噴門部癌が大きく影響しており、腫瘍の位置や大きさ及び進行状況等という要素のほか、表3のようにSXTHはすべての噴門部癌に対して胃全摘術を行い、胃を温存する噴門部切除術は1例もなか

った。一方、SMIC では噴門部癌に対して積極的に噴門側胃切除術を行っていた。噴門側胃切除術は胃の貯留能が保持されるものの、再発のリスクや逆流性食道炎で生活の質の低下が懸念される。日本は早期癌が多いので再発リスクは少なく機能温存の手術がますます重視されていて、人工 His 角作成や空腸間置などによる逆流防止の方法改善により良好な効果を得た。これらによって部分的に胃を温存して患者の生活の質を改善できることが確認された[4]。一方、中国では進行癌が多くを占め、そのうえ逆流防止効果は疑れているため、今日まで胃全摘術が標準的な方法と考えられている。

SMIC は SXTH より手術の平均時間が長かったが（P<0.05）、日本の手術操作が中国より熟練性で劣るわけではなくて、両国の修練医に対する育成方法の違いのためであった。私は SMIC の上部消化管外科にいる半年間で見学した手術の中で、修練医が教授の指導に従って執刀、手術を完遂する症例が大部分を占めた。中国では、副主任医師以上の資格を持っている医師だけに比較的複雑な手術である胃癌手術を行う資格がある。今の中国は医師と患者の関係が必ずしも良好とは言えないことに加えて、若手医師が執刀する機会が非常に少なく、ほとんど全ての手術を教授が遂行していた。一方で、日本では手術中の落ち着いた雰囲気の下で、傷は小さく、手術操作は滑らかで操作のひとつひとつが丁寧なため、時間は長かった。その結果、手術後の合併症の発生率は有意に低い結果であった。(P<0.05)(表 2)。

腹腔鏡手術は現在外科領域で幅広く行われる方法である。1980 年代に世界初の胃癌腹腔鏡手術が成功してから 30 年経過した今日では非常によく行われている手術となった。一方、中国の胃癌腹腔鏡手術はスタートが遅れていたが、2000 年以降に広く普及するようになり、SXTH では 2010 年以降に多く導入された。従って、今回の来日では腹腔鏡下胃癌手術について学習することが主要な目的でもあった。表 2 から SMIC 群と SXTH 群のデータは腹腔鏡手術率では大きな差が見られていないが、疾患ステージで層別解析すると二病院に腹腔鏡手術の適応症における大きな差が存在することが明らかであった（表 4）。SMIC では比較的早期の胃癌である 1 期、2 期の患者に腹腔鏡手術を行っている。SXTH ではその傾向はなく、ステージに関係なく腹腔内視鏡手術行っていた。日本臨床腫瘍研究グループ(JCOG)による臨床試験では早期胃癌患者に対する腹腔鏡手術および従来の開腹手術に治療成績には差がなく、傷が小さく回復も早いというメリットがあることが検証された。しかし進行期胃がんを対象とする臨床試験の研究結果はまだなくガイドラインにも示されていない。進行した胃癌における腹腔鏡手術適応について桜本教授はもとより日本は慎重な態度を持っている。一方中国では臨床研究に対する着手が遅れているが、進行胃癌患者が多く大量の臨床症例を背景に進行胃癌患者を対象に率先して臨床研究を展開している。現在、最新の無作為臨床試験[5]では進行胃癌患者に対する腹腔内視鏡手術の短期成績の安全性は示されたが、長期的な効果については今後の検証が必要である。日本の腹腔鏡手術の手技においては、操作に関してきめ細かく繊細で、さまざまな工夫も加えられている。例えば、腹腔鏡下幽門側胃切除術で吻合を行う際、SMICでは標本を切除した後で腹壁を引き上げて空間を保ち、腹腔鏡下に吻合することで、良視野の確保とともに、傷も小さくてすむ（図1）。これに対しSXTHでは開腹、標

本摘出した後で直視下に吻合を行うため、十分な腹壁の切開を加えなければならない（図 2）。このような技巧はいくつもあり、何気なく行っている手技は、桜本教授が長年の臨床経験の末に築いたものである。別の印象深いことの一つに、SMIC の医師はチーム意識が強いことがあげられる。手術を遂行しているとともに、手術に参加しない医師は切除標本を観察し、リンパ節をひろいあげ、吻合口の状態を確認する。手術を効率的に行えると同時に、標本は詳細に正確に病理組織学的な検討が行われる。一方、SXTH の医師は独立したグループに分かれているので、手術後摘出標本を処理する時間が十分に取れないまま、間もなく次の手術の準備にかかっている。その際には標本からリンパ節を拾い上げることを熟知しない病理検査技師に任せることになり、SXTH グループのリンパ節検索数が SMIC より有意に低い結果になっていた。これは SXTH が今後改善する必要があるところだ。

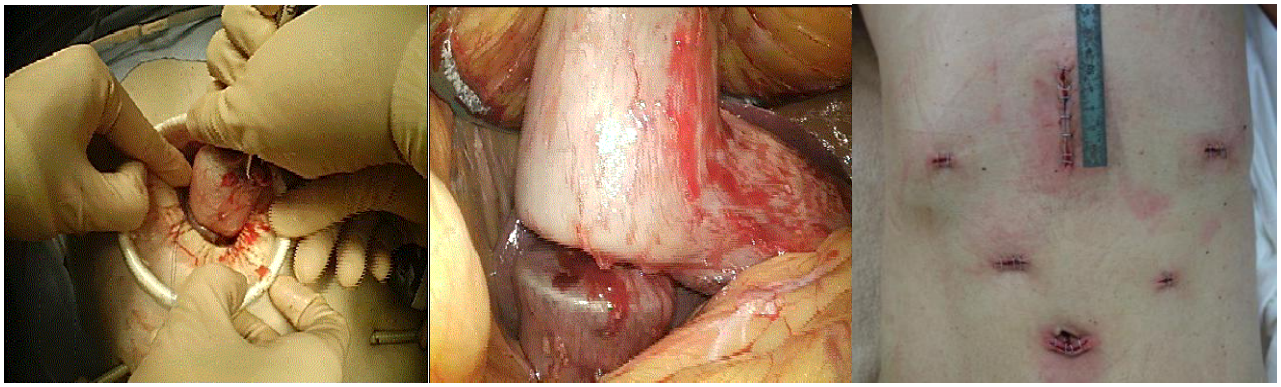

図 1　SMIC 幽門側胃切除吻合および閉腹する状況

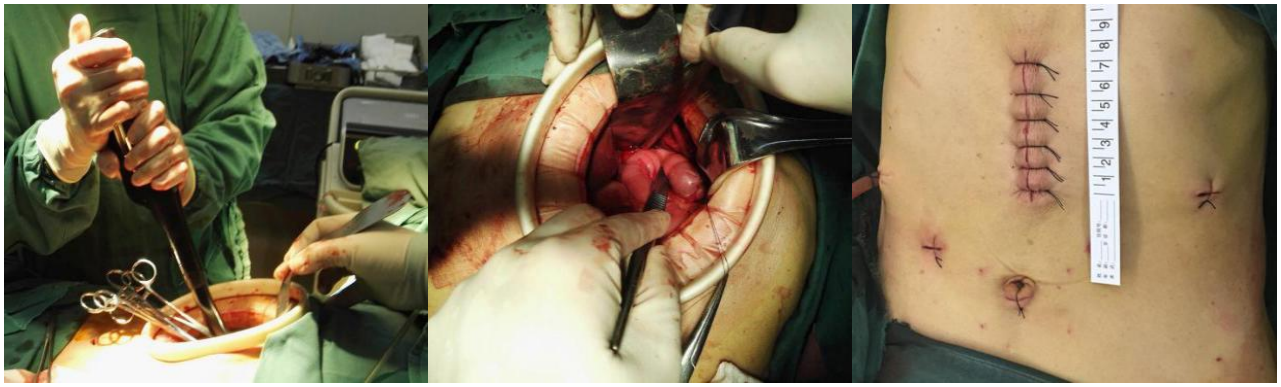

図 2　SXTH 幽門側胃切除吻合および閉腹する状況

最後に胃癌患者の術後管理について述べる。SMIC は ERAS プロトコルをよく実行していた。全身麻酔及び硬膜外麻酔の複合麻酔を行って術中管理し、術後も疼痛を軽減していた。術中の体温をモニタリングして体温管理し、下肢加圧ポンプなどで静脈血栓形成を予防した。また術後早期に胃管を抜去し、異常がなければ第 3 病日から食事摂取を開始し、約 1 週間で退院する。中国では、ERAS が強く提唱されているものの、患者は医師に対して懐疑的あり、多くの医師が過度に慎重に術後管理を行う傾向がある。SXTH では、全身麻酔を行い、術中体温の管理は注意しているが、下肢静脈血栓に対する予防は行っていない。術後約 1 週間

で胃管を抜き、消化道造影で吻合部を確認してから食事を始めるため、平均入院期間は 2 週間である。術後管理について、SMIC は術後患者の QOL を下げずに在院日数も短くできることを目の当たりにした。中国の現状を変えるために、医療環境を改善することだけではなく、外科医、麻酔医及び看護系の連携意識を増強し、チームとしての行動力を高める必要があると思われる。

まとめ

SMIC は SXTH と比べて、胃癌に対する手術治療および術後管理の方面で優れた点がみられた。この経験から学び参考にすることによって、SXTH の胃癌に対する診断と治療能力を高めたい。

文献

[1] Stewart BW, Wild CP. World Cancer Report 2014. http://publications.iarc.fr/ Non-Series-Publications/ World-Cancer-Reports/World-Cancer-Report-2014.

[2] Kusano C, Gotoda T, Khor CJ,et al.Changing trends in the proportion of adenocarcinoma of the esophagogastric junction in a large tertiary referral center in Japan. J Gastroenterol Hepatol. 2008 Nov;23(11):1662-5.

[3] 陈峻青．胃癌外科治疗的术式选择与评价．中华医学杂志，2004，84(24)：2057-2059.

[4] Takiguchi N, Takahashi M, Ikeda M, et al.Long-term quality-of-life comparison of total gastrectomy and proximal gastrectomy by postgastrectomy syndrome assessment scale (PGSAS-45): a nationwide multi-institutional study. Gastric Cancer. 2015 Apr;18(2):407-16.

[5] Sakuramoto S, Yamashita K, Kikuchi S,et al. Laparoscopy versus open distal gastrectomy by expert surgeons for early gastric cancer in Japanese patients: short-term clinical outcomes of a randomized clinical trial. Surg Endosc. 2013 May;27(5):1695-705.

[6] Hu Y, Huang C, Sun Y, et al.Morbidity and Mortality of Laparoscopic Versus Open D2 Distal Gastrectomy for Advanced Gastric Cancer: A Randomized Controlled Trial. J Clin Oncol. 2016 Apr 20;34(12):1350-7.

作成日：2017 年 02 月 19 日

表 1　全手術症例の臨床病理学的特徴の**比較**

Characteristics	SIMC group	SXTH group	P value
SEX, n			
Male	91(75.2%)	105(69.5%)	0.300
Female	30(24.8%)	46(30.5%)	
Age, years			
Mean	70.4	58.5	<0.001
Range	44-87	26-85	
Height, cm			
Mean	161	165	<0.001
Range	125-177	142-188	
Weight, Kg			
Mean	59	61	0.086
Range	32-84	35-89	
BMI			
Mean	22.4	22.4	0.088
Range	11.1-31.2	15.6-34.9	
Tumor location			
U	15(11.5%)	59(38.6%)	<0.001
M	71(54.6%)	32(20.9%)	
L	44(33.8%)	62(40.5%)	
Pathological stage, n			
Ⅰ	53(43.8%)	30(19.9%)	<0.001
Ⅱ	30(24.8%)	26(17.2%)	
Ⅲ	25(20.7%)	85(56.3%)	
Ⅳ	13(10.7%)	10(6.6%)	

表 2　　胃癌根治手術の短期成績の比較

Characteristics	SIMC group	SXTH group	P value
Surgical procedure, n			
Total gastrectomy	38(34.2%)	76(53.1%)	0.003
Partial gastrectomy	73(65.8%)	67(46.9%)	
Surgical method, n			
Laparoscopic surgery	70(63.1%)	73(51.0%)	0.057
Open surgery	41(36.9%)	70(49.0%)	
Operation time, min			
Mean	257	177	0.001
Range	99-473	90-340	
Intraoperative blood loss, ml			
Mean	124	126	0.934
Range	0-960	5-800	
Number of harvested lymph nodes, n			
Mean	37	26	<0.001
Range	15-86	3-74	
Postoperative oral intake, days			
Mean	3.4	10.3	<0.001
Range	2-19	5-51	
Postoperative hospital stay, days			
Mean	10.1	18.2	<0.001
Range	4-38	7-94	
Postoperative complication			
Anastomotic leakage	3	11	0.015
Wound problem	0	2	
Intra-abdominal bleeding	1	4	
Intraluminal bleeding	0	2	
Ileus	2	3	
Intra-abdominal abscess	1	5	

Lymphatic leakage	0	1
Pancreatic leakage	2	1
Pulmonary	2	5
Others	2	0
Total	13(11.8%)	34(23.8%)

表 3　噴門部胃癌における術式の**比較**

	Number of patients	Total gastrectomy	Partial gastrectomy
SIMC group	15	6	9
SXTH group	54	54	0

表４　　ステージ別腹腔鏡手術の**比較**

Hospital	Pathological stage		Laparoscopic surgery	Open surgery	Total	P value
SIMC group	stratification	Ⅰ+Ⅱ	65(58.6%)	18(16.2%)	83	<0.001
		Ⅲ+Ⅳ	5(4.5%)	23(20.7%)	28	
	total		70	41	111	
SXTH group	stratification	Ⅰ+Ⅱ	36(25.1%)	20(14.0%)	56	0.016
		Ⅲ+Ⅳ	37(25.9%)	50(35.0%)	87	
	total		73	70	143	

Clinicopathological features and outcomes after hepatectomy for diabetes mellitus related hepatocellular carcinoma

糖尿病に関連する肝がんの臨床病理の特徴と肝切除手術の予後

研究者氏名　梁　静（第38期笹川医学研究者）
中国所属機関　天津市第三中心医院消化器科
日本研究機関　東京女子医科大学附属病院消化器外科
指導責任者　山本　雅一　教授
共同研究者名　有泉　俊一　准教授

Abstract

Aims: To investigate cilinicopathological characteristics and surgical outcomes of DM related HCC patients who underwent liver resection.

Methods: All 189 patients of HCC with DM underwent hepatectomy and were studied retrospectively. Patients were divided into virus-HCC group (n=84), alcohol-HCC group (n=30), DM-HCC group (n=75) according to the history of patients. The cilinicopathological characteristics and surgical outcomes of HCC patients among three groups were analyzed. Moreover, the features and prognosis between DM with nonalcoholic steatohepatitis (NASH) and without NASH in background have also been compared.

Results: The patients in DM-HCC had higher age and serum PIVKA-II level than those in virus-HCC and alcohol-HCC ($P<0.05$).Comparing with virus-HCC, DM-HCC patients was associated with larger BMI, higher albumin and prothrombin activity as well as larger tumor size ($P<0.05$). After hepatectomy, 5 year recurrence free survival (RFS) rate and overall survival (OS) rate were significantly higher in DM-HCC group (22.7% and 49.3%) than in virus-HCC group (9.5%, $P<0.05$; 31.0%,$P<0.05$), whereas no difference between DM-HCC and alcohol-HCC groups (20.0%, $P=0.765$;43.3%, $P=0.578$). In DM-HCC group, both the OS and RFS in DM-HCC were longer than those in virus-HCC group ($P<0.05$). PIVKA-II>200 mAu/ml, vascular invasion and intrahepatic metastasis were independent risk factors for OS and RFS of all HCC patients after hepatectomy ($P <0.01$). Comparing with DM with NASH group, patients of DM without NASH group associated with more percentage of vascular invasion and higher PIVKA-Ⅱ level ($P<0.05$,$P<0.01$). Nevertheless, there was no difference of OS and RFS between the two groups ($P=0.59$, $P=0.76$).

Conclusion: Our study showed that the patients in DM related HCC exhibited a better liver function and lower degree of liver cirrhosis than patients with virus related HCC. Patients with DM related HCC showed favorable long-term surgical outcomes than virus related HCC after hepatectomy. PIVKA-Ⅱ could be a hopeful tumor marker of DM related HCC and prognostic factor for HCC patients with DM.

Key Words: Diabetes mellitus; hepatocellular carcinoma; nonalcoholic steatohepatitis; hepatectomy

Introduction

Many studies suggested that diabetes mellitus (DM) may play an important role in non B non C hepatocellular carcinoma [1,2]. In this study, we aim to evaluate the DM related HCC patients who underwent liver resection, with the purpose of comparing the cilinicopathological characteristics and surgical outcomes with those of virus related HCC and alcohol related HCC patients in the background of DM. Furthermore, we aim to classify DM related HCC according to pathological manifestation (NASH and non-NASH) and compare its characteristics and outcomes.

Patients and methods

Consecutive patients who received liver resection for primary HCC from January 2002 to December 2013 at Tokyo Women Medical University were recruited. The 189 HCC patients who concomitant DM were classified by etiology.77 patients were defined as DM-HCC when DM patients with viral-hepatitis, alcohol hepatitis, autoimmune hepatitis and other hereditary liver disease were excluded. Baseline clinical and laboratory parameters, clinical history of diabetes and hypoglycemic therapy were retrieved and reviewed from the hospital database. All liver specimens were re-examined by two senior pathologists who were blinded to the original diagnosis.

Result

A total of 837 HCC patients performed hepatectomy during 2002-2013, in which 189(22.6%) patients combined with diabetes mellitus. Among 189 HCC patients with DM, virus-HCC were diagnosed in 84 patients (44.4%), alcohol-HCC in 30 patients (15.9%), 75 patients (39.7%) had no other chronic liver disease were classified as DM related HCC.

Table 1 showed the cilinicopathological characteristics among three groups. HCC was diagnosed at a significantly higher age, larger BMI in DM-HCC group than virus-HCC group. The ALT and AST level was significantly lower in DM-HCC group compared with that in virus-HCC group. Patients in DM-HCC had the highest serum albumin levels and prothrombin activity which were significantly higher than those in virus-HCC group. The Maximum tumor size in DM-HCC was significantly larger than that in virus-HCC and alcohol-HCC. All 189 patients underwent a median follow-up of 46.7 months (range 1~ 183 months), 50 patients (26.5%) died from cancer recurrence, and 12 patients (6.3%) died from DM complications. A significantly longer OS and RFS at time of maximal follow up was observed in DM-HCC group with a statistically difference than those in virus-HCC group. (figure1).

All 189 HCC patients with DM were analyzed by Cox regression. Multivariate analysis identified that PIVKA-II>200 mAu/ml, vascular invasion and intrahepatic metastasis were significant risk factors for OS and RFS after hepatectomy. (figure2)

All 75 DM- HCC were divided into DM with NASH group (37cases) and DM without NASH (38cases) according to the background NASH diagnosis. DM with NASH patients showed larger BMI, higher level of HBA1c and albumin than those in DM without NASH patients. While higher PIVKA-Ⅱ level and platelet count were observed in DM without NASH group than those in DM without NASH group(Table 2). Survival analysis was also performed between two groups, but no significant difference between two groups were observed.

Discussion

Hepatocellular carcinoma is a growing concern due to its high mortality and poor progression, more attention was given to address the causal risk factors that could be preventable and treatable. Several risk factors have been identified that contribute to the occurrence and development of HCC such as chronic infection with HBV and HCV, alcoholic liver disease, NASH, DM, obesity and genetically inherited disorders. Of known risk factors for HCC, DM was considered an important risk of HCC supporting by substantial evidences [3,4]. In light of the emerging trends of increasing number of patients with DM developing HCC, there is an urgent need to clarify and strategize the HCC originating from DM. In this study we evaluated the clinical and pathological characteristics of DM related HCC patients by comparing that with other underlying etiologies patients in the background of DM

In our center from 2002 to 2013, HCC with DM patients accounted for 22.6% of all 837 HCC patients who underwent liver resection. All these patients included HCC with definite etiology such as hepatitis C, hepatitis B and

alcoholic hepatitis in which DM were considered to be a concomitant phenomenon. The remaining 75 DM related HCC patients accounted for 39.7% of all HCC with DM patients.

Comparing of the characteristics with different etiologic HCC patients, DM-HCC patients were older at HCC diagnosis. It suggest that incidence of HCC increased with age in patients with DM history. In these three groups, the BMI of DM related HCC patients group was highest, which could be speculated that obese patients are more likely to develop diabetes and hepatocellular carcinoma[5]. In DM related HCC, serum albumin levels and prothrombin activity were higher while serum ALT and AST levels decreased in the HCC group than those observed in the virus related HCC. These data suggest that the patients in DM- HCC exhibited a better liver function than patients with virus-HCC.

According to reports of features of pathology, larger tumor size and higher non-cirrhosis percentage were detected in patients of DM-HCC comparing with virus-HCC and alcohol-HCC patients. The larger tumor size was one of the characteristics of DM-HCC which was similar to the HCC associated with metabolic syndrome described in previous study [6]. The reason was thought to reflect rapid tumor growth due to hyperinsulinemia associated with DM [7]. Combined with the higher platelet levels detected in DM-HCC, we consumed that the DM-HCC patients have lower degree of liver cirrhosis and portal hypertension than virus-HCC and alcohol-HCC.

Without consideration of hepatocellular carcinoma, DM itself may result in a higher operative risk and affect the long survival after liver resection. Studies of early stage HCC patients undergoing liver resection also demonstrated significantly decreases OR and RFS in DM patients compared to non-DM patients [8]. However, there was no report about the comparison of DM related HCC and other etiological HCC with DM background. In our study 5 year OS rate was significantly higher and overall survival time was much longer in DM-HCC than those in virus-HCC group after hepatectomy. Combined with the clinical features, we suggested that the better prognosis associated with DM-HCC probably due to its better liver function and lower degree of cirrhosis in background. Therefore the patients with DM-HCC were less likely to develop decompensated cirrhosis and had more opportunity for repeat-resection or other treatment than virus-HCC patients. Furthermore, by Kaplan–Meier analysis, we found that the 5 year RFS rate and RFS time of DM-HCC patients were significant better than those of virus-HCC patient, which indicated that DM-HCC patients associated with later tumor relapse. The reason maybe speculated by the older age at diagnosis of DM-HCC and stronger carcinogenesis of HCV. Another important reason was recognized the synergistic role of DM with HCV infection in exacerbating liver disease and promoting HCC developing [9]. Therefore, we should be confident of good prognosis for DM related HCC patients after hepatectomy, although they have older ages.

Multiple reports suggested a substantial proportion of HCC arise as a result of hepatocellular injury from NASH. Insulin resistance and the resulting inflammatory cascade, which are associated with the development of NASH appears to mediate hepatocarcinogenesis in HCC. But Patients were considered to have NASH as a potential etiological factor of HCC only if there was clear evidence of steatohepatitis on pathologic review of the surgical specimens. Moreover NASH was apparently associated with several causes which share the insulin resistance as the pathologic link, such as DM, HCV and Obesity, therefore NASH was also considered to be hepatic manifestation of metabolic disease[10]. Studies reported a high prevalence of NASH in DM patients [11], yet no previous report has focused on the differences between DM-related HCC patients with NASH and those without NASH.

In our study patients of DM with NASH in background contributed to 49.3% of all DM related HCC patients, and non-NASH in background also contributed to a significant proportion (51.7%). Our study firstly compared the clinic pathological difference between DM with and without NASH. We found that DM with NASH group showed larger BMI, higher serum level ALB and HBA1c which suggested more higher BMI and hyperglycemia were more likely to

associated with NASH manifestation in the liver of DM related HCC patients. The notable histological characteristics of DM without NASH include a tendency of vascular invasion as well as larger tumor size. This result was similar to Connolly's finding that DM impacted risk of macrovascular invasion in patients of HCC [12]. However we failed to demonstrate statistical significant prognosis between DM with and without NASH groups. Clinically, it is difficult to precisely discriminate between NASH or DM as a certain cause of cirrhosis and HCC, but our study showed that there were some differences between the DM with and without NASH background. Clearly large sample study is needed to further determine the synergistic role of these two cross-talk diseases.

Though large-scale study showed DM is an independent risk factor for HCC, there is still no indicative marker to identify DM related HCC. Prothrombin induced by vitamin K absence-Ⅱ (PIVKA-Ⅱ) is an abnormal prothrombin protein that is elevated in HCC. To date, many studies have been conducted to determine the role of PIVKA-Ⅱ in patients with HCC and considered it as an important predictor of early HCC[13] . In our study, one interesting result showed that PIVKA-Ⅱ was much higher in DM-HCC patients than virus-HCC and alcohol- HCC patients, especially in DM without NASH patients. Moreover elevated level of PIVKA-Ⅱ was closely associated with poor survival and tumor recurrence. So that we speculated PIVKA-Ⅱ could be used as a hopeful tumor marker DM related HCC and a prognostic factor for HCC patients with DM.

In conclusion, we confirmed that DM related HCC associated with better liver function and distinctive pathological features, meanwhile showed favorable long-term outcomes and associated with later tumor relapse after hepatectomy.

Reference:

1 Ochiai T, Ogino S, Ishimoto T, Toma A, Yamamoto Y, Morimura R, et al. Prognostic impact of hepatectomy for patients with non-hepatitis B, non-hepatitis C hepatocellular carcinoma. Anticancer Res 2014;34:4399-4410. PMID:25075077.

2 Ali Kamkar MM, Ahmad R, Alsmadi O, Behbehani K. Insight into the impact of diabetes mellitus on the increased risk of hepatocellular carcinoma: mini-review. J Diabetes Metab Disord 2014;13:57. PMID:24918094.

3 Welzel TM, Graubard BI, Quraishi S, Zeuzem S, Davila JA, El-Serag HB, et al. Population-attributable fractions of risk factors for hepatocellular carcinoma in the United States. Am J Gastroenterol 2013;108:1314-1321. PMID:23752878.

4 Hotta N, Nakamura J, Iwamoto Y, Ohno Y, Kasuga M, Kikkawa R, et al. Causes of death in Japanese diabetics: A questionnaire survey of 18,385 diabetics over a 10-year period. J Diabetes Investig 2010;1:66-76. PMID:24843411.

5 Marengo A, Rosso C, Bugianesi E. Liver Cancer: Connections with Obesity, Fatty Liver, and Cirrhosis. Annu Rev Med 2016;67:103-117. PMID:26473416.

6 Yoshida N, Takayama T, Midorikawa Y, Higaki T, Nakayama H, Moriguchi M, et al. Surgical outcomes in patients with hepatocellular carcinoma associated with metabolic syndrome. World J Surg 2015;39:471-477. PMID:25331727.

7 Arcidiacono B, Iiritano S, Nocera A, Possidente K, Nevolo MT, Ventura V, et al. Insulin resistance and cancer risk: an overview of the pathogenetic mechanisms. Exp Diabetes Res 2012;2012:789174. PMID:22701472.

8 Ting CT, Chen RC, Chen CC, Liu MH, Chu D, Kuo NW. Diabetes worsens the surgical outcomes in cirrhotic patients with hepatocellular carcinoma. Tohoku J Exp Med 2012;227:73-81. PMID:22688467.

9 Dyal HK, Aguilar M, Bartos G, Holt EW, Bhuket T, Liu B, et al. Diabetes Mellitus Increases Risk of Hepatocellular Carcinoma in Chronic Hepatitis C Virus Patients: A Systematic Review. Dig Dis Sci 2016;61:636-645. PMID:26703125.

10 Chettouh H, Lequoy M, Fartoux L, Vigouroux C, Desbois-Mouthon C. Hyperinsulinaemia and insulin signalling in the pathogenesis and the clinical course of hepatocellular carcinoma. Liver Int 2015;35:2203-2217. PMID:26123841.

11 Shima T, Uto H, Ueki K, Takamura T, Kohgo Y, Kawata S, et al. Clinicopathological features of liver injury in patients with type 2 diabetes mellitus and comparative study of histologically proven nonalcoholic fatty liver diseases with or without type 2 diabetes mellitus. J Gastroenterol 2013;48:515-525. PMID:22911170.

12 Connolly GC, Safadjou S, Kashyap R, Chen R, Orloff MS, Hezel AF. Diabetes mellitus impacts risk of macrovascular invasion in patients undergoing transplantation for hepatocellular carcinoma. BMC Gastroenterol 2013;13:9. PMID:23317091.

13 Yu R, Xiang X, Tan Z, Zhou Y, Wang H, Deng G. Efficacy of PIVKA-II in prediction and early detection of hepatocellular carcinoma: a nested case-control study in Chinese patients. Sci Rep 2016;6:35050. PMID:27731353.

Table 1 Cilinicopathological features and outcomes of DM-HCC, Virus-HCC and Alcohol-HCC groups

	DM-HCC (n=75)	Virus-HCC (n=84)	Alcohol-HCC (n=30)
Clinical factors			
Age（years）	70.8±9.1[v,a]	66.5±8.8	66.5±7.6
Gender(male/female)	70/5	77/7	28/2
BMI(kg/m^2)	24.4±3.5[v]	22.5±3.4[a]	24.8±3.5
ICG15(%)	13.5±11.7	14.6±8.4	15.4±12.6
TBil(mg/dl)	0.6±0.3	0.7±0.7	0.7±0.3
ALT(iu/l)	37.7±20.4[v]	53.8±36.8	42.6±28.4
AST(iu/l)	39.2±22.4[v]	55.8±41.7[a]	38.4±19.1
ALB(g/dl)	3.9±0.4[v]	3.7±0.5	3.9±0.4
ALP(iu/l)	397.0±319.0	353.5±189.8	318.5±310.0
GGT(iu/l)	145.6±150.6	123.3±122.0	166.1±147.5
Child-Pugh(A/B)	70/5	74/10	29/1
PLT(10^4/ul)	19.2±7.5[v,a]	13.7±5.1	14.8±6.0
Prothrombin activity (%)	91.2±9.4[v]	87.7±9.2	87.8±10.3
HBA1c(%)	8.2±1.7	8.3±1.6	7.6±1.4
$_{LG10}$(AFPng/ml)	1.3±1.2	1.6±1.0	9.5
$_{LG10}$(PIVKA-Ⅱ mAu/ml)	2.7±1.3[v]	2.3±1.0	2.67±1.08
Pathological finding			
MaximumTumor size(cm)	6.6±4.1[v,a]	4.2±2.9	4.8±2.9
Vascular invasion (negative/positive)	56/19	59/25	22/8
Im(negative/positive)	60/15	59/25	24/6
Background liver(LC/non-LC)	10/65[v,a]	43/41	12/18
Macroscopic type(small nodular with indistinct margin, simple nodular type, simple nodular type with extranodular	64/9/2	68/10/6	21/4/5

growth/mutinodular type/mass type)			
Outcomes			
5 year overall survival rate	49.3%(37/75)[v]	31.0%(26/84)	43.3%(13/30)
5 year recurrence free survival	22.7%(17/75)[v]	9.5%(8/84)	20.0%(6/30)
Overall survival (month,median)	57.3[v]	37.7	46.4
Recurrence free survival (month,median)	53.3[V]	20.8	20.5

AST, aspartate aminotransferase; ALT, alanine aminotransferase; GGT, gamma-glutamyl transpeptidase; ALP, alkaline phosphatase; TBil, total bilirubin; PLT, platelet count;ICG15, indocyanine green retention at 15 min;HBA1c, hemoglobinA1c; AFP, alpha-fetoprotein; PIVKA-Ⅱ, protein induced by vitamin K absence or antagonist-II; Im, Intrahepatic metastasis; LC, liver cirrhosis; v: Comparison with Virus-HCC, p<0.05.a: Comparison with Alcohol-HCC, p<0.05.

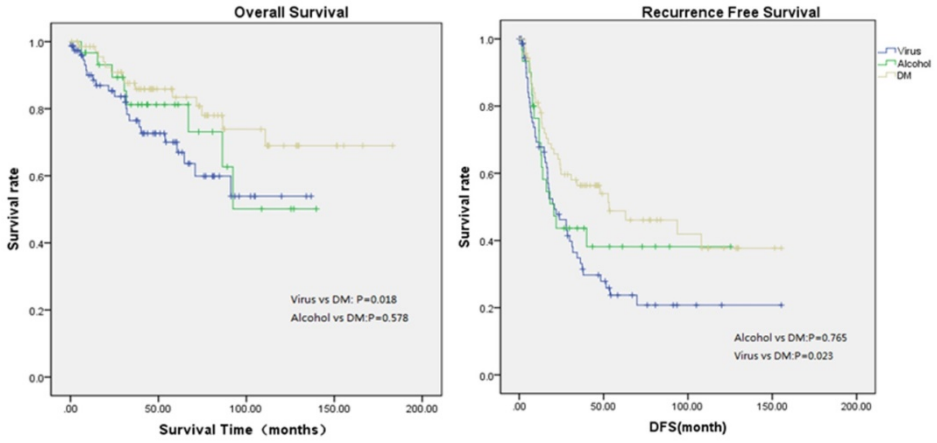

Figure1. Overall Survival and Recurrence-free Survival for Virus-HCC, Alcohol-HCC and DM-HCC

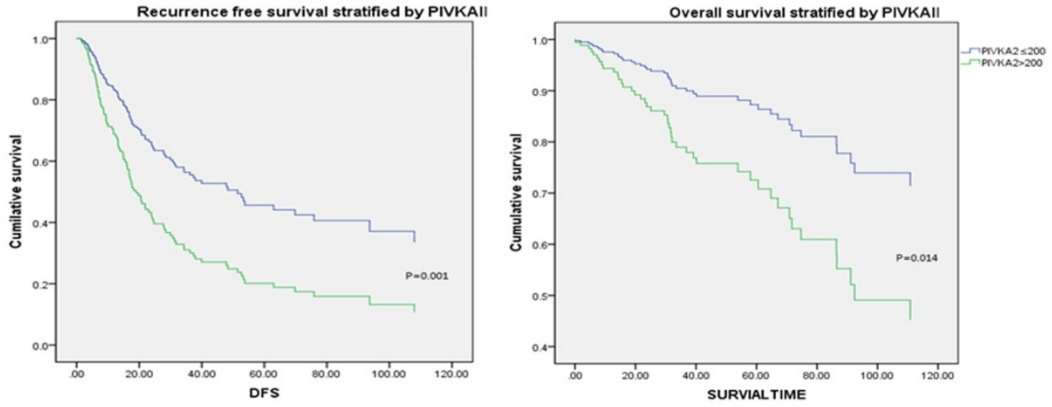

Figure 2　Overall survival and Recurrence free survival stratified by PIVKAⅡin all study population

Table 2 Cilinicopathological features and outcomes of DM-HCC with NASH and DM without NASH groups

	NASH (n=37)	Non-NASH (n=38)	P
Clinical factors			
Age（years）	71.4±9.7	70.3±8.7	0.609
Gender(male/female)	34/3	36/2	0.975
BMI(kg/m^2)	25.6±3.5	23.2±3.1	**0.002**
ICG15(%)	15.9±15.5	11.1±5.4	0.076
TBil(mg/dl)	0.7±0.3	0.6±0.3	0.164
ALT(iu/l)	41.8±22.3	33.6±17.8	0.081
AST(iu/l)	36.9±14.8	41.4±28.0	0.388
ALB(g/dl)	4.0±0.4	3.8±0.5	**0.035**
ALP(iu/l)	341.6±238.0	451.0±377.4	0.139
GGT(iu/l)	132.9±134.1	158.0±166.0	0.474
Child-Pugh(A/B)	36/1	34/4	0.371
PLT(10^4/ul)	15.9±5.2	22.4±8.0	**0.000**
Prothrombin activity (%)	91.7±7.7	90.6±10.9	0.618
HBA1c(%)	8.6±1.9	7.8±1.4	**0.031**
$_{LG10}$(AFP ng/ml)	1.1±1.0	1.6±1.4	0.056
$_{LG10}$(PIVKA-Ⅱ mAu/ml)	2.3±1.1	3.1±1.4	**0.005**
Pathological finding			
MaximumTumor size(cm)	4.7±3.2	8.5±4.2	**0.000**
Vascular invasion (negative/positive)	33/4	23/15	**0.015**
Im(negative/positive)	32/5	28/10	0.273
Background liver(LC/non-LC)	29/8	36/2	0.081
Macroscopic type(small nodular with indistinct margin, simple nodular type, simple nodular type with extranodular growth/mutinodular type/mass type)	31/6/0	34/3/2	0.144
outcomes			
5 year overall survival	56.8%(21/37)	42.1(16/38)	0.204
5 year recurrence free survival	27.0%(10/37)	18.4%(7/38)	0.373
Overall survival (month, median)	68.8	40.0	0.721
Recurrence free survival (month, median)	45.1	23.5	0.467

AST, aspartate aminotransferase; ALT, alanine aminotransferase; GGT, gamma-glutamyl transpeptidase; ALP, alkaline phosphatase; TBil, total bilirubin; PLT, platelet count;ICG15, indocyanine green retention at 15 min;HBA1c, hemoglobinA1c; AFP, alpha-fetoprotein; PIVKA-Ⅱ, protein induced by vitamin K absence or antagonist-II; Im, Intrahepatic metastasis; LC, liver cirrhosis

作成日：2017 年 2 月 23 日

Genetic analysis for disease causing mutations through combinatory use of various methods
複数の解析手法を組み合わせた効率的な遺伝子診断

研究者氏名　盧　永平（第38期笹川医学研究者）
中国所属機関　遼寧省計画生育科学研究院分子遺伝科
日本研究機関　東京女子医科大学統合医科学研究所
指導責任者　山本　俊至　准教授
共同研究者　恩藤　由美子

Abstract:

Genetic analysis is necessary for patients who are suspected as having genetic disorders which can be diagnosed only by molecular investigation. For efficient and speedy diagnosis, combinatory use of the equipment would be required. In this study, we could get molecular diagnosis for 5 patients using Sanger sequencing, the next-generation sequencing (NGS), and chromosomal microarray testing. A novel *PLP1* mutation was identified in a patient with Pelizaeus-Merzbacher disease (PMD), an X-linked recessive hypomyelination disorder. An adult patient with hypomyelination showed no mutation in the targeted genes by NGS but showed a novel *TUBB4A* mutation by Sanger sequencing. NGS revealed three mutations in the genes related to Sotos phenotype in 3 patients. All 3 mutations were de novo origin. As presented here, combinatory use of the different and suitable methods would be time-effective for early diagnosis of the patients with unknown disorders.

Key Words:

exome sequencing; leukoencephalopathy; hypomyelination with atrophy of the basal ganglia and cerebellum (H-ABC); tubulin; extra-pyramidal movement.

Introduction:

Genetic analysis is important to get precise diagnosis for patients with unknown etiologies. If clinical diagnosis was correct and the responsible genes for the diseases were restricted, candidate gene approach would be beneficial. On the other hand, if there were many genes which may be responsible for the patients' conditions, comprehensive genetic analysis using the next-generation sequencing (NGS) would be rather beneficial than candidate gene approach by Sanger sequencing. Comprehensive genetic analysis by use of NGS would be also beneficial for patients with unknown etiologies.

Here, we present recent our achievement to get molecular diagnosis for patients with neurodevelopmental disorders.

Materials and methods

This study was performed in accordance with the declaration of Helsinki and was approved by the ethics committee of Tokyo Women's Medical University. After receiving informed consent, we obtained blood samples from the patient and his parents and extracted genomic DNA for sequence analysis. Next-generation sequencing (NGS) was performed using the TruSight One v1.0 sequencing panel (Illumina, San Diego, CA). The extracted data was mapped to a reference genome (GRCh37/hg19) using the BWA Enrichment v1.0 software (Illumina) and annotated and filtered by the Variant Studio software (Illumina). Chromosomal microarray testing using the Agilent 60K Human Genome CGH Microarray platform (Agilent Technologies, Santa Clara, CA) was performed in accordance with the manufacturer's

protocol. Sanger sequencing using specific primers for each genes was performed in accordance with standard method.

Results:

Patient 1

A 3-year-old boy showed pendular nystagmus soon after birth. Because he had feeding difficulties due to laryngeal wheezing, tube feeding was initiated. Brain magnetic resonance imaging at 6 months of age revealed a hypomyelination pattern. The patient exhibited severe developmental delay with no head control or meaningful language development. From these findings, connatal type Pelizaeus-Merzbacher disease (PMD; MIM #312080) was suggested as a candidate diagnosis. Because most of the patients with PMD show the proteolipid protein 1 gene (*PLP1*) duplications, we first performed chromosomal microarray testing and there was no abnormality. Then, Sanger sequencing was performed and a missense mutation was identified in exon 6 of *PLP1* (Fig. 1). The patient's mother was heterozygous for this mutation, indicating that this mutation was maternally inherited. The prediction scores of this mutation were evaluated using wANNOVAR the results were damaging. From these findings, identified mutation was considered to be disease-causing.

注：本症例部分は 2017 年1月5日Human Genome Variationに誌上発表しました.

Patient 2

A 21-year-old Japanese male patient with an unremarkable family history. His abnormal gait was first observed beyond adolescence when he was 17 years old. Neurological examination showed spasticity in his lower extremities. Brain MRI showed an abnormal intensity in the white matter. Owing to unknown etiology for his clinical condition, NGS was performed. However, no possible candidate variants were detected through NGS. Since *TUBB4A*, the gene responsible for hypomyelinating leukodystorophy, was not included in the panel, Sanger sequencing for all *TUBB4A* exons was performed. As a result, a missense mutation was detected. This was considered as a de novo mutation because both parents did not carry this mutation. The prediction scores of this mutation, which was evaluated by wANNOVAR, suggested this mutation was "damaging".

For a better understanding of the genotype-phenotype correlation, the FirstGlance in Jmol macromolecular visualization tool was used to process data from the Protein Data Bank (PDB). All of the previously reported *TUBB4A* mutations were mapped to the bovine αβ-tubulin protein crystal structure (PDB identification code: 1JFF) which is similar to the human αβ-tubulin protein structure (Fig. 2).

注：本症例部分は現在論文投稿中です.

Patient 3, 4, and 5

Three patients were suspected as having Sotos syndrome. Because the nuclear receptor SET domain-containing protein 1 gene (*NSD1*), the gene responsible for Sotos syndrome, is too large to analyze by Sanger sequencing, we used NGS. Then, possible mutations were identified in these patients. For re-confirmation of these mutations in the patients and to check inheritance pattern, Sanger sequencing was performed for the patients and their parents.

Patient 3 is a 9-year-old girl. At birth, cleft lip and palate was noted. He showed developmental delay with head control at 6 months. Her height, weight, and occipitofrontal circumference (OFC) were within normal limits. His developmental level was evaluated as moderately delayed. This patient showed de novo missense mutation in NSD1.

Patient 4 is a 10-year-old boy was diagnosed as having autistic features and hyperkinetic behaviors. At 5 years, he showed overgrowth with over 2 standard deviation score. He showed distinctive facial features including flat nasal bridge and inverted triangular face, typical for Sotos syndrome. One-bp insertion was identified in *NSD1* gene, which

leads to a frame shift.

Patient 5 is a boy at 4 years and 6 month old, who showed developmental delay since early infancy. There was no distinctive facial finding. He showed autistic features and moderate global developmental delay. A de novo mutation was identified in exon 2 of *NFIX* gene.

The effect of the mutations and insertion for protein features was predicted by following web-based prediction tools: SIFT, Polphen-2 and Mutation Taster. The prediction results of the three variants showed suspected to be disease-causing by these algorithms.

注：本症例部分は現在論文投稿準備中です.

Discussion:

In this study, two patients showed hypomyelination. Patient 1 showed typical findings of PMD. PMD is an X-linked recessive disorder caused by mutations in *PLP1* located on chromosome Xq22.[1,2] More than 100 mutations have been reported in PMD, including duplications, point mutations, insertions and deletions[3]. Among them, *PLP1* duplications are the major mutation in PMD patients. Thus, we first performed chromosomal microarray testing for patient 1. Owing to no duplication, then, Sanger sequencing for *PLP1* was performed. Since the *PLP1* mutation identified in patient 1 has never been reported previously, we determined it to be a novel mutation. Because the patient's mother was a carrier of this mutation, this result can be used for future prenatal diagnosis.

Clinical features of patient 2 were complicated. We could not get tentative diagnosis by clinical information. This is the reason for the use of NGS analysis but no mutation was identified through NGS. Re-evaluation of the clinical findings of the patient suggested possible contribution of *TUBB4A*, a disease causing gene for H-ABC[4,5,6], which is not included in the NGS panel. Thus, we performed Sanger sequencing for *TUBB4A*. This suggests that targeted Sanger sequencing is still necessary in this NGS era. Although there is no therapeutic method for this disorder, the final diagnosis by genetic analysis will be beneficial for the patient and his family.

Final diagnosis was obtained through NGS for patients 3-5. Sotos syndrome[7,8] due to *NSD1* mutation is well-known and clinical features of Sotos patients are recognizable; however, clinical features of patient 3 and 4 were different. Patient 4 showed typical overgrowth; however, patient 3 did not. Such difference may be derived from genotypic difference. Patient 5 was diagnosed as having Malan syndrome due to de novo mutation in *NFIX*. Although this syndrome is also recognized as Sotos 2, clinical features of this syndrome are not easy to be reconnized. This suggests comprehensive genetic analysis using NGS is cost- and time-effective.

In this study, we used various genetic analysis methods as a system of molecular diagnosis for each patient. Combinatory use of these methods is necessary for molecular diagnosis.

References:

1. Koeppen AH, Robitaille Y. Pelizaeus-Merzbacher disease. J Neuropathol Exp Neurol 2002; 61: 747–759.

2 Inoue K. PLP1-related inherited dysmyelinating disorders: Pelizaeus-Merzbacher disease and spastic paraplegia type 2. Neurogenetics 2005; 6: 1–16.

3 Shimojima K, Inoue T, Hoshino A, Kakiuchi S, Watanabe Y, Sasaki M et al. Comprehensive genetic analyses of PLP1 in patients with Pelizaeus-Merzbacher disease applied by array-CGH and fiber-FISH analyses identified new mutations and variable sizes of duplications. Brain Dev 2010; 32: 171–179.

4. Hamilton EM, Polder E, Vanderver A. 2014. Hypomyelination with atrophy of the basal ganglia and cerebellum:

further delineation of the phenotype and genotype-phenotype correlation. Brain 137:1921-1930.
5. Van der Knaap, M. S. et al. New syndrome characterized by hypomyelination with atrophy of the basal ganglia and cerebellum. AJNR. American journal of neuroradiology 23, 1466-1474 (2002).
6. Shimojima K, Okamoto N, Yamamoto T. 2016. A novel TUBB3 mutation in a sporadic patient with asymmetric cortical dysplasia. Am J Med Genet A 170A:1076-1079.
7. Sotos, J. F., Dodge, P. R., Muirhead, D., Crawford, J. D. & Talbot, N. B. Cerebral Gigantism in Childhood. A Syndrome of Excessively Rapid Growth and Acromegalic Features and a Nonprogressive Neurologic Disorder. The New England journal of medicine 271, 109-116, doi:10.1056/NEJM196407162710301 (1964).
8. Tatton-Brown, K. et al. Genotype-phenotype associations in Sotos syndrome: an analysis of 266 individuals with NSD1 aberrations. American journal of human genetics 77, 193-204, doi:10.1086/432082 (2005)

Figure legends:

Fig. 1. Electropherograms of Sanger sequencing. The patient 1 shows T>C missense mutation and his mother is a heterozygous carrier of this mutation.

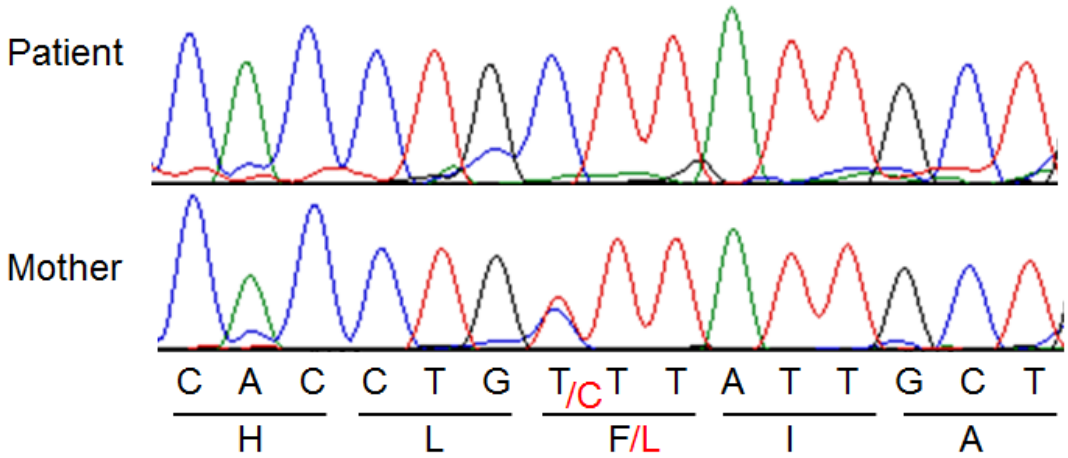

Fig. 2. Mapping TUBB4A mutations to the 3-D protein crystal structure of the bovine αβ-tubulin heterodimer.

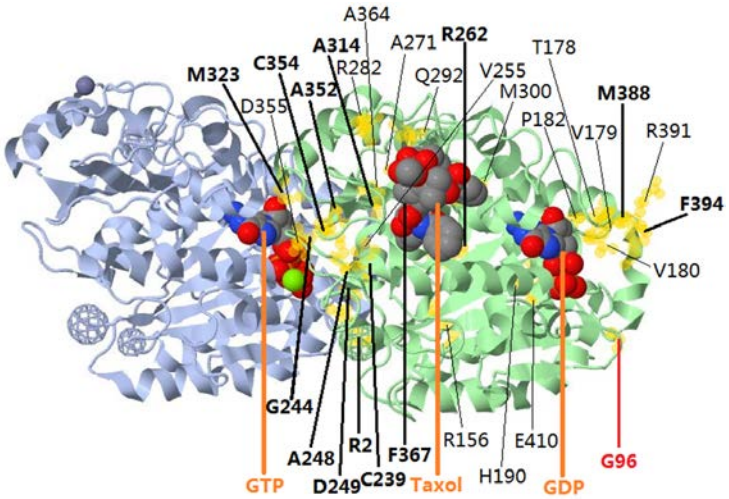

作成日：2017年 2月 23日

Boiogito attenuates progression of nonalcoholic steatohepatitis in mice

非アルコール性脂肪肝炎のマウスモデルによる防己黄耆湯の治療効果

研究者氏名	鄭　佳連（第38期笹川医学研究者）
中国所属機関	遼寧中医薬大学附属医院感染科
日本研究機関	名古屋大学医学系研究科消化器内科
指導責任者	後藤　秀実　教授
共同研究者名	石上　雅敏　講師，本多　隆　助教

Abstract:

Background: Non-alcoholic steatohepatitis (NASH), including inflammation, fibrosis and damage of hepatocyte is the more severe stage of Nonalcoholic fatty liver disease (NAFLD). More worse, patients with NASH may suffer from cirrhosis even hepatocellular carcinoma (HCC) without any drug intervention or changes of lifestyle[1]. So the treatment of NASH is drawing more attention. Boi-ogi-to (BOT), one of the Kampo formula, has been shown to improve serum lipid level and down-regulate inflammatory factors in rat liver[2].To observe the effect of BOT on NASH mouse model and explore for the possible mechanism,this experiment was implemented.

Method :C57BL/6J male mice were fed with choline-deficiency high-fat（CDHF）diet for 8 weeks as the model group, CDHF mixed with either 1.93% or 9.65% BOT powder as the intervention group, choline-sufficient high-fat (CSHF) diet as the control group. Serum biochemical and histological indexes were evaluated.

Results: CDHF elevated the liver/body weight, ALT, AST, serum lipid level and caused steatosis and fibrosis pathologically. BOT improved them and the 5 times dose was more effective.

Conclusion: BOT prevented the development of NASH in mice induced by CDHF, of which the 5 times dose was more effective.

Key words:

Choline-Deficient High-Fat diet, Non-alcoholic steatohepatitis, Boiogito, Kampo formula,

Introduction:

More and more experts and scholars are paying close attention on NAFLD for its poor prognosis and no proven treatment so far. NASH is the only treatment opportunity before cirrhosis or even hepatocellular carcinoma. As an

organic whole and less side-effect, natural drugs acquire more and more attention. BOT, traditionally used to treat obesity of the “asthenic type” in China, Japan and other Asian countries, had been proven to suppress visceral fat accumulation and subcutaneous fat in TSNO mice which will develop Type Ⅱ Diabetes Mellitus spontaneously[3]. Ogi, one main component of BOT, had an effect on hypercholesterolemia in NAFLD rats[4]. The effects of BOT on NASH have never been studied.Our aim is to evaluate the treatment effects of BOT on NASH model in mice.

Methods:

Materials and methods

Animals and Drugs

Seven-week-old male C57BL/6J mice were obtained from SLC Japan (Hamamatsu, Japan). All the mice were housed in a controlled environment (12h light/12h dark cycle, humidity 50±10%, temperature 23±1℃) with free access to water and CE2 diet (CLEA Japan, Inc., Tokyo, Japan). The experiment started from the second week after 1 week of acclimation.

BOT (TJ-20, Tsumura&Co, Tokyo, Japan) were well-distributed mixed with CDHF diet (Oriental Yeast CO., Tokyo, Japan). The concentration of 1.93% was equivalent with the amount of a 60Kg adult (dose translation according to the previous reference [5].The concentration of 9.65% was the 5 times BOT.

Experimental Design

There were 4 groups which were the CDHF diet group (CDHF), the CSHF diet group(CSHF), the 1×BOT group(1×BOT)and the 5×BOT group(5×BOT). CSHF(Oriental Yeast CO., Tokyo, Japan) was as the control diet. The mice were fed with respective diet for 8 weeks. All the studies were approved by the Animal Care and Research and Development Committees of the Division of Experimental Animals of Nagoya University.

Biochemical Analyses

All the mice were anesthetized with intraperitoneal injection of pentobarbital sodium(1%) after 12-h fast. Blood was collected from the heart quickly after anesthesia for serum biochemical analyses which were entrusted to SRL,Inc. (Tokyo,Japan). Total protein, albumin, total bilirubin, glucose, total cholesterol, AST, ALT were evaluated.

Histological Examination

Liver tissue was fixed in 4% paraformaldehyde phosphate buffer solution for 16 h, or rapidly frozen in lipid nitrogen and stored at -80℃for histological analyses. After dehydrated and embedded in paraffin, liver tissue was sliced into 3μm sections then stained with hematoxylin and eosin (H&E) and Sirius red(Sigma-Aldrich, St Louis, MO) for histological examination. The ratio of the hepatic steatosis and Sirius red-positive areas was calculated from 10 microscopic fields for each tissue sections, using the BZ-ⅡIage Analysis Application(KEYENCE, Osaka, Japan). For hepatic steatosis: 0 is none; 1 is up to 33%; 2 is 33-66%; 3 is more than 66%. For inflammatory cell infiltration: 0 is none; 1 is 1 to 2 foci/field; 2 is up to 4 foci/field; 3 is more than 4 foci/field[6].The staging of hepatic fibrosis was investigated by Sirus Red staining as follows: 0 is none; 1 is expanded portal tracts; 2 is periportal fibrosis; 3 is bridging fibrosis with nodular architecture; 4 is cirrhosis[7].

Determination of Liver Lipid Levels

Total liver lipids were extracted according to the method of Folch[8]. 18mg frozen liver tissue were homogenized in Bertin Precellys 24 (Bertin Technologies Co.,France) and extracted twice with the methanol:chloroform (1:2 v/v)solution. The organic layer was resuspended in isopropanol for the determination of lipids mass. TG and cholesterol levels were determined using a commercial colorimetric method(Wako Pure Chemicals Industries, Osaka, Japan).

Statistics

All analyses were performed using the statistical package for social sciences(SPSS), version 23. The data were shown as mean±SD. Comparison among groups were using the one-way analysis of variance (ANOVA). The p value was considered to be statistical significance when less than 0.05.

Results:

CDHF Diet Induced NASH Model in mice

Liver/body weight was significantly higher in CDHF than in CSHF in which though the body weight was even higher. Serum ALT, AST, TG, TBil level in CDHF were significantly higher than that of CSHF. Glucose level was higher in

CSHF than CDHF, because choline deficiency exacerbates fatty liver but improves glucose tolerance[9-10]. NASH is characteristic of inflammation and fibrosis. The livers of CDHF showed pronouced steatosis and abundant inflammatory cells in the H&E staining. Nas score in CDHF which was significantly higher than that of CSHF was more than 5 which supported the diagnosis of NASH. Correspondingly, the hepatic lipid level (TG, TC) was also measured. The livers in CDHF contained more lipid (TG, TC) compared with that of CSHF. Also, CDHF increased the level of fibrosis staging and positive red area which were significantly lower in CSHF.

BOT Ameliorated Liver Injury in CDHF mice .

BOT decreased liver/body weight though no difference in the mice body weight compared with CDHF. It effectively improved serum ALT, AST, Tbil, serum and hepatic TG. For serum and hepatic TC, there was no difference between the intervention groups and CDHF. In the histological examination, BOT both ameliorated steatosis (NAS score) and fibrosis (fibrosis staging and positive red area). There were less steatosis, inflammation infiltration and periportal or pericellular fibrosis in the two intervention groups compared with CDHF.

Between the two doses, 5×BOT was more effective.

Between the two intervention groups, only 5×BOT improved the liver/body weight and hepatic TG level. Serum ALT, serum and hepatic TG and histological Nas score level were significantly decreased in the two intervention groups between which 5×BOT was significantly lower. There was no difference between the two groups about the serum AST, FFA, fibrosis staging and positive red area. About the serum TBil, 1×BOT is lower than 5×BOT which has no difference with CDHF. There was less steatosis, inflammation infiltration in the livers of 5×BOT shown by the H&E staining.

The analysis results suggested that BOT ameliorated liver injury in CDHF and 5 times was more effective.

Discussion:

Choline is a kind of vitamin containing in foods and involved in some crucial processes such as the biogenesis of the major membrane component -phosphatidylcholice[11].Our experiment showed that CDHF diet decreased glucose level

in mice compared with CSHF diet. It accorded with Gengshu Wu's experiment in which choline deficiency significantly attenuated high-fat-diet-induced weight gain but improved glucose tolerance in ob/ob mice[12]. In another experiment,Peter J[13]etal found that CDHF diet did not effect body weight but amplified fatty liver and improved glucose tolerance which was also in accordance with our result .There was no difference between CDHF and the intervention groups about the body weight but the liver/body weight was significantly lower in 5×BOT compared with CDHF .Glucose level in CSHF was significantly higher than that of the other 3 groups .

BOT did not have evident effect on the serum or hepatic content of total cholesterol. However, BOT decreased both serum and hepatic content level of triglyceride. The results suggested that BOT may take part in the metabolism of triglyceride instead of total cholesterol.

The serum Tbil level of 5×BOT which had no difference with CDHF was significantly higher than 1×BOT and CSHF .Whether BOT have side effect still needs further research.

References:

1.Karima Begriche et al. Mitochondrial dysfunction in NASH:Caucses,consequences and possible means to prevent it. Mitochndrion, 2006;6:1-28.

2.Weibin Qian,Junichi Hasegawa,Satoshi Tsuno.Effects of Kampo Formulas on the Progression of hyper cholesterolemia and fatty liver induced by high-cholesterol diet in Rats.Yonago Acta medica,2014;57:147-158.

3.Tsutomu Shimada,"Preventive effect of Boiogito on metabolic disorders in the TSOD mouse,a model of spontaneous obese type □diabetes mellitus,"Evidence-Based Complementary and Alternative Medicine,vol 2011,June 2011

4.Weibin Qian,"Components of Boiogito suppress the progression of hypercholesterolemia and fatty liver induced by high-cholesterol diet in rats",Yonago Acta medaca.2016;59:67-80

5.Shannon Reagan-Shaw, Minakshi Nihal and Nihal Ahmad. Dose translation from animal to human studies revisited. The FASEB Journal. 2007; 22: 659-661.

6.Kleiner DE, Brunt E, Van Natta M et al:Design and validation of a histological scoring system for nonalcoholic fatty liver disease. Hepatology 41:1313-1321,2005

7.Brunt EM, Janney CG, Di Biscegli AM et al:Nonalcoholic steatohepatitis:A proposal for grading and staging the

histological lesions.Am J Gastroenterol 94:2467-2474, 1999.

8.Folch J,Lees M,Sloane Stanley GH.A simple method for the isolation and purification of total lipids from animal tissues.J Biol Chem.1957;26:497-509.

9. Wu G,Zhang L,Li T,Lospaschuk G,Vance DE,Jacobes RL.Choline deficiency attenuates body weight gain and improves glucose tolerance in ob/ob mice.J Obes.2012;2012:319172.

10. PJ Raubenheimer, MJ Nyirenda, BR Walker.A Choline-Deficient Diet Exacerbates Fatty Liver but Attenuates Insulin Resistance and Glucose Intolerance in Mice Fed a High-Fat Diet.Diabetes 2006 Jul; 55(7): 2015-2020.

11.Ficher LM, daCosta KA, Kwock L, et al.Sex and menopausal status influence human dietary requirements for the nutrient choline, Am J Clin Nurt.2007;85:1275-1285.

12.Wu G,Zhang L,Li T,Lopaschuk G,Vance DE,Jacobs RL.Choline deficiency attenuates body weight gain and improves glucose tolerance in ob/ob mice.J Obes.2012;2012:319172

13.Peter J,Raubenheimer,Moffat J,Nyirenda and Brian R.Walk.A Choline-Deficiency Diet Exacerbated Fatty Liver but Attenuated Insulin Resistance and Glucose Intolerance in Mice Fed a High-Fat Diet. Diabetes,2006,6;55:2015-2020

作成日：2017 年 2 月 28 日

Clinical Management of Salvage Esophagectomy Following definitive Chemoradiotherapy On patients with Squamous Cell Carcinoma of Esophagus

根治的化学放射線療法失敗した食道扁平上皮癌患者におけるサルベージ手術の臨床管理

研究者氏名　趙　宏波（第 38 期笹川医学研究者）
中国所属機関　河南省安陽市腫瘤医院
日本研究機関　国立がん研究センター
指導責任者　日月 裕司　科长

Abstract

Although the inherent advantage of non-invasive feather of definitive chemoradiotherapy (CRT) and its favorable short-time outcomes in treatment of esophageal cancer have made it an increasing popular treatment solution among both clinical oncologists and patients compared with traditional invasive procedure, the tendency of loco-regional failure after definitive CRT, in form of recurrence or residual, usually put doctors and patients in a dilemma in deciding whether to proceed this treatment. The future modality trends in patients with esophageal cancer may well be going towards non-surgical therapies even if patients are suitable for surgery. Presently, surgical interventions especially salvage esophagectomy is still generally viewed as an effective alternative with curative intention in treating loco-regional failure after definitive CRT. With increasing number of patients with esophageal cancer being definitive CRT as an initial treatment, more and more patients fitting for salvage esophagectomy will maybe refer to surgeons. However, salvage esophagectomy has been found to be associated with significantly increased incidence of mortality and morbidity. Therefore, great efforts should be put on how to optimize the current chemoradiotherapy regimens, how to select qualified candidates for salvage surgery and how to reduce the perioperative morbidity and mortality for the sake of long-term outcomes.

Key Word: Esophageal cancer ;definitive chemoradiotherapy (CRT); salvage esophagectomy;

Introduction

Esophageal cancer is the eighth most common malignant tumor worldwide, the sixth most common cause of cancer-related deaths, and the fifth most common cause of cancer-related deaths among human [1]. There are two most important types of esophageal cancer: adenocarcinoma and squamous cell carcinoma. Adenocarcinoma is the dominant histologic type of esophageal cancer in western countries, while squamous cell carcinoma is the more common type in the highest-risk area, often referred to the “esophageal cancer belt,” which stretches from northern Iran through the Central Asian republics to north-central China [2]. Various surgical procedures had always played a predominant role in treatment of patients with esophageal cancer during the past decades, until two landmark randomized trials, RTOG 85-01 and FFCD 9102, clearly documented that definitive CRT may provide an equally curative effect for patients suffering from esophageal malignant tumor [3, 4].

Current advancement in definitive chemoradiotherapy for esophageal cancer

Neither chemotherapy nor radiotherapy alone is recommended as a curative modality for patients with esophageal cancer, since neither of them can provide a trend to favorable long term outcomes. Two randomized clinical trials, RTOG8501 and FFCD9102, had confirmed that definitive CRT can obtain comparable results compared with surgery alone. Definitive CRT has been an initial selective option for patients who decline to receive surgery or were evaluated as being not able to tolerate thoracotomy since then. New advancement in definitive CRT for esophageal cancer has

come to a stage of exploring how to maximize efficacy and minimize toxicity.

Viewed from the point of chemotherapy, an important measure to maximize the efficacy of definitive CRT is to apply more effective cytotoxic agents into treatment of esophageal cancer. Chemotherapy regimen consisting of Cisplatin and 5-fluorouracil has been widely used for many years and is recommended as the standard treatment in concurrent chemoradiotherapy previously [5-10]. The regimen is always correlated to considerable adverse effect though the curative effective of which is still satisfied. Taxanes were recent found to be promising antitumor agents. Hamai et al. showed that the toxicity of docetaxel and 5-fluorouraci was essentially mild, that the postoperative complications were acceptable, and the rates of complete resection and survival rate were favorable [11]. They documented that docetaxel and 5-fluorouraci with concurrent radiotherapy was safe, and it seemed that it has a favorable antitumor effect for esophageal cancer. Now a prospective, randomized, multicenter and open arms trial, which aims to appraise the complete resection rate and severe postoperative morbidity rate associated with two different chemotherapeutic regimens (carboplatin-paclitaxel or fluorouracil-oxaliplatin-folinic acid) when each is combined with the radiation regime in operable esophageal and gastro-esophageal junctional cancer, is ongoing [12]. Japan Clinical Oncology Group (JCOG) initiated a three-arm Phase III trial, which tries to confirm the superiority of docetaxel, cisplatin plus 5-fluorouracil over cisplatin plus 5-fluorouracil and the superiority of cisplatin plus 5-fluorouracil with chemoradiotherapy over cisplatin plus 5-fluorouracil as preoperative therapy for squamous cell carcinoma of esophagus [13].

Besides, radiotherapy, combining targeted agents such as tyrosine kinase inhibitors, antibodies, and immune modulators, should be introduced into treatment of esophageal cancer. Another trial that aims to determine if trastuzumab can increase disease-free survival when combined with tri-modality treatment for patients with HER2-overexpressing esophageal adenocarcinoma is advancing [14]. The findings of these three trials are worthy of attention.

Due to the frequent presence of loco-regional failure after definitive CRT, dose-escalation has been a subject to look into in the setting of definitive CRT [6]. Unsatisfactorily, a randomized Intergroup 0123 trial, which aimed to investigate of the correlation between dose and efficacy failed to observe improvement in survival in dose comparisons of 64.8 Gy versus 50.4 Gy, however, an unexpected high deaths rates and increased grade toxicities were occurred [15]. Dose of 50.4 Gy is now widely accepted as standard in definitive tri-modality treatment of esophageal cancer [9]. A recent CROSS trial adopting a dose of 41.4 Gy achieved pathological complete response rate of 29%, which was similar with regimens utilizing dose of 50.4 Gy [16]. The result should be interpreted carefully because 75% of patients enrolled suffer from adenocarcinoma. Moreover, theoretically, Proton therapy enjoys in advantage in treatment of esophageal cancer due to its slight toxicity on surrounding of normal-tissue. Welsh at al. from the US confirmed that intensity-modulated proton therapy further reduces normal tissue exposure during definitive therapy for esophageal cancer [17].

Surveillance on patients after definitive chemoradiotherapy

Indeed, definitive CRT has significantly increased the short-term remission rate in the past decades and won a favorable reception in large scale. Statistical data from Japan Clinical Oncology Group (JCOG) shows that complete response rate of 62.2% was observed for stage II/III esophageal squamous cell carcinoma [18].

However, unsuccessful control of loco-regional disease after definitive CRT is an issue that cannot be ignored. Decreased performance after definitive CRT may cause patients to adopt a “watch and wait” strategy. In fact, a

significant number of patients who undertook complete response after definitive CRT have to face up to the dispiriting reality of loco-regional failure in spite of approving complete response rates at the beginning [3, 6, 19-23]. It was reported that the figure in the presence of recurrence or residual after definitive CRT ranged from 13% to 50% [3, 6, 19, 20], and the figure even can reach as high as almost 60% [4, 6, 24]. Salvage esophagectomy is possibly the sole treatment option available that can offer a chance of favorable long-term outcome with patients who had underwent definitive CRT but unfortunately not achieved loco-regional control [21]. On the contrary, once lost the chance of detecting the recurrence or residual at the beginning and accepting potentially beneficial salvage therapy, most of those patients experienced a gloomy prognosis [25-27]. Several studies had documented that a reasonable fraction of patients who experienced failed loco-regional control could anticipate a promising survival by receiving salvage surgery compared with other therapy measures [28-32].

Actually, it is only a very narrow window from loco-regional disease to unresectable disease that allows the surgeons to have opportunity to intervene from the viewpoint of surgery. As a result, the importance of surveillance on patients after definitive CRT cannot be overstated. In another word, there is not much doctor can do for patients who develop local aggressive or distant metastasis in short interval after definitive CRT. Moreover, the frequency and method of surveillance for patients treated with definitive CRT can affect the surgeon's ability to offer resection. Local-regional failure unrecognized will progress to a point of non-resectability even in situation where there is no evidence of distant metastasis. From the point of clinicians, this should be considered as the ultimate failure of therapy.

Active systematic surveillance includes time-related visit and technology-related follow-up. On the time dimension, follow-up strategies vary widely with various clinical centers. The authors did not find prospective relevant research on superiority of different strategies. The following surveillance strategies are normally recommended in a majority of researches: patient visits after definitive CRT should be carried out once every 3 months for the first year, then once 6 months for the following 2 years, and then once a year for at least the following 5 years [22, 31, 33, 34]. Hofstetter recommended patients should undergo endoscopy with ultrasound along with PET imaging every four months during the first 1-2 years after definitive CRT, followed by surveillance at 6-12 months interval thereafter [35]. Noticeably, Urschel et al. reported that up to 95% of patients will recur within two years after receiving definitive CRT treatment, and almost all within three years (99%) [36]. Therefore, special emphasis should be laid on the first 3 years after definitive CRT so as to find patients with loco-regional disease as many as possible. A prospective, single arm, multicenter, and diagnostic trial, which arms to identify the presence or absence of residual tumor that could be predicated reliably 6 or 12 weeks after completion of neoadjuvant chemoradiotherapy, is currently ongoing [37].

With regard to technology-related surveillance, except for conventional thoracoabdominal computed tomography, endoscopy mucosal with biopsies of primary tumor site and radial endo-ultrasonography (EUS) in cases of suspected patients, periodic positron emission tomography scanning (PET) has been adopted by clinicians recent years due to its advantages in finding the slight trace of loco-regional failure from the metabolic perspective, despite there were still some controversy regarding the effectiveness of FDG-PET imaging in assessing histopathologic response of the primary tumor to definitive CRT [38-47]. Several studies reported the variability of role of PET-CT, which possibly were subjected to smaller cohorts of patients [45, 48-50]. A number of researches had confirmed that PET had better ability to differentiate residual primary tumor from post therapy scar after definitive CRT [51, 52]. Goense et al. revealed that the sensitivity of PET-CT ranges between 89% and 100% and the specificity between 55% and 94% respectively in detecting recurrent after definitive CRT in the systematic review and meta-analysis [53]. Moreover, Kato et al. documented that SUV was one of the most responsible prognosticators of response in accessing clinical value of

therapy prior to CRT [54]. A multivariate analysis also showed that SUV before CRT was an independent predictor for clinical complete response [55]. In spite of the limitation of lower specificity of PET-CT, its higher sensitivity may conduce to the earlier diagnosis of recurrent tumors, which may, in turn, prolong survival of patients with recurrent after definitive CRT. As a result, PET should be introduced as a further examination in the postoperative follow-up to include or exclude patients who were suspected loco-regional disease after definitive CRT. Nevertheless, the ideal PET parameters used to assess response have not been clearly established.

Recently, the attempt of chemokines as a predictor in long-term survival of esophageal squamous cell carcinoma patients is highlighted. A latest study revealed that chemokines CCL4 has been demonstrated to be an independent predictive marker of survival of patients with esophageal squamous cell carcinoma, which, in combination with CCL20, was of significant prognostic value [56]. Provided that the value of those independent predictive makers has been validated in clinical practice, by monitoring of chemokines, we can feasibly choose eligible candidates who are expected to achieve a favorable long-term survival after salvage esophagectomy from those patients who had failed dCRT while avoiding the high mortality and morbidity of salvage surgery.

To sum up, Special emphasis should be laid on the quality of the active investigations during follow-up after definitive CRT as mentioned before. On the other hand, new measures should be introduced to improve accuracy of diagnosis. PET-CT may be a good choice in detecting loco-regional disease and in assessing the stage because it can provide metabolic information.

Qualified candidates for salvage esophagectomy

That to properly select patients for salvage esophagectomy following definitive CRT is a major challenge in clinical practice. Theoretically, all those patients who have been determined to have residual tumor or recurrent cancer after definitive CRT, and show no evidence of systemic disease, can be qualified candidates for salvage esophagectomy. As a matter of fact, salvage esophagectomy is well known to be correlated with impressing mortality and morbidity albeit it renders a possibility of long-time survival for patients with failed dCRT. Literatures have documented that morbidity rates were in a wide range from 50% to 79% [57-63], and mortality rates range from 6% to 22.2% [31, 57-62, 64-67]. Meanwhile, long-term survival situation of patients after salvage esophagectomy is unsatisfactory up to date, with 5-year survival rates ranging from 0 to 33% [31, 57, 59, 60, 62, 65, 66]. Considering the embarrassing situation at present, it should be cautious in identifying qualified patients for this high risk treatment modality.

Above all, proper assessment of individual performance status after definitive CRT is a noticeable issue. As is well known, esophageal cancer's incidence rate is higher in relative elder patients. In general, elderly patients have limited ability to tolerate intensive treatments compared to nonelderly patients because of various medical comorbidities and reduced functional reserve of vital organs. Various comorbidities such as predominantly cardiovascular diseases, pulmonary diseases and diabetes, which generally increase with age, may increase the risk of salvage surgery. It seems reasonable to speculate that chemoradiotherapy may further aggravate any previous cardio-respiratory co-morbidity and cause problems that were not overt previously. Takeuchi et al. reported that toxicities tend to be more substantial in elderly patients, and that the elderly groups show a higher recurrence rate (47.6%) after pathological complete response than nonelderly group (33.7%) [68]. Several researches disclosed the acute and late toxicity after definitive CRT on patients with esophageal cancer, some of the side effects were occasionally fatal [21, 68-72]. Ishikura et al. reported that the incidence of grade ≥ 3 pericarditis after definitive CRT in their study was 10%, some patients died as a result of heart failure [69]. What is noteworthy is that the negative impaction organism caused by definitive CRT is a long and

constant course, which probably will overlap with salvage surgery, and further increases the risk of surgery. Therefore, it is advisable to comprehensively consider patients' comorbidities, age, and possible toxicity caused by definitive CRT when selecting qualified candidates for salvage esophagectomy. In addition, detailed protocols on assessment of individual performance status after definitive CRT need to be explored and developed in future.

Furthermore, that the doctors need to consider not only from the view of safety of salvage surgery itself but also from the view of prognosis when identifying candidates for salvage esophagectomy is a very important issue. Patients who are assessed to probably have a dismal prognosis after definitive CRT should be precluded from this highly invasive procedure. Therefore, the beneficial prognostic factors that influence favorable long-term outcomes probably are also strong indicators for suitability of salvage esophagectomy. Swisher et al. previously revealed that early pathologic stage (T1N0, T2N0), complete resection without residual tumor (R0) , and prolonged time to relapse (>12 months) were associated with long-term survival [57]. However, a recent study deemed that the interval between definitive CRT and surgery were not associated with postoperative morbidity, pathologic complete response, or overall survival [73]. Watanabe et al. argued that R0 resection and patients with pT0–2 tumors were independent, and favorable prognostic factors after salvage esophagectomy [63]. Miyata et al. found that pretreatment T and N status, pathological T stage, and R0 resection were significant prognostic factors [66]. And interestingly, Marker et al. revealed that residual after definitive CRT was associated with poorer survival compared with recurrent [74]. It is also supported by some other studies which hold the same view [58, 65, 75]. It is not difficult to understand that a more favorable long term prognosis could be anticipated with those patients who showed a better response to definitive CRT from the view of biological feathers of carcinoma.

To sum up, patients who are preoperatively assessed to be in an early pathologic stage, have prolonged time to relapse (>12 months), recurrent disease and possibility of total mediastinal dissection and R0 resection, regardless of the patients' individual performance, are better indications of that they should accept salvage surgery even at a risk of a high treatment-related mortality. Notably, it is a common consensus that R0 resection is the most favorable independent factor predicting long-term survival, so salvage esophagectomy should be reconsidered cautiously if R0 resection is not anticipated during pre-surgical evaluation unless presenting of serious upper digestive tract obstruction.

Therefore, qualified candidates should be patients who can tolerate the surgery itself well and have the possibility to achieve long-term survival. How to find the optimal balance point between curability and safety is another urgent challenge for thoracic surgeons in dealing with the situations of loco-regional failure after definitive CRT.

Salvage esophagectomy

Pulmonary complications and mortality

Various pulmonary complications after esophagectomy are much frequently observed, and they remarkably increase the intensive care unit readmission rate, the length of hospital stay, and the mortality rate [81, 82]. Postoperative pulmonary complications rates after esophagectomy were reported to be in a wide range of 13–38 % [83-91].

Notably, hospital deaths caused by pulmonary complication account for up to 64% of overall hospital deaths [90, 92, 93]. Schieman et al. maintained that major pulmonary complications were implicated in the vast majority of perioperative mortality, and should remain the focus of efforts to improve clinical outcomes [94]. A report which mostly based on esophageal adenocarcinoma revealed that use of advanced radiation technologies (intensity modulated radiation therapy and proton beam therapy) were also associated with a pulmonary complication rate of 24% [95]. And radiation field will become wider to the lung in patients with squamous cell carcinoma which located in more proximal

esophagus. A pooled analysis confirmed the incidence of pulmonary complications significantly increases in the salvage esophagectomy group [96]. Swisher revealed the numbers of perioperative pulmonary adverse events after preoperative chemoradiation therapy [97]. Similarly, our previous study also confirmed that preoperative therapy was an independent predictive factor for development of postoperative pulmonary complications [98]. A recent study by Takeuchi et al. showed that postoperative morbidity, including pulmonary complications, has a significant impact on the long-term survival after salvage esophagectomy, which can be explained from immunological aspects in their opinions [31]. It seems to be a certainty that pulmonary complications after salvage esophagectomy will see a significant increase compared with simple esophagectomy without preoperative treatment.

Importantly, secondary non-malignant tracheobronchial fistula is an extremely serious pulmonary complication after esophagectomy, and it frequently results in respiratory failure or even death. D'Journo et al. documented that preoperative chemoradiotherapy for local advanced tumors was a dangerous factor to secondary non-malignant tracheobronchial fistula and local peritracheal ischemia after extensive peritracheal dissection, and that it was associated with the presence of secondary non-malignant tracheobronchial fistula [99]. A considerable factor responsible for this complication is the grade of ischemia suffered by the trachea and bronchial during radical mediastinal lymphadenectomy. Considering the close anatomical relationship between the trachea, the bronchial and the esophageal, it is not difficult to deduce that surgical procedures have non-negligible impact on devascularization of trachea and main bronchi more or less in severing esophagus and conducting the extended mediastinal lymphadenectomy. Furthermore, microcirculation and epithelium mucosae are rendered vulnerable by the radiation and chemical drugs.

In such a situation, how to reduce perioperative pulmonary morbidity, including fatal tracheobronchial fistula, is a crucial issue in further reducing treatment-related mortality after salvage esophagectomy. A recent Germany research showed that the vagus nerve plays an important role as it mediates afferent effects triggered by inflammatory mediators and it also interacts with visceral organs by efferent activity [100]. Therefore, pulmonary branches of the vagal nerve should be preserved as far as possible during operation. Except for such routing measures as sufficient preoperative preparation, enhancement the pertinence of antimicrobial drugs, and strengthen the postoperative pulmonary nursing, to our knowledge, preservation of bronchial artery and pulmonary nerves during operation is an advisable option to counteract the devasularization of surgical injury, and thus contribute to reduce the postoperative pulmonary complications. The strategies to reduce the pulmonary complications after salvage surgery need to be further explored.

Where to reconstruct the upper digestive tract during operation: posterior mediastinal or retrosternal?

Cancer resection and esophageal reconstruction following resection are two usual steps of esophagectomy. The stomach is the first choice substitute used for replacement after esophagectomy when the stomach is available [101, 102]. Variety of routes had been explored to maintain restoration of alimentary continuity after esophagectomy. Subcutaneous, retrosternal, left or right intrathoracic and posterior mediastinal routes are the main routes available for reconstruction after esophagectomy now [103]. Among the numerous choices for esophageal reconstruction for patients undergoing an esophagectomy for esophageal cancer, retrosternal and posterior mediastinal routes are regularly chosen to reconstruct the upper digestive tract in most cases [104, 105]. Nevertheless, which model should be the first-rank between retrosternal and posterior mediastinal route is still under debate.

Many researches have documented the advantages and disadvantages of the aforementioned reconstructive routes after esophageal resection. Some conclusions of these researches are even contradictory. With regard to the length of different routes, Coral et al. reported that posterior mediastinal route was a little shorter of time than retrosternal route [106], while Yang et al. got a contrary result. As far as pulmonary complications after esophagectomy are concerned,

Kunisaki et al. found that posterior mediastinal route will result in lower occurrence rate of pulmonary complication compared with that of retrosternal route [107]. But Zheng et al. obtained nearly the same incidence rate of pulmonary complications between those two reconstruction routes after esophagectomy [106]. Zheng et al. recommend posterior mediastinal route as a conventional choice because their study demonstrated that reconstruction by posterior mediastinal route reduces incidence of postoperative pulmonary complications provided survival is not affected [108]. However, Mannell et al. showed a higher occurrence of pulmonary complications in posterior mediastinal route than in RS route [109]. Regarding whether a different approach would affect the leakage rate, a previous meta-analysis by Urschel et al. revealed that the choice of reconstruction route will not affect the frequency of anastomotic leakage [110], which is consistent with a meta-analysis conducted by Markar [111]. however, Mei-Lin Chan et al. demonstrated that the leakage rate was remarkably lower for patients who received posterior mediastinal reconstruction compared with those received retrosternal reconstruction [112]. Regarding the mortality after salvage surgery, Orringer et al. and Gawad et al. insisted that patients who underwent posterior mediastinal route had lower rates of morbidity and mortality after esophagectomy compared with those underwent retrosternal route [113, 114]. Urschel and his colleagues also show that no obvious differences were observed in morbidity and mortality after comparing the two approaches in their meta-analysis [110].

Therefore, it would be a more complex and challenging problem when taking preoperative definitive CRT and the possibility of recurrence or residual after salvage esophagectomy into account. Due to the aforementioned controversial viewpoints on the two different routes, it is not surprising that surgeons usually make a choice between posterior mediastinal and retrosternal route largely depending on their preference and experience. Advocates of the posterior mediastinal route as the preferred choice of conduit transposition maintain that the retrosternal route of conduit transposition will increase postoperative morbidity rate. They support the hypothesis that when the esophageal replacement is not in position of normal esophageal bed, it will lack brace from adjacent structures, which probably will result in a considerable incidence rate of anastomotic leakage. Those proponents who believe the retrosternal route should be the preferred choice of conduit transposition probably mainly base their view upon the perception that the gastric conduit will be outside the tumor bed in case of recurrent or residual after esophagectomy.

Besides, different pathological type and frequent location of esophageal cancer between eastern and western countries contribute to several of construction approaches. To our knowledge, we preferred to the posterior mediastinal route at the beginning of the salvage esophagectomy. Unfortunately, we observed the significant presence of anastomotic leakage in salvage esophagectomy, especially in patients who accepted irradiation dose over 50Gy. Mediastinal abscess caused by leakage easily extended to the tracheal and destroyed the posterior wall of tracheal, which in turn increased the hospital mortality after esophagectomy. After these critical experiences, we changed to the retrosternal route during salvage esophagectomy and witnessed declining hospital mortality. However, in western countries, tumors locate in the lower esophagus and the field of irradiation usually not extend to the upper mediastinum. It is quite different from our salvage esophagectomy in Japan.

In spite of the merits and demerits of the two different routes of reconstruction after esophagectomy shown by a number of studies, there is still lack of evidences to show overwhelming superiority of one route over another from several meta-analysis or randomized controlled trials [110, 115, 116]. To Maintain a quality living and prolong the survival time as much as possible are the two common primary objectives that both the doctors and patients tried to achieve. Considering from the perspective of quality living, posterior mediastinal route after salvage esophagectomy seems to be a good choice since it fits with the original anatomical structure and physiological characteristics. However, taking high aggressive characters of tumor with loco-regional failure after definitive CRT into consideration, the

esophageal bed which posterior mediastinal route got through is more likely to become vulnerable again. Moreover, posterior mediastinal route may bring concerns on the subsequent treatment, especially possible radiation. Considering from the perspective of oncologic surgery, the retrosternal route should be highly recommended as the first choice if R1 or R2 resection are potentially anticipated during intraoperative evaluation.

To our knowledge, posterior mediastinal route could be attempted only if R0 resection could be anticipated. Besides, Juloori et al. newly revealed that patients anastomosed inside the radiation field had an obvious higher incidence of leakages when compared to anastomosis that were placed outside of the radiation field [117]. From the view of this, we strongly recommend retrosternal as a routine route for reconstruction, which also conformed to our past practice.

In short, the choice of an individualized and proper route on a given patient depends upon the intraoperative assessment, resectability and possible postoperative therapy.

Conclusion

Patients who are qualified for salvage esophagectomy after failed definitive CRT represent a highly selected group of patients with potentially favorable outcomes. Meanwhile, indications of salvage esophagectomy should be well discussed multidisciplinary team setting, and the guaranteeing surgery can only be performed in experienced high-volume center.

Reference

1. Ferlay J, Shin HR, Bray F, Forman D, Mathers C, Parkin DM: **Estimates of worldwide burden of cancer in 2008: GLOBOCAN 2008**. *Int J Cancer* 2010, **127**(12):2893-2917.
2. Wheeler JB, Reed CE: **Epidemiology of esophageal cancer**. *Surg Clin North Am* 2012, **92**(5):1077-1087.
3. Cooper JS, Guo MD, Herskovic A, Macdonald JS, Martenson JA, Jr., Al-Sarraf M, Byhardt R, Russell AH, Beitler JJ, Spencer S *et al*: **Chemoradiotherapy of locally advanced esophageal cancer: long-term follow-up of a prospective randomized trial (RTOG 85-01). Radiation Therapy Oncology Group**. *JAMA* 1999, **281**(17):1623-1627.
4. Bedenne L, Michel P, Bouche O, Milan C, Mariette C, Conroy T, Pezet D, Roullet B, Seitz JF, Herr JP *et al*: **Chemoradiation followed by surgery compared with chemoradiation alone in squamous cancer of the esophagus: FFCD 9102**. *J Clin Oncol* 2007, **25**(10):1160-1168.
5. Ajani JA, Barthel JS, Bentrem DJ, D'Amico TA, Das P, Denlinger CS, Fuchs CS, Gerdes H, Glasgow RE, Hayman JA *et al*: **Esophageal and esophagogastric junction cancers**. *J Natl Compr Canc Netw* 2011, **9**(8):830-887.
6. Minsky BD, Pajak TF, Ginsberg RJ, Pisansky TM, Martenson J, Komaki R, Okawara G, Rosenthal SA, Kelsen DP: **INT 0123 (Radiation Therapy Oncology Group 94-05) phase III trial of combined-modality therapy for esophageal cancer: high-dose versus standard-dose radiation therapy**. *J Clin Oncol* 2002, **20**(5):1167-1174.
7. Kleinberg L, Gibson MK, Forastiere AA: **Chemoradiotherapy for localized esophageal cancer: regimen selection and molecular mechanisms of radiosensitization**. *Nat Clin Pract Oncol* 2007, **4**(5):282-294.
8. Yamasaki M, Miyata H, Miyazaki Y, Takahashi T, Kurokawa Y, Nakajima K, Takiguchi S, Mori M, Doki Y: **Perioperative therapy for esophageal cancer**. *Gen Thorac Cardiovasc Surg* 2014, **62**(9):531-540.
9. Tepper J, Krasna MJ, Niedzwiecki D, Hollis D, Reed CE, Goldberg R, Kiel K, Willett C, Sugarbaker D, Mayer

R: **Phase III trial of trimodality therapy with cisplatin, fluorouracil, radiotherapy, and surgery compared with surgery alone for esophageal cancer: CALGB 9781**. *J Clin Oncol* 2008, **26**(7):1086-1092.

10. Walsh TN, Noonan N, Hollywood D, Kelly A, Keeling N, Hennessy TP: **A comparison of multimodal therapy and surgery for esophageal adenocarcinoma**. *N Engl J Med* 1996, **335**(7):462-467.
11. Hamai Y, Hihara J, Emi M, Murakami Y, Kenjo M, Nagata Y, Okada M: **Results of Neoadjuvant Chemoradiotherapy With Docetaxel and 5-Fluorouracil Followed by Esophagectomy to Treat Locally Advanced Esophageal Cancer**. *Ann Thorac Surg* 2015, **99**(6):1887-1893.
12. Messager M, Mirabel X, Tresch E, Paumier A, Vendrely V, Dahan L, Glehen O, Vasseur F, Lacornerie T, Piessen G *et al*: **Preoperative chemoradiation with paclitaxel-carboplatin or with fluorouracil-oxaliplatin-folinic acid (FOLFOX) for resectable esophageal and junctional cancer: the PROTECT-1402, randomized phase 2 trial**. *BMC Cancer* 2016, **16**:318.
13. Nakamura K, Kato K, Igaki H, Ito Y, Mizusawa J, Ando N, Udagawa H, Tsubosa Y, Daiko H, Hironaka S *et al*: **Three-arm phase III trial comparing cisplatin plus 5-FU (CF) versus docetaxel, cisplatin plus 5-FU (DCF) versus radiotherapy with CF (CF-RT) as preoperative therapy for locally advanced esophageal cancer (JCOG1109, NExT study)**. *Jpn J Clin Oncol* 2013, **43**(7):752-755.
14. Safran H, Dipetrillo T, Akerman P, Ng T, Evans D, Steinhoff M, Benton D, Purviance J, Goldstein L, Tantravahi U *et al*: **Phase I/II study of trastuzumab, paclitaxel, cisplatin and radiation for locally advanced, HER2 overexpressing, esophageal adenocarcinoma**. *Int J Radiat Oncol Biol Phys* 2007, **67**(2):405-409.
15. Gaspar LE, Winter K, Kocha WI, Coia LR, Herskovic A, Graham M: **A phase I/II study of external beam radiation, brachytherapy, and concurrent chemotherapy for patients with localized carcinoma of the esophagus (Radiation Therapy Oncology Group Study 9207): final report**. *Cancer* 2000, **88**(5):988-995.
16. van Hagen P, Hulshof MC, van Lanschot JJ, Steyerberg EW, van Berge Henegouwen MI, Wijnhoven BP, Richel DJ, Nieuwenhuijzen GA, Hospers GA, Bonenkamp JJ *et al*: **Preoperative chemoradiotherapy for esophageal or junctional cancer**. *N Engl J Med* 2012, **366**(22):2074-2084.
17. Welsh J, Gomez D, Palmer MB, Riley BA, Mayankkumar AV, Komaki R, Dong L, Zhu XR, Likhacheva A, Liao Z *et al*: **Intensity-modulated proton therapy further reduces normal tissue exposure during definitive therapy for locally advanced distal esophageal tumors: a dosimetric study**. *Int J Radiat Oncol Biol Phys* 2011, **81**(5):1336-1342.
18. Kato K, Muro K, Minashi K, Ohtsu A, Ishikura S, Boku N, Takiuchi H, Komatsu Y, Miyata Y, Fukuda H: **Phase II study of chemoradiotherapy with 5-fluorouracil and cisplatin for Stage II-III esophageal squamous cell carcinoma: JCOG trial (JCOG 9906)**. *Int J Radiat Oncol Biol Phys* 2011, **81**(3):684-690.
19. Herskovic A, Martz K, al-Sarraf M, Leichman L, Brindle J, Vaitkevicius V, Cooper J, Byhardt R, Davis L, Emami B: **Combined chemotherapy and radiotherapy compared with radiotherapy alone in patients with cancer of the esophagus**. *N Engl J Med* 1992, **326**(24):1593-1598.
20. Minsky BD, Neuberg D, Kelsen DP, Pisansky TM, Ginsberg R, Benson A, 3rd: **Neoadjuvant chemotherapy plus concurrent chemotherapy and high-dose radiation for squamous cell carcinoma of the esophagus: a preliminary analysis of the phase II intergroup trial 0122**. *J Clin Oncol* 1996, **14**(1):149-155.

注：本研究は 2017 年 2 月<Gastroenterology Report>にて発表した

作成日：2017 年 2 月 22 日

Intravenous polymyxins: revival with puzzle

ポリミキシン点滴静注の再興と論争

研 究 者 氏 名　　俞　芸（ 第 38 期笹川医学研究者）
中国所属機関　　上海交通大学医学部附属新華病院
日本研究機関　　東京大学医学部附属病院肝胆膵外科
指 導 責 任 者　　国土　典宏 教授
共同研究者名　　唐子　堯（東大・医），潘　曙明（交大・新華）

Abstract

With the increasing incidence of multi-drug resistant strains, especially carbapenem resistant strains, polymyxsins based regimens seem to be revival as an effective treatment of last resort in these infections. Evidence from 47 clinical trials or case series we reviewed showed that polymyxins based regimens are effective and with less toxicity compared with previous trails. But there’re still controversies in dosing strategies, and combination regimens and so on. Prospective trials of lager sample are needed.

Keywords

intravenous; polymyxins; colistin; polymyxin B;

1. Introduction

Polymyxins are bactericidal drugs that exhibit their antibacterial activity by disrupting bacterial cell membranes, leading to cell lysis. There’re two commercially available polymyxin antibiotics: polymyxin B and colistin (also known as polymyxin E) available in two forms, colistin sulphate and the prodrug colistin methanesulfonate (CMS). The lack of treatment options for MDR gram-negative bacilli(GNB) has leaded to the re-emergence of polymyxin as an antimicrobial therapy. We try to review clinical evidence of intravenous polymyxins in clinical practice.

2. Method

We conducted a comprehensive literature search in database of PubMed, without year or language restriction, using the following terms: “colistin” or “polymyxin E” or “polymyxin B”, and “intravenous or systemic” as well as their combinations in the terms of “case reports, clinical conference, clinical study, clinical trial, comparative study, controlled clinical trial, evaluation studies, editorial, letter, meta-analysis, multicenter study, observational study, pragmatic clinical trial, randomized controlled trial, review, or systematic reviews”. We listed 47 clinical trials or case series out of a total of initially identified 281 references updated on October 2016.

3. Result

The cure rates of colistin based regimens are reported to be 53.7-79.1% in GNB infections[1], a clinical response rate of

43.1-79%[2-5], and a microbiological response rate of 66.7%(34/51)[2]. IV polymyxins therapy can be used either as monotherapy or in combination with other antibiotics.

3.1. Monotherapy

It's indicated that the mortality of monotherapy ranged from 0% to 74.3%[4,6-21], clinical response(cure and improve) rate was 7–82.1%, and microbiological eradication 27.3–73.9%[7,17-22]. Some studies indicated that colistin appeared to be as safe and as effective as other antimicrobials in GNB infection[14,16,23,24]. But a larger sample sized study discovered that colistin was less effective and more toxic than β-lactam antibiotics[13]. It's reported that polymyxin B treatment in the currently recommended dosage may be inferior to other drugs in the treatment of VAP and tracheobronchitis caused by organisms tested as susceptible in vitro to this agent[12]. Kwon SH et al. reported that in *A. baumannii* infection, microbiological negative conversion rate was significantly higher in the colistin group than the tigecyclin group, but with no statistically significant difference in in-hospital mortality rate[20]. While another retrospective study found an excess mortality of 16.7% in MDR *A. baumannii* pneumonia treated with tigecycline[25].

3.2. Combination Therapy

The effect of combination therapy in severe infections with MDR GNB was proved early[3]. A study including 104 patients with carbapenem-resistant(CR) bacteria infection indicated polymyxin B combination therapy with all-cause mortality of 47% for the hospitalization and 77% after 6 months[26]. Is combination therapy better than monotherapy? What's the optimal combination for the clinic practice?

3.2.1. Combination Therapy vs. Monotherapy

It's reported that there were no differences in outcome variables between colistin monotherapy and combination therapy[2,19]. But there're other studies indicated that combination therapy result in a better clinical and microbiological outcome than monotherapy[8,27].

An early retrospective study indicated that the effectiveness of colistin monotherapy did not appear to be inferior to that of colistin–meropenem combination therapy for patients with MDR bacterial infections[10]. While another studiy showed that clinical cure rates or bacteriological clearance rates were better in the colistin/sulbactam combination therapy than colistin monotherapy, although with no statistical significance[18]. In clinic practice, clinical outcomes did not differ between patients treated with colistin plus vancomycin and those treated with colistin alone[28]. But it's also indicated in the study that when this combination lasted ≧5 days, it was associated with a higher survival rate [11].

Aydemir H et al. reported that clinical, laboratory, radiological and microbiological response rates were better in the colistin-rifampicin combination group, although these differences were not significant[29]. But another multicenter, parallel, randomized, open-label trial found no clinical benefit, but increased rate of *A. baumannii* eradication with colistin-rifampicin combination treatment was also found[30]. Then, colistin-fosfomycin combination therapy group was also found to have a trend toward more favorable clinical outcomes and lower mortality compared with colintin monotherapy group[31].

3.2.2. Different combination therapies

Shields et al [32] and reported that colistin-carbapenem combination therapy 80%(4/5) of the transplant recipients with

XDR *A. baumannii* infections were treated successfully. Yilmaz GR et al. also [15] reported that clinical and microbiological response was better in colistin-carbapenem group than colistin-sulbactam group. But other studies indicate that there were no better clinical or microbiological outcome in patients receiving colistin-carbapenem combination treatment[27,33].

Khawcharoenporn T et al. reported that the 28-day survival rate and mean length of hospital stay were not statistically different between colistin-tigecycline group and colistin-carbapenem group[33]. While another prospective, multicenter study found an increased 14-day mortality in colistin-tigecycline therapy compared with colistin-carbapenem thrapy[34]. A retrospective study suggested an equivalency of regimens that contained high-dose, 4-h infusion of doripenem plus fosfomycin versus colistin plus fosfomycin for treatment of CR *P. aeruginosa* pneumonia, indicating feasible, effective and well tolerated[35]. Petrosillo N et al. found no different in 30-day mortality, in the 4 groups as follows: colistin alone, colistin-glycopeptide, colistin plus other anti-GNB drugs, colistin-glycopeptide plus other anti-GNB drugs[11]. Three uncontrolled clinical studies have assessed the safety and clinical efficacy of the colistin-rifampicin combination, showing very high overall response rates[36-38]. Despite the lack of a control group and the limited number of patients, colistin in association with rifampicin appears to be effective.

Colistin-based combinations, with or without the addition of carbapenems, have been considered the milestone of the treatment. Then, a case series reported 4 patients treated with colistin-vancomycin-meropenem combination had a positive outcome with no infection relapses. Maybe it's an alteration when come up with poor clinical response [39].

3.3. Toxicities

The most common adverse effect of polymyxins is nephrotoxicity which is particularly more common in patients with high baseline creatinine at the initiation of treatment, while neurotoxicity, ranging in severity from reversible paresthias to respiratory failure, is a less common side effect [40]. On the other hand, the reported frequency and severity of nephrotoxicity is lower as compared to the figures reported in 1970s[40]. This maybe because of the more purified formulations of the drug as well as the closer monitoring of the paitients.

The reported incidence of IV-colistin-related nephrotoxicity decreased from 36% in the 1960s to 14–19% in the 1990s, before rising to 24%[41]. Reported rates of nephrotoxicity vary widely from 0-59.6% of patients treated with polymyxins. This maybe because these data are generated from a number of small, non-comparative studies or case series, with heterogeneous patient populations, and varying dosing schemes. It's also because different definitions of nephrotoxicity, such as AKIN (Acute Kidney Injury Network) criteria[28,42], RIFLE[17,18,27,30,31] , KIDIGO[33], and other criteria[2,20,23]. So it's difficult to compare nephrotoxicity between trials.

Several studies indicated that no neurological side effects of were noted[29,31,38,43] with IV or inhaled colistin. While two studies noted very low incidence of neurotoxicity, 3 (0.14 %)patients[27], and 1(0.99%) patient[30], respectively. In a retrospective study neurotoxicity was observed in 2 (6%)patients who received IV polymyxin B[44].

4. Conclusion

As carbapenem resistance is now increasingly worldwide, polymyxsins based regimens seem to be revival as an

effective treatment of last resort. Although polymyxsins have been used for over half century, there're still many issues to be confirmed . In spite of treatment success, persistence of bacterial growth and emerging resistance raises concern for long-term efficacy of polymyxin monotherapy. Though the clinical benefits have been subject to controversy, combination therapy is still recommended for two main reasons. Firstly, to prevent the selection of heteroresistant strains, secondly, to get potential synergic effects. There have been no more side effects of combination therapy than monotherapy except colistin-vancomycin combination. The optimal dosing strategies and combination regimens are still controversial. Most of the data came from retrospective or small sample sized prospective trails, so prospective trials of lager sample are needed.

Refrences:

1. Falagas ME, Rafailidis PI, Ioannidou E, et al. Colistin therapy for microbiologically documented multidrug-resistant Gram-negative bacterial infections: a retrospective cohort study of 258 patients. *International journal of antimicrobial agents.* 2010;35(2):194-199.
2. Simsek F, Gedik H, Yildirmak MT, et al. Colistin against colistin-only-susceptible Acinetobacter baumannii-related infections: Monotherapy or combination therapy? *Indian journal of medical microbiology.* 2012;30(4):448-452.
3. Markou N, Apostolakos H, Koumoudiou C, et al. Intravenous colistin in the treatment of sepsis from multiresistant Gram-negative bacilli in critically ill patients. *Critical care (London, England).* 2003;7(5):R78-83.
4. Paksu MS, Paksu S, Karadag A, et al. Old agent, new experience: colistin use in the paediatric Intensive Care Unit--a multicentre study. *International journal of antimicrobial agents.* 2012;40(2):140-144.
5. Karbuz A, Ozdemir H, Yaman A, et al. The use of colistin in critically ill children in a pediatric intensive care unit. *The Pediatric infectious disease journal.* 2014;33(1):e19-24.
6. Elias LS, Konzen D, Krebs JM, Zavascki AP. The impact of polymyxin B dosage on in-hospital mortality of patients treated with this antibiotic. *The Journal of antimicrobial chemotherapy.* 2010;65(10):2231-2237.
7. Karnik ND, Sridharan K, Jadhav SP, et al. Pharmacokinetics of colistin in critically ill patients with multidrug-resistant Gram-negative bacilli infection. *European journal of clinical pharmacology.* 2013;69(7):1429-1436.
8. Rigatto MH, Behle TF, Falci DR, et al. Risk factors for acute kidney injury (AKI) in patients treated with polymyxin B and influence of AKI on mortality: a multicentre prospective cohort study. *The Journal of antimicrobial chemotherapy.* 2015;70(5):1552-1557.
9. Binh NG, Hayakawa K, Co DX, et al. The efficacy and nephrotoxicity associated with colistin use in an intensive care unit in Vietnam: Use of colistin in a population of lower body weight. *International journal of infectious diseases : IJID : official publication of the International Society for Infectious Diseases.* 2015;35:18-23.
10. Falagas ME, Rafailidis PI, Kasiakou SK, Hatzopoulou P, Michalopoulos A. Effectiveness and nephrotoxicity of colistin monotherapy vs. colistin-meropenem combination therapy for multidrug-resistant Gram-negative bacterial infections. *Clinical microbiology and infection : the official publication of the European Society of Clinical Microbiology and Infectious Diseases.* 2006;12(12):1227-1230.
11. Petrosillo N, Giannella M, Antonelli M, et al. Clinical experience of colistin-glycopeptide combination in critically ill patients infected with Gram-negative bacteria. *Antimicrobial agents and chemotherapy.* 2014;58(2):851-858.
12. Rigatto MH, Ribeiro VB, Konzen D, Zavascki AP. Comparison of polymyxin B with other antimicrobials in the treatment of ventilator-associated pneumonia and tracheobronchitis caused by Pseudomonas aeruginosa or Acinetobacter baumannii. *Infection.* 2013;41(2):321-328.
13. Paul M, Bishara J, Levcovich A, et al. Effectiveness and safety of colistin: prospective comparative cohort study. *The Journal of antimicrobial chemotherapy.* 2010;65(5):1019-1027.
14. Reina R, Estenssoro E, Saenz G, et al. Safety and efficacy of colistin in Acinetobacter and Pseudomonas infections: a prospective cohort study. *Intensive care medicine.* 2005;31(8):1058-1065.
15. Yilmaz GR, Guven T, Guner R, et al. Colistin alone or combined with sulbactam or carbapenem against A. baumannii in ventilator-associated pneumonia. *Journal of infection in developing countries.* 2015;9(5):476-485.
16. Garnacho-Montero J, Ortiz-Leyba C, Jimenez-Jimenez FJ, et al. Treatment of multidrug-resistant Acinetobacter baumannii ventilator-associated pneumonia (VAP) with intravenous colistin: a comparison with

imipenem-susceptible VAP. *Clinical infectious diseases : an official publication of the Infectious Diseases Society of America.* 2003;36(9):1111-1118.
17. Kalin G, Alp E, Coskun R, Demiraslan H, Gundogan K, Doganay M. Use of high-dose IV and aerosolized colistin for the treatment of multidrug-resistant Acinetobacter baumannii ventilator-associated pneumonia: do we really need this treatment? *Journal of Infection and Chemotherapy.* 2012;18(6):872-877.
18. Kalin G, Alp E, Akin A, Coskun R, Doganay M. Comparison of colistin and colistin/sulbactam for the treatment of multidrug resistant Acinetobacter baumannii ventilator-associated pneumonia. *Infection.* 2014;42(1):37-42.
19. Jang HJ, Kim M-N, Lee K, Hong S-B, Lim C-M, Koh Y. The Comparative Efficacy of Colistin Monotherapy and Combination Therapy Based on in vitro Antimicrobial Synergy in Ventilator-associated Pneumonia Caused by Multi-drug Resistant Acinetobacter baumannii. *Tuberc Respir Dis.* 2009;67(3):212-220.
20. Kwon SH, Ahn HL, Han OY, La HO. Efficacy and safety profile comparison of colistin and tigecycline on the extensively drug resistant Acinetobacter baumannii. *Biological & pharmaceutical bulletin.* 2014;37(3):340-346.
21. Balkan, II, Batirel A, Karabay O, et al. Comparison of colistin monotherapy and non-colistin combinations in the treatment of multi-drug resistant Acinetobacter spp. bloodstream infections: a multicenter retrospective analysis. *Indian journal of pharmacology.* 2015;47(1):95-100.
22. Dalfino L, Puntillo F, Mosca A, et al. High-dose, extended-interval colistin administration in critically ill patients: is this the right dosing strategy? A preliminary study. *Clinical infectious diseases : an official publication of the Infectious Diseases Society of America.* 2012;54(12):1720-1726.
23. Betrosian AP, Frantzeskaki F, Xanthaki A, Douzinas EE. Efficacy and safety of high-dose ampicillin/sulbactam vs. colistin as monotherapy for the treatment of multidrug resistant Acinetobacter baumannii ventilator-associated pneumonia. *The Journal of infection.* 2008;56(6):432-436.
24. Gounden R, Bamford C, van Zyl-Smit R, Cohen K, Maartens G. Safety and effectiveness of colistin compared with tobramycin for multi-drug resistant Acinetobacter baumannii infections. *BMC infectious diseases.* 2009;9:26.
25. Chuang YC, Cheng CY, Sheng WH, et al. Effectiveness of tigecycline-based versus colistin- based therapy for treatment of pneumonia caused by multidrug-resistant Acinetobacter baumannii in a critical setting: a matched cohort analysis. *BMC infectious diseases.* 2014;14:102.
26. Crusio R, Rao S, Changawala N, et al. Epidemiology and outcome of infections with carbapenem-resistant Gram-negative bacteria treated with polymyxin B-based combination therapy. *Scandinavian journal of infectious diseases.* 2014;46(1):1-8.
27. Batirel A, Balkan, II, Karabay O, et al. Comparison of colistin-carbapenem, colistin-sulbactam, and colistin plus other antibacterial agents for the treatment of extremely drug-resistant Acinetobacter baumannii bloodstream infections. *European journal of clinical microbiology & infectious diseases : official publication of the European Society of Clinical Microbiology.* 2014;33(8):1311-1322.
28. Garnacho-Montero J, Amaya-Villar R, Gutierrez-Pizarraya A, et al. Clinical efficacy and safety of the combination of colistin plus vancomycin for the treatment of severe infections caused by carbapenem-resistant Acinetobacter baumannii *Chemotherapy.* 2013;59(3):225-231.
29. Aydemir H, Akduman D, Piskin N, et al. Colistin vs. the combination of colistin and rifampicin for the treatment of carbapenem-resistant Acinetobacter baumannii ventilator-associated pneumonia. *Epidemiology and infection.* 2013;141(6):1214-1222.
30. Durante-Mangoni E, Signoriello G, Andini R, et al. Colistin and rifampicin compared with colistin alone for the treatment of serious infections due to extensively drug-resistant Acinetobacter baumannii: a multicenter, randomized clinical trial. *Clinical infectious diseases : an official publication of the Infectious Diseases Society of America.* 2013;57(3):349-358.
31. Sirijatuphat R, Thamlikitkul V. Preliminary study of colistin versus colistin plus fosfomycin for treatment of carbapenem-resistant Acinetobacter baumannii infections. *Antimicrobial agents and chemotherapy.* 2014;58(9):5598-5601.
32. Shields RK, Kwak EJ, Potoski BA, et al. High mortality rates among solid organ transplant recipients infected with extensively drug-resistant Acinetobacter baumannii: using in vitro antibiotic combination testing to identify the combination of a carbapenem and colistin as an effective treatment regimen. *Diagnostic microbiology and infectious disease.* 2011;70(2):246-252.
33. Khawcharoenporn T, Pruetpongpun N, Tiamsak P, Rutchanawech S, Mundy LM, Apisarnthanarak A. Colistin-based treatment for extensively drug-resistant Acinetobacter baumannii pneumonia. *International journal of antimicrobial agents.* 2014;43(4):378-382.

34. Cheng A, Chuang YC, Sun HY, et al. Excess Mortality Associated With Colistin-Tigecycline Compared With Colistin-Carbapenem Combination Therapy for Extensively Drug-Resistant Acinetobacter baumannii Bacteremia: A Multicenter Prospective Observational Study. *Critical care medicine.* 2015;43(6):1194-1204.
35. Apisarnthanarak A, Mundy LM. Carbapenem-resistant Pseudomonas aeruginosa pneumonia with intermediate minimum inhibitory concentrations to doripenem: combination therapy with high-dose, 4-h infusion of doripenem plus fosfomycin versus intravenous colistin plus fosfomycin. *International journal of antimicrobial agents.* 2012;39(3):271-272.
36. Petrosillo N, Chinello P, Proietti MF, et al. Combined colistin and rifampicin therapy for carbapenem-resistant Acinetobacter baumannii infections: clinical outcome and adverse events. *Clinical microbiology and infection : the official publication of the European Society of Clinical Microbiology and Infectious Diseases.* 2005;11(8):682-683.
37. Motaouakkil S, Charra B, Hachimi A, et al. Colistin and rifampicin in the treatment of nosocomial infections from multiresistant Acinetobacter baumannii. *The Journal of infection.* 2006;53(4):274-278.
38. Bassetti M, Repetto E, Righi E, et al. Colistin and rifampicin in the treatment of multidrug-resistant Acinetobacter baumannii infections. *The Journal of antimicrobial chemotherapy.* 2008;61(2):417-420.
39. Ceccarelli G, Oliva A, d'Ettorre G, et al. The role of vancomycin in addition with colistin and meropenem against colistin-sensitive multidrug resistant Acinetobacter baumannii causing severe infections in a Paediatric Intensive Care Unit. *BMC infectious diseases.* 2015;15:393.
40. Falagas ME, Kasiakou SK. Toxicity of polymyxins: a systematic review of the evidence from old and recent studies. *Critical care (London, England).* 2006;10(1):R27.
41. Gauthier TP, Lantz E, Frederick C, et al. Variability within investigations of intravenous colistin: the scope of the problem. *Clinical infectious diseases : an official publication of the Infectious Diseases Society of America.* 2014;58(9):1340-1342.
42. Alan S, Yildiz D, Erdeve O, et al. Efficacy and safety of intravenous colistin in preterm infants with nosocomial sepsis caused by Acinetobacter baumannii. *American journal of perinatology.* 2014;31(12):1079-1086.
43. Isguder R, Agin H, Ceylan G, Bayram N, Devrim I. Safety and efficacy of intravenous colistin use for the treatment of nosocomial multidrug-resistant Acinetobacter baumannii infections in a pediatric intensive care unit. *American journal of infection control.* 2016;44(6):734-735.
44. Holloway KP, Rouphael NG, Wells JB, King MD, Blumberg HM. Polymyxin B and doxycycline use in patients with multidrug-resistant Acinetobacter baumannii infections in the intensive care unit. *The Annals of pharmacotherapy.* 2006;40(11):1939-1945.

作成日：2017 年 2 月 21 日

Purification and Activity Assessment of Plasma Membrane Ca^{2+}-ATPase
細胞膜カルシウム輸送 ATP アーゼの精製と活性測定

研究者氏名　魏 霞蔚（第 38 期笹川医学研究者）
中国所属機関　四川大学華西医院
日本研究機関　東京大学分子細胞生物研究所
指導責任者　豊島　近　教授
共同研究者名　小川　治夫　准教授

Abstract

Ca^{2+} is fundamental to cell signaling and acts as a universal messenger in cell regulation. The plasma membrane Ca^{2+}-ATPase (PMCA) is a high-affinity Ca^{2+} transporting system in the plasma membranes, ejecting Ca^{2+} out of eukaryotic cells. In the present study, we conducted the activity assessment of PMCA microsomes and aimed to prepare purified PMCA from COS-7 cell membranes by HaloTag-based purification or by calmodulin affinity chromatography. First, PMCA over-expressed COS-7 cell membrane was used for ATPase activity assessment and the ATPase activation by calmodulin was confirmed. Then, the optimized condition for PMCA solubilization was studied. The concentrations of lipids and detergents during the purification process were also characterized. PMCA was successfully purified by HaloTag-based purification and the ATPase activity of the purified enzyme showed a restore after being incubated in excessive amounts of lipids and detergents. The further purification of PMCA with calmodulin-affinity column was also performed. To better understand the double bands of PMCA protein on the SDS-PAGE gel after the purification, they were further characterized by western blotting.

Key Words:

Plasma membrane Ca^{2+}-ATPase, Calmodulin, HaloTag-based purification

Introduction:

Calcium signaling plays fundamental role in regulating and maintaining homeostasis in cells. Ca^{2+} transporting system is vital for regulating the amount of Ca^{2+} within all eukaryotic cells. As the large transmembrane electrochemical gradient of Ca^{2+} drives the entry of the ion into the cells, it is important that Ca^{2+} transporting systems maintain low concentrations of Ca^{2+} by pumping them out of the cell [1]. The plasma membrane Ca^{2+}-ATPase (PMCA) is a transport protein in the plasma membrane which functions to remove Ca^{2+} from the cell and is the main regulator of the intracellular Ca^{2+}concentration [2].

Like the sarco/endoplasmic reticulum Ca^{2+}-ATPases (SERCAs), PMCA belongs to the P-type ion-motive ATPase [3]. This class of ATPase forms a phosphorylated intermediate (an aspartyl phosphate) during the reaction cycle and Ca^{2+} is bound to the enzyme in the high-affinity conformation (E_1), followed by the phosphorylation of the catalytic aspartic acid by ATP [4]. The two families of Ca^{2+} pump share essential basic properties, such as their high affinities for Ca^{2+}, the similar membrane topographies and the resembled organizations of the catalytic domain.

However, PMCA also has some unique properties such as the numerous regulatory mechanisms, which involve the auto-inhibitory function of C-terminal, as well as its regulation by protein kinases, membrane phospholipids *etc.* [5] The best understood regulatory mechanism of the pump is its activation by Calmodulin (CaM), which interacts with the

C-terminal tail with a high affinity, reducing the $K_{m(Ca2+)}$ of the pump to submicromolar values [6]. In the absence of CaM, CaM-binding domain located in the C-terminal tail interacts with the main body of the pump and keeps it inhibited, whereas, CaM could restore the activity by removing the domain from these sites [7]. Although much has been studied concerned with the basic mechanistic properties of PMCA, three-dimensional structure of PMCA remains unexplored. In the previous study, we have prepared PMCA4a microsomes from Halo-tagged ATP2B4 (human PMCA4a) over-expressing COS-7 cells. Here we aim to obtain purified PMCA4a protein by HaloTag-based purification or calmodulin-affinity chromatography, and which might be used for further crystallization of PMCA4a protein.

Methods

Activity assessment of PMCA4a

The plasma membrane Ca^{2+} ATPase activity was measured spectrophotometrically, using a coupled enzyme assay. The medium contained 120 mM KCl, 60 mM Hepes (pH 7.0 at 37°C), 3 mM $MgCl_2$, 2 mM ATP, 0.2 mM NADH, 0.5 mM phosphoenolpyruvate, 10 μM A23187, 5 mM NaN_3, 6 μM thapsigargin (TG), 0.1 μM ouabain, 24 U/ml of pyruvate kinase, 18 U/ml of lactate dehydrogenase, 500 μM EGTA, 500 μM HEDTA. The ATPase activity was followed by measuring continuously the difference in absorbance under 340 nm using a spectrophotometer. Calmodulin (purchased from Merck) was used at a concentration of 10 μg/ml. Different amounts of $CaCl_2$ were added to obtain free Ca^{2+} concentrations from of 0.1 μM ~100 μM. After the pre-incubation of the assay medium for 10 min at 37°C, 200 μl medium was added to 10 μg of membrane protein (PMCA microsome) each well to start the reaction.

Solubilization of PMCA4a

The PMCA4a microsomes were diluted to the concentration of 1~4 mg/ml in a solubilization buffer containing 50 mM MOPS-KOH (pH 7.0), 20% (w/v) glycerol, 100 mM KCl, 8 mM $CaCl_2$, 3 mM $MgCl_2$, 0.25 mM DTT, and proteinase inhibitor was added. Detergents including n-dodecyl-D-maltoside (DDM), Octaethylene Glycol Monododecyl Ether ($C_{12}E_8$), $C_{12}E_{10}$ were added at various concentrations to determine the optimized condition. Sample was vortexed 20s for three times and kept on ice for 60 min, then, centrifuged at 50k rpm for 30min. The Supernatant was moved to another tube, and the same volume of solubilization buffer was added to the pellet. Both parts were used for further detection.

HaloTag-based purification of PMCA4a

HaloTag-based purification was conducted in both batch and column method essentially as described [8]. The collected sample was further determined by SDS-PAGE, BCA protein assay and ATPase activity measurement.

Calmodulin-affinity column purification of PMCA4a

Calmodulin Sepharose 4B was purchased form GE Healthcare Life Sciences. Calmodulin-affinity column purification of PMCA4a was performed in batch method according to product instruction. Briefly, calmodulin sepharose 4B was added to a tube and balanced with wash buffer: 10 mM MOPS (pH7.0), 20% (w/v) Glycerol, 50 mM NaCl, 1 mM $CaCl_2$, 1 mM $MgCl_2$, 0.25 mM DTT, 0.032% $C_{12}E_8$, 0.067mg/ml Brain extract phospholipids (BE). The solubilized supernatant of PMCA or HaloTag purified PMCA sample was added to the Sepharose resin and incubated for 1 h at RT. The flow through was discarded and wash buffer was added for 3 times. PMCA was finally purified with elution buffer containing 2 mM EGTA. The collected sample was further determined by SDS-PAGE, BCA protein assay and ATPase activity measurement.

Western blotting

The HaloTag purified PMCA sample was loaded at 0.5μg/lane. The anti-calcium pump pan PMCA ATPase antibody [5F10] was purchased from Abcam (1:1000). The the anti-PMCA4a C-terminus antibody was ordered from Sigma (both diluted as 1:1000). Anti-mouse IgG, HRP-linked antibody and Protein A HRP conjugate were used as secondary antibody (both diluted as 1:1000). After transblotting onto the PVDF, membranes were incubated in Blocking One for 30 min, followed by incubation in primary antibody and secondary antibody for 30 min each before imaging.

Results

The assessment of PMCA4a activity

In order to confirm that we have successfully obtained PMCA4a microsomes from PMCA4a-overexpressing COS-7 cells, we have determined the ATPase activity of the microsomes. The assay was carried out with a coupled enzyme assay according to the previous work by Niggli et al. The free Ca^{2+} concentration varies between 0.09 μM- 62.1μM, and the activity was detected both in/without the presence of calmodulin. The inhibitors including NaN_3, ouabain and TG were added to reduce the activities of other ATPases in the background. The results showed that we have successfully determined the activity of PMCA4a and which showed an increased in its activity in a Ca^{2+} concentration-dependent manner (Figure 1a). Moreover, the activation of PMCA4a by calmodulin was also confirmed (Figure 1b).

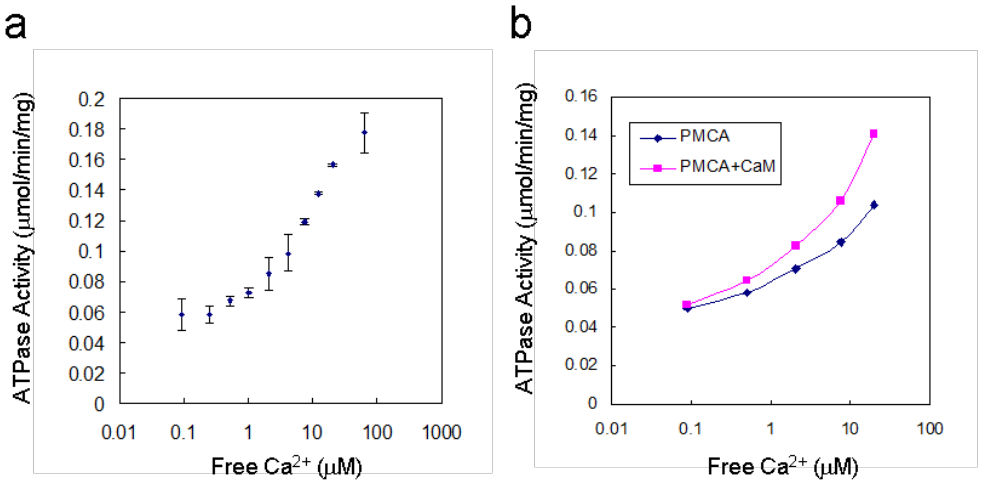

Figure 1. The Activity of PMCA in the presence of different concentrations of free Ca^{2+} (a) and after the stimulation by calmodulin (b).

Study on the solubilization condition of PMCA4a

To determine the optimized solubilization condition for PMCA4a, various detergents have been adopted including DDM, $C_{12}E_8$ and $C_{12}E_{10}$. The efficacy of solubilization was determined by SDS-PAGE and ATPaes activity assessment. The results of ATPase activity measurements showed that both 1.0% $C_{12}E_8$ and 1.0% $C_{12}E_{10}$ elicited a high ATPase activity in the supernatant and might be most efficient during PMCA4a solubilization (Figure 2a-c). Furthermore, we have determined the effects of pH, the addition of ADP, vortex time and the concentration of KCl on the solubilization efficiency. The results showed that pH7.0+ADP group yields the highest ATPase activity in the supernatant both after $C_{12}E_8$ and $C_{12}E_{10}$ treatment and the activities were maintained high even after being kept in such condition for 72 h (Figure 3a, b), whereas the times of vortex and KCl concentration had minor effects on the solubilization efficiency (Figure 3c). Therefore, 1.0% $C_{12}E_{10}$ was used for PMCA solubilization in the further experiments.

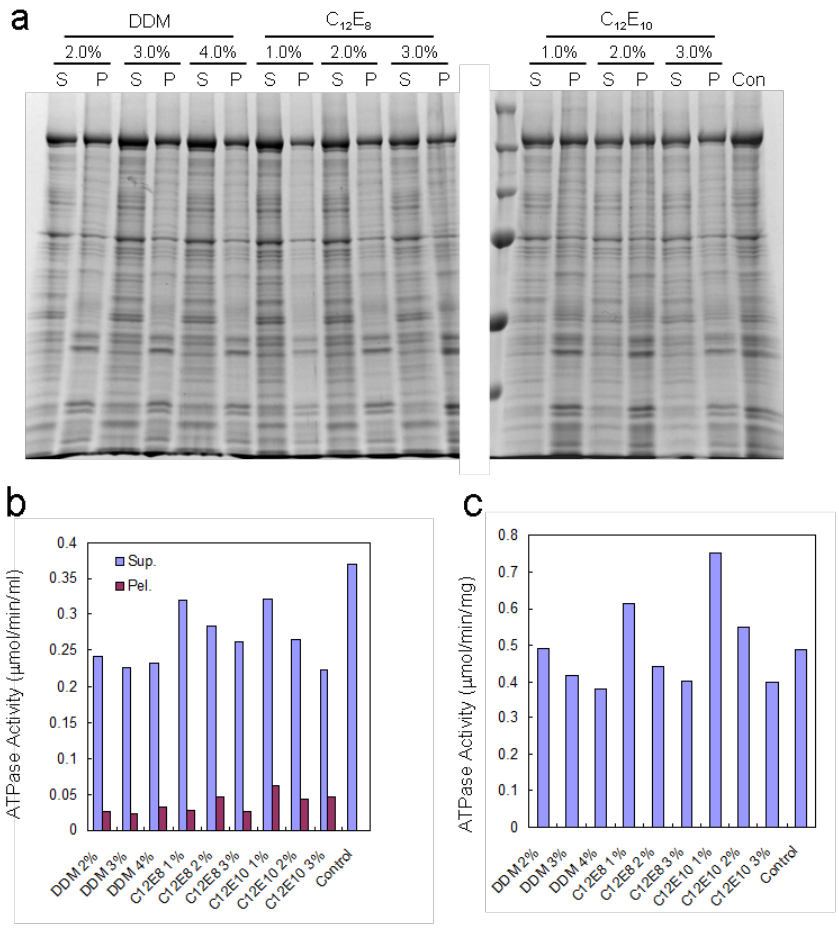

Figure 2. The SDS-PAGE image (a) and the ATPase activities (b, c) of the solubilized PMCA4a under different concentrations of DDM, $C_{12}E_8$ and $C_{12}E_{10}$. Control group represents the unsolubilized sample.

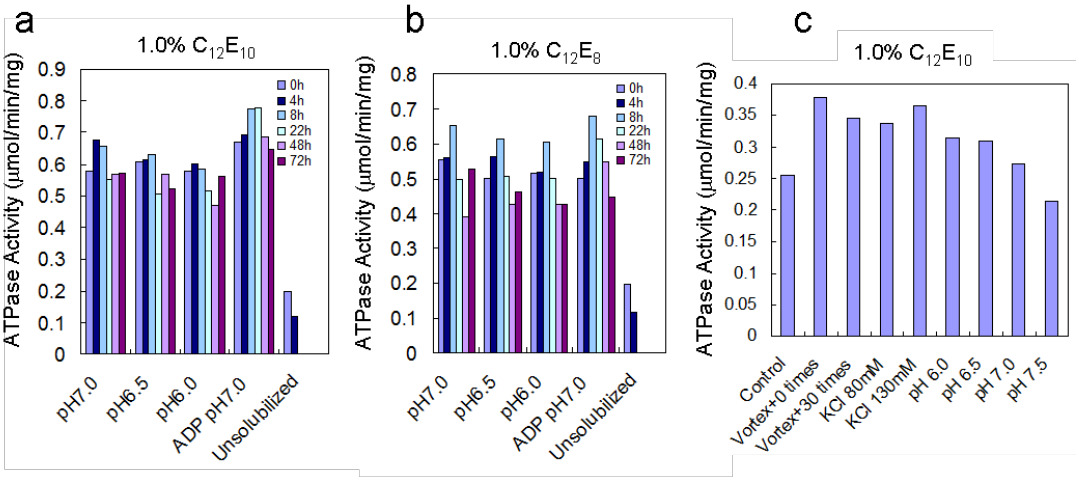

Figure 3. The ATPase activities of PMCA at different time points after being solubilized under pH 6.0-7.0 condition (a, b). The ATPase activities of PMCA after being solubilized by 1.0% $C_{12}E_{10}$ with 3 times of vortex, 30 times of vortex, in the presence of 80 mM/ 130 mM of KCl, or under different pH conditions (c).

HaloTag-based purification of PMCA4a

The preferable conditions of lipids and detergents during the purification process help to maintain the ATPase activity

of PMCA. In the meantime, the incubation of purified PMCA in the presence of excessive lipids and optimized concentrations of detergents also help to restore the enzyme activity.

In order to find the preferable condition for HaloTag-based purification of PMCA, we first investigated the best concentration of lipids and detergents for the purified PMCA to restore its activity. For the pre-experiment, PMCA was purified in the presence of 0.25 mg/ml Heart extract phospholipids (HE) and 0.1 % $C_{12}E_{10}$. The solubilized supernatant was first loaded on to the Halolink resin, washed, digested with TEV Cleavage solution and the final elution was collected. First Elution (E_0, 0.19 mg/ml protein), was used for the further determination of ATPase activity after the incubation with different amounts of detergents and lipids (Figure 4a). The reaction took place in 50 µl volume of reaction mix buffer with the addition of 2 µl of E_0. Reaction buffer containing various concentrations of lipids and detergents were added soon before the start of the reaction. The results showed that purified PMCA elicited higher activity after being incubated with Brain extract phospholipids (BE) rather than HE (Figure 4b), and ATPase activity increased with the increase of BE concentration under 0.25% $C_{12}E_8$ or 0.25% $C_{12}E_{10}$ (Figure 4c). In addition, under the same concentration, $C_{12}E_8$ helped to restore a higher PMCA activity while compared to $C_{12}E_{10}$ and the optimized concentration of $C_{12}E_8$ has been determined as 0.05% in the present study (Figure 4d).

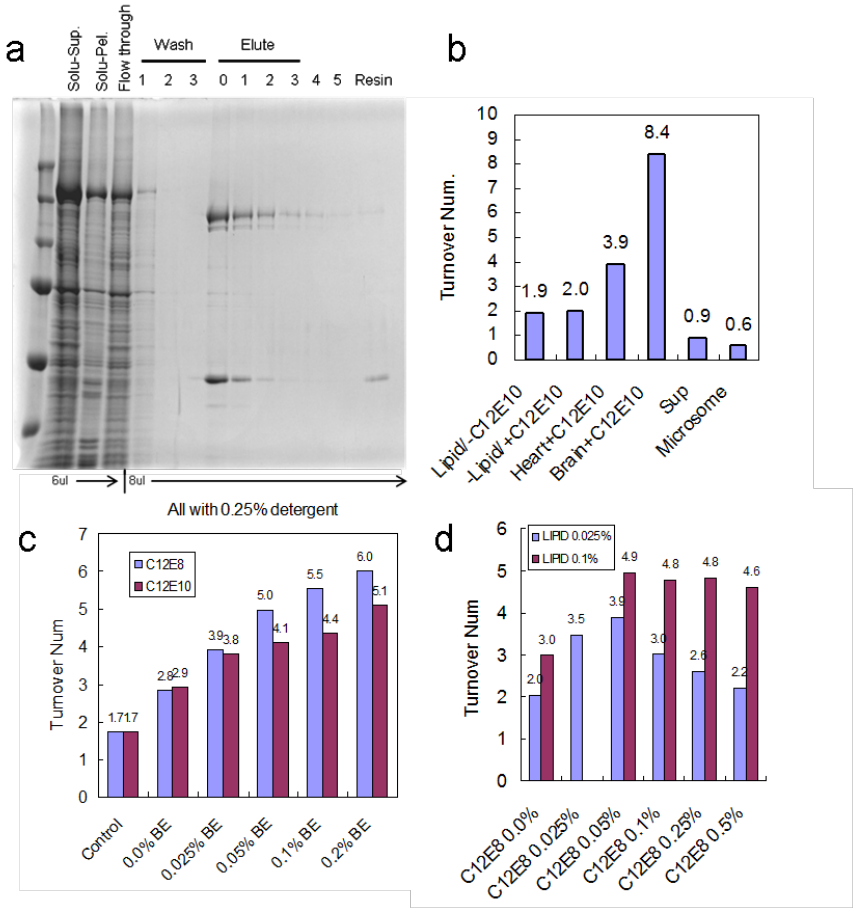

Figure 4. The SDS-PAGE image of PMCA protein after the HaloTag-based purification (a). The ATPase activities of purified PMCA after the incubation with different concentrations of detergents and lipids (b).

Next, we have investigated the optimal concentrations of $C_{12}E_8$ and BE during the purification process. PMCA purified under 0.1% $C_{12}E_8$ and 0.025% BE condition was compared with that purified under 0.033% $C_{12}E_8$ and 0.0067% BE. The eluted PMCA was used for ATPase activity assay and PMCA in both groups restored the activity while determined in the optimal condition with 0.05% $C_{12}E_8$ and 0.2% BE (Figure 5a). Moreover, the purified PMCA showed

higher activities after being incubated with 10 times of $C_{12}E_8$ and BE (0.5% $C_{12}E_8$ and 2% BE) for 30 min before assessment (Figure 5b) and the ATPase activity didn't drop even after 22 h of storage on ice (Figure 5c). As the reduction in detergents and lipids to 0.033% $C_{12}E_8$ and 0.0067% BE did not affect the ATPase activity, we further used the condition in the large scale purification of PMCA. The remove of TEV protease with the nickel resin was also carried out with 0.033% $C_{12}E_8$ and 0.0067% BE.

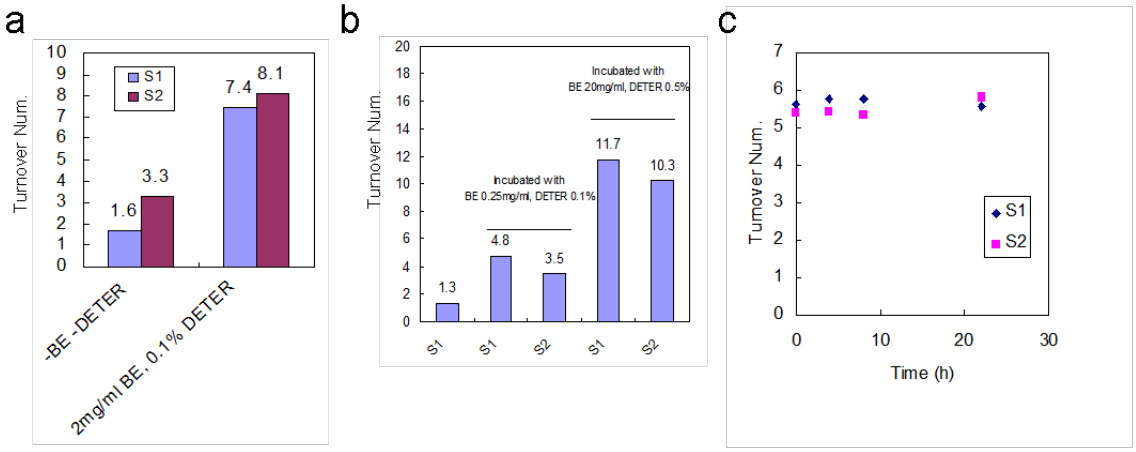

Figure 5. The ATPase activities of HaloTag-purified PMCA after the incubation with different concentration of detergents and lipids. S1 represents PMCA purified with 0.05% $C_{12}E_8$ and 0.2% BE, and S2 represents the 0.033% $C_{12}E_8$ and 0.0067% BE group.

The large scale purification of PMCA4a was carried out on a column using ÄKTA Protein Purification System. The SDS-PAGE image and the recovery percentages calculated according to ATPase activities were presented in Figure 6. As a result, we successfully obtained 51.0% recovery of PMCA4a from the microsomes after HaloTag-based purification.

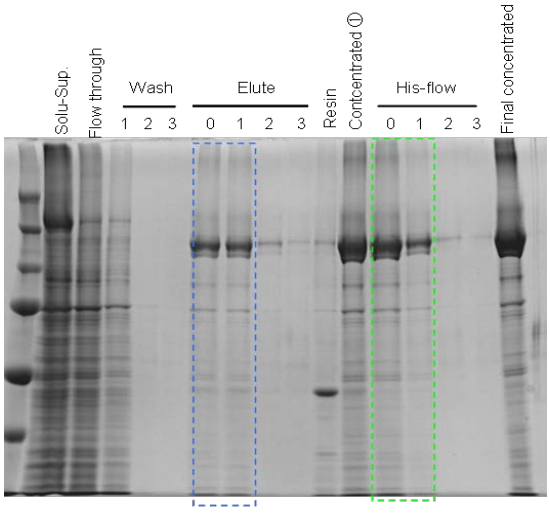

	Conc. (mg/ml)	Volume (ml)	Protein (mg)	ATPase Activity (/umol/min/mg)	Turnover Num	Recovery (%)
Micro-C12E10	2.952	1.5	4.428	0.400	0.889	
Micro-C12E8	2.829	1.5	4.243	0.358	0.796	
Sup-C12E10	2.419	1.4	3.386	0.590	1.310	solu %=112%
Sup-C12E8	2.583	1.4	3.616	0.400	0.889	solu %=95%
Pel-C12E10	0.538	1.4	0.753	0.057	0.127	
Pel-C12E8	0.667	1.4	0.933	0.015	0.034	
	combined sup:		6.990	0.495	1.100	100%
TEV0#	0.265	1.5	0.398	3.678	8.174	42.3%
Elution1#	0.209	2	0.418	4.859	10.797	58.7%
Concentrated 1	0.554	1.3	0.721	3.525	7.834	73.5%
His-flow0#	0.385	1	0.385	4.558	10.128	50.8%
His-flow1#	0.148	0.2	0.030	5.612	12.470	4.8%
Final concentrated	1.661	0.2	0.332	5.310	11.801	51.0%

Figrue 6. Purification of PMCA using HaloTag-based purification. SDS-PAGE image (left) and PMCA activity at each step (right).

Purification of PMCA by calmodulin-affinity column

The SDS-PAGE results showed that HaloTag purified PMCA4a seemed to contain other unwanted proteins. We

attempted to remove these proteins with a secondary purification using calmodulin-affinity chromatography. Purified PMCA was incubated with calmodulin sepharose 4B for 1 h in the presence of 1 mM $CaCl_2$ to allow the biding of PMCA to the resin. In the next step, flow through was discarded and resin was washed. Then, PMCA was eluted in the presence of 2 mM EGTA to be released form the resin. The elution was collected and examined with SDS-PAGE (Figure 7a). The non-targeted proteins were removed after secondary purification.

Furthermore, we noticed that the purified PMCA showed two bands on the SDS-PAGE gel in the region of ~124kD (Figure 7b), to detect whether they are both the PMCA proteins or part of the PMCA protein, we performed Western blotting to identify the double bands of HaloTag purified PMCA and calmodulin sepharose 4B purified PMCA. The anti-calcium pump PMCA antibody targeting 719-738 residues of PMCA4a (5F10, Abcam) and the anti-PMCA4a C-terminus antibody targeting final residues of the C-terminus of PMCA4a were used. The results showed that the second band, other than main band of PMCA4a, appears to be negative for anti-PMCA4a C-terminus antibody, and might be a form of PMCA4a without a C-tail.

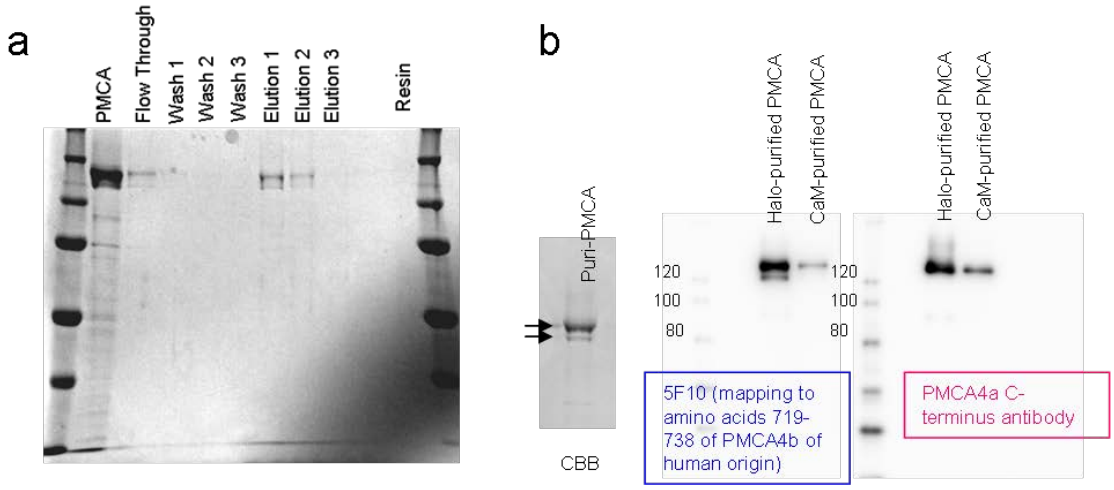

Figure 7. SDS-PAGE image of the purified PMCA after a secondary purification using calmodulin sepharose 4B (a) and the western blot image of the purified PMCA4a (b).

Discussion

Several observations have been made in the present study concerning PMCA, HaloTag-based purification, ATPase activity *etc.* We have obtained the PMCA4a-overexpressing COS-7 cell membranes and confirmed their ATPase activities. The stimulation of PMCA activity by calmodulin was also confirmed. The optimal solubilization condition of PMCA has been studied and 1% $C_{12}E_{10}$ was selected for eliciting the highest ATPase activity in the supernatant and was used in the further experiments. Next, we have investigated the preferable condition for HaloTag-based purification of PMCA, including the concentration of detergents and lipids for ATPase recovery after purification, as well as their concentration during the purification process. The results suggested a preferable concentration of 0.05% $C_{12}E_8$ and 0.2% BE could fully activate the purified pump, and 0.033% $C_{12}E_8$ and 0.0067% BE might be enough for the purification process. PMCA4a has been successfully purified from the cell membrane using the HaloTag-based purification, and a further secondary purification was also performed with calmodulin Sepharose 4B. The double bands in the SDS-PAGE of purified PMCA4a were characterized with antibodies to the N-domain or the C-terminus of PMCA, and the second band was identified as the PMCA4a without the C-tail.

To date, the three-dimensional structure of the PMCA pump has not been solved. Although PMCA shared many basic

properties of SERCA, however, PMCA as a membrane protein appears to have more obstacles in the protein purification process. In the present study, we attempted to purify PMCA4a from the PMCA4a over-expressing COS-7 cell membrane by two methods, namely, HaloTag-based purification and calmodulin-affinity chromatography. However, from the SDS-PAGE result of the purified PMCA4a sample, many unwanted proteins still remained in the final elution. Several attempts have been made to improve the current status to get higher purity of PMCA, including increasing the wash buffer volume and wash times, increasing the percentage of lipids and detergents in the purification process and screening a better detergent at the stage of solubilization *etc*. However, none of them resulted in a satisfactory result in the purification of PMCA4a. Moreover, the double bands of PMCA4a characterized after HaloTag-based purification suggested another form of PMCA4a without a C-tail after the purification. Thus, much work remains to be done before we could obtain a high purity PMCA4a sample which could be used in the crystallization of PMCA4.

References

1. Carafoli, E. "The Ca^{2+} pump of the plasma membrane." *J Biol Chem* 267.4 (1992): 2115-2118.
2. Carafoli, E. "Biogenesis: plasma membrane calcium ATPase: 15 years of work on the purified enzyme." *The FASEB Journal* 8.13 (1994): 993-1002.
3. Lopreiato, Raffaele, Marta Giacomello, and Ernesto Carafoli. "The plasma membrane calcium pump: new ways to look at an old enzyme." *Journal of Biological Chemistry* 289.15 (2014): 10261-10268.
4. Carafoli, Ernesto, and Marisa Brini. "Calcium pumps: structural basis for and mechanism of calcium transmembrane transport." *Current opinion in chemical biology* 4.2 (2000): 152-161.
5. Niggli, V., et al. "Purified (Ca^{2+}-Mg^{2+})-ATPase of the erythrocyte membrane. Reconstitution and effect of calmodulin and phospholipids." *Journal of Biological Chemistry* 256.1 (1981): 395-401.
6. James, Peter, et al. "Identification and primary structure of a calmodulin binding domain of the Ca^{2+} pump of human erythrocytes." *Journal of Biological Chemistry* 263.6 (1988): 2905-2910.
7. Di Leva, Francesca, et al. "The plasma membrane Ca^{2+} ATPase of animal cells: structure, function and regulation." *Archives of biochemistry and biophysics* 476.1 (2008): 65-74.
8. Toyoshima, Chikashi, et al. "Crystal structures of the calcium pump and sarcolipin in the Mg^{2+}-bound E1 state." *Nature* 495.7440 (2013): 260-264.

作成日：2017 年 2 月 25 日

日中笹川医学奨学金制度第38期研究者名簿

No.	氏名	中国所属機関	研究先	指導責任者
3801	葛　海燕	復旦大学附属華東医院 呼吸科 主治医師	北海道大学大学院医学研究科 呼吸器内科学	西村　正治　　教授
3802	鄭　衛青	南昌市疾病予防控制中心 媒介生物防制科 検験技師	帯広畜産大学 原虫病研究センター	玄　学南　　教授
3803	楊　光	山西省腫瘤医院 外科 医師	埼玉医科大学 国際医療センター	小山　勇　　病院長
3804	魏　霞蔚	四川大学華西医院 老年医学研究室 助理研究員	東京大学 高難度蛋白質立体構造解析センター	豊島　近　　教授
3805	孫　長博	中国医科大学附属第一医院 胸外科 住院医師	東京大学医学部附属病院 呼吸器外科	中島　淳　　教授
3806	兪　芸	上海交通大学医学院附属新華医院 急診科 主治医師	東京大学医学院附属病院 肝胆膵外科	國土　典宏　　教授
3807	王　煜	内蒙古医科大学附属医院 生殖中心 主治医師	東京大学医学部附属病院 産婦人科	藤井　知行　　教授
3808	梁　静	天津市第三中心医院 消化器内科 副主任医師	東京女子医科大学 消化器外科	山本　雅一　　教授 講座主任
3809	盧　永平	遼寧省計画生育科学研究院 分子遺伝室 助理研究員	東京女子医科大学 統合医科学研究所	山本　俊至　　准教授
3810	許　文成	湖北省中医院 薬事部 主管薬師	東京薬科大学 和漢薬物学	山田　陽城　　特任教授
3811	趙　宏波	河南省安陽市腫瘤医院 胸五科 主治医師	国立がん研究センター中央病院 食道外科	日月　裕司　　科長
3812	成　顕	西安交通大学第二附属医院 耳鼻咽喉頭頸外科 主治医師	独立行政法人国立病院機構　東京医療センター 耳鼻咽喉科	加我　君孝　　臨床研究センター・ 名誉センター長
3813	胡　瓊英	成都中医薬大学附属医院 検験科 主管技師	金沢医科大学 糖尿病・内分泌内科学	古家　大祐　　教授
3814	羅　蕾	四川省腫瘤医院 淋巴瘤病区 主管護師	静岡県立静岡がんセンター	鶴田　清子　　副院長
3815	鄭　佳連	遼寧中医薬大学附属医院 感染科 主治医師	名古屋大学 消化器内科学	後藤　秀実　　教授
3816	韓　瑩	黒龍江中医薬大学 中薬材GAP研究中心 助理研究員	名古屋市立大学 生薬学	牧野　利明　　教授
3817	劉　鉄	首都医科大学附属北京朝陽医院 骨科 副主任医師	国家公務員共済組合連合会名城病院 整形外科・脊椎脊髄センター	川上　紀明　　センター長
3818	李　文雅	中国医科大学附属第一医院 胸外科 主治医師	京都大学大学院 放射線遺伝学	武田　俊一　　教授
3819	胡　沁	四川大学華西医院 手術室 護師	兵庫県立大学 地域ケア開発研究所	山本　あい子　　教授
3820	顧　文奇	上海市第六人民医院東院 骨科 医師	奈良県立医科大学 整形外科学	田中　康仁　　教授
3821	張　立民	滄州市中心医院 麻酔科 医師	岡山大学 麻酔・蘇生学	森松　博史　　教授
3822	陳　富強	山東省血液中心 弁公室 主管技師	広島大学 免疫学	菅野　雅元　　教授
3823	張　含鳳	四川省腫瘤医院 放療病区 護師	広島大学 看護開発科学	宮下　美香　　教授
3824	張　尋	北京市疾病予防控制中心 栄養与食品衛生所 微生物検験師	香川大学医学部 分子微生物学	桑原　知巳　　教授
3825	馮　浩	中国医科大学附属第一医院 眼科 主治医師	九州大学 眼科学	園田　康平　　教授